AN INVESTIGATION OF THE DESIGN AND FUNCTION OF KNEE JOINT-SPARING MASSIVE ENDOPROSTHESES

By

REIHANEH POURSAEIDI

UNIVERSITY COLLEGE LONDON

Submitted for the Degree of Doctor of Philosophy in the University of London

SEPTEMBER 2017

I, Reihaneh Poursaeidi confirm that the work presented in this thesis is my own. Where information has been derived from other sources, I confirm that this has been indicated in the thesis.

Abstract

Distal femoral and proximal tibial joint-sparing bone tumour implants allow to preserve the knee, in limb salvage surgery. The aim of this thesis was to compare implant survival, functional outcomes, acceptance, proprioception and gait in patients with knee sparing implants and conventional knee sacrificing implants. Using FEA, a distal femoral implant and cadaver bone were modelled and parametrised to find the design that improves implant fixation.

A survivorship study of 104 consecutive patients following knee sparing surgery (mean follow-up 36.1 ± 11.0 months) found an implant survival rate of 78% and this is comparable to the reported survival for joint sacrificing prostheses. Younger patients showed improved implant survival compared to older individuals. Plate fracture was not observed and aseptic loosening was the main reason for revision. Radiographic analysis indicated that implantation accuracy increased implant survival.

Patient questionnaires showed that patients with knee sparing implants had more normal functional outcome and acceptance compared with patients with knee sacrificing implants. However, proprioception (joint position sense) was reduced in these patients.

Using optoelectronic gait analysis system, hip, knee and ankle joint angle in 19 patients and 3 healthy subjects were measured. Ground reaction force and time in stance were also investigated. Joint symmetry in the joint sacrificing group was improved compared to the joint-sparing group, however overall, the joint-sparing tibial group demonstrated a more normal gait pattern.

FEA results indicated that lower resection levels, reduced plate thickness and implant materials with lower modulus, decreased the stresses in the bone adjacent to the implant while loaded the bone more to reduce risk of stress shielding.

To conclude, knee sparing endoprostheses provide a reliable alternative to knee sacrificing implants in limb reconstruction in selected patients. However, the current design of joint-sparing implants can be optimised to potentially improve bone remodelling and implant fixation.

Acknowledgments

I am privileged to have worked alongside some remarkable people whom I acknowledge and am grateful for their contributions and support.

Prof. Gordon Blunn- Thank you for your guidance throughout the project. Your deep understanding of a broad range of topics never failed to amaze me and gave me the confidence that I was in safe hands. Most of all, thank you for giving me the opportunity to do this PhD.

Dr. Melanie Coathup- Thank you for your patience, encouragement and guidance. Thank you for making yourself available whenever I needed your help. Your attitude to research and life inspired me and gave me the confidence and energy to carry on.

Dr. Paul Fromme and Mr. Matt Thornton- Thank you for your support and for sharing your immense knowledge and experience. Without your guidance this project could not be completed.

Thank you to Stanmore Implants Ltd, for making this PhD possible and for their contribution to this project. Special thanks to Dr. Paul Unwin and Mr. Jon Charters.

Special thanks to my partner, Ben. Thank you for consistently loving me and for supporting me in everything I do. Thank you for your patience throughout all the years it took me to complete this PhD.

This thesis is dedicated to my parents for their love, strength and undying support. Thank you both Maman and Baba!!!

Contents

Figures

Tables

Chapter 1 Introduction

Massive bone tumour implants are commonly used for reconstruction of the limb following removal of a tumour. A joint-sparing massive bone tumour implant is a design that allows the knee joint to be spared. Additional potential advantages of joint-sparing implants include preservation of the knee and natural range of motion as well as eliminating failures associated with artificial joint replacements.

Knee joint-sparing endoprostheses are unique to the orthopaedic manufacturing company Stanmore Implants (Elstree, UK). During the last 13 years, over 100 patients have been treated with this implant, however no study has investigated survivorship greater than 5 years follow up. This thesis is therefore the largest follow up study investigating within this unique cohort of patients. No other study has investigated limb function and gait in patients with a joint-sparing implant.

This thesis examined the different design approaches used for joint sparing implants, investigated the survivorship, function, proprioception and gait in patients with these designs. Using Finite Element Analysis (FEA) the final part of this thesis investigated

the optimum design parameters and material properties required to ensure long-term fixation.

The following literature review evaluates the published information relevant to massive bone tumour implants and develops the rationale for the use and development of knee joint-sparing implants that were investigated in this thesis.

1.1 Bone Tumours and Bone Lesions

The term 'bone tumour' includes both malignant and benign lesions. The malignant bone tumour may be primary in origin or secondary where tumours develop at remote sites following metastasis from other non-osseous tissue sites to bone. Benign lesions remain localized within the bone and do not metastasize to other tissues or organs, but can limit joint function (Tsuchiya et al. 2007) or cause pathological fractures (Mattos et al. 2012). Although benign lesions can invade and destroy normal bone tissue, they do not metastasize to other anatomical sites and prognosis for this group of patients, with or without surgery, is usually favourable (Schwartz 2007).

1.1.1 Primary Malignant Tumours

Primary bone cancer is one of the most common types of cancer in children, teenagers and adolescents, occurring in the long bones of the upper and lower limb (Dorfman and Czerniak 1995). Bone cancer accounts for 10.6% of all cancers in 10 to 14 year olds and 8.1% of all cancers in 15 to 19 year olds (Bosetti et al. 2010). Osteosarcoma (56%) and Ewing's sarcoma (24%) are the most common bone cancers diagnosed in patients under the age of 29 (Kent and Trafton 2013) with a reported incidence of 4.8 (Gorlick et al. 2013) and 3 (Esiashvili, Goodman, and Marcus 2008) cases per million individuals per year. Bone cancers are relatively rare and occur predominantly before

the third decade of life (Teo and Peh 2004; Boffetta et al. 2014). An epidemiological study published by Siegel et al., reported that less than 0.2% of all cancers diagnosed yearly originated within bone, causing an estimated 1,440 deaths in 2013 (Siegel et al. 2013).

In adults, over 40% of primary sarcomas of the long bone are chondrosarcomas, followed by osteosarcomas (28%) and Ewing's sarcoma (8%). ('American Cancer Society Information and Resources for Cancer: Breast, Colon, Lung, Prostate, Skin' 2014). Despite the low incidence rates of osteosarcoma reported in individuals between 25 and 59 years of age, its prevalence rises again in individuals over 60 years of age with a frequency similar to that seen during adolescence (Mirabello et al. 2009; Gorlick and Khanna 2010). A study that compared the prevalence of osteosarcoma in adults and adolescent patients showed that a greater proportion of older individuals had tumours in axial sites, low-grade tumours, surface lesions, and rare presentations such as at extra-osseous sites (Gorlick and Khanna 2010). These differences in presentation of the disease suggest that the underlying pathogenesis of osteosarcoma in adults and adolescents is not identical. Factors such as Paget's disease or prior radiation exposure have been identified as risk factors particular to older patients (Mirabello et al 2009).

Other types of skeletal sarcomas occur less frequently in adults including, Fibrosarcoma (5%), Fibrous Histiocytoma (1-5%) and Angiosarcoma (less than 1%) (Schwartz 2007). Figure 1.1 shows the incidence rate of primary bone cancer relative to all other cancer types by age.

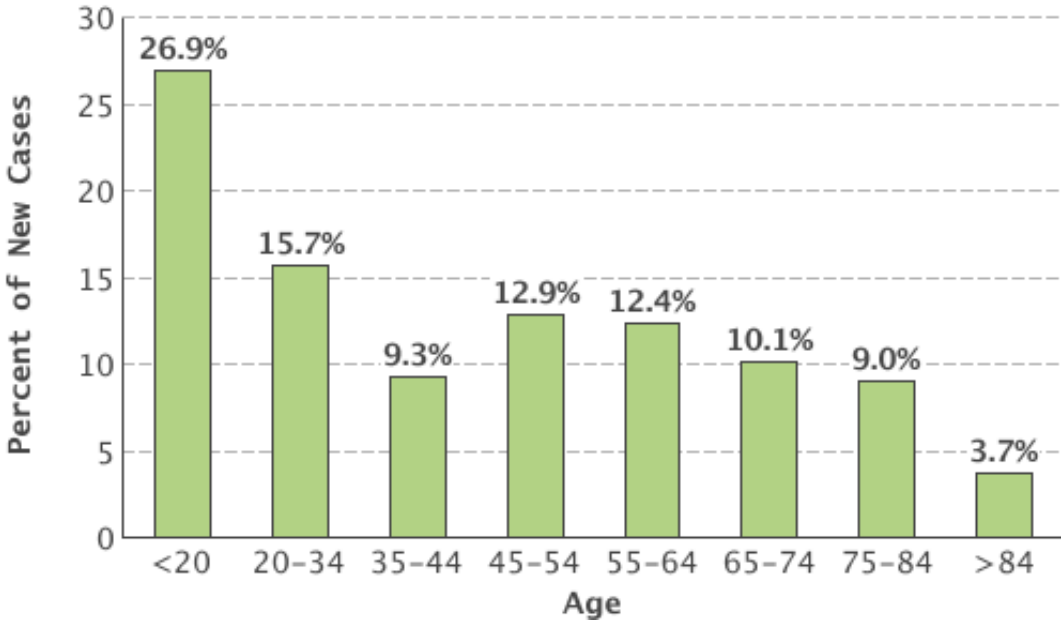

Figure 1.1 Incidence of primary bone tumours relative to all cancers by age. Source: ('Cancer of the Bones and Joints - SEER Stat Fact Sheets' 2011)

Although bone tumours can develop in any part of the body, they commonly occur in the lower (68%) and upper (10%) extremities (Kent and Trafton 2013), in particular in the metaphyseal portion of bone around the knee. Around half of all osteosarcomas develop around the knee (Gorlick and Khanna 2010); 36% in the distal femur and 17% in the proximal tibia (Geller and Gorlick 2010; Kent and Trafton 2013). Ewing's sarcoma can also affect any bone in the body, but the pelvis and femur are mostly affected (Rana et al. 2015), with the tumour often occurring in the diaphysis or occasionally in the metaphysis of long bones (Hefti 2015).

Secondary malignant bone tumours are more common than primary bone cancers (Weber et al. 2008). Cancers that most commonly metastasize to bone are breast and prostate cancers. Seventy to 85% of all secondary bone tumours are reported to have started in one of these soft tissue sites (Coleman 2001; Coleman 2006; Galasko 1982).

1.2 Diagnosis and Treatment

Initial symptoms of bone cancer often appear as prolonged and progressive but non-specific aches and pains which often occur at rest or at night (Weber et al. 2008). Characteristics such as swelling or decreased joint range of motion are other indicators of bone tumours (Weber et al. 2008). Radiographic assessment of the affected area is the first step towards diagnosis with over 80% of cases correctly diagnosed following radiographic review (Jan van der Woude and Smithuis 2014). Needle biopsies are performed to confirm the diagnosis and open biopsies are sometimes necessary in order to obtain an adequate quantity of biopsy material (Kent and Trafton 2013).

Treatment for bone cancer often includes preoperative neoadjuvant chemotherapy and radiotherapy followed by definitive surgery and adjuvant chemotherapy (Arpaci et al. 2005; Marina et al. 2004). Although improvements in the chemotherapeutic agents used has significantly increased patient survival rates, surgical resection of the tumour and the surrounding tissue remains an essential part of the treatment (Grimer 2005). Bone cancer does not have a clearly defined cause. However some studies have reported that exposure to high doses of radiation can increase the risk of developing osteosarcoma, particularly in children (Le Vu et al. 1998). Underlying bone abnormalities, such as the Paget's disease, and genetic predisposition are other causes of osteosarcoma (Qureshi et al. 2013). Ewing's sarcoma has not been associated with any heredity, congenital or previous radiation exposure (Pizzo and Poplack 2006).

1.2.1 Amputation

In the past, amputation was the standard method of treatment for patients with sarcomas of the extremities (Refaat et al. 2002). In the 1970s, with advances in chemotherapy and improved diagnostic methods, orthopaedic surgeons embarked on

limb-salvage procedures instead of amputation. By the early 1980s, pre-operative or neoadjuvant chemotherapy was introduced and the positive response of primary lesions led to introduction of many limb-salvage protocols (Enneking 2000).

Although limb-salvage procedures are the common method of treatment of bone tumours, amputation may still be necessary in cases where a wide excision is not possible without the limb becoming non-functional (Nagarajan et al. 2002). Progression of the tumour during chemotherapy, tumour recurrence and the failure of limb reconstruction are other indications for amputation (Schwartz 2007).

1.2.2 Rotationplasty

Rotationplasty is an alternative surgical technique to primary amputation in patients with bone deficiency in the lower limb, particularly in the distal femur or proximal tibia (Gupta et al. 2012). It is more commonly carried out in adolescent patients with remaining growth potential, (Fuchs and Sim 2004) where limb reconstruction can result in a leg length discrepancy over time, due to growth of the non-affected limb.

This technique involves an intercalary resection, followed by 180° rotation of the distal limb to allow the ankle to function as a knee joint when fitted with a modified below-knee amputation prosthesis (Nagarajan et al. 2002). The major requirements for optimal prosthetic function in this type of surgery is an intact major nerve, such as the sciatic nerve (Gupta et al. 2012; Fuchs and Sim 2004; Heise and Minet-Sommer 1993), a sensate foot that has an adequate plantar flexion strength and a good range of motion of the ankle (Gupta et al. 2012). Figure 1.2 shows a patient who has undergone rotationplasty surgery.

Rotationplasty is less common compared to other treatment methods, due to major concerns regarding the post-operative psychological effect of this procedure. Many studies have reported mixed results with regards to the quality of life and psycho-social outcomes of these patients in terms of body image and appearance (Veenstra et al. 2000; Gupta et al. 2012; Akahane et al. 2007). Limb salvage surgery where a wide resection of the tumour and surrounding tissues followed by reconstruction using a metal implant with the aim of retaining function of the affected limb, is currently the most common treatment for patients with bone tumours of the extremities (Grimer et al. 1997; Orlic et al. 2006). Over 85% of patients diagnosed with osteosarcoma in the UK are treated using limb salvage surgery (Grimer 2005).

Figure 1.2 Rotationplasty; the tumour and knee have been removed and the lower leg is connected to the thigh. The foot (now rotated 180°) replaces the knee joint, resulting in similar function to a below-knee amputation. Source: (Grimer 2005)

In the past concerns were reported when performing limb salvage surgery, over a conceivable increase in local tumour recurrence leading to metastasis and a decrease in patient survival when the affected limb was retained. However, studies have since

shown that limb salvage procedures do not shorten the disease-free interval or compromise the long-term survival of patients (Simon et al. 2005; Plötz et al. 2002). Results have also shown that preservation of the limb produced improved psychological and functional outcomes in patients (Jeys et al. 2003).

Improvements in surgical techniques, anaesthesia, neo-adjuvant chemotherapy and innovative imaging techniques such as Computer Tomography (CT) scans and Magnetic Resonance Imaging (MRI), have made the ability to accurately determine the disease free margins of bone adjacent to the tumour (Veth et al. 2003). Neo-adjuvant chemotherapy, is a treatment given as a first step to reduce the size of a tumour before the surgery and prevents the development of metastases (Wodajo et al. 2003). This is important, because it reduces the amount of bone and soft tissue resected during the limb salvage procedure (Grimer 2005).

Many surgical techniques are used during limb salvage reconstruction including endoprosthetic metallic implants, osteoarticular or intercalary allografts and composite endoprosthetic allografts where the resected joint and bone are replaced with an allograft from a donor individually or in combination with a massive endoprosthesis (Nagarajan et al. 2002). With most sarcomas of the bone involving the knee joint (Lietman and Joyce 2010), limb reconstruction that provides sufficient soft tissue coverage while restoring the extensor mechanism of the knee can be challenging, due to the knee's complicated anatomy (Ek et al. 2011). In cases where active mobility of the artificial joint cannot be achieved due to major muscle excision, a resection arthrodesis also known as joint fusion, may be inevitable (Veth et al. 2003).

1.3 Biological Reconstruction Methods

Osteoarticular and intercalary allografts are biological reconstruction methods used in reconstructive limb salvage surgery. Frozen and irradiated allografts are obtained from tissue bank facilities and can be used alone or combined with vascularised fibular (VF) autografts to fill the defect caused by tumour resection (Puri et al. 2009). In this method, an intercalary segment of the fibular with intact nutrient vessels and its periosteal cuff is harvested at a larger length than the gap that requires filling. The autogenous fibula is then inserted into the medullary canal of the tibial stump, distally and at the centre of the metaphysis or epiphysis, proximally. The graft is then secured in place using screws before a massive allograft is placed around it longitudinally (Figure 1.3) (Capanna et al. 2007). Massive allografts can be used for reconstruction without the vascularised fibular autograft. Although massive allografts with strong cortical bone provide a rigid fixation and excellent functional results, there is a risk of non-union at the allograft-host junction and subsequent fracture of the allograft (Li et al . 2010). This is due to the time required for revascularization of the allograft (Berrey et al. 1990). On the other hand, although the VF graft contains the essential blood supply and living cells to offer an alternative to the allograft (Taylor et al. 1975), it is a thin and weak bone that does not provide the structural strength for the weight bearing lower limb reconstructions and has high fracture rates (de Boer and Wood 1989). Combining the two methods that was first described by Capanna et al., utilises the advantages of both reconstruction methods (Capanna et al. 1993). The allograft provides early mechanical stability and bone stock and the VF graft enhances the biological properties of the reconstruction (Li et al. 2010). Although use of massive allograft and vascularised fibular autograft is an established method of reconstruction, studies have reported high early failure rates. Complications include; infection (8.6%),

fracture (34.3%) and non-union (25.7%) of the construct at the mean follow up of 7.2 years (Deijkers et al. 2005). This is believed to be associated with poor bone remodelling of the allograft leaving dead bone which is then susceptible to these failure modes.

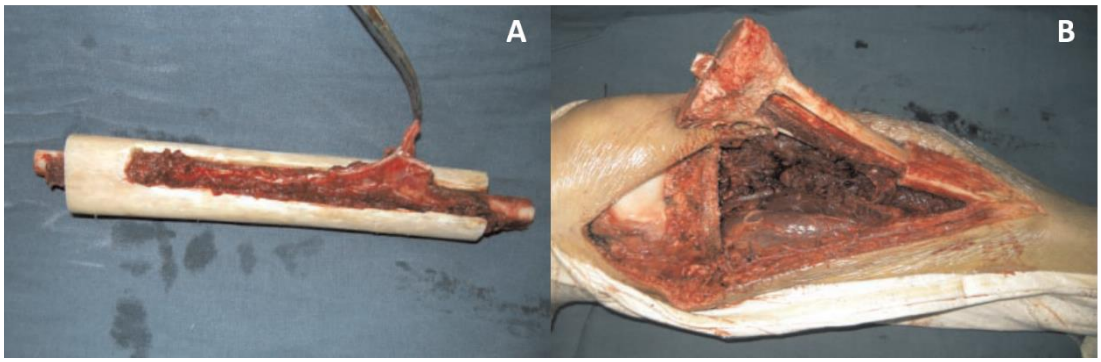

Figure 1.3 [A] Vascularized fibular flap, harvested to be placed into the medullary canal of the allograft. [B] Ipsilateral pedicle vascularized fibula being placed into the medullary canal of the allograft (Li et al. 2010).

Extracorporeal irradiation and re-implantation of bone is another reconstructive method of choice (Davidson et al. 2005). During this technique, bone is stripped from the soft tissues, washed with saline and wrapped in sterile towels before it is sterilised and re-implanted. The various methods of sterilization reported in the literature are boiling, autoclaving, gamma irradiation, microwave, pasteurization and the use of liquid nitrogen (Sharma et al. 2013; Singh et al. 2010). Various fixation methods, such as conventional or custom plates, nails and segmental metal prostheses may be used to securely attach the bone graft to the non-affected segments of bone (Agarwal et al. 2010).

These segmental, intercalary bone allografts or autografts, are sometimes combined with use of implants, to retain the natural limb function (Figure 1.4) (Capanna et al. 2007; Chang and Weber 2005; Agarwal et al. 2010).

Irradiation can increase the risk of fracture. There are reports that irradiation of more than 30,000 Gy reduces torsion and bending strength to 65% of normal, while breaking strength remains at 80% to 90% with radiation of less than 30,000 G (Rödl et al. 2000)

One of the main disadvantages in using devitalized autograft such as autoclaved, pasteurized, or irradiated bone is that it takes a long time for revascularisation and incorporation into the surrounding bone (Ogura et al. 2015). Bone graft healing has a similar mechanism to fracture healing and is initiated by an inflammatory response followed by vascular invasion from the host that facilitates the recruitment of mesenchymal stem cells (MSCs) (Zhang et al. 2005). In the case of autograft, both graft and host bone contribute osteogenic cells (Burchardt 1987), however as allograft does not contain any live cells, healing relies on invasion of the graft by host cells and tissues (Koefoed et al. 2005). Vascularization and remodelling of cancellous bone occurs rapidly due to its porous texture, with osteoblastic bone formation occurring first on the surface of necrotic trabeculae followed by osteoclastic bone remodelling. This process gradually resorbs the entrapped dead trabeculae and eventually replaces the entire graft with new living bone (Zhang et al. 2005). In contrast, vascularization of cortical bone is slow and requires an initial phase of bone resorption. Union of cortical graft begins at the host–graft junction and gradually spreads toward the mid-shaft of the structural graft. Any imbalance between resorption and bone formation can lead to bone loss and graft failure (Zhang et al. 2005). In the case of large structural allografts, remodelling along the allograft is limited. Failure rates of 25 to 35% failure rate due to non-union and fracture have been directly associated with this limited remodelling (Burchardt 1987; Berrey et al. 1990). Complications that required revision surgery or amputation were as high as 27.7% at a mean follow up of 9 years (Capanna et al. 2007). Forty-five percent of patients experienced complications related that did

not require further surgery at a mean follow up of 2 years and 10 months (Li et al. 2010).

The use of allograft for reconstruction is not always possible as obtaining bone graft may require ethical approval and is subject to availability. In addition, in vascularised fibular autograft reconstructions, instability and valgus deformity of the ankle joint can be caused if the fibular osteotomy is too close to the ankle joint (Capanna et al. 2007).

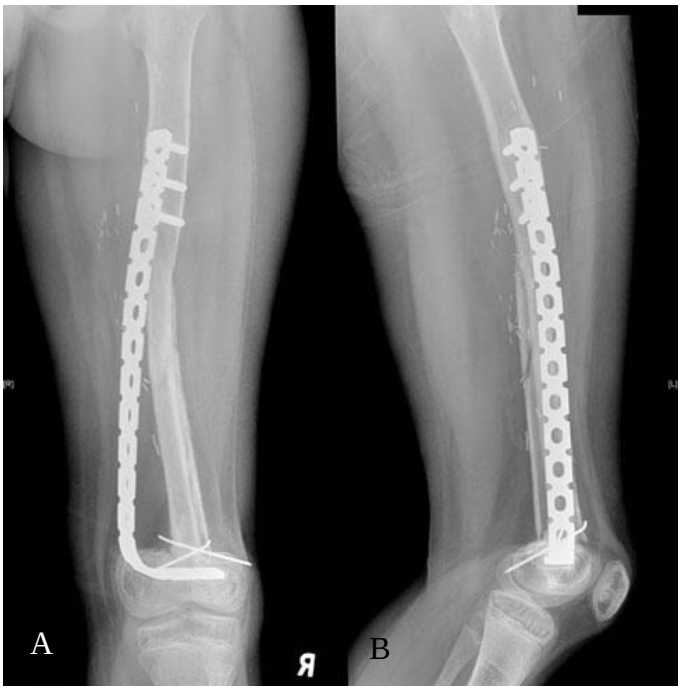

Figure 1.4 A combined allograft and vascularized fibula in a diaphyseal defect in the AP view [A] and the ML view [B]. An L-plate was used to stabilise the construct. Source: (Agarwal et al. 2010).

1.4 Use of Metal Endoprostheses in Limb Salvage Surgery

The earliest published example of an endoprosthetic reconstruction following treatment of a giant-cell tumour dates to the 1940's, where a custom proximal femoral component manufactured from Vitallium, a Cobalt-Chromium-Molybdenum alloy, was implanted into a patient (Hwang et al. 2014). Since then, custom-made massive

endoprostheses manufactured from metal, have been widely and successfully used in reconstructive surgery for bone tumours (Henshaw and Malawer 2001).

Early implants used to treat bone sarcomas were custom made, designed and manufactured to suit patients' skeletal size and planned surgical resection levels. They have been developed to safely and reliably reconstruct all major anatomical joints and adjacent bone (Schwartz 2007).

Concerns have been raised over the time required between diagnosis and manufacture of a custom implant, which can be several weeks and may have a negative impact on patient survival (Henshaw and Malawer 2001). Custom implants have also been criticised for their lack of intra-operative flexibility. The planned resection levels cannot be fully controlled and dimensions may need revising during the surgical procedure as tumour size may have increased during the time required for implant manufacture. Additionally, there may be a difference between the images provided to the design team for measurement preoperatively and the patient's actual anatomical dimensions. These errors can result in inaccurate manufacture of the implant (Henshaw and Malawer 2001) and can occur due to an inaccurately placed calibration device, producing magnification errors when imaged (Personal communication with Stanmore Implants, Elstree, UK).

These issues led to the introduction of modular, off-the-shelf endoprostheses in the mid-1980s. The Howmedica Modular Replacement System (HMRS, Howmedica International) was the first generation of modular endoprostheses that included an uncemented intramedullary (IM) stem supported by external flanges and trans-cortical fixation screws with a simple hinge mechanism to mimic the knee joint (Wiesel 2012).

The current designs of modular endoprosthetic systems are composed of a series of component combinations, designed for a wide variety of resection levels and sizes to be selected and combined to allow for the most suitable reconstruction (Croci et al. 2000). Modular systems provide flexibility during the operation. They include trial components that allow the surgeon to create the best reconstruction option prior to selecting and assembly of the actual, definitive endoprosthesis (Malawer et al. 2001).

Standardization of components in modular systems enables the manufacturers to increase the level of quality control greatly, while reducing the overall costs. As a result manufacturers can reduce overall inventory and time to delivery while providing a large choice of prosthetic shapes and sizes. Modular systems permit hospitals to maintain an on-site inventory that has allowed these systems to be available immediately as a backup option for selected non-oncologic patients, such as those undergoing difficult joint revision surgery or patients with significant peri-articular fractures (Malawer et al. 2001). However, retaining a full inventory of modular implants can be costly for hospitals due to the large number of components and the storage space required. Although the use of modular implants provides flexibility at the time of surgery, it can also increase the complexity of the mechanical construct thereby increasing the risk of failure associated with the individual components or the sum of all components (Croci et al. 2000). Disassociation and wear of the components are examples of failures that have occurred at the modular junctions (Henshaw and Malawer 2001).

Modular implants, cannot completely replace the use of custom implants. The aim of limb-salvage surgery is not only to obtain oncological clearance but to also preserve the maximum amount of bone and limb function following tumour resection. The

requirement of individual patients varies and modular implants cannot always address all specifications. Modular implants are only available to treat tumours located at common sites, such as the femur and reconstruction that involves bone of irregular geometry is only achievable with custom-made prostheses. Custom implants are fabricated for patients' exact size and resection levels, whereas a modular implant is only a close match. A study that evaluated the suitability of modular implants for use in a group of bone tumour patients reported that only 24% of all patients would be suitable for implantation of a modular implant without a compromise in design requirements (Unwin 2006).

1.4.1 Fixation of Massive Endoprostheses

Limb reconstruction using metallic endoprostheses is the preferred method of choice for limb salvage procedures in the UK (Jeys et al. 2008). The use of massive bone tumour implants allows full weight-bearing post-surgery which enables the patient to return to their daily physical activities rapidly (Jeys et al. 2005). Additional advantages when compared to allograft and composite endoprosthetic allografts include availability, reliability and cost-effectiveness (Grimer et al. 1997).

Stanmore Implants (Elstree, UK), previously part of the John Scales Centre for Biomedical Engineering, University College London has been designing and manufacturing custom-made massive implants since 1949 (Unwin et al. 1996). Implants are designed and manufactured on a case-by-case basis. The current design of implants that replace the knee joint, such as the distal femoral and the proximal tibial endoprostheses include a cemented or un-cemented intramedullary stem that is fixed within the medullary bone canal. Based on the anatomy of the patient, the required resection levels and the surgeon's opinion the stem is shaped to follow the

natural curvature of the intramedullary (IM) canal. The IM stem and the shaft of the implant are made from titanium alloy (Ti 318, Ti6Al4V). Titanium and its alloys have been reported to be more biocompatibility than other alloys which have suitable strengths. Titanium oxide, which is present on all titanium surfaces, allows absorption of proteins. It is thought that the immune system recognises the proteins covering the implant surface and so identifies the implant as part of the body. This reduces the risk of the immune response to the implant (Jansson et al. 2001). Cemented IM stems are fixed using polymethylmethacrylate (PMMA) bone cement. The chosen method of fixation must provide implant longevity and meet the patient's short and long term needs (Farfalli et al. 2009). Although a cemented stem may provide immediate post-operative recovery by means of a stable load bearing fixation, its long-term durability is often compromised by aseptic loosening. On the other hand, uncemented stems provide a durable biological fixation through potential bone growth and have a lower risk of aseptic loosening in the long term providing the implant is initially well fixed. However, they have a longer recovery period and can cause stress shielding of the cortical bone (Wyatt et al. 2014; Coathup et al. 2013).

The Compress® Compliant Pre-Stress Implant (Zimmer Biomet, Warsaw, IN) (Figure 1.5) is a novel bone tumour implant that generates a compressive force using a series of spring washers, which compresses the implant at the transection site onto the bone surface (O'Donnell 2009). The self-adjusting compression forces produced, promote biologic fixation at the interface while simultaneously transmitting stress to the cortex, inducing bone hypertrophy and minimizing stress shielding (Farfalli et al. 2009). Compression also seals the IM canal from inflammatory particulate debris thereby avoiding osteolysis (Blunn and Coathup 2014). In a retrospective study of 124 patients fixation of a traditional press-fit uncemented implant and Compress® endoprostheses

were compared. All patients were treated for primary tumours of the distal femur or for revision of failed distal femoral tumour reconstruction at a minimum follow up time of 2 years (Farfalli et al. 2009). Implant survival was estimated at 85% and 88% at 5 years for the uncemented press-fit and Compress® implants respectively. While aseptic loosening was the major cause of failure in the uncemented press-fit group, the main mode of failure in the Compress® group was fracture of the femoral bone, followed by failure of the mechanism (Farfalli et al. 2009). A matched-case study of the Compress® implant with traditional cemented IM implants described the early results of using the Compress® as safe and effective (Bhangu et al. 2006), however the long term outcomes remain unclear.

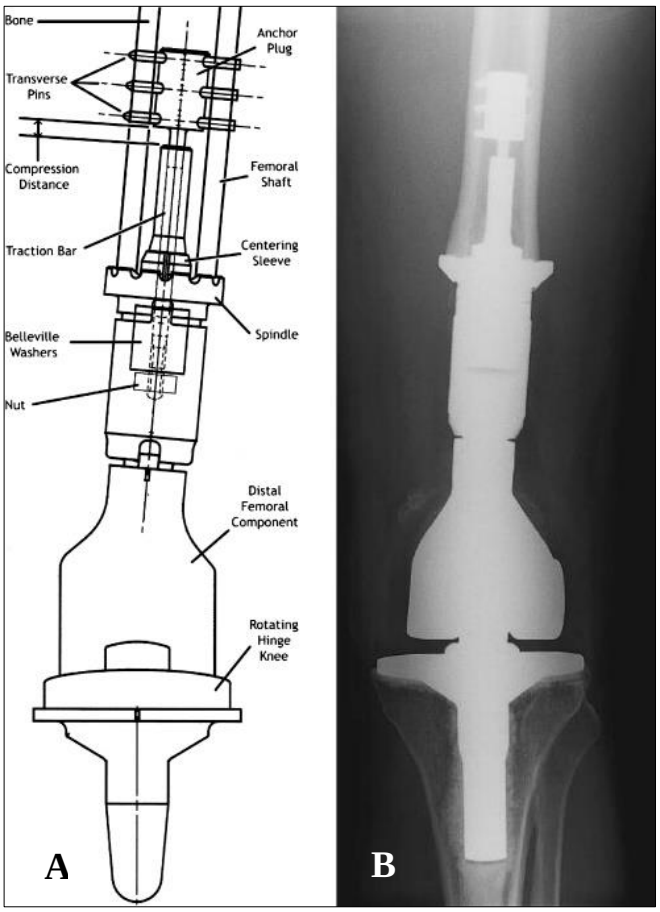

Figure 1.5 [A] Schematic diagram of the Compress® implant. [B] Antero-posterior radiograph of a distal femoral Compress® device (Bhangu et al. 2006)

1.4.2 Fixed and Rotating Hinged Knee Designs

Until 1992, the Stanmore fixed hinged knee was used for reconstruction of the joint. The Stanmore knee is a first generation highly constrained hinged total knee replacement that only allowed for simple flexion and extension of the joint. On loading, highly constrained knee designs transfer high stresses, particularly torque, on the stem-cement interface resulting in early aseptic loosening of the implant. Other designs of constrained knee replacements include the Wallidius and Guepar knee that were introduced in 1951 and 1969 respectively (Manning et al. 2005). Second generation hinged knees followed with design modifications that decreased prosthetic constraint by including varus/valgus motion and axial rotation to a linked design of the hinge, similar to that of the natural knee joint. These less constrained designs include the Sheehan®, Herbert®, Attenborough®, Spherocentric®, Noiles®, and Kinematic® rotating hinge prostheses (Sheehan 1979; Murray et al. 1977; Kershaw and Themen 1988; Kester et al. 1988; Matthews et al. 1986; Shindell et al. 1986; Shaw et al. 1989).

Although modern-generation rotating-hinge knee implants mitigate complications related to pain and range of movement (Biswas et al. 2013), aseptic loosening, infection, peri-prosthetic fractures and failure of the hinge mechanism are failures related to the hinge mechanism (Springer et al. 2004; Pour et al. 2007; Schwarzkopf et al. 2011). Third generation modifications include modularity of the endoprosthesis, deepening of the anterior femoral groove to improve patellar tracking, variable metaphyseal sizing for an improved fit and the use of bony ingrowth collars (Manning et al. 2005).

Since 1992, the Stanmore Modular Individualised Lower Extremity System (SMILES) rotating hinge knee replacement, a third generation hinged knee, made from cast cobalt-chromium-molybdenum alloy, has been used following resection of the joint (Coathup et al. 2013). The rotating hinge knee articulation includes a bevelled polyethylene bearing surface that is placed on the tibial plate and limits rotational movement to ±5°. Hyperextension of the knee is constrained by a bumper that acts as a secondary bearing surface (Maruthainar et al. 2006). Since introduction of the rotating hinge knee, a significant reduction in aseptic loosening (3-24% in 10 years) has been reported when compared with the fixed hinge knee design (46% in femoral replacements at 10 years follow-up) (Myers et al. 2007a, 2007b; Maruthainar et al. 2006; Unwin et al. 1996). This reduction in aseptic loosening is thought to have occurred due to a more physiological load distribution and a reduction in stresses within the IM fixation. Other third generation total hinged knee replacements include the Finn® (Biomet Inc, Warsaw, IN), NexGen THK® (Zimmer, Warsaw, IN) and S-ROM®, which is a modified version of the Noils® knee (DePuy Orthopaedics Inc, Warsaw, IN) (Manning et al. 2005). Figure 1.6 shows a distal femoral and a proximal tibial massive modular prostheses with a SMILES knee.

Although the rotating hinged knee provides a near normal range of motion and improved implant survival, fixed hinged knee replacements are still used in certain limb salvage operations. Removal of significant amounts of soft tissue around the joint, during wide resection of a tumour reduces stability and in these cases use of a constrained hinge is often more suitable (Merchán et al. 1994).

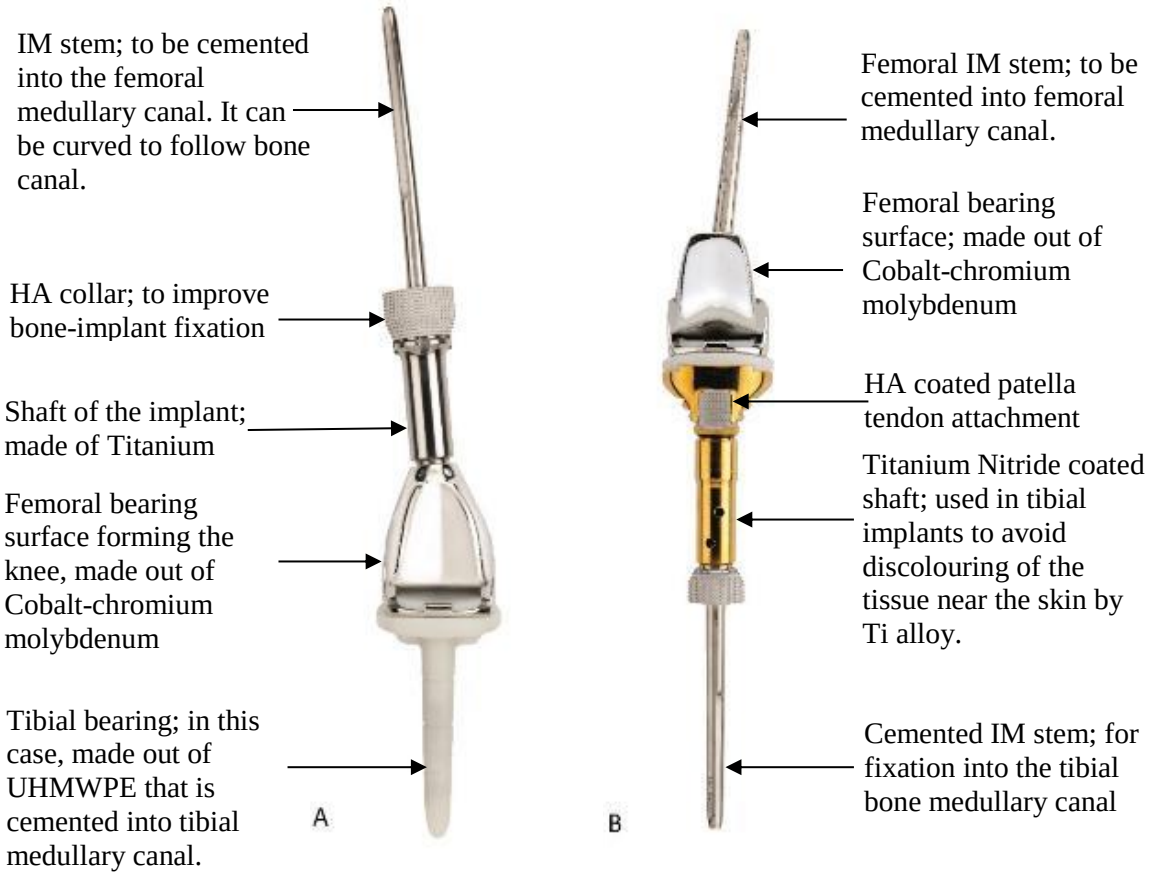

Figure 1.6 [A] A distal femoral and [B] a proximal tibial modular bone tumour endoprostheses. Both manufactured with a SMILES rotating hinge knee.

1.4.3 Complications of Massive Bone Tumour Endoprostheses

Although endoprosthetic reconstruction can provide good physiological and functional outcomes, there are a number of complications and high revision rates associated with this method of reconstruction. Complications may either be biological in origin, such as deep infection or mechanical in origin, such as implant fracture (6.1%) (Jeys et al. 2008). Aseptic loosening accounts for over 28% of failures and in massive implants is usually associated with adverse loading and failure of the cement mantle. In total hip replacements aseptic loosening is attributed to a biological reaction linked to the generation of wear particles and the subsequent cellular reaction leading to bone

resorption. It is not clear whether debris particles contribute significantly to the loosening of massive implants.

1.4.3.1 Infection

Deep infection is a major complication associated with the use of massive implants. Infection causes pain, a longer rehabilitation period, poor functional outcome, bone loss leading to repeat surgical procedures and often amputation (Jeys et al. 2003; Jeys et al. 2005). Risk of infection varies depending on the site of surgery. Some locations such as the tibia, have a reported higher infection rates when compared to distal or proximal femoral replacements (Pala et al. 2013) due to inadequate soft tissue coverage (Hay 2006). However, studies have shown a 50-75% reduction in risk of infection in proximal tibial replacements, when the "gastrocnemius flap" technique was used for reconstruction (Grimer et al. 1999; Myers et al. 2007b).

The most common pathogenic organisms known to cause deep infection following limb salvage surgery are coagulase-negative Staphylococcus and Staphylococcus Aureus respectively (Jeys and Grimer 2009). Although the risk of infection has been reduced in recent years with the aid of antibiotic loaded cement and silver coated megaprostheses (Hardes et al. 2010), infection remains one of the major challenges of limb salvage surgery (Jeys and Grimer 2009). A recent study reported an infection rate of 3.5% at a mean follow up of 6.6 years after a limb-salvage procedure using a massive endoprosthesis. The study also reported that 30.6% of amputations following a limb salvage procedure were caused by infection (Schwartz et al. 2014). Another retrospective study with a mean follow up period of 5.8 years, reported a higher infection rate of 11% and a higher amputation rate following limb salvage surgery due to infection (37%) (Jeys et al. 2005).

Peri-prosthetic infection rates following limb-salvage surgery using massive implants are considerably higher than those reported for typical total knee and hip arthroplasty. Studies have reported infection rates ranging from 0.46% to 1.90% (Amin et al. 2015; Gehrke et al. 2015; Kurtz et al. 2009) following primary total knee arthroplasty (TKA) with risk of infection reducing after 2 years (Kurtz et al. 2009). Similarly, the incidents of peri-prosthetic infection following hip replacement surgery have been reported between 0.67% and 2.4% (Kurtz et al. 2012; Bozic et al. 2014). Immunological deficiency in patients undergoing limb-salvage caused by the neo-adjuvant chemotherapy, absence of adequate soft tissue surrounding the affected area, the long operation time and the size of the implant are suggested to be possible causes of increased infection rates in bone tumour patients when compared with conventional arthroplasty (Morii et al. 2010). These factors may promote the formation of biofilms that can also increase the risk of infection following massive tumour surgery (Mavrogenis et al. 2011).

1.4.3.2 Wear of the Bearing Surfaces in the Joint

Another complication related to use of conventional knee-replacing massive implants, is wear of the prosthetic's bearing surface. The surgery to replace the bearing surfaces without revising the implant is known as rebushing (Myers et al. 2007b). Rebushing is often required when the implant has been *in situ* for an extended period of time and the polyethylene bushes have worn. As a result, rebushing is more commonly carried out in younger, more active patients. Failure of bushes can cause varus-valgus instability and locking and clicking in some cases, however it is often painless (Capanna et al. 1994). Rebushing replaces the worn plastic components and the metallic alloy axle that form the bearing surfaces with new components. Although surgically simple, this procedure still carries the risk of introducing infection (Myers

et al. 2007b). A rebushing rate of 10% has been reported in custom distal femoral replacements with a rotating hinge knee in a retrospective follow up study by Myers et al. (2007a). In this study, the mean time from implantation to rebushing was 11 years (range: 1 to 15 years) with some patients undergoing multiple rebushing procedures (Myers et al. 2007a). Capanna et al. reported a rebushing rate of 42% at an average of 64 months in patients treated with the KMFTR® fixed hinge modular tumour endoprosthesis by Kotz (Capanna et al. 1994). The reduced rate of rebushing required in the Stanmore SMILES knee has been associated with use of rotating hinge knee implants (Myers et al. 2007a). This rate was higher (16%) in proximal tibial replacements with a fixed hinge knee than in the rotating hinge knee design. The time from implantation to rebushing ranged between 3.7 and 17.7 years (Myers et al. 2007b). Replacement of the polyethylene bushes also reduced the incidence of mechanical failure and revision of the implant (Maruthainar et al. 2006).

1.4.3.3 Aseptic Loosening

Aseptic loosening is a principal mode of failure of the IM stem in massive implants, in particular in distal femoral replacements (Unwin et al. 1993). Aseptic loosening is defined as failure of the bond between an implant and bone in the absence of infection (Cedars-Sinai 2015). It often initiates with cortical bone loss at the bone-implant junction adjacent to the shoulder of the implant (Blunn and Wait 1991; Blunn et al. 2000). Osteolysis progresses over time and can be recognised in radiographic images by the presence of radiolucent lines adjacent to the IM stem or at the interface of the cement and bone. This can eventually lead to aseptic loosening and failure of the implant (Ward et al. 1997, 1993; Coathup et al. 2015).

Over the years, changes to the design of conventional implants such as the introduction of a grooved hydroxyapatite (HA) coated collar located at the shoulder of the implant, and use of a rotating hinge knee, have dramatically reduced the incidence of aseptic loosening (Myers et al. 2007a, 2007b; Coathup et al. 2015; Coathup et al. 2013). Variable revision rates (10% to 24% in 12 years), have been reported for custom distal femoral replacements with a rotating hinge knee joint (Maruthainar et al. 2006; Myers et al. 2007a). Revision rates due to aseptic loosening of proximal tibial replacements with a rotating hinged knee was reduced to 3% in 10 years from 46% in implants with fixed hinge knees (Myers et al. 2007b). The age of the patient at the time of operation and resection levels have both been indicated as major contributing factors to aseptic loosening (Unwin et al. 1996). Unwin et al., investigated 1001 patients with custom massive bone tumour implants and showed that younger patients with distal femoral and proximal tibial replacements were more likely to experience aseptic loosening. Aseptic loosening rates of 13.6% and 6.4% in patients under the age of 20 with distal femoral and proximal tibial replacements, respectively were reported in this study. In comparison, patients aged between 20 and 60 years, had loosening revision rates of 7.3% and 5.5%. The study by Unwin et al also found that aseptic loosening increased in relation to the percentage of the bone resected. Patients with over 60% of their tibia or femur removed were at higher risk of aseptic loosening.

Studies have reported that other factors may contribute to the incidence of aseptic loosening. Ward et al. (1997) suggested that aseptic loosening is associated with osteolysis caused by the presence of wear debris generated at the artificial bearing surfaces. Design modifications that promote extra-cortical bone bridging at the bone-implant junction with osteointegration may seal the interface and prevent the migration of wear particles (Rahbek et al. 2005) thereby reducing the risk of aseptic loosening

(Ward et al. 1997; Revell 2008). Other studies showed that extra-cortical bone bridging with ingrowth to the implant shaft reduced stresses on the IM stem by preserving load transfer at the shoulder thereby reducing aseptic loosening (Blunn and Wait 1991; Taylor et al. 1997; Chao et al. 2004; Coathup et al. 2015). A telemetric study by Taylor et al. (1997) showed that load distribution over the post-operative period gradually reduced within the shaft of the implant and gradually increased at the stem tip. Aseptic loosening is known to begin at the shoulder of the implant where bone loss is seen radiographically as radiolucent lines, and slowly progress towards the tip of the stem. Finite Element analysis has shown that the stresses on the IM stem and the cement mantle are reduced where there is extra-cortical bone bridging and integration of bone with the implant surface (Chao and Sim 1990; Fromme et al. 2017). This stress transfer at the cortical bone-implant junction and consequently, the reduction of resultant forces within the stem-cement interface has been associated with significant improvements in long-term implant fixation to bone and reducing the risk of aseptic loosening (Chao and Sim 1992). These findings suggest that bony ingrowth at the shoulder of the implant may maintain load distribution at the shaft of the implant, thereby reducing risk of aseptic loosening of the stem (Taylor et al. 1997).

1.5 Extra Cortical Bony Bridging

Various methods, such as HA coated ingrowth collars and porous coated implant shafts have been introduced to achieve osteointegration of extra-cortical bone in order to improve long term survival of the implant (Coathup et al. 2013). These composite implants were designed to encourage bone growth at the shoulder of the implant with direct contact and integration at the implant surface. Extra cortical bone formation at the shoulder of the implant is dependent on the immediate stability of the implant as provided by a cemented IM stem, while osteointegration and long-term fixation is

achieved through the ingrowth onto the collar positioned at the shoulder of the implant (Chao, 1989). Extra-cortical bone bridging has been reported to be enhanced by autogenous bone-grafting, which was shown to induce the formation of extra-cortical bone across a porous-coated implant shoulder (Chao et al. 2004).

Several radiographic analysis and histological studies of extra-cortical bone formation reported that bone bridging occurs consistently, however evidence of direct osteointegration of the ingrowth collar is limited (Blunn and Coathup, 2016; Unwin et al. 1995; Meirelles et al. 2015; Heck et al. 1986). Tanzer et al. compared bone growth to an ingrowth collar both radiographically and histologically in five implants retrieved from patients. Although the radiographs appeared to show osteointegration into the porous segment of all implants, histological analysis of the prostheses revealed that none of the extra-cortical bone had grown into the porous-coated segment of the implant but the porous surface was instead ingrown with fibrous tissue (Tanzer et al. 2003).

1.5.1 Hydroxyapatite Coated Collar

Many massive endoprosthetic replacements are manufactured from titanium alloy; however, osteointegration of titanium alloy is limited. Osteointegration is the direct contact between living bone and an implant. Histologically it is defined as the direct anchorage of an implant by the formation of bony tissue around the implant without the growth of fibrous tissue at the bone–implant interface (Albrektsson and Johansson 2001). Studies have reported limited direct bone-implant contact to titanium (Brånemark et al. 1983; Meirelles et al. 2015), and mechanical and chemical surface modifications are required to increase osteointegration and promote the bone-implant bond (Matena et al. 2015; Huang et al. 2015). Modifications include; surface

roughening (Barfeie et al. 2015; Hacking et al. 2012), the application of a porous coating (Bellemans 1999) and in the case of custom joint-sparing implants, grooved hydroxyapatite coated collars (Sanghrajka et al. 2005; Coathup et al. 2013).

The application of a hydroxyapatite ($Ca_5(OH)(PO_4)_3$) coating onto the implant surface has shown to significantly augment osteointegration (Drnovsek et al. 2012). Hydroxyapatite (HA) coatings, that have commonly been used in clinical practice, are osteoconductive due to its similar chemical composition to natural bone (Drnovsek et al. 2012). An osteoconductive compound is one that promotes bone growth on its surface (Albrektsson and Johansson 2001).

The HA collar located at the shoulder of the implant, was introduced by the Centre for Biomedical Engineering, UCL, Stanmore, during the early 1990's to improve bone-implant fixation (Unwin et al 1995; Blunn et al. 2000). The surface of the collar is grooved to facilitate extra-cortical bone growth and osteointegration of the implant surface. This ingrowth collar has circumferential and longitudinal grooves 1.5mm deep, 1.0mm apart, and 1.0mm wide (Figure 1.6). The surface of the collar is plasma sprayed with a 50μm thick highly crystalline hydroxyapatite coating (>85% crystallinity) (Plasma Biotal, Plasma Coatings, Tideswell, United Kingdom).

A recent study showed that bone ingrowth and osteointegration into the HA coated collar increased implant survival from 75% to 98% at 18 years (Coathup et al. 2013). A study by Myers et al. showed that HA collars reduced the incidence of aseptic loosening in patients with distal femoral prostheses. This retrospective study of 192 patients at a mean follow-up of 12 years, investigated and compared aseptic loosening in custom-made distal femoral replacements with HA collars to earlier designs of distal

femoral replacements without a HA collar at the shoulder of the implant. The study showed that the rate of aseptic loosening was reduced to 0% in implants with a HA collar from 24% in implants without a HA collar over a 10 year period (Myers et al. 2007a). Coathup et al. radiographically investigated 22 pair-matched patients with two types of implants, with and without a HA collar. The authors reported that nine of 11 patients had osteointegrated HA collars, whereas only one patient in the non-collar group had osteointegration. The study also reported fewer radiolucent lines, that can result in aseptic loosening, in the HA collar group when compared with the non-collar group (Coathup et al. 2015). In another study that histologically investigated the correlation between osteointegration and aseptic loosening, Coathup et al. (2013) found that when a grooved hydroxyapatite-coated structure was used, direct bone contact with the surface of the implant was seen whereas when no collar was present, the extra-cortical bone that formed at the shoulder did not osteointegrate but was instead separated from the surface of the implant by a layer of fibrous tissue. The study also showed that distal femoral massive bone tumour prostheses with a hydroxyapatite coated collar located at the shoulder of the implant had a lower revision rate due to aseptic loosening compared to those without a HA collar (Coathup et al. 2013).

1.6 Extra-Cortical Plate Fixation

Metallic plates are commonly used in orthopaedic surgery, particularly for the internal fixation of bone used for alignment and healing after fracture (Pakula et al. 2013). Use of plates for the fixation of massive bone tumour implants was first reported in the 1950s, before the development of bone cement for fixation of an IM stem (Burrows et al. 1975). In cases where extensive resection of bone is required, the remaining segment of bone is small and the IM stem has to be fixed within a wide-diverging canal and surrounded by relatively weak cancellous bone. In such cases, fixation of the IM

stem may be enhanced by use of extra-cortical plates which are fixed to the periosteal surface of the bone with screws (Cobb et al. 2005).

The natural growth of long bone is accompanied by remodelling and centrifugal growth with bone formation on the periosteal surface such that the intramedullary cavity increases in diameter as does the overall bone diameter. This remodelling is continuous throughout life and in older individuals this increase in girth is accompanied with thinning of the cortex. This natural remodelling can further facilitate extra-cortical plate fixation (Blunn and Coathup 2016).

Design of the extra-cortical plates used by Stanmore Implants was based on the results of a study by Coathup et al. that investigated the optimal geometric and surface properties that encouraged ingrowth and bonding of bone to an extra-cortical plate in an *in vivo* animal model (Coathup et al. 1999). The surface modifications investigated included a roughened titanium alloy surface, a plasma sprayed HA coating of low crystallinity, a solution precipitated calcium phosphate coating and a plasma sprayed highly crystalline hydroxyapatite. The results of this study indicated that a highly crystalline plasma sprayed hydroxyapatite coating, encouraged significantly greater bone-implant contact when compared to the other surfaces investigated. Additionally and for optimal bone ingrowth into the plates, the presence of either holes or slots along the length of the plate was required (Coathup et al. 1999).

As a result of this initial study, extra cortical plate fixation was further investigated in a caprine model where plates were used to fix a massive segmental implant to bone following the removal of a 50mm mid-tibial segment of bone (Coathup et al. 2000). Bone apposition on the external surface of the plates occurred through a combination

of periosteal bone production, invasion of bone through slots in the plate, and bone growth over the ends of the plates. The presence of slots within the plates improved bone ingrowth onto the plates. Finite element analysis demonstrated that extra-cortical plate fixation to the bone surface altered the stresses locally. In models with 3 or 6 plates, the second moment of area that indicated stiffness was increased, leading to stress shielding of the bone adjacent to the plate. The least amount of stress shielding was seen in response to the 2-plate design (Coathup et al. 2000).

The extra-cortical plate design developed for fixing massive bone tumour implants to longer segments of bone in patients, was later implemented in the design of joint-sparing implants where bone length was limited.

1.7 Joint-Sparing Diaphyseal Resection

Resection of the tumour and the surrounding bone with a wide margin, free from invasion of the tumour, is the first principle of limb salvage surgery. The recommended margin is 3cm from the bony extent as seen on the MRI scan (Kawaguchi et al. 2004). As described earlier in this chapter, the majority of bone tumours occur within the metaphysis of long bones close to the articulating joint. When the distal femur or the proximal tibia is affected, resection often includes the knee joint in order to obtain satisfactory surgical margins (Malawer and Sugarbaker 2001).

In some patients tumours localise to the metaphysis without involving the joint. These situations allow the surgeon to resect the tumour within an adequate margin without sacrificing the joint or the growth plate (Agarwal et al. 2010). With the aid of more accurate imaging techniques and surgical advances surgeons have been able to achieve closer tumour margins with confidence (Gillespy et al. 1988). This has increased the

options available to the surgeon who may wish to avoid resection of the joint. This is particularly advantageous around the knee due to the high failure rates reported in distal femoral and proximal tibial replacements (Sharma et al. 2006) and with the complications involved in achieving a successful extensor mechanism, especially following a proximal tibial replacement (Titus and Clayer 2008). Reconstruction of the proximal tibia is particularly challenging due to its anatomical limitations (Puri 2014). The close proximity of the neurovascular structures in the popliteal fossa and peroneal nerve at the lateral aspect of the leg, insufficient soft tissue coverage and the need to reattach the extensor mechanism following resection of the tibial tuberosity involved with the tumour, are complications involved with the reconstruction of tibia (Mavrogenis et al. 2012). The patella tendon is attached to the tibial tuberosity and passes through the anterior aspect of the knee. It is also embedded in the quadriceps tendon that is responsible for extension of the knee joint (Martini 2006). Failure to achieve appropriate reattachment of the patellar tendon will lead to lack of an extensor mechanism which will alter the biomechanics of the knee and can result in patella alta, atrophy of the quadriceps and altered gait with an extensor lag (Oddy et al. 2005).

Numerous options for the reconstruction of the extensor mechanism of the knee following proximal tibial and extra-articular knee resections have been reported (Mavrogenis et al. 2012). These include direct reattachment of the patellar tendon to a megaprosthesis (Oddy et al. 2005; Pendegrass et al. 2004), osteoarticular allografts or allograft prosthesis composites (Ek et al. 2011; Clatworthy and Gross 2001), and augmentation techniques with synthetic materials, autologous bone graft or synthetic substitutes, tendon transfers and muscle flaps, and combined techniques.

In some cases, during a joint-sparing reconstruction, the growth plate can also be spared. Saving the distal femoral and proximal tibial growth plates in adolescent patients are especially beneficial allowing normal growth of the affected limb (Agarwal et al. 2010). However, limb-reconstruction near the knee and achieving secure implant fixation to small segments of bone is a challenging procedure with limited reconstruction options. Custom, knee sparing metallic endoprostheses preserve the knee joint and have the potential to preserve gait and in young patients retain the growth plate.

1.8 Custom Knee Joint-Sparing Implants

Preservation of the natural joint can eliminate the issues related to joint replacements, such as limited range of motion (Frink et al. 2005) and wear of the artificial knee (Henshaw and Malawer 2001; Myers et al. 2007b; Maruthainar et al. 2006; Myers et al. 2007a). Achieving a normal ROM in conventional massive implants has been one of the challenging areas in limb salvage surgery using massive implants that replace the joint (Frink et al. 2005; Tsauo et al. 2006). In addition and where possible, any future leg length discrepancy caused by removal of the epiphyseal plate in adolescent patients can be avoided (Agarwal et al. 2010), provided that the physis is not damaged by extra-cortical plate and screw fixation.

Knee sparing massive endoprostheses were introduced in the late 1990s by Stanmore Implants, Elstree, UK. They allowed for intercalary, metaphyseal reconstruction where the implant is fixed to the remaining segment of bone using extra-cortical plates. Joint-sparing prostheses provide an alternative method of fixation in cases where insufficient bone is available for fixation using IM stems (Agarwal et al. 2010). Another advantage of using a knee joint-sparing implant is that fixation of the implant is limited to the

affected bone only. When conventional knee sacrificing implants are inserted, surgery requires not only removal of the affected bone and joint but additional bone is removed in the tibia for a distal femoral replacement and in the femur for a proximal tibial replacement, for fixing the rotating hinge.

To achieve a secure initial fixation, extra-cortical plates are fixed to bone using either uni-cortical or bi-cortical screws. Bi-cortical screws lock the plates to both cortices and improve fixation especially in cases where the cortical bone is deficient, as is the case in many revision cases. The optimum number of screws required to achieve a long lasting successful fixation is dependent on the shape and size of the implant and the amount of residual bone, which often varies from patient to patient. Failure to obtain a secure primary fixation can result in loosening of the implant (Cobb et al. 2005). Figure 1.7A shows an A/P radiographic image obtained from a 43 year old female patient at 62 months follow-up, with a proximal tibial joint-sparing implant in her left leg. The radiograph shows plate fixation with uni-cortical screws and slotted cutting fins on the plateau of the implant. Figure 1.75B is an A/P radiograph obtained from a 23 year old male patient at 46 months follow-up, with a distal femoral joint-sparing implant in his right leg. The plateau of the implant includes spikes for improved fixation in addition to extra-cortical plate fixation with screws.

A knee sparing implant can only be used if there is no involvement of the popliteal neurovascular structures or invasion of the joint by the tumour to allow safe plate fixation of the prosthesis (Gupta et al. 2006). The remaining segment of bone after the resection must be long enough to secure the implant using extra-cortical plates. The resection level must be clearly planned using MRI scans preoperatively to ensure no

interference with the tumour and to verify that a joint-sparing implant is suitable for use (Gupta et al. 2006).

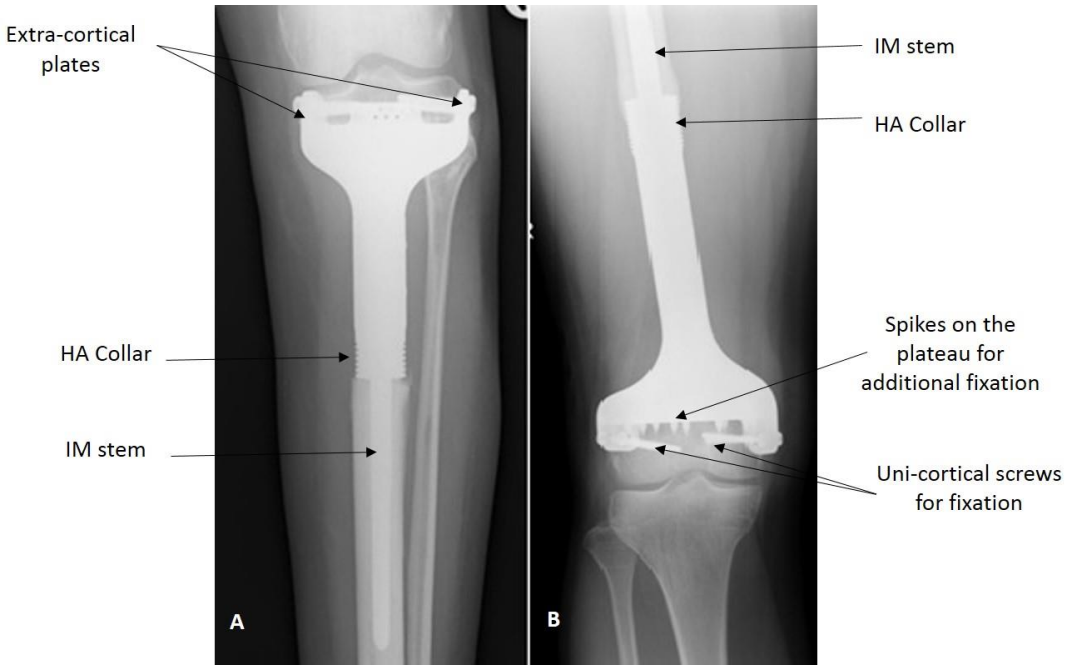

Figure 1.7 [A] An A/P radiographic image of a 43 year old female patient at 62 months follow-up, with a proximal tibial joint-sparing implant. The radiograph shows plate fixation with uni-cortical screws and slotted cutting fins on the plateau of the implant. [B] An A/P radiograph obtained from a 23 year old male patient at 46 months follow-up, with a distal femoral joint-sparing implant. The plateau of the implant includes spikes for additional fixation.

1.8.1 Resection Accuracy

Creating a construct that can reliably grip and hold the remaining small segment of bone with anatomically accurate dimensions and good function of the limb postoperatively, are the major challenges in knee sparing implant surgery (Agarwal et al. 2010, Wong et al. 2012).

As knee sparing implants are custom-made, their success is dependent on correct resection of the diseased bone prior to insertion of the implant. Resection of the bone

is technically demanding as the surgeon is required to ensure the surgical margin is sufficiently wide for complete removal of the tumour, and that the plane and orientation of the resection match that of the custom prosthesis precisely (Wong and Kumta 2013).

While most surgeons rely on various imaging techniques such as MRI and CT-scans combined with their knowledge and experience to make an accurate cut, others use computer assisted navigation methods to obtain a precise resection (Lin et al. 2015; Wong and Kumta 2014). In computer aided surgery, MRI and CT images are fused, allowing the surgeon to produce a pre-operative surgical plan by defining the extent of the tumour and resection levels (Wong and Kumta 2014). Intra-operatively, a tracker is attached to the bone for registration. This means that the operative anatomy is matched precisely with the images of the pre-operative surgical plans and involves matching selected bony landmarks and points chosen on the exposed surface of the bone. Once the accuracy of the registration is confirmed, the "navigation" probe and the instruments mounted with the navigation trackers are calibrated to allow for real-time spatial location of the instruments in relation to the patient's anatomy and to create accurate resections according to the preoperative surgical plans (Wong et al. 2007).

A simpler technique to help achieve resection accuracy is by using a patient-specific computer-aided designed/computer-aided-manufactured (CAD/CAM) surgical jig. The jig, identifies both the distal and proximal resection points using distal and proximal cutting blocks that are positioned on the bone surface at the planned resection sites without translation. The slits on the cutting blocks have the same orientation as

the resection planes on the joint-sparing implant, allowing the surgeon to create a cut that matches the implant precisely (Wong et al. 2012).

1.8.2 Clinical Outcomes of Joint-Sparing Implants

The first study to report on the clinical use of joint-sparing implants and extra-cortical plates in four anatomical locations; proximal tibia, distal femur, distal humerus and mid-shaft humerus, was by Cobb et al. in 2005. Tri-plate endoprostheses were implanted into 14 patients who either underwent revision surgery following failure of the intramedullary (IM) stem fixation or in primary surgery, where the remaining segment of bone was too small for fixation using an IM stem. All patients undergoing revision surgery had previously been treated for bone tumours and as a result had poor bone stock, making implant fixation more challenging. In such cases revision to another cemented device was only a viable option if sufficient bone stock remained for adequate fixation. The success rate of a revised implant is often lower than primary implants (Cobb et al. 2005). This is due to osteolysis at the bone-implant junction resulting in the reduced Young's modulus of the bone surrounding the cemented stem (Blunn and Wait 1991) that gradually progresses along the bone-cement interface resulting in aseptic loosening (Coathup et al. 2015). This bone loss means that the quantity and quality of bone is reduced and therefore the revised implant is more likely to fail. Use of extra cortical plates, not only makes implant fixation to short bone segments possible, but by altering the stress distribution on the bone, can strengthen the bone that has previously been weakened (Cobb et al. 2005). All implants investigated in the study were designed and manufactured by Stanmore Implants Worldwide Ltd (Elstree, UK). The extra-cortical plates were manufactured 12mm wide, with a tapering thickness of 3mm to 2mm and were of variable length depending on their location. Patients were followed up prospectively and their functional

outcomes were measured. Functional scores showed that all patients regained their original level of function within 5 months of surgery. In addition, radiographic analysis showed bone remodelling with bone growth seen over the plates and integration at the bone-plate interface. Cobb et al., reported a survival probability of 89% at a follow-up period of 99 months. With the high survival probability and good functional and surgical outcomes, this study further encouraged the use of extra-cortical plate fixation and joint-sparing surgery using massive implants.

Following the promising results reported by Cobb et al., a prospective study of 8 patients who met all criteria for receiving a distal femoral knee joint-sparing implant was carried out by Gupta et al. (2006). All patients were diagnosed with a malignant bone tumour that had not crossed the physis of the distal femur. Implants were custom-made distal femoral joint-sparing implants with intramedullary stems that were either cemented or uncemented within the femoral bone. Implants were fixed to the remaining small segment of distal femur using 2 or 3 extra-cortical plates attached to bone using screws. Postoperatively all patients were followed up and assessed radiographically and limb function was semi-quantified using the Musculoskeletal Tumour Society Score (MSTS) (Enneking et al. 1993). Although the functional results reported by Gupta et al. 2006 were promising (mean score: 80%, range 57-97%), knee stiffness in flexion (only 20°) was observed in one patient (12.5%). Good overall function was reported for all other patients, with no reports of fracture, infection, recurrence, aseptic loosening or amputation at the 2 year follow-up (mean: 24 months, Range: 20-31 months). Radiographic evidence of new bone formation and plate incorporation was also reported, suggesting that extra-cortical plate fixation is a viable alternative to IM stem fixation in massive implants (Gupta et al. 2006).

Another follow up study by Spiegelberg et al. (2009), investigated 6 patients with joint-sparing tibial replacements. Range of motion (ROM) and overall function was assessed using the MSTS and revised Oxford Knee Score (OKS) (Murray et al. 2007) at a mean follow-up of 35 months. Results showed that the prosthesis allowed preservation of the knee joint with good overall function (Mean: MSTS= 79%, OKS= 40 out of 48) and with no early evidence of aseptic loosening (Spiegelberg et al. 2009).

When knee sparing implants were compared to bone graft as a method of preserving the knee joint, custom prostheses with plate fixation were found to produce an improved function, durability and recovery time (Agarwal et al. 2010).

While there are a number of studies that have assessed functional outcomes in patients with a joint-sparing implant using questionnaires, no investigation using more objective methods such as gait analysis has been made to quantifiably assess and compare their function with that of the joint sacrificing endoprostheses.

1.9 Gait Analysis and Applications

Gait Analysis is the systematic review of human walking, using the eye and brain of experienced observers, augmented by instrumentation for measuring body movements, body mechanics and the activity of the muscles (Levine et al. 2012). The most commonly known clinical application of gait analysis is in the treatment of neuromuscular disorders such as cerebral palsy (Gage et al. 1996). Precise examination of gait in patients with cerebral palsy can enable the surgeon to assess the pathological components and to carry out all corrections during one surgical operation. This reduces the risk of post-operative complications due to a fewer number of procedures and consequently avoids unnecessary pain to the patient. Identifying the pathological

components of the gait prior to surgery can also reduce the post-operative rehabilitation period (Gage et al. 1996). Gait or motion analysis has applications beyond investigating gait in individuals with cerebral palsy. Other medical pathologies, such as those related to upper extremities or reconstructive surgery of the lower extremities may benefit in a similar manner ('Research Council' 2015).

Computerized gait analysis is used as a functional outcome assessment tool instead of or in combination with traditional clinical evaluations or questionnaires (Kilgore 2005). Historically, most orthopaedic surgeons and rehabilitation specialists have relied primarily on static examination and observational gait analysis to assess outcomes. Computerized gait analysis is an accurate, precise and valid method of quantifying movement and therefore can be an effective functional outcome measure ('Research Council' 2015).

The patellar tendon and the extensor mechanism that is often compromised in patients with knee-sacrificing implants, is preserved in patients with joint-sparing endoprostheses. Therefore a near normal gait in joint-sparing patients is expected, following their full post-operation recovery. This is the first study that investigated patients' gait to establish whether an improved gait is achieved in lower limb reconstruction with joint-sparing endoprostheses.

1.9.1 Normal Gait

In order to identify gait pathology in patients, gait assessment often includes a comparison of pathologic gait with "normal gait". Normal gait is a pattern which has been generalised from the general public across many variables, including age and sex (Fish and Nielsen 1993). A complete gait cycle is often divided into several phases,

however, it consist of two main phases; the stance, which is 60% of the cycle, and the swing phase that makes up the remaining 40% of the cycle. A complete gait cycle is from the heel strike to the next heel strike of the same foot (Gage 1993). The Initial Single support phase starts after the opposite toe off and at the start of the commonly known mid-stance phase. Terminal single support ends with the opposite initial contact where pre-swing phase starts (Figure 1.8

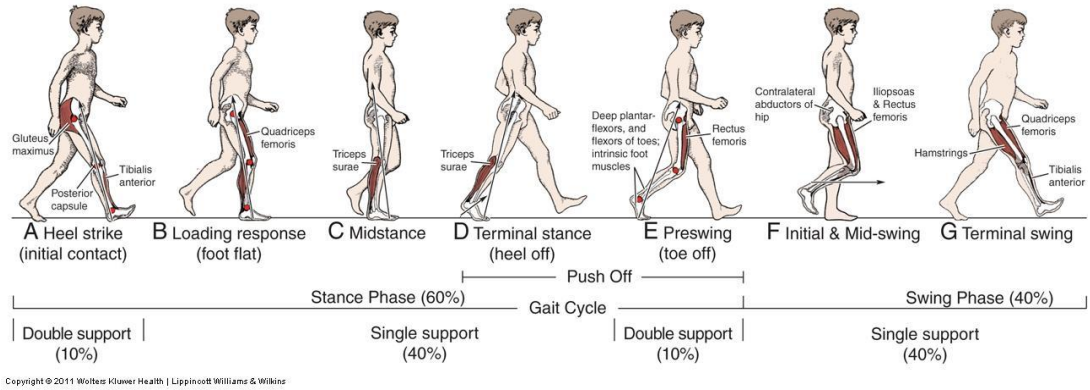

).

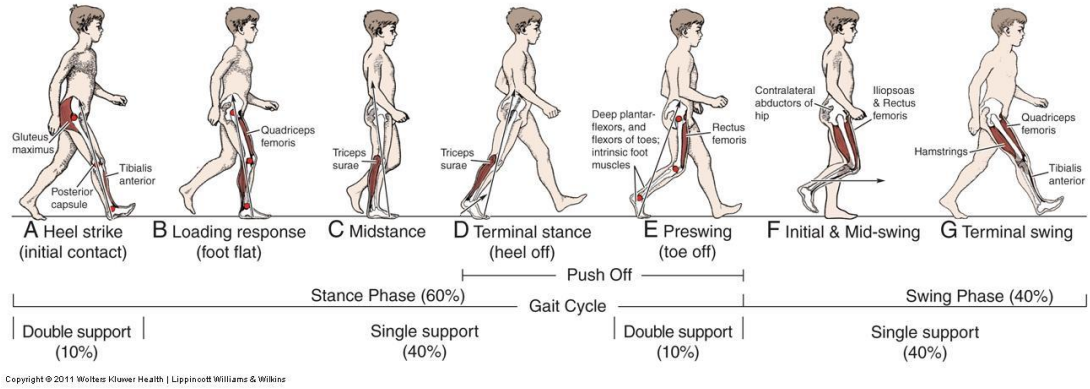

Figure 1.8 Demonstration of the gait cycle ('Gait in Prosthetic Rehabilitation - Physiopedia, Universal Access to Physiotherapy Knowledge.' 2016)

1.10 Material Properties of Skeletal Tissue

Any implant design must take into account bone remodelling as differences in Young's modulus between the implant and the bone can affect bone formation an

resorption. In order to understand bone remodelling the material properties of the bone need to be understood and the way that bone remodels and the stimuli associated with remodelling need to be comprehended.

Bone consists of living cells, organic collagen fibres and inorganic hydroxyapatite crystals. The bone cells include osteoblasts (bone-building cells), osteoclasts (bone-resorbing cells) and osteocytes (bone-maintaining cells). The combination of hydroxyapatite crystals and collagen fibrils gives bone its compression and tension characteristics, respectively (Tortora and Grabowski 1993). For this reason bone tissue has biphasic characteristics; it is both flexible and stiff. Cortical bone is denser and less porous than cancellous bone, has a high Young's modulus, and is stronger in compression than in tension (Hench and Jones 2005). Thicker regions of cortical bone are usually found in areas where stresses are applied in relatively few directions and are therefore heavily stressed. Cancellous bone is weaker compared to cortical bone and due to its low density, reduces the overall weight of bone. Regions of cancellous bone are usually not heavily stressed or are subject to stresses from many directions (Tortora and Grabowski 1993).

Bone tissue is inhomogeneous, which means that its material properties vary with location. The material properties of bone also vary with direction (anisotropic) and the load magnitude (nonlinear) (Carter 2008).

1.10.1 Bone Modelling and Remodelling

Bone is a living organ that undergoes remodelling throughout life. Bone modelling and remodelling is an adaptive process resulting in a change in the geometry or material properties of bone (Carter 2008). Bone modelling incurs a change in geometry

or density of bones and refers to the dependent action of osteoclasts and osteoblasts, whereby new bone is added along some surfaces and removed from others. The adaptation of a bone's shape and size is important in long bones as well as in response to varying mechanical loads throughout life (Office of the Surgeon General (US) 2004). Bone remodelling, on the other hand, refers to the combined action of osteoclasts and osteoblasts to repair or replace old or damaged bone. The process of bone remodelling serves to maintain bone health as it undergoes repetitive loading throughout life (Feng and McDonald 2011). Defects such as micro cracks are repaired by the coupling of osteoclasts and osteoblasts. In a homeostatic equilibrium resorption and formation are balanced so that old bone is continuously replaced by new tissue so that it adapts to mechanical load and strain (Frost 1990).

Osteoclasts and osteoblasts closely linked in the remodelling process in what is called a basic multicellular unit (BMU). The osteocytes which are osteoblasts that have become embedded in bone are believed to have a role in the control of remodelling, supressing osteoblastic action by the secretion of sclerostin. The organization of the BMUs in cortical and trabecular bone differs, but these differences are mainly morphological rather than biological (Hadjidakis and Androulakis 2006). The remodelling cycle consists of three consecutive phases: resorption, reversal, and formation. Resorption begins with the migration of partially differentiated mononuclear preosteoclasts to the bone surface where they form multinucleated osteoclasts. After the completion of osteoclastic resorption, there is a reversal phase when mononuclear cells appear on the bone surface. These cells prepare the surface for new osteoblasts to begin depositing bone and provide signals for osteoblast differentiation and migration. The formation phase follows with osteoblasts laying down bone until the resorbed bone is completely replaced by new. When this phase is

complete, the surface is covered with flattened lining cells and a prolonged resting period begins until a new remodelling cycle is initiated (Hadjidakis and Androulakis 2006).

1.10.1.1 Strain as a Bone Remodelling Stimulus

Bone cells, like many other cell types, respond to alterations in their external environment. The physiological mechanism by which the mechanical loading applied to bone is sensed by the tissue and the mechanism by which the sensed signal is transmitted to the cells, have not been fully identified. In 1873, Wolff who researched the structure of the bone, stated "The law of bone remodelling is that mathematical law according to which observed alterations in the internal architecture and external form of bone occur as a consequence of the change in shape and/or stressing of bone" (Wolff 2012) and established the concept of bone adaptation occurring in response to mechanical stress (Brand 2010).

Strain refers to the relative change in length or deformation in bone tissue when a bone is loaded in compression, tension, or torsion. Frost's mechanostat theory describes the relationship between bone remodelling and mechanical environment (Frost 1987). It describes a window of strain which is considered physiological and maintains the bone in homeostasis. In the disuse window (DW), where strains are below the physiological threshold, bone is resorbed by increased remodelling thereby increasing strain. In the overuse window (OW), where strains exceed the upper boundary of the physiological domain, bone is formed (Liedert et al. 2005; Jang et al. 2008) and becomes stiffer, reducing strain. The remodelling threshold (1000-1500 microstrain) is known as the lazy zone (Dunlop et al. 2009) in which a uniform stable strain state is achieved and bone mass is maintained. Outside this zone, bone resorption or bone apposition will

occur. It has been stated that for long bones, bone formation occurs primarily on the periosteal (outer) surface of the cortical bone and bone resorption occurs primarily on the endosteal (inner) surface. Many quantitative studies in the simulation of bone remodelling have used a strain energy density based approach to bone remodelling for the characterization of internal bone morphology (Huiskes et al. 1987; Tsili 2000; Fyhrie and Carter 1986).

In healthy adults, bone homeostasis occurs when osteoblasts form new bone and osteoclasts resorb existing bone maintaining a constant rate of remodelling. In the absence or reduction of mechanical stimuli, bone mass is decreased (Liedert et al. 2005). Fracture healing, where bone is renewed from soft tissue, is also subject to mechanical regulation. The stiffness of the fixation influences the healing process in which ossification occurs (Goodship et al. 1998). Interfragmentary micromotion during flexible fixation can stimulate callus formation improving the healing process, whereas unstable fixation can prevent the repair process (Aspenberg et al. 1992). The direction of loading is also an important factor is fracture repair; moderate axial loading stimulates bone formation (Larsson et al. 2001). Computational methods such as Finite Element Analysis (FEA) have been utilised to predict bone reaction to materials of different moduli, forces and direction of loading to improve fracture healing and design of orthopaedic implants and associated bone remodelling. FEA is also used to investigate stress and strains in implants to predict if they lead to failure. In this thesis FEA was used to investigate the effect of using extracortical plates in joint-sparing implants on the strain distribution in the surrounding bone and the stresses in the implant.

1.10.2 Finite Element Analysis

Finite element methods (FEM) are numerical techniques for approximating the solutions of mathematical problems that are usually formulated in order to precisely state an idea of some aspect of physical reality. FEM was originally developed for solving structural analysis problems relating to mechanics, civil and aeronautical engineering and it is best understood from its practical application, known as Finite Element Analysis (FEA) (Turner et al. 1956). FEA is a computational tool for performing engineering analysis and predicting how a complex geometry reacts to real-world forces such as, vibration, heat and other physical effects. FEA uses mesh generation techniques where the geometry is divided into finite number of small elements that are called 'finite elements'. In addition to geometry in FEA, loads and constraints, as well as material properties of the structures and their combinations are specified to achieve accurate solutions. Powerful FEA software programs, coded with FEM algorithms are widely used in almost all engineering disciplines (Saurabh and Yadav 2016). FE simulations have become a powerful tool in the field of orthopaedic surgery and traumatology, enabling surgeons to have a better understanding of the biomechanics, both in healthy and pathological conditions. FE simulations predict the biomechanical changes and bone responses to these changes that occur following the implantation of endoprostheses. It can also calculate the changes in the stress distribution around the implant and can predict subsequent bone remodelling. FE can be used to simulate the effects of different material properties of implants, the effect of implant position, design of implant on both the adjacent bone and stresses within the implant (Herrera et al. 2012). This information can be used when creating novel implant designs.

1.10.3 Orthopaedic Materials

1.10.3.1 Titanium Alloy

Titanium alloy (6% aluminium ,4% vanadium) also known as Ti 6-4 is important in the context of joint-sparing prostheses as this alloy is used for the construction of the implant shaft and extra-cortical plates. Trabecular bone has a stiffness between 10.4 ± 3.5GPa and 14.8 ± 1.4GPa, while the stiffness measured for cortical bone is between 18.6 ± 3.5GPa and 20.7 ± 1.9GPa (Rho, Ashman, and Turner 1993). Titanium has a stiffness approximately half of stainless steel (E=200 ± 20GPa) or cobalt chrome (E=250 ± 10GPa) which are often used for manufacture of prosthetic hips and knees, (Ganesh et al. 2005) and therefore it is less likely to cause stress shielding. Titanium, in its commercially pure form is relatively soft and weak. Therefore, for many biomedical applications titanium alloys that include aluminium and vanadium (Ti6Al4V) and have similar biocompatibility to pure Ti but are stronger, are used (Ratner et al. 2012). Titanium and its alloys are relatively soft when compared to stainless steel and cobalt chrome alloys and for this reason are not used as bearing materials.

1.10.3.2 Porous Titanium

Conventionally stiff metal implants can induce bone atrophy and stress shielding due to the absence of mechanical stress (Sumitomo et al. 2008) associated with inappropriate load transfer. Stress shielding causes loosening of implants such as massive endoprostheses and joint replacements and can cause fracture as part of the bone resorbs and becomes weaker. Therefore the Young's modulus of metallic implants in contact with bone should emulate the stiffness of the bone as closely as possible (Niinomi 2011). Although titanium and its alloys possess a lower modulus than some other metallic biomaterials commonly used in orthopaedic applications,

research into low modulus materials to replace the conventional metallic implants is an important area (Niinomi 2011). However, Young's modulus is not the most important mechanical properties of the implants. Fatigue strength, tensile properties, wear resistance, fracture toughness and biological compatibility are also important factors for the practical medical application of the alloys (Niinomi 2008).

Changing the structural design of the titanium alloys by introducing porosity into the alloys is an effective method for reducing the Young's modulus. This method provides control of the Young's modulus by variation of the porosity. The Young's modulus of approximately 30% porous titanium made from powdered titanium is reported to be equal to Young's modulus of cortical bone (Oh et al. 2002). Additionally pores of appropriate size could enhance bone ingrowth. The disadvantage of using porous implant is that both fatigue strength and the ultimate strength are reduced. Titanium alloy is classified as being a notch sensitive material and the introduction of porosity where notches are introduced may affect its fatigue performance.

Surface morphology is an important factor in determining the long-term implant stability. Many studies have reported improvement of bone-implant contact and promotion of initial and long term implant stability in using porous metals (Pilliar et al. 1986; Li et al. 2007). Porous materials provide biological anchorage for the bone tissue via the ingrowth of mineralized tissue into the pore spaces (Simmons et al. 1999).

1.10.3.3 PEEK

Poly-ether-ether-ketone (PEEK) is one of the Polyaryletherketones (PAEK) group of polymers that has a stiffness similar to that of bone, which has made it an attractive

biomaterial for a bone implant. PEEK is used in trauma and spinal orthopaedic implants. Polyaromatic ketones are stable at high temperatures exceeding 300°C, are resistance to chemical and radiation damage and have the ability to be reinforced by other materials (May 2002; Kurtz 2011). PEEK has also shown to be resistant to degradation and damage caused by lipid exposure (Kurtz and Devine 2007).

Viability and proliferation of normal human osteoblasts onto PEEK has been studied extensively. Researchers have concluded that pure PEEK is non-toxic and that cell proliferation was inhibited when β-TCP was present. This suggests that PEEK possesses good biological interaction even without the addition of traditionally bioactive components as enhancements (Petrovic et al. 2006). Due to interest in further improving implant fixation, PEEK biomaterials research has also focused on compatibility of the polymer with bioactive materials, including hydroxyapatite, either as a composite filler, or as a surface coating (Fan et al. 2004; Ha et al. 1997; Yu et al. 2005).

Despite the relatively rigid molecular chain structure, PEEK has considerable ductility and can accommodate large deformation plastic flow in both uniaxial tension and compression. At small strains and room-temperature PEEK displays a linear relationship between stress and strain in both tension and compression. Furthermore, the PEEK transition in compression is 30-40% higher than in tension. Beyond the yield transition, PEEK displays varying post-yield hardening or softening characteristics in tension and compression, depending upon the temperature and strain rate (Kurtz and Devine 2007).

Despite gradual changes in surgical technique and implant design, metallic locking plates and intramedullary nails continue to dominate the field of internal fracture fixation. The biomechanics of fracture fixation and presence of stress shielding depends upon the bending stiffness of the bone-implant complex, not simply the elastic modulus of the implant. The bending stiffness of an implant can be altered by changing its moment of inertia, as well as by modifying its elastic modulus, to improve these affects (Cordey et al. 2000). Stiffness will also dictate the shear strains at the interface; low stiffness means the increase of micromovement at the bone- implant contact.

1.11 Aim and Hypotheses

The aims of this thesis were to describe different design variables for joint-sparing prostheses and to investigate the perceived advantages and disadvantages regarding the implantation of knee-sparing endoprostheses such as, durability of the plate fixation and safety of bone resection with close margins.

It is logical to assume that as joint-sparing implants retain the knee joint, the joint function will be more normal than with a replaced knee. However, no studies have quantified these differences. The objectives of this thesis were to investigate the functional outcomes, gait and proprioception in patients with knee sparing implants, joint sacrificing implants and healthy controls.

As joint-sparing implants are customised for individuals, their design varies from one implant to another. However, the effect of these variations in design, on the bone adjacent to the extra-cortical plate and the implant are unknown. The aim of this thesis was also to investigate the strain and stresses generated within the bone and the implant using the Finite Element Analysis (FEA) method.

Therefore, it was hypothesised that:

1. Following bone tumour surgery, knee joint-sparing implants have similar or reduced revision rates compared to conventional knee sacrificing implants.
2. Extra-cortical plates are a durable method of attaching a knee joint-sparing prosthesis to the fragmental proximal tibia or distal femur.
3. Patients with joint-sparing implants have improved proprioception due to the retention of soft tissues such as the knee ligaments which have been shown to contain sensory nerve endings .
4. Patients with joint-sparing implants have improved function and acceptability of their implant compared to patients with knee sacrificing implants.
5. Knee joint-sparing massive implants produce a more normal gait in comparison to conventional knee-sacrificing implants.
6. FEA shows that extra-cortical plates do not cause stress shielding of the bone.
7. Use of materials with lower Young's modulus, such as porous titanium and PEEK do not increase risk of implant or plate fracture and can enhance bone formation adjacent to the prosthesis.

Chapter 2 The Design and Manufacture of Joint-Sparing Implants

2.1 Introduction

Patient-specific knee-sparing massive endoprostheses were introduced by Stanmore Implants (Elstree, UK) in 1997 to preserve joint function, wherever possible, by sparing the articulating segment of the bone and the related muscle attachments in patients undergoing a limb-salvage procedure (Figure 2.1). Advanced design and manufacturing technology is employed to create custom implants that closely match the patients' anatomy, both in size and shape. Design considerations that specifically relate to individual needs, in relation to anatomy of the knee joint and the mechanics of the bone, are taken into account by the implant designers.

2.2 Objectives

The aim of this chapter is to review the design concepts used when manufacturing joint-sparing implants. This chapter will explain how various implant features aim to facilitate restoration of knee joint function and improve stability of the construct.

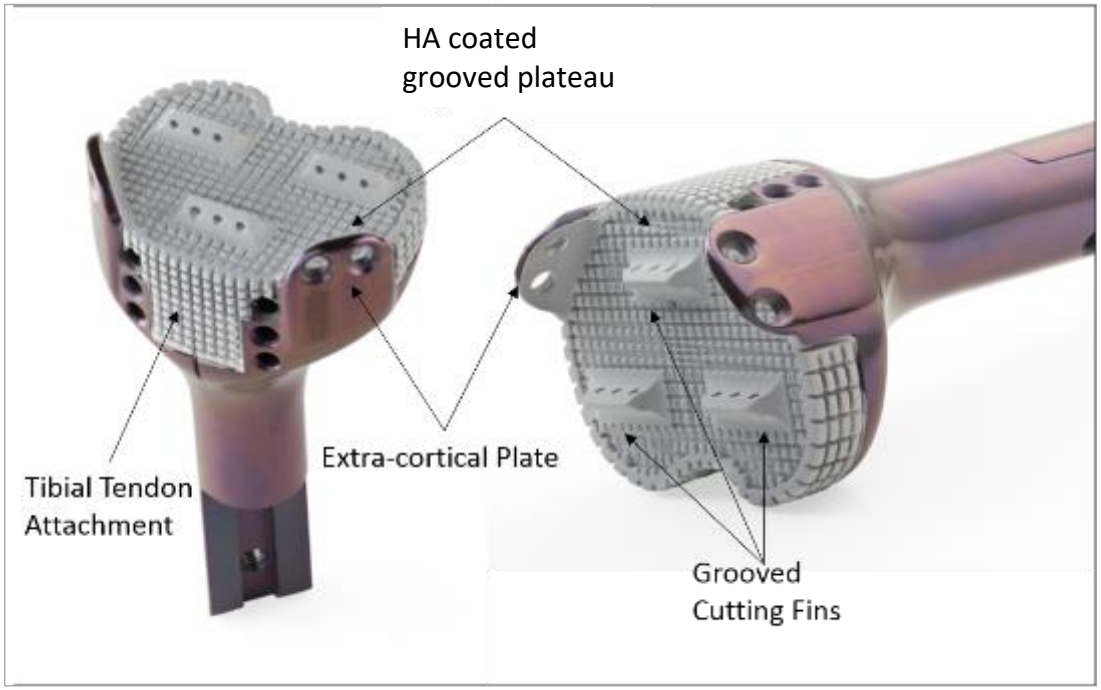

Figure 2.1 A photograph of a proximal tibial joint-sparing implant. The plateau of the implant is grooved and hydroxyapatite (HA) coated. Three grooved cutting fins on the plateau are also HA coated. The two extra-cortical plates have holes for screw fixation and are HA coated on the inside of the plate only. The anterior tendon attachment is also grooved and HA coated. The surface of the implant has been modified using Agluna® silver treatment to aid in reducing risk of infection.

2.3 Method

2.3.1 Medical Design Input

The majority of patients who receive joint-sparing implants are young and active and are predicted to return to an active life style following surgery. The use of a joint-sparing implant is decided by the surgeon, where the primary consideration is the resection of the tumour and of the bone so that an appropriate safe margin is achieved. Other considerations include; careful assessment of the patient's survival probabilities, activity levels and the MRI and CT images of the affected site. MRI scans enable the surgeon to evaluate the neurovascular structures around the knee and any involvement of soft tissues with the tumour. Intact, tumour free popliteal neurovascular structures are crucial for patients to receive a joint-sparing implant (Gupta et al. 2006). The CT

images will allow the surgeon to decide (i) bone resection levels for each patient, (ii) whether the joint surface is intact and (iii) if a sufficient length of the bone is predicted to remain following resection, thereby allowing for extra-cortical attachment.

Prior to implant design and manufacture, information such as the patient's clinical history, growth rate and recent radiographic images of both the affected and unaffected, contralateral limb are considered by the implant designer. This information is used to create implants that will account for both current and future requirements needed by the patient. For example, extendible endoprostheses are commonly used in adolescent patients when the growth plate is removed during surgery and the contralateral limb has remaining growth potential. In order to prevent future leg length discrepancy, extendible implants are used that allow for reconstruction of the limb at the time of treatment and also address the issues associated with limb length as the patient grows.

2.3.2 Design Objectives

The main design objectives for a limb salvage implant are to create a stable construct following replacement of the affected site, and to preserve limb function for the lifetime of the patient. In custom design, objectives vary from case to case, however, the common objectives for joint-sparing implants are as follow;

- Preservation of natural knee function through preserving the joint and soft tissue attachments.
- Identifying the optimum location and geometry of extra-cortical plates in order to produce a stable initial fixation.

- Reduce stress shielding within bone adjacent to the extra-cortical plates by optimising plate thickness and adding slots and holes to decrease plate stiffness.
- Designing an implant that is mechanically appropriate, where for example fatigue fracture of the extra-cortical plates does not occur.
- Ensure the articulating surface of the joint is intact and not damaged by the implant to avoid pain in patients.
- To use an appropriate implant size to ensure adequate soft tissue coverage.
- Improve natural implant fixation by choosing the optimum resection level.
- Ease of implantation and intraoperative flexibility, wherever possible

2.3.3 Pre-Design Assessment

Joint-sparing implants are designed using a Computer Assisted Design and manufacturing (CAD-CAM) method from Computer Tomography (CT) images obtained from patients pre-operatively. As the size of the tumour may change in a short period of time, it is essential that images are taken within one month of the proposed surgery. To begin with, a 3D model of bone from 2D CT images is developed using an image processing software (Mimics®, Materialise, Belgium). This software is used to design an implant that closely matches the geometry of the affected bone. The software contains in-built segmentation Hounsfield unit (HU) threshold ranges calibrated to a grey-level scale. Hounsfield units (HU) are standard numbers that originate from conventional multi-slice computed tomography (MSCT) imaging and represent the relative density of bodily tissues according to a calibrated grey-level scale, based on normalized HU for air (-1000 HU), water (0 HU) and dense bone (1000HU) (Nackaerts et al. 2011). The software operator can choose any one of the

built-in default HU threshold ranges available within the software or alternatively customise the HU threshold range to select the voxels belonging to a particular type of tissue to create a series of 2D images that only include the chosen voxels, called a "Mask". Masks can also be edited manually to exclude any voxels that are not part of the desired geometry but have the same HU. Each mask can then be converted to a 3D model that can be exported to Computer Assisted Design (CAD) software. Figure 2.2 shows a mask that was created by customising the HU threshold range, to include both cancellous and cortical bone tissue, and the 3D model created from the same mask.

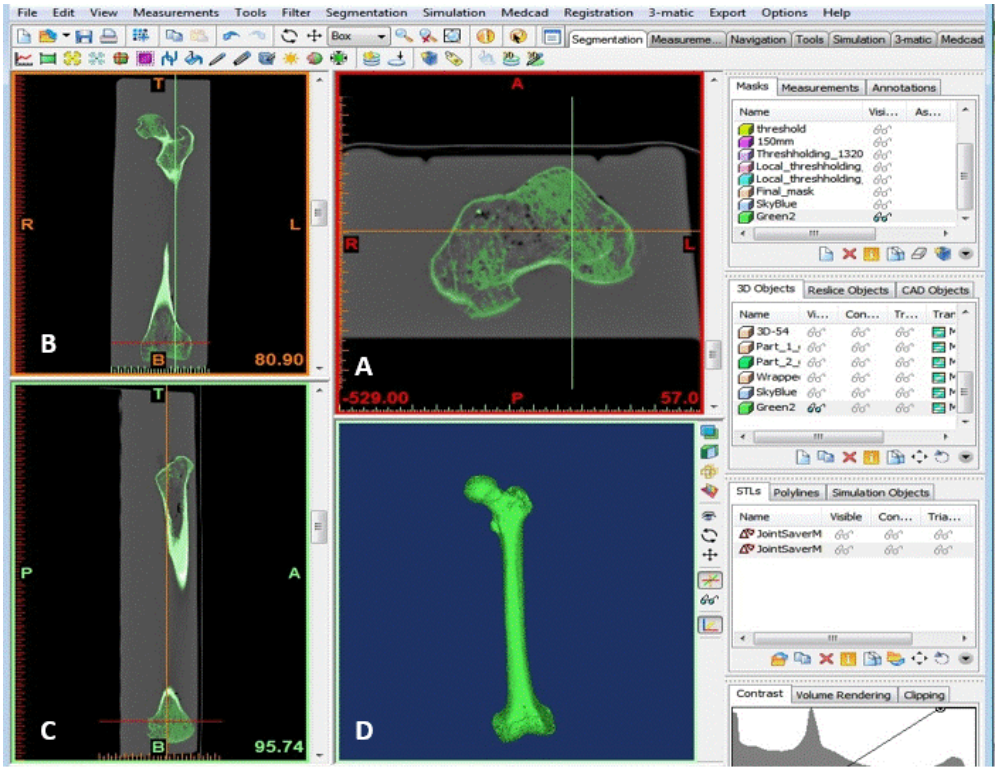

Figure 2.2 A photograph showing segmentation of CT images of a femoral bone shown in three planes; [A] transverse plane, [B] frontal plane, [C] sagittal plane and [D] the 3D bone model created from the green mask.

2.3.4 Determination of the Resection Plane

Although the treating surgeon provides details of the measurements required for adequate resection of the bone tumour by combining the original CT and MRI images

and the 3D model created, the designers can also locate the appropriate resection that allows for sufficient tumour margins and ensures preservation of soft tissue and muscle attachments.

Resection levels for knee joint-sparing implants can be categorised into three main zones, indicated in Figure 2.3. The ideal transection location for the insertion of a knee-sparing implant is in Zone 2 as there is a sufficiently large cross sectional area of cancellous bone available for contact and fixation with the implant plateau. Adequate bone-implant contact in this region would result in a more physiological distribution of load within adjacent trabeculae (Ohyama et al. 2013). This region also has the optimum geometry for close positioning of the extra-cortical plates onto the bone surface.

Resection of bone within zone 1, may result in a bone-implant construct that is less stable, due to a smaller cross sectional area of bone available for fixation and a lack of cancellous bone. Additionally, dense cortical bone can make the attachment of plates more challenging as the insertion of screws becomes more difficult. Implantation of the prosthesis is impossible in the proximal region above the femoral condyle eminence, as the extra-cortical plates will not follow the contour of the bone and adequate fixation is not possible.

Due to the small amount of bone remaining, resections made in zone 3 often result in inadequate extra-cortical plate attachment. Joint-sparing implants requiring a resection in this zone are not recommended and patients often receive a conventional joint-sacrificing endoprosthesis. Resection in zone 3 may result in the removal of essential muscle attachments and tendons. Additionally, short extra-cortical plates (no less than

1.00 mm) may not hold the remaining bone adequately which can result in an unstable implant fixation. If the plates are too long and exceed the length of the remaining bone, they can damage the joint's surface and cause pain.

A similar principle applies for resection of bone within the tibia; plate fixation becomes less optimal further away from the joint. The irregular shape of bone in this region results in the inability of the plate to locate fully onto the bone surface. However, in resections too close to the joint, there is a risk of removing the tibial tuberosity and compromising the knee function (Martini 2006). The quadriceps tendon attaches to the quadriceps femoris muscles to the superior aspect of the patella and is responsible for extending the knee. The patella tendon attaches the apex of the patella to the tibial tuberosity (Martini 2006). Failure to preserve the patellar tendon will lead to lack of an extensor mechanism which will alter the biomechanics of the knee and compromise its function gait (Oddy et al. 2005).

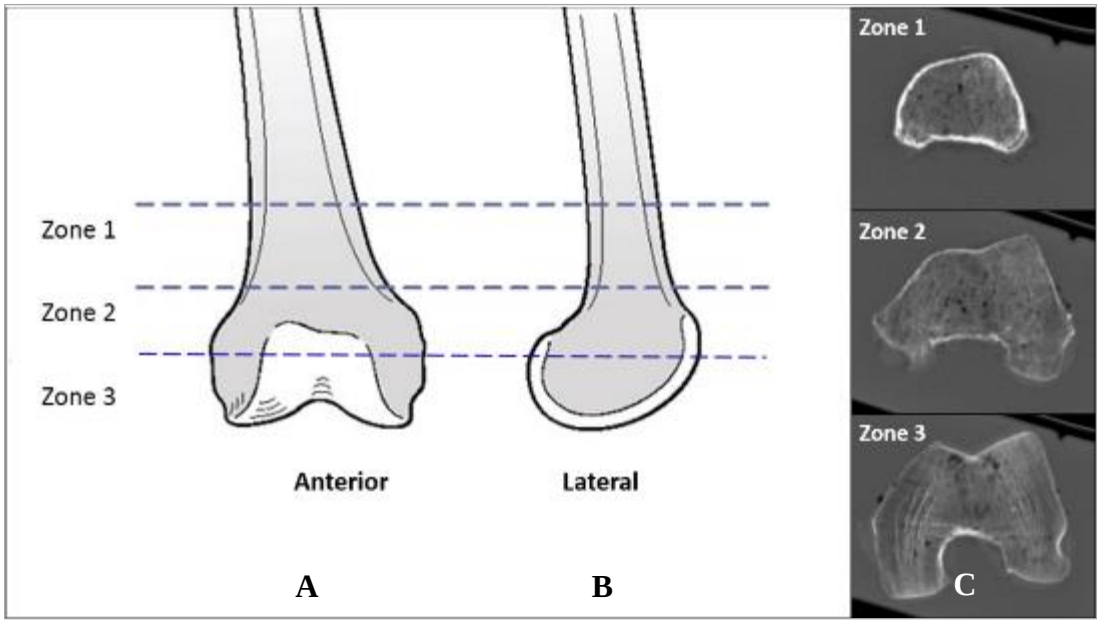

Figure 2.3 Femoral resection zones in [A] Anterior-Posterior and [B] Medio-Lateral views and in the transvers plane [C].

During the design of most joint-sparing implants, the plane of resection is accurately measured as an offset of a datum plane. The datum plane is parallel to the plane that connects the two condyles of the respective bone and is tangential to both of them. The bone on the opposite side of the joint can be used to confirm the position and the orientation of the datum plane. The plane of resection furthest from the joint and any other planes required to form the body of the implant and match the shape of the bone are also parallel to the datum plane (Figure 2.4). The resection plane in proximal tibia, is horizontal and perpendicular to the shaft of the tibia, which anatomically lies almost completely vertical. However when inserting a femoral implant, the resection plane must allow for the 5 to 7° degree angle between the anatomical axis of the femur and the mechanical axis of the lower limb (Pickering and Armstrong 2015).

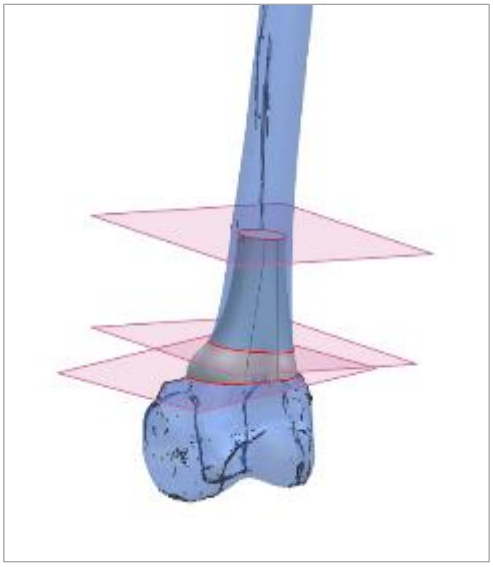

Figure 2.4 Image showing the three planes that form the basis of the implant design

2.3.5 Design of Extra-Cortical Plates

Correct location of the extra-cortical plates is key in designing knee joint-sparing implants. Shorter (longitudinally), wider plates are usually used in shorter segments of

the bone to avoid contact of the plate with the articulating surface. Ideally, the extra-cortical plates are positioned on a part of the cortex where there is a relatively flat surface. Such flat surfaces are usually found on the anterior-medial and anterior-lateral side of the femoral condyles and on the medial and anterior-lateral side of the tibial condyles, as marked on the transverse view of a right femoral and a left tibial condyle shown in Figure 2.5. These locations vary slightly depending on the resection level.

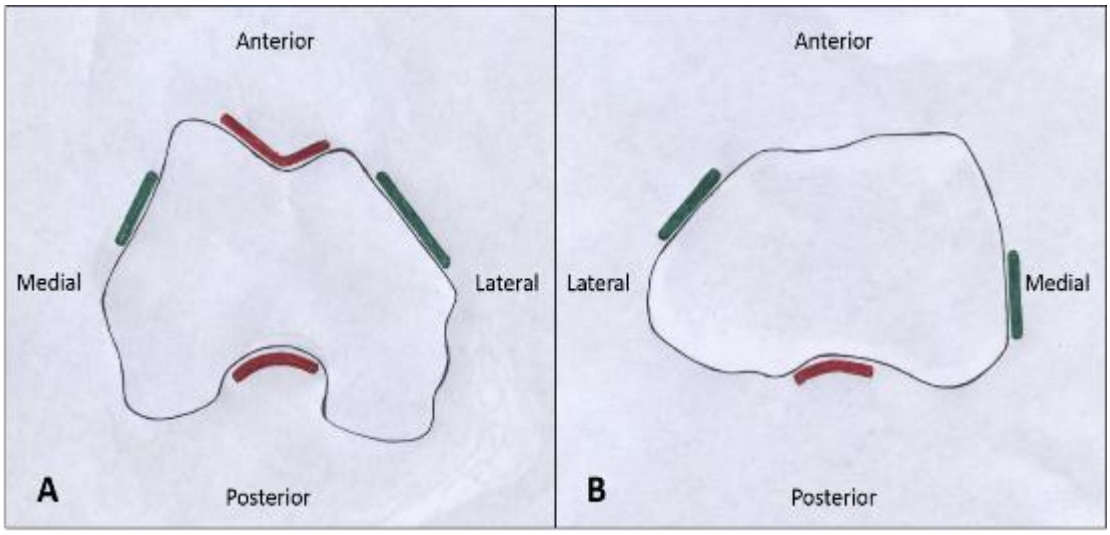

Figure 2.5 Sketch showing the cross-sectional area of the femoral condyle [A] and tibial condyle [B], indicating areas most suitable for plate fixation. Green plates (lines) represent suitable areas while areas most unsuitable or less likely to be used for plate fixation are shown in red.

Extra-cortical plates are designed to follow the shape of the bone, and to lie flush on the cortical surface. Maximal bone-plate contact is required for optimal initial implant stability following surgery. Using the 3D bone model created from the CT images, the implant designers can create a ‘sheet’ parallel to the line of resection on the cortex of the bone and the profile of the implant at the plateau to form the basis of the size and location of the plates. By trimming and thickening the sheet, the desired plate size can be created. Plates are usually 3mm thick with varying width and length. In some cases, extra-cortical plates are designed with tapering thickness, from 3mm at the plateau to

1.5mm at the tip in order to reduce bulkiness around the knee, and improve soft tissue coverage. The tapered plate design reduces plate stiffness and may in turn decrease bone loss in areas immediately adjacent to the plate (Cobb et al. 2005). As the plate becomes thinner the structural rigidity reduces. The relationship between plate thickness and rigidity is defines by the expression in Equation 2.1.

$$\boldsymbol{Rigidity\ of\ the\ plate = Et^3} \qquad \textbf{Equation 2.1}$$

Where *E* is the Young's modulus of the material and *t* is the thickness of the plate.

Critical contact stresses can inhibit bony incorporation of an implant. Rreducing plate thickness and therefore its stiffness can yield a more homogeneous stress distribution to the surrounding trabecular bone (Simon et al. 2003). Studies have also shown that less stiff implants yield better osseointegration (Huiskes et al. 2000). Additionally, extra-cortical plates are often manufactured with slots or holes to increase their flexibility and allow for greater vascularisation which may encourage bony integration such that the plates become incorporated within a remodelled cortex (Coathup et al. 2000). Incorporation of the plates within the load bearing structure may provide better implant stability and achieve consistent longer term fixation (Cobb et al. 2005).

The number of extra-cortical plates manufactured can vary between two and four plates per implant, depending on bone quality, length of the remaining bone and variations in bone geometry (Spiegelberg et al. 2009). Low quality and shorter segments of the bone often require more plates. Shorter and wider plates are used when the remaining segment of bone is greatly reduced and where plate fixation can still be used without the implant breaching the articulating surface. Prior to implantation, the inner surface of all extra-cortical plates are plasma-sprayed with a highly crystalline

(> 85%), thin (50 micron) hydroxyapatite (HA) coating. The extra-cortical plates also include grooves or holes that can be used for screw fixation. Grooves encourage bone ingrowth into the plate. Use of screws provide initial stability post-operatively and reduce micro-movements that decrease ossointegration (Søballe et al. 1992). In order to increase intraoperative flexibility, the number, type, length and direction of screws used can be decided by the surgeon at the time of operation.

The earlier designs of knee joint-sparing implants included a shorter posterior plate to prevent implant rotation (Figure 2.6). However, this method of fixation has been replaced with other design features that augment a secure fixation. These design features include HA coated grooves (1mm in depth, width and length), spikes and cutting fins located on the plateau of the implant.

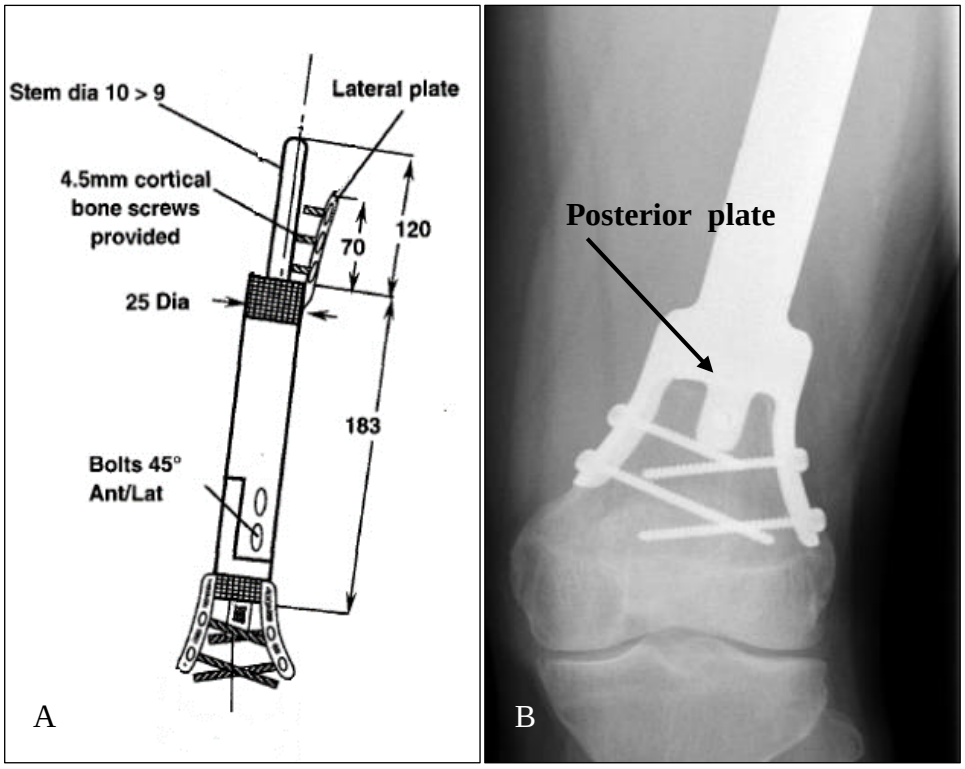

Figure 2.6 [A] A design diagram of a distal femoral knee-sparing replacement with three extra-cortical plates. [B] The radiographic image of the same implant after implantation in a male patient, 8 years post-surgery. Proximally, the implant is fixed

using a cemented IM stem and an extra-cortical plate. The shorter posterior plate and the uni-cortical screws are visible in the radiographic image.

Following the introduction of extra-cortical plates in implant design by Stanmore Implants (Elstree, UK), other plate designs such as LISS® plates were designed and developed. LISS® plates that are anatomically shaped, reduce stress on the bone while optimising screw position.

2.3.6 Design of the Implant Plateau

The plateau of the implants include various features to improve implant stability. Since bone ingrowth onto the implant requires a rough surface (Coathup et al., 1999), the plateau at the bone-implant interface has grooves, measuring 1 mm deep that are organised orthogonally to each other and plasma coated with HA. This pattern for organisation of the grooves is also used in the HA collars on the shoulder of the implant.

As the increased mechanical interlock will promote and allow secondary bony ingrowth to the implant surface and osseointegration (Biemond et al. 2011), the plateau in some implants includes small, HA coated protrusions known as "cutting fins". Cutting fins are smaller in length and width than the extra-cortical plates and have a sharp edge that is designed to provide anchorage for the implant for a more secure fixation by penetrating into the cancellous bone. This increases the bone-implant contact surface area, reduces micromotion and promotes the potential for bone attachment and implant fixation. The length of the cutting fins is dependent on the length of the remaining bone so that they do not penetrate the cortex and damage the joint surface, causing pain. Cutting fins are positioned in such way that they do not interfere or obstruct the insertion of the screws used for extra-cortical plate fixation.

The majority of implants reported in this thesis included three cutting fins (30%), however the number of cutting fins can vary between 2 and 4 (used in 21% and 1% of cases reported in this thesis) depending on the available surface area on the plateau. Figure 2.7 shows a diagram of a femoral joint-sparing implant that includes cutting fins and a radiographic image of the same implant after implantation.

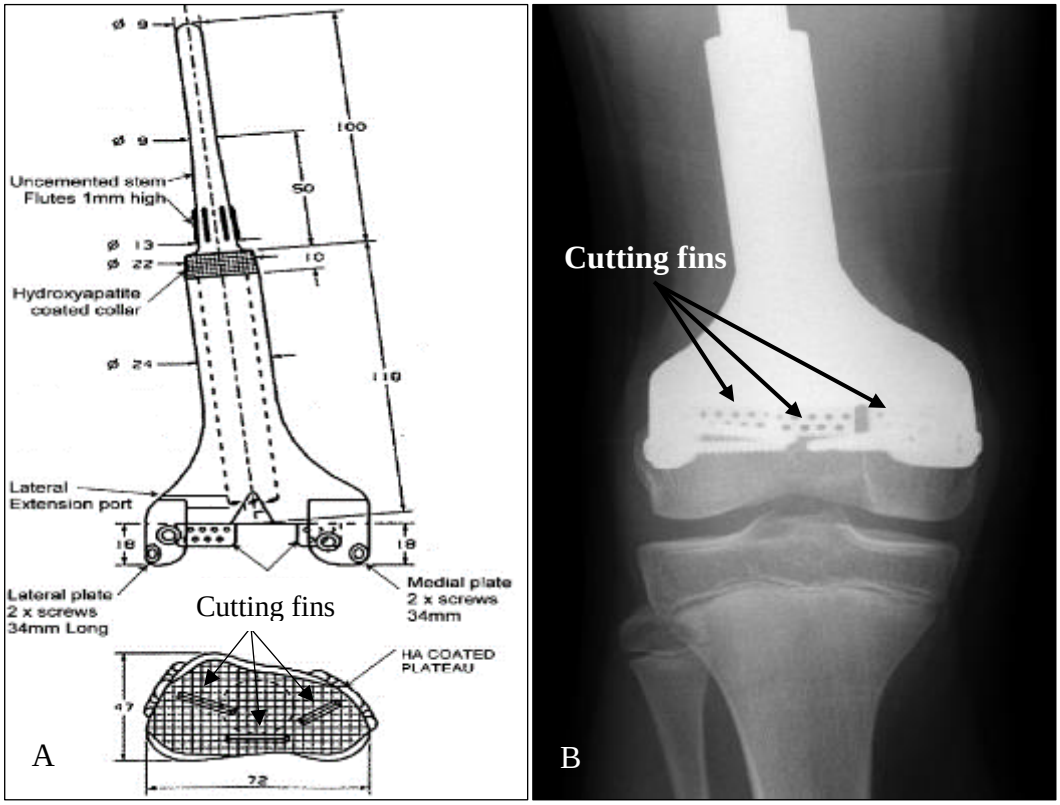

Figure 2.7 [A] A diagram of an extendible femoral joint-sparing implant with three cutting fins on the plateau. [B] A radiographic image of the same prosthesis after implantation.

The grooved plateau with cutting fins is not designed and manufactured for all cases; 56 of the implants reviewed in this thesis, had cutting fins.

Between 1998 and 2013, 103 joint-sparing implants were designed, out of which five had 4 to 9 sharp "spikes*"* on their plateau, depending on the available surface. Spikes are typically 8mm long and are HA coated. Similar to cutting fins, spikes were

designed to anchor the implant into the bone and improve fixation. Figure 2.8 shows a diagram of a knee joint sparing implant with spikes. Due to the difficult and often time-consuming manufacturing process involved in creating the spikes, their design is now obsolete.

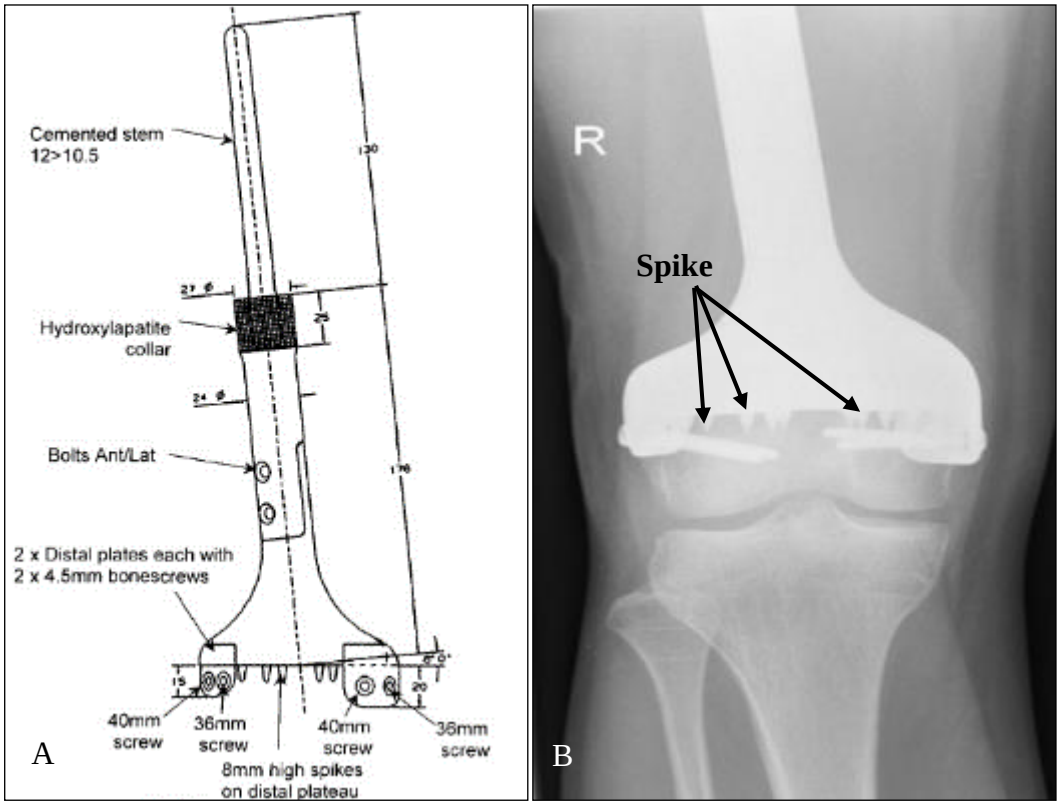

Figure 2.8 [A] A diagram of a split-shaft distal femoral joint-sparing implant with spikes located on the implant plateau. [B] An antero-posterior radiographic image of the same prosthesis in a male patient, 35 months post-implantation.

Another fixation feature that is more commonly designed where resection levels are required further from the joint, is a short stem that is larger in diameter (typically 18mm) than an intramedullary stem and is known as an "obturator stem". The length of an obturator stem varies and depends on the length of the remaining bone. However, stems longer than 45mm are not used. The cross sectional shape of the stem is rectangular to limit implant rotation while anchoring the implant at the same time.

Obturator stems can be cemented or uncemented depending on the length of the remaining bone and the surgeon's preference. Cemented stems have cement grooves while the uncemented stems are HA coated to promote bone growth and better fixation. This type of fixation is more commonly used in older patients where the growth has completed and the insertion of the obturator stem will not disrupt the fused and remodelled growth plate.

2.3.7 Shaft of the Implant

The cylindrical main body of the implant is known as the "shaft", often comprises of two parts (split-shaft) that are bolted together and can be assembled and disassembled at the time of surgery (Figure 2.6 and Figure 2.8). The split-shaft feature facilitates partial revisions, allowing the surgeon to remove and replace the section of the implant that requires replacement while leaving the well-fixed section *in situ.* This minimise damage and disruption to the bone. In this way the surgeon could potentially replace the joint-sparing implant with a knee joint replacement, should a revision be required.

All implants have a grooved "HA coated collar" located at the shoulder of the implant at the bone-implant junction.

2.3.8 Intramedullary Stem Fixation

Intramedullary (IM) stems are commonly used to attach massive bone tumour implants to the remaining segment of the bone. All cemented IM stems, have 4 longitudinal and parallel cement grooves, stretched along two thirds of the length of the stem. These grooves are manufactured in order to improve the mechanical bond between implant and cement and to reduce torsional motion. For cemented stems, an approximately 2mm margin is allowed for the cement mantle (Malawer and Sugarbaker 2001).

However, this varies based on the size of a patient's bone, with smaller margins allowed for smaller patients. The diameter of an IM stem is determined by the inner diameter of the cortex or the medullary canal and often has a tapering diameter of 13 to 9mm in adults. The stem length, in femoral implants, provided sufficient length of the bone is remaining, is typically 150 mm. Massive endoprostheses with a cemented stem and a grooved HA coated collar have been reported to have low revision rates caused by aseptic loosening (Coathup et al. 2013). In some cases, an uncemented stem is used where fixation relies on osteointegration and bone remodelling. The design of uncemented IM stems include cutting flutes of 1mm height and 15mm length (Figure 2.7), located near the shaft of the implant that penetrate into the bone for improved initial fixation.

When distal femoral implants are designed, the IM stem length is manufactured not too close to the greater trochanter in case a hip replacement is required in the future. In cases where inadequate stem length is available, one or more extra-cortical plates are designed to provide additional reinforcement of fixation (Figure 2.6). Figure 2.9 shows a sketch of a joint-sparing implant with its various design features. In tibial replacements, the IM stem is often 140 mm in length. The stem must not be too close to the ankle joint to interfere with its structure and function. Extra-cortical plates can also be used in this type of prosthesis if a stem of inadequate length is designed.

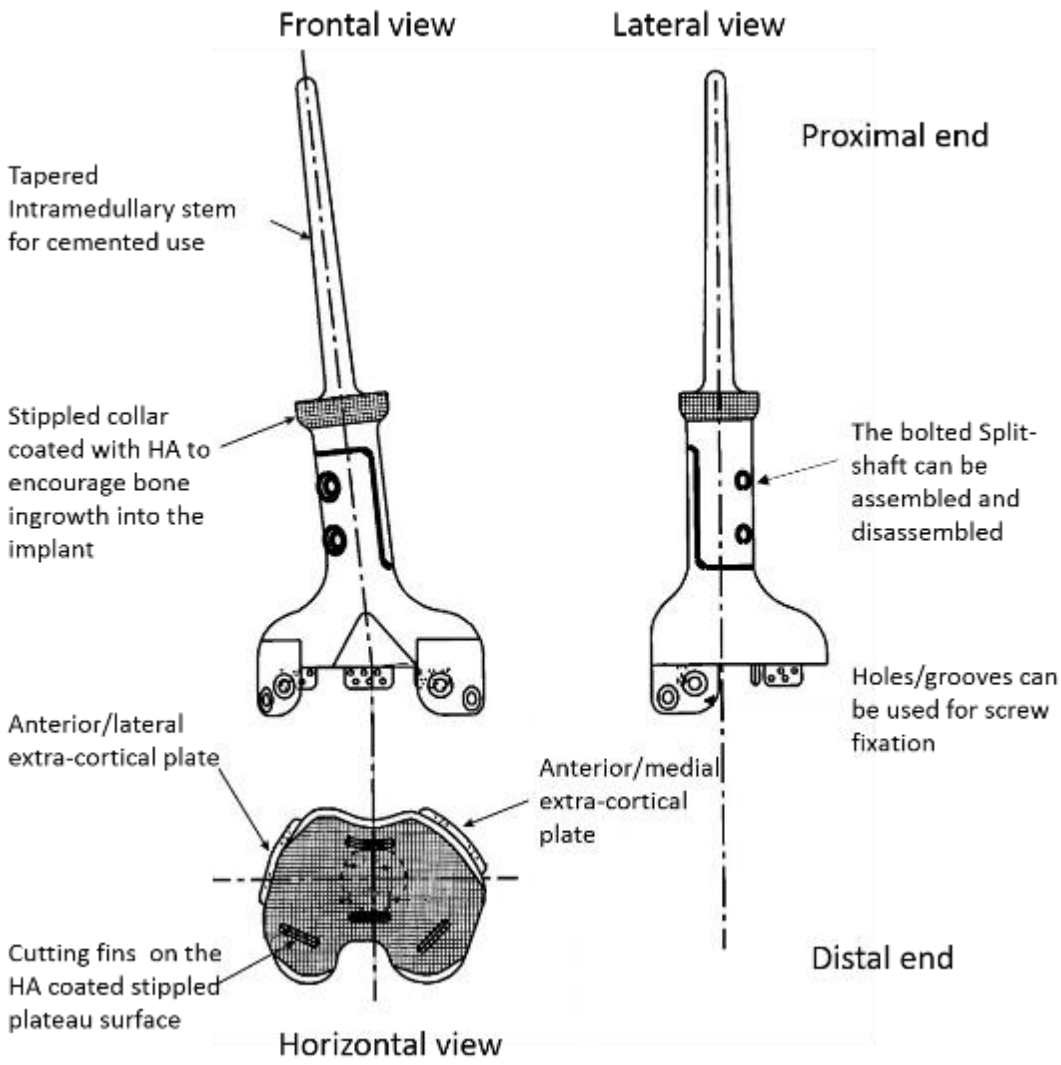

Figure 2.9 A diagram of a split-shaft femoral joint-sparing implant, with a HA collar and cutting fins (Source of the image: Gupta et al., 2006).

2.3.9 Manufacturing

All parts of a joint-sparing implant are fabricated from medical grade 5 titanium alloy (Ti-6Al-4V). The main body of the implant and the extra-cortical plates are manufactured with a computer aided manufacturing method from individual pieces of titanium alloy. The stem is made by conventional machining and is fitted into the main body of the implant using the shrink fit method at high temperatures before it is cleaned and sterilised. Less commonly, all parts are made from one solid bar.

In the majority of cases and at the surgeons' request, the IM stem of the implant is curved to follow the natural arc of the bone, using a mechanical press. A 1:1 scale image of the patient's leg in lateral view is used as reference for shaping the stem.

The particle sizes used for the HA coating are 15, 30 and 50 micron and the nominal value of coating thickness is 50 to 200μm, however the actual thickness may vary depending on device geometry. The plasma spraying method involves ultrasonically cleaning and degreasing all surfaces of the implant using detergents prior to coating. Areas that are not HA coated are masked for protection while HA surfaces are grit blasted with white alumina grit and are passivated in nitric acid prior to plasma spraying (Tsui et al. 1998). HA-sprayed coatings are applied onto the implant using a Vacuum Plasma Spraying (VPS) technique. A mixture of gases such as Argon and Hydrogen is heated with a high energy arc up to 20,000°C and ionised. The heated gas is then ejected through a nozzle at a high speed and the powdered coating is melted in this high energy plasma jet and is deposited onto the implant surface ("Plasma Spray - Thermal Spray Coating Process" 2015).

2.4 Conclusion

To summarise, the key design objectives for knee-sparing implants are that:

- The knee joint and soft tissue attachments are preserved by employing accurate imaging and image processing techniques in order to preserve natural joint function.
- Positioning the extra-cortical plates on relatively flat surfaces of the bone and away from the curvature of the condyles provides a stable initial fixation which in turn will improve long term bone-implant attachment.

- Producing a tapered plate thickness will decrease the risk of stress shielding of the underlying bone.
- Grooved extra-cortical plates, increase plate flexibility to encourage osteointegration and therefore initial stability and increased exposure to a vascular supply.
- A suitable length of the fixation features on the plateau is used; such as spikes and cutting fins to ensure that the articulating surface of the joint is intact.
- The HA coated grooved surface of the plateau, the spikes or the cutting fins, can increase initial fixation, reduce micromotion and improve implant fixation through increasing osteointegration.
- Using several screw holes offers intraoperative flexibility, by allowing the surgeon to choose the location, orientation and type of screws, based on possible unforeseen circumstances.

In this chapter the design objectives for knee-sparing implants was outlined and the design consideration and features that are implemented to meet these objectives were described. The design and manufacturing processes, from image processing to HA coating applied, aim to produce a reliable endoprostheses with a secure initial fixation and one that preserves natural knee function. Part of this thesis will investigate whether the use of these implants is a safe alternative to their knee sacrificing counterparts, and if the extra-cortical plates can securely fix the implant onto the remaining bone in order to preserved the natural knee function.

Chapter 3 Joint-Sparing Implants: A Survivorship and Radiographic Study

3.1 Introduction

Although many studies have reported on the survivorship and complications of conventional joint sacrificing implants (Hardes 2013; Pala 2014; Pala 2013; Ahlman 2006), there are only limited clinical studies that have reported on proximal tibial and distal femoral joint-sparing endoprostheses, all with follow-up of less than 4 years. Although these studies reported encouraging results in a small number of patients (Gupta et al. 2006; Spiegelberg et al. 2009; Wong and Kumta 2013; Agarwal et al. 2010), there are no known studies that have investigated the mid- to long-term survival of joint-sparing megaprostheses.

One of the major challenges of sarcoma surgery is to resect the tumour with an oncologically safe margin and to reconstruct the skeletal defect to the exact anatomical dimensions necessary for good function (Wong et al. 2012). Accurate bone resection that matches the dimensions of a custom endoprosthesis that fits the exact shape of the remaining bone, can ensure a suitable bone-implant alignment and provide a superior function (Wong et al. 2012). Various studies of reconstructive orthopaedic surgery,

particularly around the hip and the shoulder have shown improved radiological outcomes with increased surgical accuracy (Anderson et al. 2005; Gregory et al. 2013, Baauw et al. 2015). In this chapter, the long-term survival of the knee joint-sparing implants and the complications associated with the use of these implants was assessed. The fixation and loosening of these prostheses was also investigated in a retrospective, post-operative radiographic analysis.

3.2 Objectives

The aim of this chapter was to evaluate patient and implant survival rates in surgical treatment with knee-sparing implants used to treat bone cancers. 104 patients, treated in 22 different centres, were investigated retrospectively. All patients were treated with knee joint-sparing implants designed and manufactured by Stanmore Implants (Elstree, UK). These implants were first introduced in 1998. This chapter also aimed to identify the common modes of failure of proximal tibial and distal femoral joint-sparing implants and investigated whether failure rates vary with patients' age, anatomical site and implant design. The relevant Clinical Audit approval was obtained for this investigation (Title: A Comprehensive audit of Joint Sparing Prostheses). A comprehensive list of all patients who were treated with distal femoral and proximal tibial knee joint-sparing endoprostheses was obtained and routed to their treatment institution. Patient medical files and post-operation radiographic images were reviewed for information including: age, diagnosis, treatment regime, date of surgery, complications and revisions. Information regarding the design of each implant such as, length of resection, number, size and location of extra-cortical plates and IM stem fixation was also obtained. Survival analysis was carried out for different patient outcomes and compared for different bony locations and patients' age group, to establish whether the outcome of using knee-joint sparing implants was different

depending on patients' groups. Using the sequential radiographic images available, an observational study was carried out to investigate the changes to the surrounding bone and fixation of knee joint-sparing implants.

Additionally, this chapter aimed to correlate implantation accuracy and implant longevity by comparing the positional precision in failed endoprostheses and those that remained *in situ*. Accuracy of implantation was determined by quantifying bone-implant alignment and comparing the amount of the remaining bone and implant position in pre-operative surgical plans with that achieved, measured on postoperative radiographs.

3.3 Hypothesis

It was hypothesized that;

- Prostheses survival in joint-sparing implants is equivalent to those reported in the literature for conventional joint-sacrificing implants around the knee.
- The rate of local recurrence in patients undergoing limb reconstruction using knee-sparing implants is no higher than those reported in the literature for conventional knee joint-sacrificing implants.
- Inaccurate implantation of joint-sparing implants increases the risk of early mechanical failure such as implant fracture and loosing, such that implant duration is inversely correlated to implantation error.

3.4 Method

3.4.1 Patient Follow-up

A retrospective follow up of 104 patients undergoing primary or revision limb salvage surgery between September 1997 and January 2013, using knee-sparing implants designed and manufactured by Stanmore Implants Worldwide Ltd. (Elstree, UK) was carried out. All patients were treated for a bone tumour around the knee joint and one patient was treated bilaterally, resulting in a total of 105 implants investigated in this study. Seven patients were treated for failed intercalary endoprostheses or allografts. All the remaining patients underwent primary limb salvage surgery. Surgery was carried out in 22 centres worldwide and by 26 surgeons. The mean age of patients at the time of surgery was 22.8 ± 1.8 years (range: 3 to 72 years) where 41 patients were female and 63 male. No patients were recalled specifically for this study and data was obtained from the medical records and radiographs.

This study investigated 59 distal femoral, 43 proximal tibial and three total femoral endoprostheses. Forty-six implants were fixed into the intramedullary canal with uncemented stems (26 femoral and 20 tibial implants) and 56 (33 femoral and 23 tibial) with cemented stems. The mean age of patients who received proximal tibial replacements was 28.8 ± 3.1 years (range: 7 to 72 years) and the mean age in patients with a distal femoral replacement, including the three with total femoral replacements, was 18.7 ± 2.0 years (range: 3 to 67 years). Forty eight (46.2%) patients were treated for osteosarcoma, 9 (8.7%) for Ewing's sarcoma, 3 (3.0%) for chondrosarcoma, one for a bone metastasis and 37 (35.6%) for other rare types of bone and soft tissue tumours. Seven implants (6.7%) were inserted at revision surgery and their primary diagnosis was unknown. Thirty-five implants contained an extension mechanism as

these patients were skeletally immature with remaining bone growth potential. Of these growing prostheses, 27 implants were minimally-invasive extendible implants that required key-hole surgery for implant extension. Eight implants contained an extension mechanism where lengthening occurred non-invasively. These implants used an external electromagnetic field generated by a drive unit, to extend the prosthetic shaft in the outpatient department (Meswania et al. 2008). In addition to the extra-cortical plates, the implant fixation was augmented with additional design features: seventeen endoprostheses had obturator stems of varying lengths, ranging from 18mm to 40mm; 57 implants had cutting fins and 5 implants were manufactured with spikes on the plateau of the implant. The remaining 26 implants had no additional fixation feature on the plateau apart from the HA coated grooved surface.

At the end of the follow-up period (mean= 36.1 ± 3.9 months, range: 3 to 151 months), 8 patients (7.77%), 7 with femoral and 1 with proximal tibial endoprostheses, had died of causes unrelated to the implant. Seventeen patients were lost to follow-up; of these, 9 patients had a femoral and 8 a tibial knee-sparing replacement. One patient underwent amputation due to infection.

3.4.2 Implantation Accuracy

Only a limited number of radiographs could be obtained for this study and therefore retrospective sequential radiographic images of 11 patients with a distal femoral joint-sparing implant (4 female and 7 male) and 10 patients (5 female and 5 male) with a proximal tibial joint-sparing implant, were investigated. Radiographs were obtained from the archives of the Royal National Orthopaedic Hospital (Stanmore, UK) and University College Hospital (London, UK). All patients had been treated for primary bone tumours of the lower limb; eleven for osteosarcoma (6 with distal femoral and 5

with proximal tibial replacements), six for Ewing's sarcoma (3 distal femoral and 3 proximal tibial replacements) and the remaining four patients (2 distal femurs and 2 proximal tibias) were treated for other rare types of bone tumours.

All radiographic images were analysed for accuracy of the resection levels and implant orientation in order to establish whether there was a relationship between the accuracy of implantation and failure of extra-cortical plates, and compare that to those implants that remained *in situ*. The accuracy of the resection level was determined by measuring the length of the residual bone near the joint, from the earliest post operation radiographs and comparing this measurement with the length of the remaining bone stated necessary by the implant design engineers on the operational drawing for each patient (Figure 3.1).

Radiographic images in the antero-posterior (AP) view, where the patients' knee was fully extended and minimal rotation was detected, were used. Knee flexion and rotation of the leg in radiographs were detected by measuring the length and width of the implant's image and comparing them to implant measurements in the operational drawings of the same endoprosthesis. Shorter length of the image of the implant and smaller width indicated knee flexion and leg rotation, respectively. Measurements were taken using a standard ruler with an accuracy of ±0.5mm and the diameter of the cylindrical implant shaft was used to calibrate each radiograph. The distance from the bottom of each condyle to the line of resection was measured and an average value was calculated for each patient. The difference between the actual resection length and the required value stated by the design engineer was calculated as the percentage error.

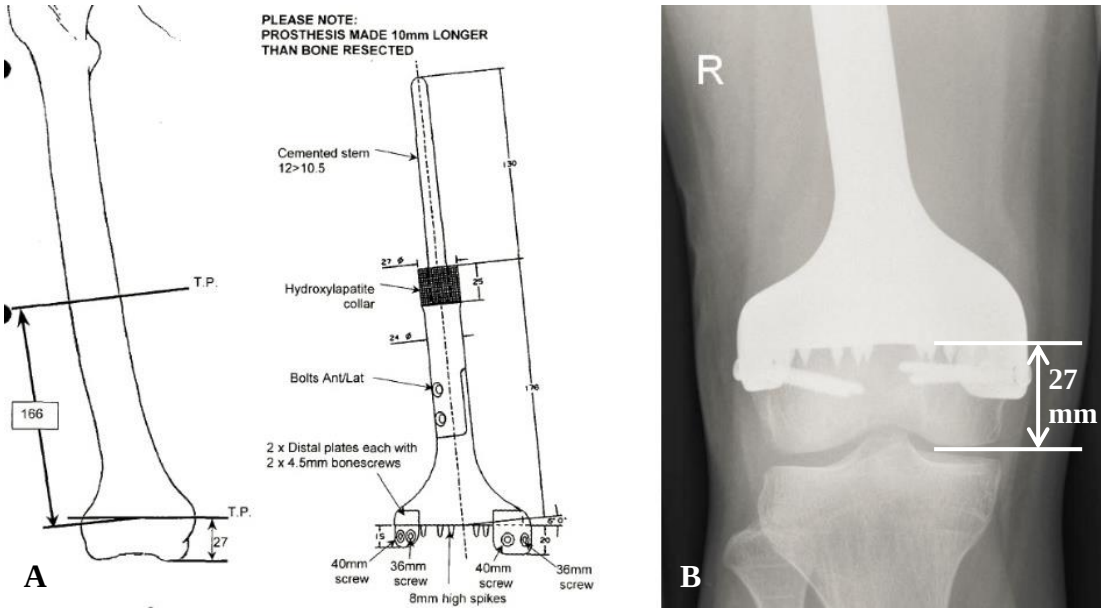

Figure 3.1 [A] Operational drawing that was provided by the implant design engineer, indicating the resection levels and the amount of remaining bone available for extra-cortical fixation. [B] The post-surgery A/P radiograph used to quantify implantation accuracy. The length of the remaining bone was measured as shown.

The angle between the mechanical and anatomical axes for both tibial and femoral endoprostheses was measured using AP view radiographic images. The anatomical axis of the femur creates an angle of 5˚ to 7˚ with the mechanical axis of the lower limb while the anatomical axis of tibia corresponds to the mechanical axis of the lower limb (Figure 3.2) (Cherian et al. 2014). Implant alignment was quantified by measuring the angle between the shaft of the implant and the line perpendicular to the line of the joint (Figure 3.3). As the anatomical axis of tibia corresponds to the mechanical axis of the lower limb, the tibial axis is almost completely vertical. The angle between the axis of the implant shaft and the line connecting the tibial condyles was measured to determine implant orientation and was expected to be approximately 90°.

Implant malalignment can be caused by incorrect fixation of the implant, mispositioned angle of the IM stem and incorrect position and angle of the resection.

Figure 3.2 image showing the angle between the anatomical and mechanical axes in femur ("Biomechanics of the knee joint" 17 June 2015).

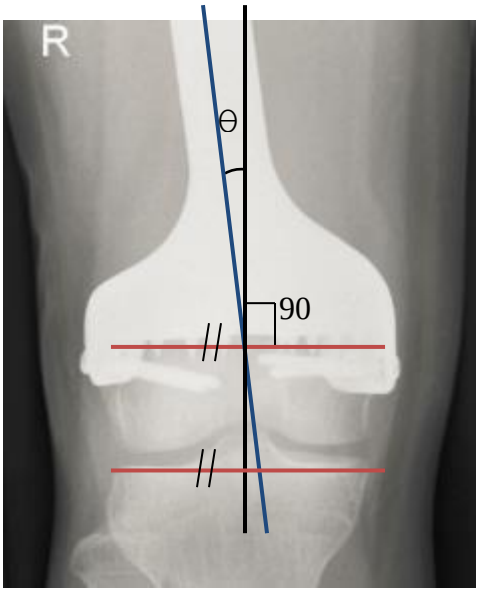

Figure 3.3 An A/P radiograph showing the method used to measure the angle between the mechanical and anatomical axis of the femur. The red line indicates the line of resection, parallel to the line joining the tibial condyles. The blue line is the axis of the femur or shaft of the implant. The black line demonstrates the line perpendicular to the red line that anatomically would cross the centre of the femoral head. The angle formed by the blue and the black line, is the same as the angle between the mechanical and anatomical axis.

3.4.3 Statistics

Endoprosthetic failure was defined as the need for complete revision of the component and conversion to a different prosthesis. Amputation due to locally recurrent disease was not included in the implant survivorship analysis as this was unrelated to the durability of the prosthesis. Loosening secondary to sepsis was classified as failure resulting from infection. The duration of follow-up was calculated from the time of surgery to the time of the latest evaluation. Implant survival was calculated using Kaplan-Meier analysis starting from the date of the original surgery with prosthesis failure, failure due to infection, fracture or aseptic loosening as the end point. Those without failure were censored either at patient death or date of last follow-up. Age at the time of surgery and duration of follow-up were univariately assessed for association with failure over the follow-up period using the chi-squared (χ^2) test. The Spearman's Rank coefficient was used to assess correlation between pairs of continuous variables. A p value < 0.05 was considered significant in all tests (version 10.1; SPSS, Chicago, Illinois).

3.5 Results

3.5.1 Implant Modes of Failure and Complications

3.5.1.1 Failure of the Endoprostheses

A total of 24 implants were revised (22.86%) at a mean follow-up of 36.1 ± 11.0 months (3 to 151 months). Seven (6.67%) implants were revised due to aseptic loosening of the intramedullary (IM) stem at a mean follow-up of 22.1 ± 8.5 months (3 to 61 months), four of which were uncemented stems. Five implants (4.76%) were revised for loosening of the extra-cortical plate fixation adjacent to the knee at a mean follow-up of 22.5 ± 14.2 months (4 to 69 months). Revision was necessary in five

(4.76%) patients due to infection at 8, 12, 14, 29 and 151 months post-surgery (mean follow-up= 42.8 ± 27.3 months).

One implant (0.95%) was revised due to local recurrence at 32 months post-operation and one patient with a proximal tibial replacement had various issues unrelated to the implant, including infection, an unhealed wound and a common peroneal nerve dysfunction, and underwent amputation. Limited knee flexion was also reported in one patient, however the implant was not revised.

Fracture of a screw was reported in one case. The fracture resulted in loosening of the extra-cortical plate fixation around the knee at 47 months post-operation, necessitating the revision of the implant to a conventional joint sacrificing distal femoral implant. One patient had an accident while playing rugby and fractured the shaft of his joint-sparing femoral implant at 77 months post-operation. As the patient's physis had been spared in the initial operation, a significant growth was observed in this patient post-operatively and therefore the fractured implant was replaced with a diaphyseal replacement. The telescopic shaft of a joint-sparing tibial replacement fractured at 144 months post-operation (Figure 3.4). However, as the IM stem was well fixed into the medullary canal and the extra-cortical plates were incorporated within the bone, the endoprosthesis was not revised. Revising a well fixed implant is a complex procedure that can cause significant damage to a patient's bone stock and can increase the risk of infection caused by the increased operation time and the size of incision. A cemented over-sleeve was provided by the implant manufacturer in order to fix the fractured shaft through a surgical procedure without revising the whole or part of the implant.

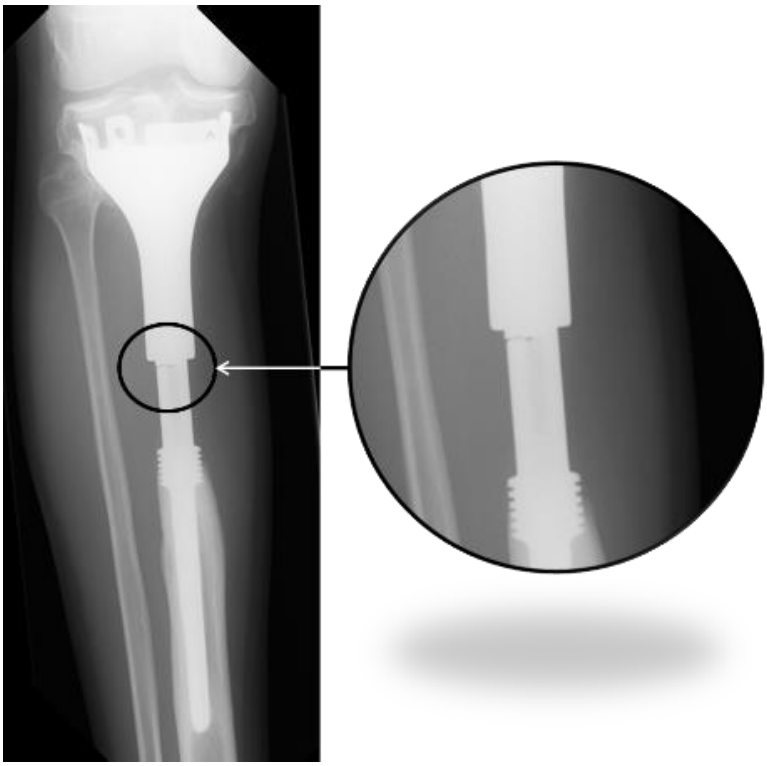

Figure 3.4 Fractured telescopic shaft of a proximal tibial joint-sparing implant at 144 months post-operation. The IM stem and the extra-cortical plates are fixed firmly, therefore the implant was not revised.

Implants with an obturator stem had the highest revision rate with 7 out of 17 (41.18%) implants being revised at a mean follow-up of 28.7 ± 9.1 months (5- 77 months). This was followed by implants with no additional fixation features on the plateau of the implant where 29.36% (8 out of 27) failed at a mean follow-up of 54.1 ± 19.5 months (3 to 151 months). 17.54% (10 out of 57) of implants with cutting fins failed at a mean follow-up of 37.3 ± 12.6 months (4 to 144 months). None of the implants with spikes were revised and all remained *in situ* at the end of the study period. A summary of the results is given in Table 3.1.

3.5.1.2 Implant Complications

Of the 27 patients with minimally invasive extendible prostheses, 5 implants collapsed (18.51% of minimally extendible implants) at 46, 52, 87, 119 and 139 months post

operation (mean= 79.6 ± 18.2 months), resulting in shortening of the limb following extension. None of the collapsed extendible prostheses were revised, however, surgical procedures were necessary to correct the leg length discrepancy. In all cases a C-shaped titanium alloy component was placed on the telescopic shaft of the extendible implant to hold the shaft at the correct length and prevent it from collapsing.

Five (4.76%) patients expressed discomfort around the knee caused by the screws used to fix the extra-cortical plates being too close to the skin or irritating the iliotibial band. In one case the lateral screw was removed due to the pain it was causing during knee flexion and in another case the implant was revised (Table 3.1).

Table 3.1 Summary of the patient follow-up results

		No of cases	No of revisions		Fractured implant or screw		Aseptic loosening- IM stem		Loosening- Extra cortical plates		Infection		Collapsed extension	
Site	Femur	62	16	25.81%	3	4.84%	6	9.68%	2	3.23%	4	6.45%		
	Tibia	43	6	13.95%	1	2.33%	1	2.33%	3	6.98%	1	2.33%		
Age	Adult	34	6	17.65%	1	2.94%	2	5.88%	3	8.82%	1	2.94%		
	Juvenile	71	16	22.54%	3	4.23%	5	7.04%	2	2.82%	4	5.63%		
Diagnosis	Osteosarcoma	48	12	25.00%	3	6.25%	3	6.25%	1	2.08%	3	6.25%		
	Ewing's sarcoma	9	3	33.33%	0	0.00%	0	0.00%	1	11.11%	1	11.11%		
	Other primary tumours	41	6	14.63%	0	0.00%	4	9.76%	3	7.32%	1	2.44%		
	Revision	7	1	14.29%	1	14.29%	0	0.00%	0	0.00%	0	0.00%		
Gender	Female	41	7	17.07%	0	0.00%	4	9.76%	1	2.44%	2	4.88%		
	Male	64	15	23.44%	4	6.25%	3	4.69%	4	6.25%	3	4.69%		
Fixation features	No fixation on plateau	27	8	29.63%	1	3.70%	2	7.41%	1	3.70%	2	7.41%		
	Cutting fins	57	8	14.04%	1	1.75%	3	5.26%	3	5.26%	2	3.51%		
	Spikes	4	0	0.00%	0	0.00%	0	0.00%	0	0.00%	0	0.00%		
	Obturator stem	17	6	35.29%	2	11.76%	2	11.76%	1	5.88%	1	5.88%		
Grower type	None	71	16	22.54%	2	2.82%	5	7.04%	5	7.04%	4	5.63%	n/a	
	Minimally invasive	26	5	19.23%	2	7.69%	1	3.85%	0	0.00%	1	3.85%	3	11.54%
	Non-invasive	8	1	12.50%	0	0.00%	1	12.50%	0	0.00%	0	0.00%	0	0.00%
Stem fixation	Uncemented	48	12	25.00%	2	4.17%	4	8.33%	3	6.25%	2	4.17%		
	Cemented	56	10	17.86%	2	3.57%	3	5.36%	2	3.57%	3	5.36%		

*Four implants did not include stem fixation; one implant was fixed using extra-cortical plates, both distally and proximally, and three are total femurs and include a hip replacement

3.5.2 Implant Survivorship

3.5.2.1 Age Groups: Juveniles and Adults

Implant survival analysis was carried out in both adult and juvenile patients with various end point criteria, including implant revision for any reason, revision due to infection, aseptic loosening and fracture of the implant. Implant survival rate at 120 months when fracture of the implant, extra-cortical plates or fixation screws was the end point was 100% and 90% for adults and juveniles, respectively. This rate decreased to 50% and 45% at 150 months post-surgery (Figure 3.5). When aseptic loosening of the IM was the end point, the probability of implant survival in adults and juvenile patients at 150 months was 92% and 89%, respectively (Figure 3.6) and 95% and 93% when infection was the end point (Figure 3.7). The overall probability of implant survival with failure for any reason as the end point in adults and juvenile patients, was 40% and 32% at 150 months (Figure 3.8). With death as the end point, survival was 87% and 77% in adults and juveniles at 150 months. No significant differences were found when the results of these two groups were compared. However, when survival was compared when loosening of the extra-cortical plates was the end point, results were significantly different at 150 months post-operatively; implant survival for adults and juveniles was 85% and 93%, respectively (p= 0.023) (Figure 3.9).

3.5.2.2 Anatomical location: Femoral and Tibial Replacements

Implant survival rates were compared in the two anatomical sites. Probability of survival was 92% and 89% at 150 months, for the femoral and tibial replacements respectively when the end point was loosening of the extra-cortical plate fixation (Figure 3.10). Probability of survival was 83% and 91% at 150 months for femoral and tibial replacements when failure due to aseptic loosening of the IM stem was the end

point (Figure 3.11). Survival rates of 100% and 77% were found for tibial and femoral replacements when the end point was fracture of the implant or screws (Figure 3.12). The probability of survival was 92% and 96% at 150 months for the femoral and tibial implants, when the end point was infection. No significant difference in implant survival was found when the different end points were compared in the two anatomical locations. The probability of survival for revision of the implant for any reason was 48% for femoral and 81% for the tibial replacements, at 150 months follow-up. Results were not significantly different (Figure 3.13). When the end point was patients' death, the survival rate was 65% and 97% for the femoral and tibial groups at 150 months post-surgery. No significant difference was found.

3.5.2.3 Gender

Implant survival rate at 120 months when fracture of the implant, extra-cortical plates or fixation screws, was the end point was 100% and 70% for female and male patients respectively. This rate decreased in male patients to 35% while survival rate remained at 100% in female patients at 150 months post-surgery but was not significant (Figure 3.14). When aseptic loosening of the IM was the end point, the probability of implant survival in female and male patients at 150 months was 93% and 87% respectively (Figure 3.15) and 95% and 93% when infection was the end point. The overall probability of implant survival with revision for any reason as the end point, for female and male patients was 80% and 24% at 150 months. With death as the end point, survival was 89% and 30% in female and male patients, at 150 months. Survival at 150 months post-surgery was compared when failure occurred due to loosening of the extra-cortical plates; implant survival in female patients was 96% while in male patients was 87% (Figure 3.16).

Although overall female patients presented improved probability of survival compared to male patient, no significant differences were found when the results of these two groups were compared.

3.5.2.4 Overall Implant Survivorship

The overall probability of survival for all implants and all age groups, when the fracture of the implant or screws was the end point was 54% at 150 months (Figure 3.17). With an end point of aseptic loosening of the IM stem, survival was 88% at 150 months (Figure 3.18). When failure of the extra-cortical plate fixation was investigated, the probability of survival was 91% at 150 months (Figure 3.19). The overall probability of survival for all implants, when the end point was total or partial revision of the implant for any reason was 39% at 120 months (Figure 3.20).

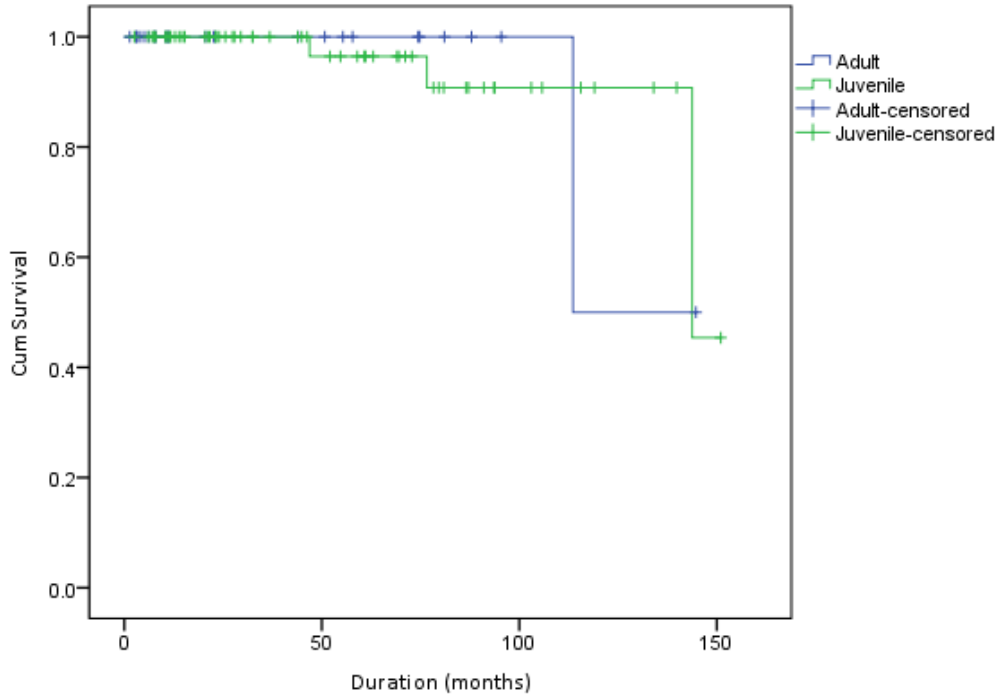

Figure 3.5 Kaplan-Meier survival curve for implant or screw fixation fracture in juvenile and adult patients. Survival rate was approximately halved for both groups at 150 months. At 100 months post-surgery, 2 adult and 8 juvenile patients remained. Fracture of the implant occurred in one adult at 145 months, and in one juvenile patient at 144 months.

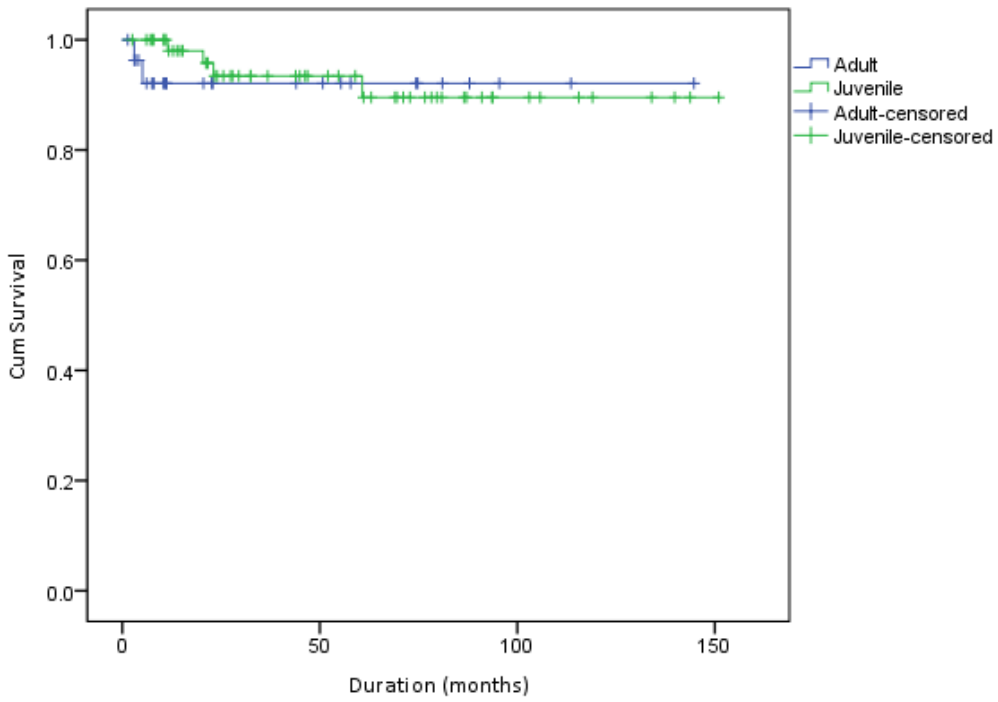

Figure 3.6 Kaplan-Meier survival curve for adults and juvenile patients. The probability of survival was 92% in adults and 89% in juveniles for aseptic loosening of the IM stem as the end point.

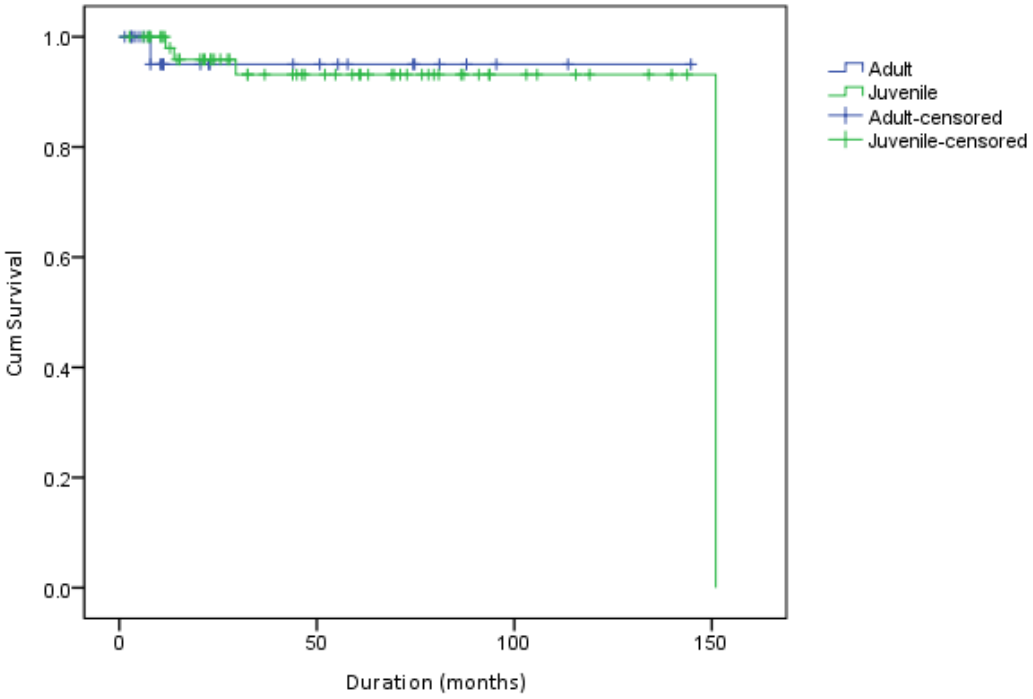

Figure 3.7 Kaplan-Meier survival curve for adults and juveniles at 150 months. Probability of survival was 92% and 89%, respectively with infection as the end point.

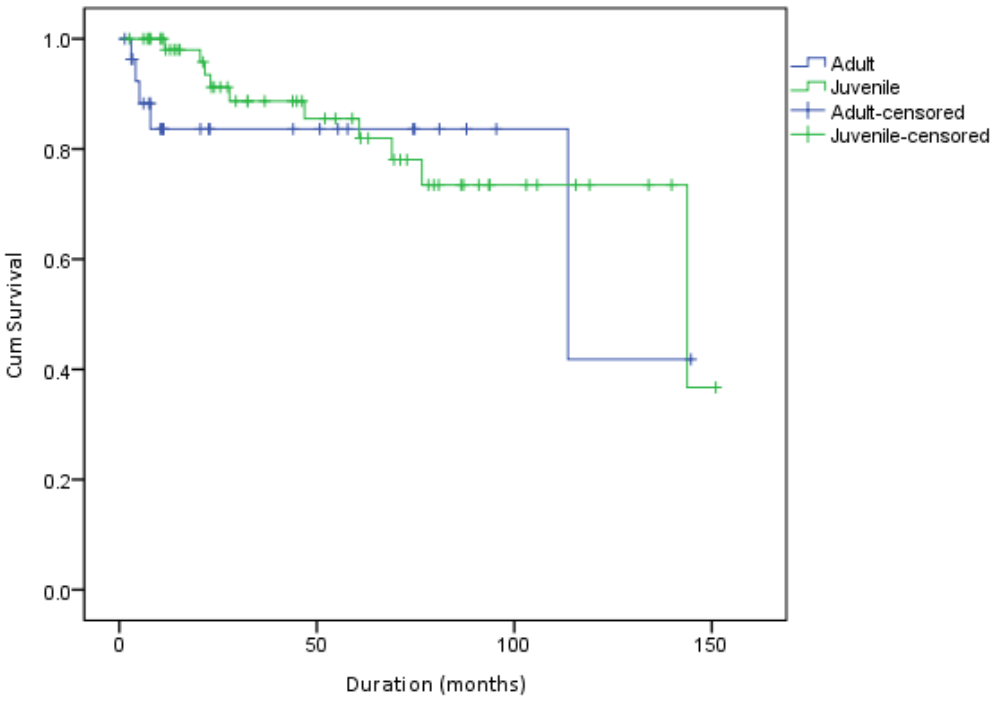

Figure 3.8 Kaplan-Meier survival curve for juvenile and adults when the end point was revision of the implant for any reason. Survival at 120 months was 40% in adults and 65% in juvenile patients.

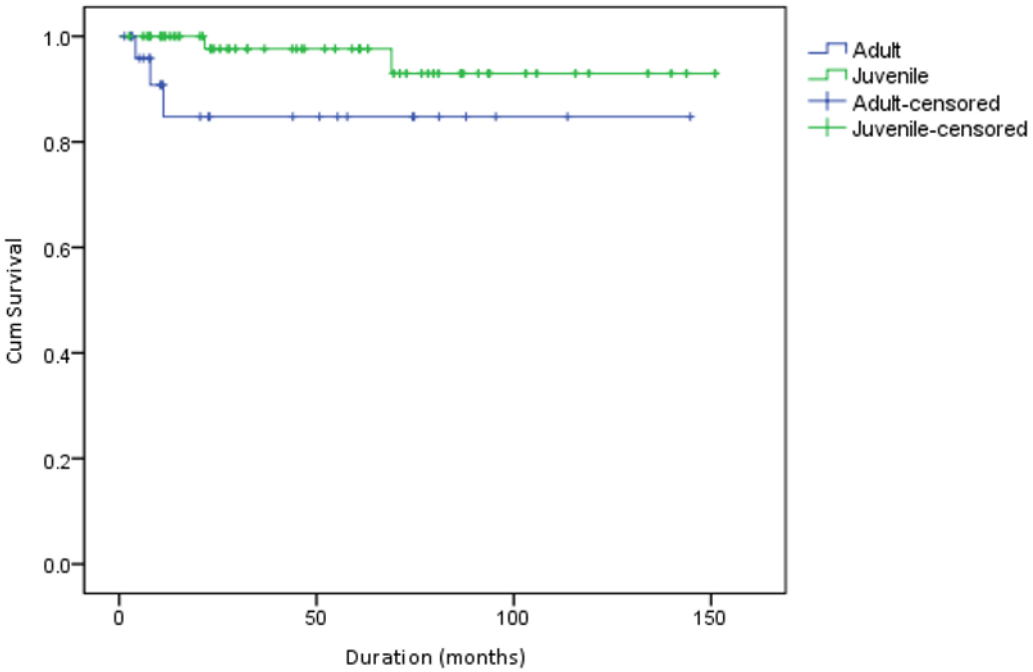

Figure 3.9 Kaplan-Meier survival curve for juvenile and adult patients when loosening of extra-cortical plates was the end point. The results were significantly different at 150 months post-operation (*p*=0.023).

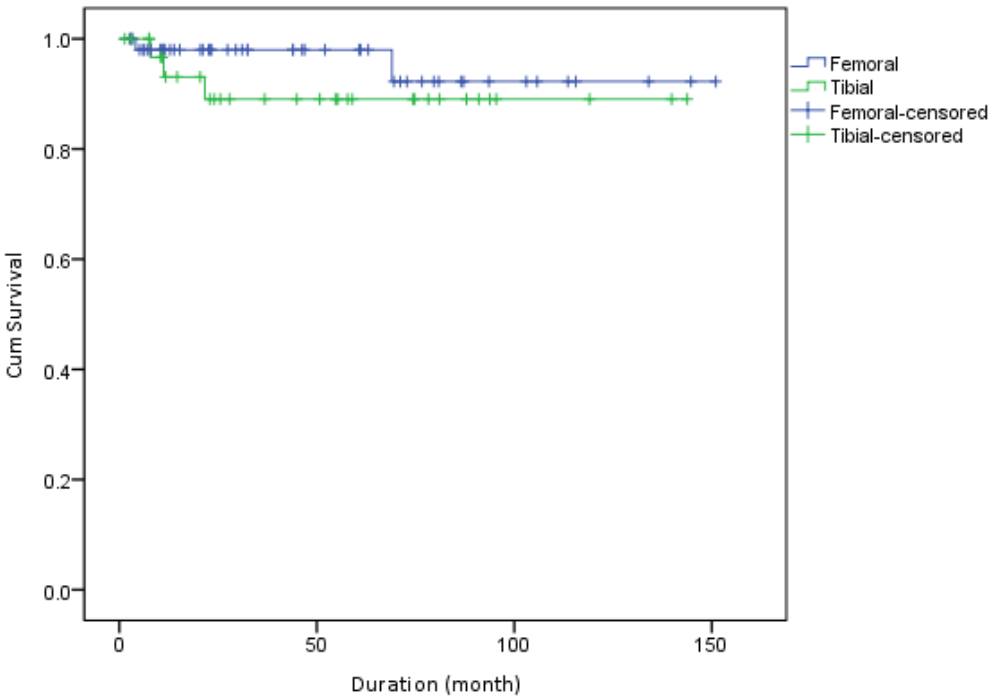

Figure 3.10 Kaplan-Meier survival curve for femoral and tibial replacements when loosening of extra-cortical plates was the end point. Survival at 150 months was estimated to be 92% and 89%, respectively.

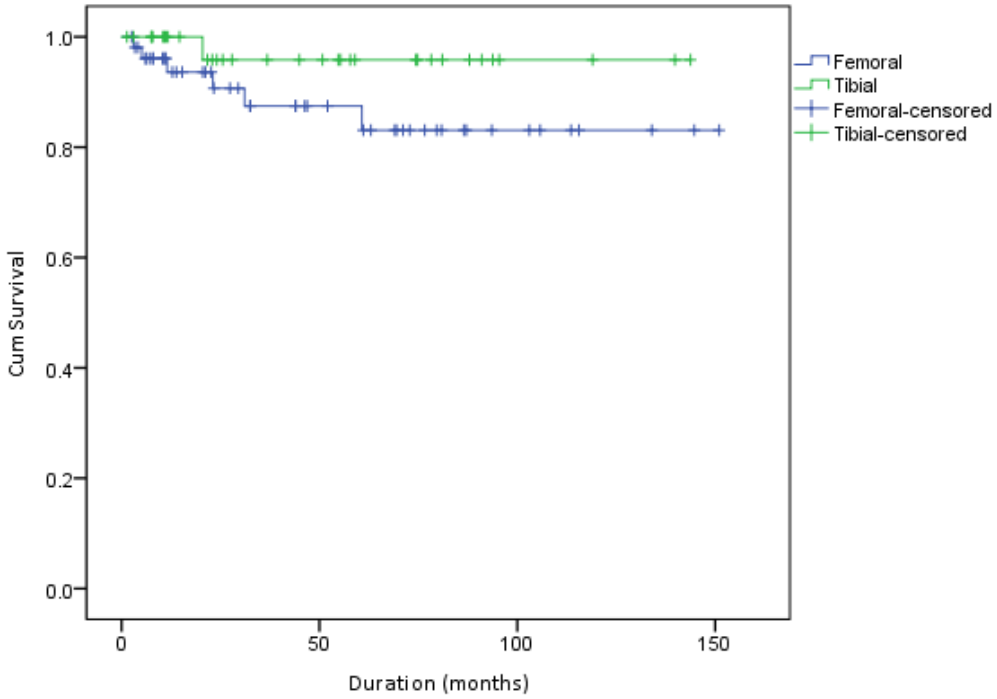

Figure 3.11 Probability of survival was 83% and 91% at 150 months for femoral and tibial replacements when aseptic loosening of the IM stem was the end point.

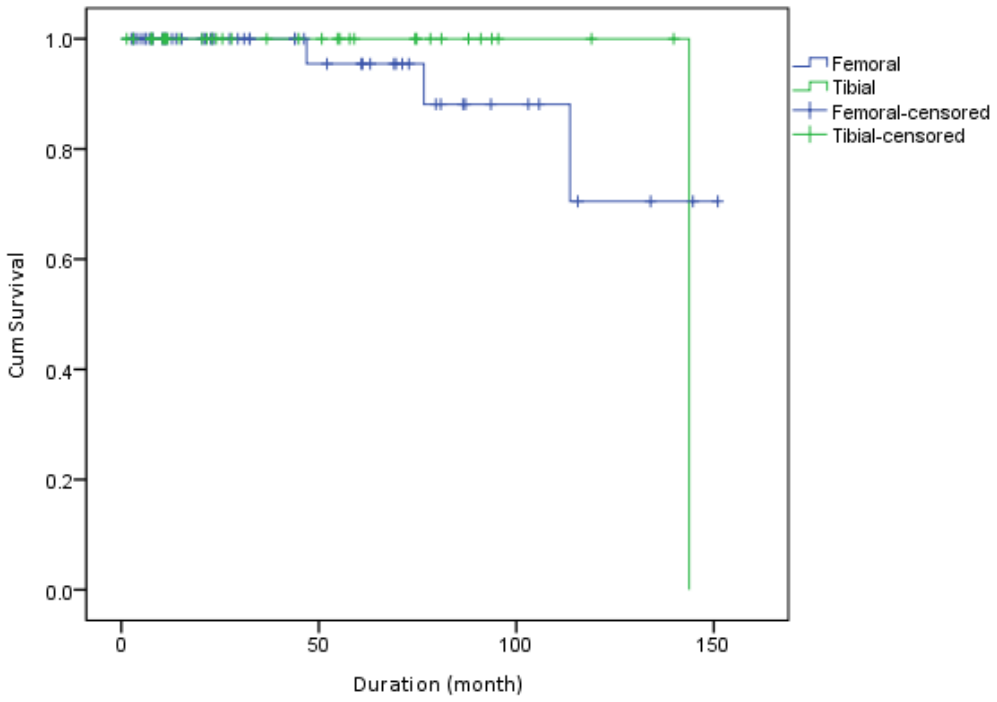

Figure 3.12 Kaplan-Meier survival curve for femoral and tibial replacements when the end point was fracture of the extra-cortical plates or the screws. Survival rate was 77% and 100% at 150 months.

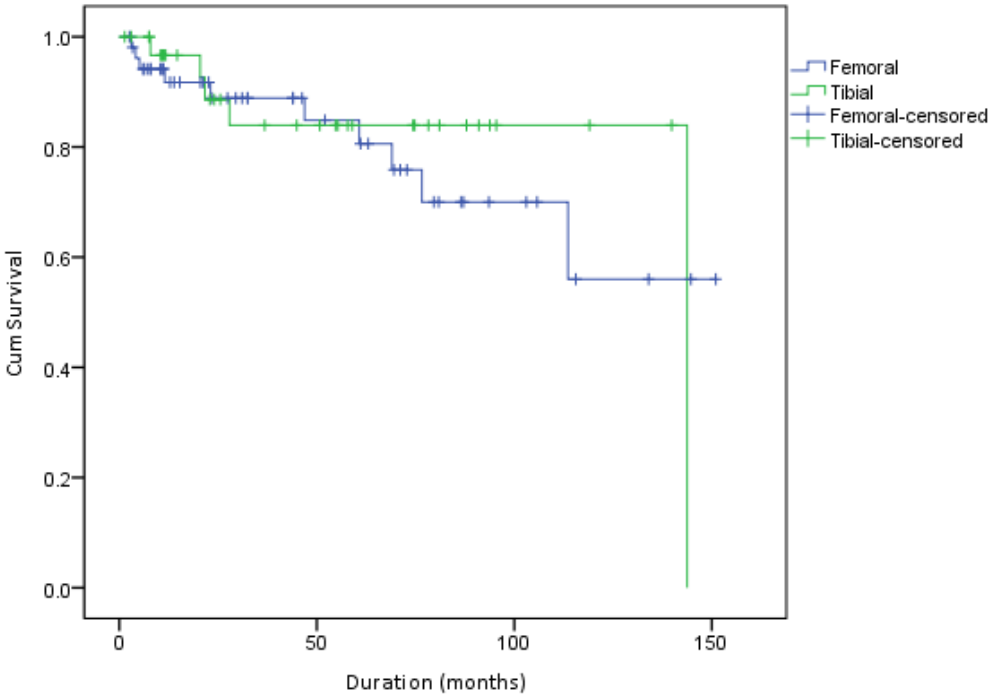

Figure 3.13 Kaplan-Meier survival curve for femoral and tibial replacements when the end point was revision of the implant for any reason. Probability of survival for the femoral and tibial replacements was 48% and 81%, respectively at 150 months.

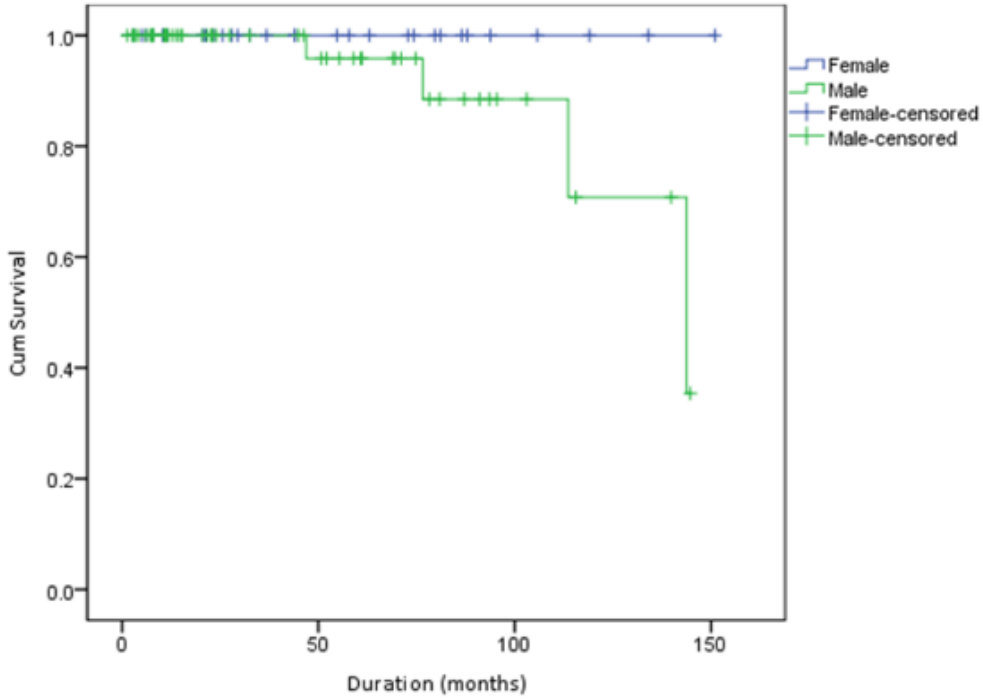

Figure 3.14 Kaplan-Meier survival curve in female and male patients when the end point was implant fracture. Survival rate in male patients reduced to 35% at 150 months while it remained at 100% in female patients. However, this was not significant.

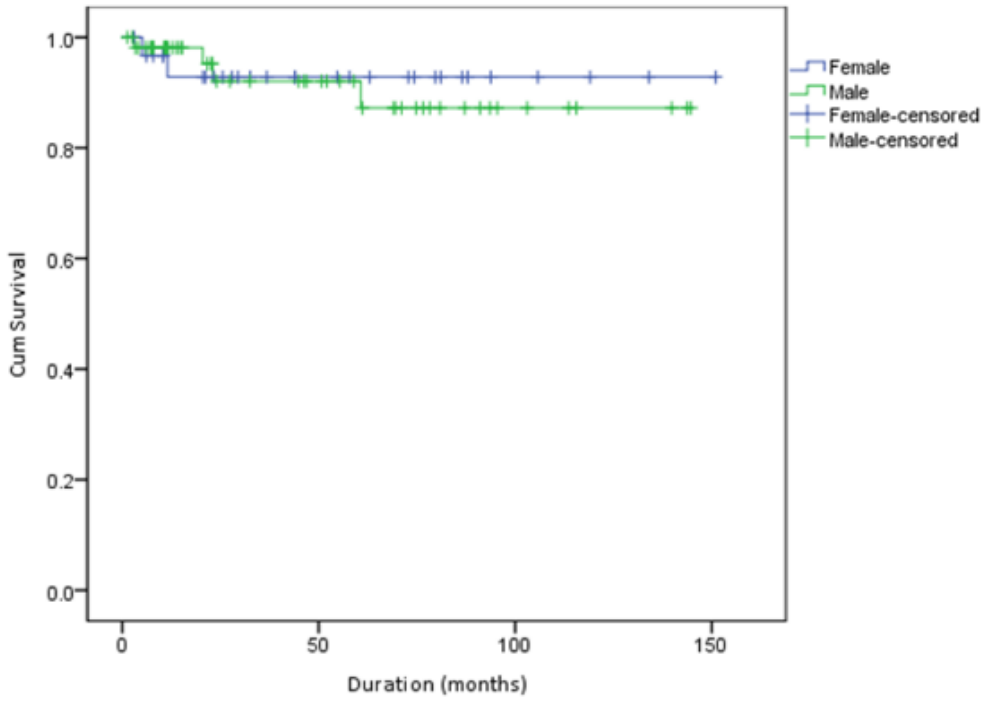

Figure 3.15 Kaplan-Meier survival curve for female and male patients when aseptic loosening of the IM stem was the end point. The probability of survival was 93% in female patients and 87% in male patients.

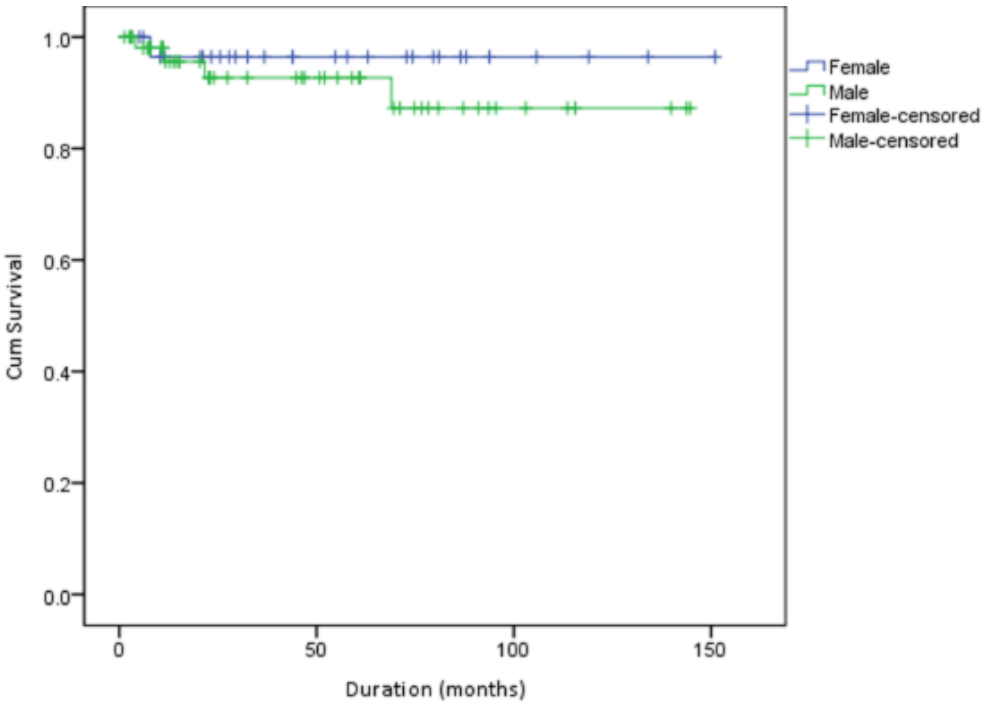

Figure 3.16 Kaplan-Meier survival curve for female and male patients when failure due to loosening of the extra-cortical plates was the end point. Probability of survival was 96% in female patients and 87% in male patients.

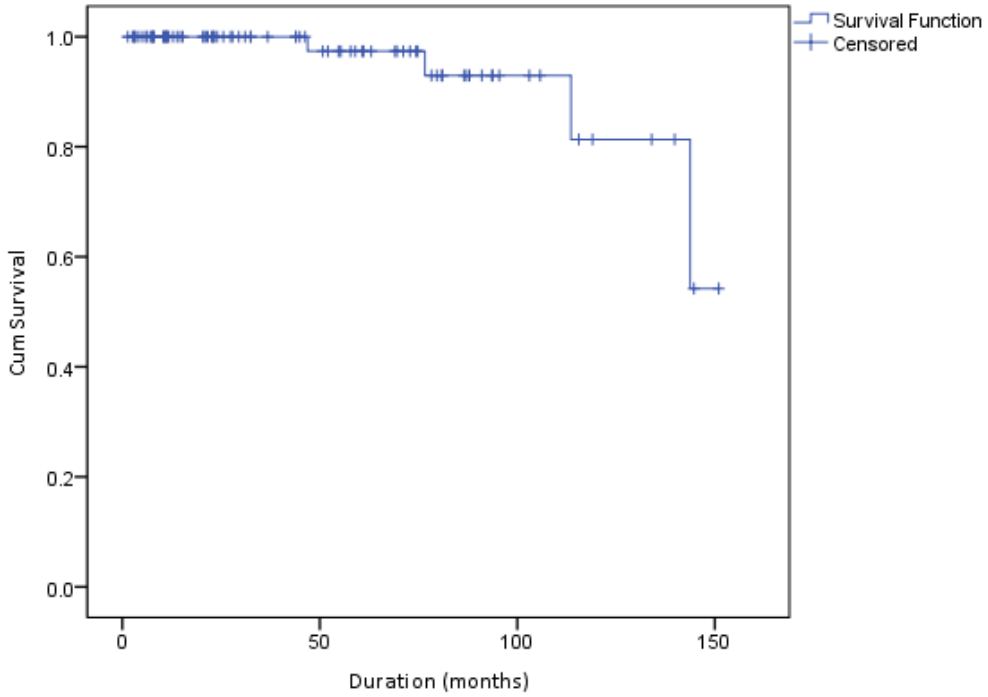

Figure 3.17 Kaplan-Meier survival curve; probability of survival for all implants was 81% at 120 months and 54% at 150 months when end point was the fracture of the extra-cortical plates or the screws.

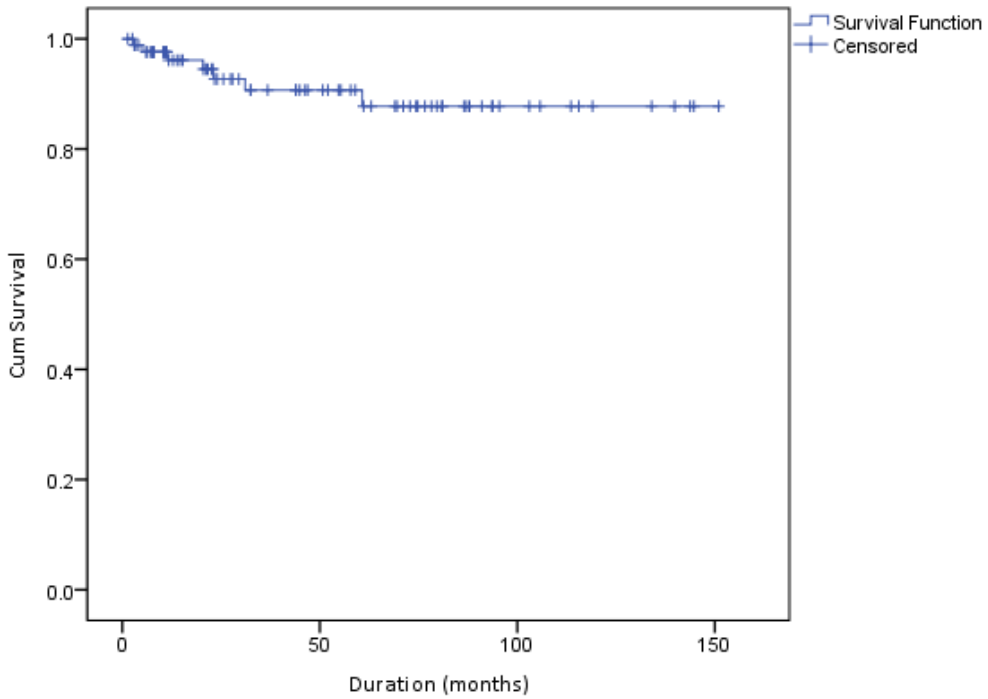

Figure 3.18 Kaplan-Meier survival curve showing the probability of survival for all implants was 88% at 150 months when end point was aseptic loosening of the IM stem.

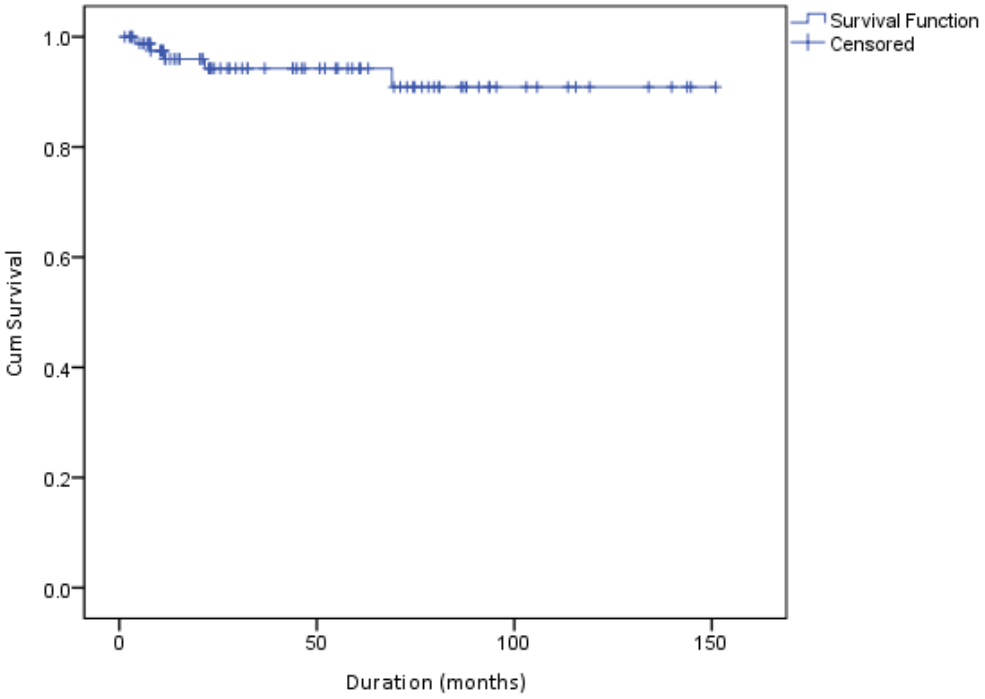

Figure 3.19 A Kaplan-Meier survival curve showing the probability of survival for all implants where failure of the extra-cortical plates was defined as the end point. Probability of survival was 88% at 120 and 150 months.

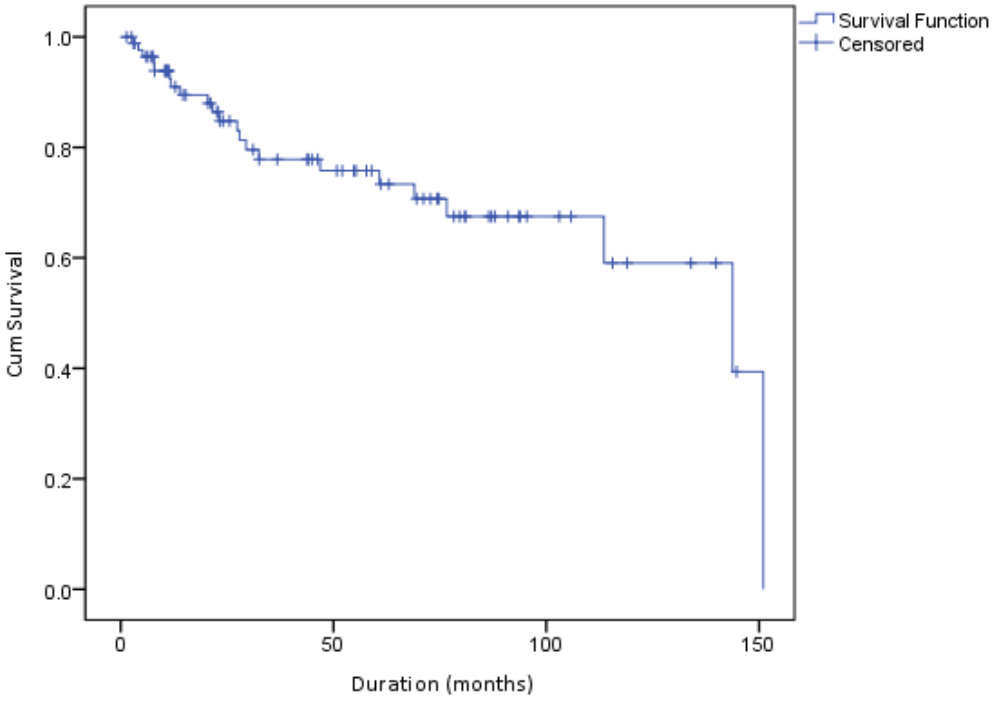

Figure 3.20 Kaplan-Meier survival curve for all implants where the end point was revision or partial revision of the implant for any reason. Probability of survival at 10 years was 39%.

3.5.3 Qualitative Analysis of Extra-Cortical Plate Fixation and Resection Length

Loosening around the extra-cortical plates was observed in three tibial implants at 1, 7 and 12 months post-operation. All three cases were later revised. The mean resection amount for the three failed implants was 32.5 ± 5.8% (range: 21- 41%) of the total tibial length; the mean resection length for the remaining 7 patients whose fixation remained stable was 52.9 ± 7.8% (range: 31- 86%). When the average resection amount in patients with a stable fixation and those that were revised were compared, no significant differences were found.

One implant that included an obturator stem was leaning laterally, one month post operation. Twelve months post-operation, radiographic images of the implant showed that the prosthesis was not aligned with the tibial shaft and radiolucent lines were visible around the IM stem. Bone remodelling in form of increased bone diameter along the IM stem was visible and the plate fixation appeared unstable with the implant leaning laterally (Figure 3.21).

In another patient that experienced instability of plate fixation, initial signs of loosening were visible at 7 months post-operation. A radiolucent line was visible between the posterior extra-cortical plate and the bone and the implant appeared to lean anteriorly. Fixation in this case was achieved with three extra-cortical plates and 4 uni-cortical screws. As the resection in this case was close to the diaphysis, extra-cortical plates were attached to the tibial shaft. Increased malalignment of the implant with the tibial bone was more apparent in 10 month post-operation radiographs, where the implant appeared to have leaned further anteriorly. At 12 months post-operation, radiographic images revealed instability of the implant; screw migration, implant

malalignment and growth of the residual bone segment was evident (Figure 3.22). The implant was later revised and replaced with a diaphyseal replacement. Implant fixation to the residual proximal aspect of the tibial bone was achieved with an IM stem.

The third case of extra-cortical plate fixation failure was in a proximal tibial implant that was secured using three extra-cortical plates and 5 uni-cortical screws. Although the immediate and 4 month post-operative radiographs showed a stable fixation, at 12 months, migration of the implant was evident. The visible radiolucent area between the proximal residual segment of the tibia and the plateau of the implant that was noted in earlier images had disappeared at 12 months and 18 months post-operation. However, this was not due to bone growth as the distance between the tip of the medial plate and the line of the joint had decreased, suggesting that migration of the implant had occurred. The change in orientation of the screws indicated screw migration. Fracture of one of the screws through the medial plate was noted at 18 months post-surgery (Figure 3.23). This implant was later revised and replaced with a diaphseal implant where fixation was achieved with IM stems.

Figure 3.21 A/P radiographs, showing a proximal tibial replacement at [A] 4 months post- operation and [B] at 12 months post-surgery. The implant is leaning laterally, causing malalignment of the knee joint.

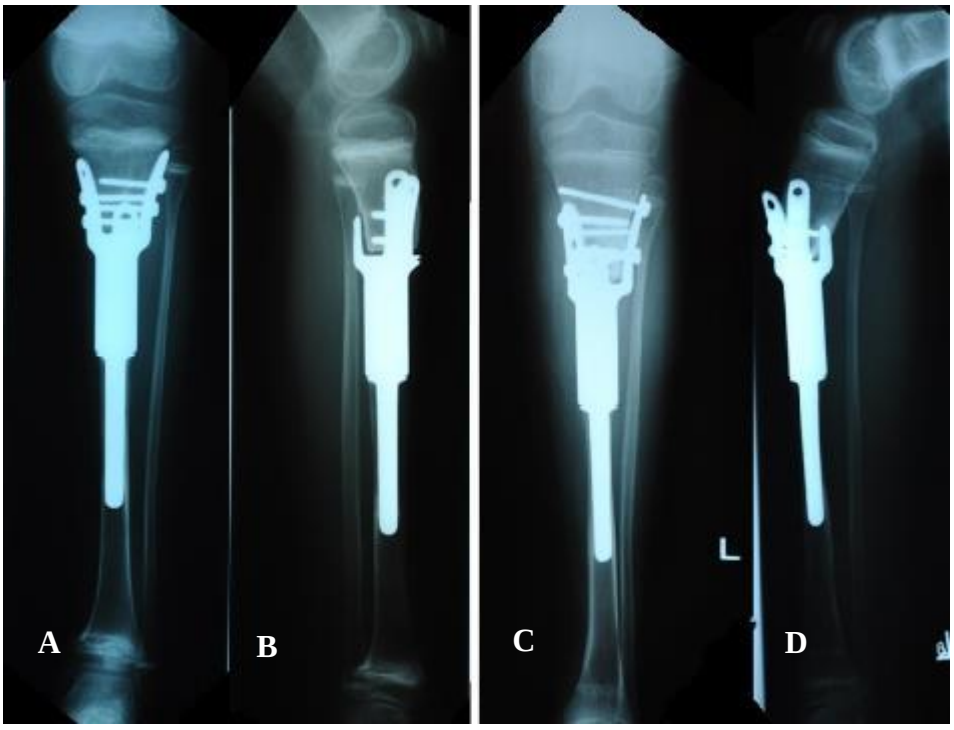

Figure 3.22 Radiographs of the implant at 5 months post-operation [A] in A/P and [B] M/L view. [C] and [D] show the same implant at 12 months post-operation in the A/P and M/L views, respectively. Screw migration and implant malalignment by leaning anteriorly are visible.

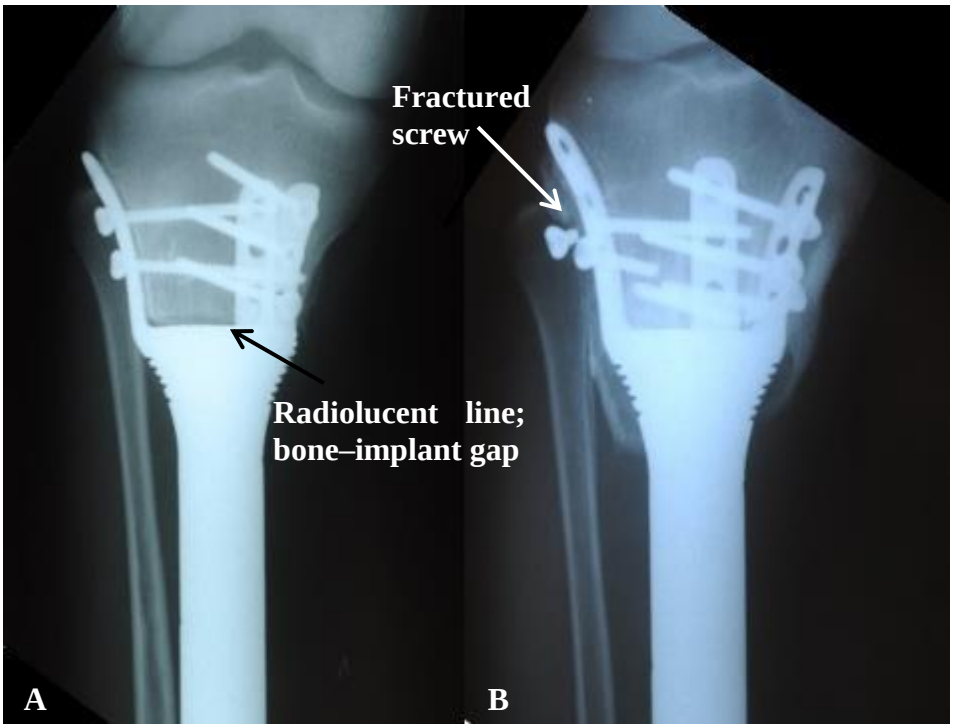

Figure 3.23 [A] A/P Radiographs of a tibial joint-sparing implant 4 months post-operation. A radiolucent line between the bone and the implant is visible. [B] Shows the same implant at 18 months post-operation where one of the screws was fractured and implant migration is visible.

3.5.3.1 Aseptic loosening

Aseptic loosening of the intramedullary stem of a distal femoral replacement in a 5 years old male patient was the reason for revision. At three months post-operation, the IM stem had migrated laterally. After 12 months, radiographical signs of loosening became evident with proximal migration of the implant. At 36 months post-operation, fragmentation of the residual proximal femoral bone was detected and approximately 48 months post-operation the IM stem of the implant was revised and replaced with triple-plate fixation (Figure 3.24).

Although revision due to aseptic loosening of the IM stem was not observed in any of the other implants reviewed for this part of the study, radiolucent lines around the

cemented and uncemented IM stems that could indicate initiation of aseptic loosening were noted in eleven patients. Radiolucent lines were detected in post-operative radiographs in three cases, two tibial (both cemented) and one femoral implant (uncemented). During the first 3 months post-surgery, the presence of radiolucent lines was noted in 4 cases, one femoral (uncemented) and 3 tibial replacements (2 cemented and 1 uncemented). The remaining cases showed signs of radiolucency between 36 and 60 months post-operation.

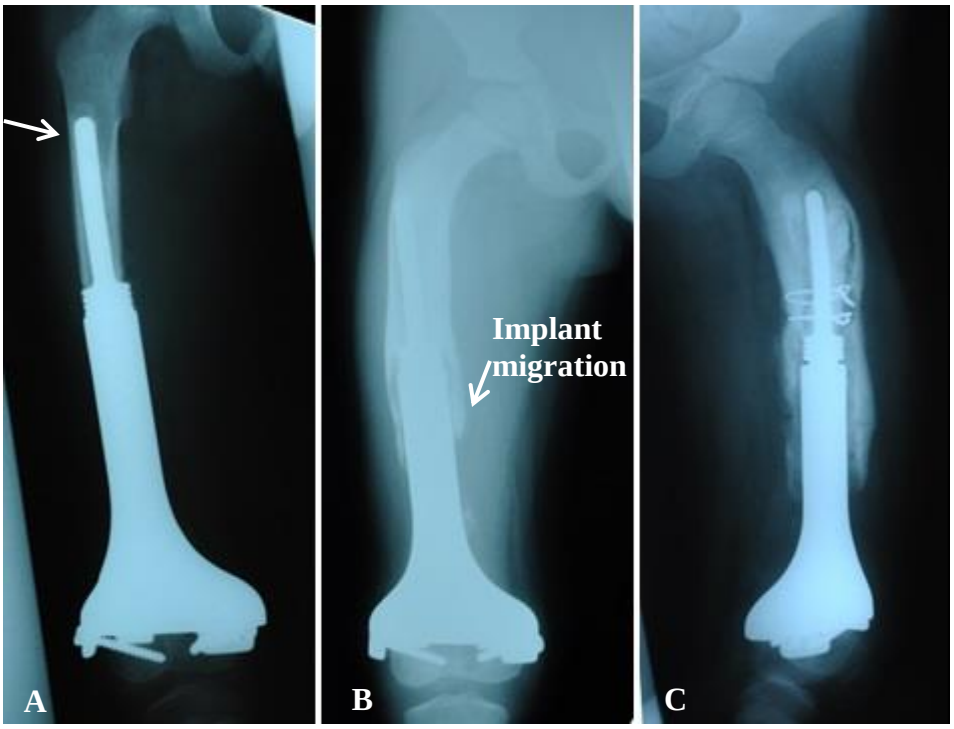

Figure 3.24 Radiographs showing loosening of the IM stem in a patient with a distal femoral implant; [A] A/P view radiograph, 3 months post-surgery the IM stem had slightly migrated laterally. [B] A/P view radiograph at 12 months post-surgery, the implant had migrated proximally as well. [C] M/L view radiograph at 36 months post-surgery, peri-prosthetic bone loss of the femoral bone is visible.

3.5.3.2 Bone remodelling

Bone remodelling was observed in more than half of all cases reviewed radiographically. In five cases, bone growth had occurred within 12 months of implantation. Bone growth was detected after 12 months post-surgery and between 24 and 60 months post-operation in 5 tibial and 4 femoral replacements. Extra-cortical bone growth around the HA collar was observed in 6 patients, 4 with a femoral and 2 with a tibial implant (Figure 3.26). In four cases, where a gap between the implant and the bone was noted in earlier radiographic images, the gaps were filled in by bone formation in later radiographs (Figure 3.27). In addition to bone remodelling, heterotrophic ossification could be detected near the HA collar in 4 cases (Figure 3.28).

Two femoral replacements displayed signs of bone loss at the bone-implant junction at the shoulder of the implant at 2 months and 12 months post operation (Figure 3.25). Cortical narrowing adjacent to the uncemented stems was observed in a tibial endoprosthesis at 10 months post-surgery (Figure 3.25). In later radiographs, hypertrophy on the opposite side of the narrowing was evident (Figure 3.29).

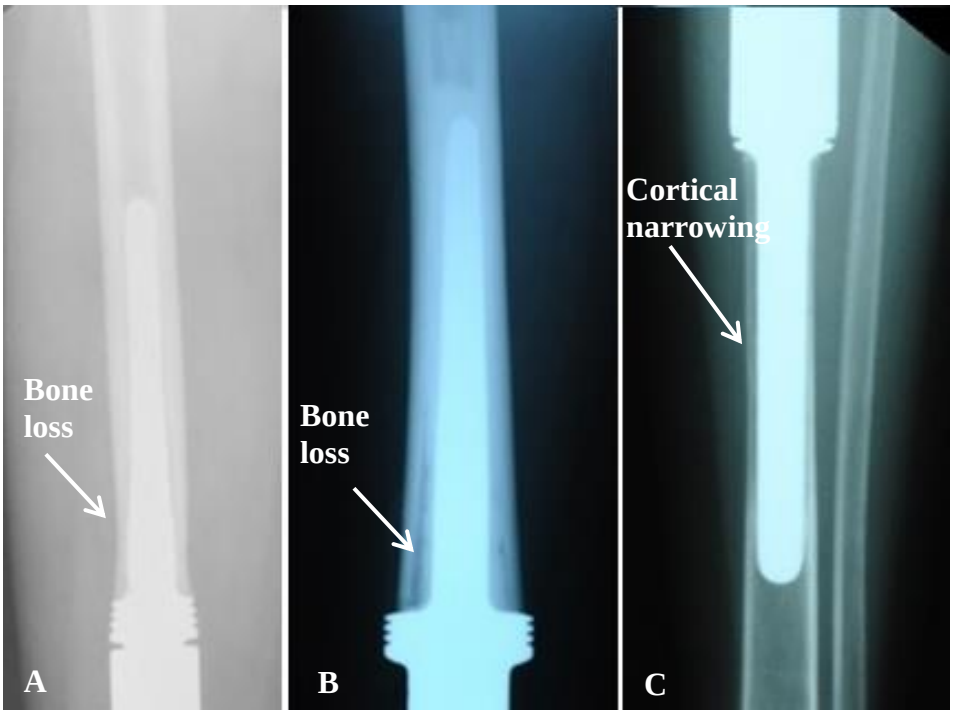

Figure 3.25 A/P radiographs [A] and [B] show two femoral joint-sparing implants with bone loss at the implant shoulder-bone junction at 12 months and 2 months post-operation, respectively. [C] An A/P radiograph shows a tibial joint-sparing implant with cortical narrowing adjacent to the uncemented stem at 10 months post-operation.

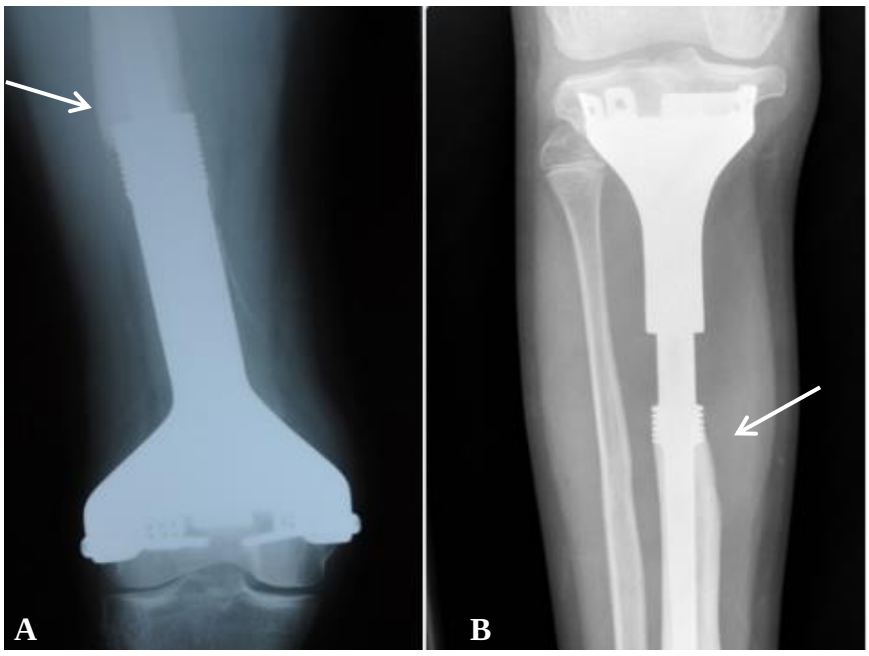

Figure 3.26 [A] An A/P radiograph of a distal femoral joint-sparing implant at 6 months post-operation. [B] An A/P radiograph of a tibial joint-sparing implant at 12 months post-operation. Arrows indicate extra-cortical bone growth onto the HA collar.

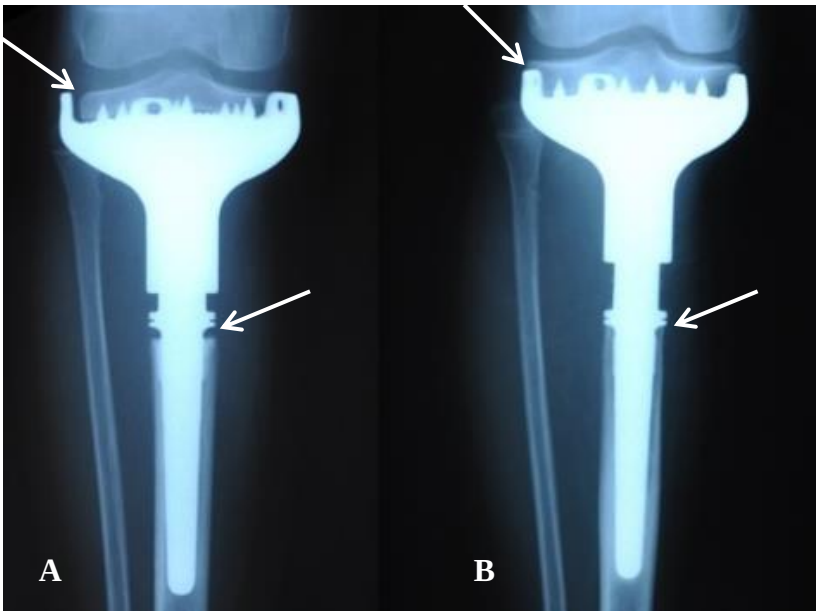

Figure 3.27 A/P radiographs of a proximal tibial implant at [A] 3 months post-surgery and [B] 30 months post-surgery. The gaps between the bone and the implant collar and the extra-cortical plate (arrows) appear to be filled at 30 months post-surgery. The gap closure could be a result of bone formation at the collar or the sinking of the implant into the bone. The disappearance of the gap between the bone and the extra-cortical plate could be a result of bone formation or caused by the angle of exposure (rotated leg).

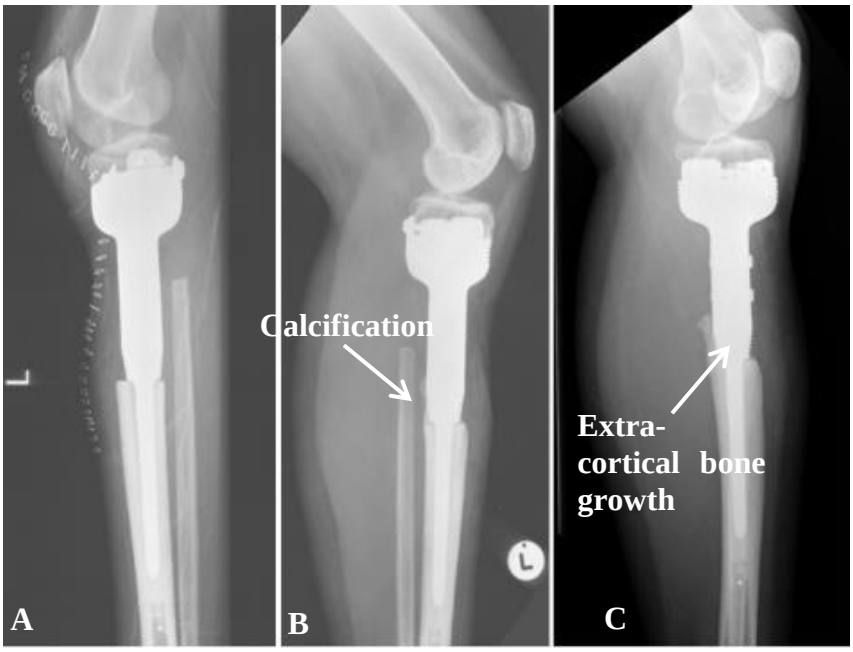

Figure 3.28 M/L radiographs of a joint-sparing tibial replacement [A] post-surgery and [B] at 2 months post-operation. Heterotrophic ossification adjacent to the HA collar is visible. [C] Shows extra-cortical bone growth into the HA collar, at 36 months post-surgery.

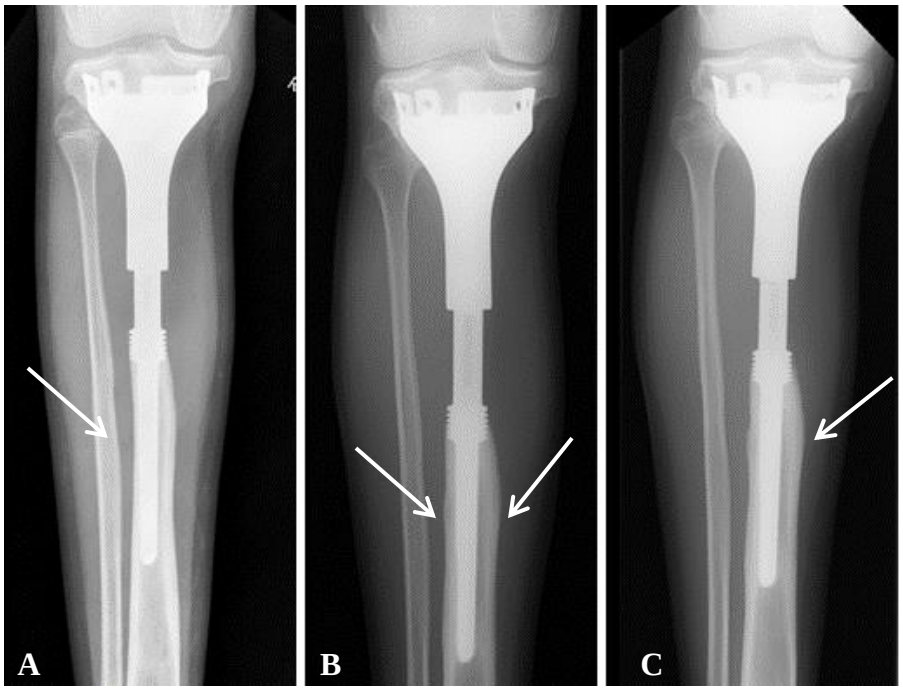

Figure 3.29 A/P radiographs a proximal tibial implant at, [A] 60 months post-operation, showing cortical narrowing adjacent to the stem. [B] At 96 months post-surgery, extra-cortical bone growth into the HA collar and bone hypertrophy is visible. [C] At 132 months post-surgery further bone remodelling is visible.

3.5.4 Implantation accuracy

Mean percentage error for resection in failed implants was 3.7 ± 2.0% (range: 1 to 8%) and the mean alignment error was 2.5 ± 1.1° (range: 0.9 to 4.7°). The mean percentage error for resection in the non-failure implants was 13.9 ± 9.5% (range: 0 to 65%) and the mean alignment error was 3.0 ± 0.5° (range: 1.5 to 4.3°).

The mean planned resection level in the femoral group was 37.5 ± 7.9mm (range: 14.5 to 96.0mm), when measured from the articulating surface of the bone at the knee joint. The average percentage error in resection level for all femoral replacements was 28.1 ± 9.1% (range: 0.2 to 103.1%) and the mean error in angle between the mechanical and anatomical axes was 3.3 ± 0.6° degrees (range: 0° to 5.4°). The average time *in*

situ for all femoral replacements included in the radiographic analysis was 75 ± 9 months (range: 28 to 118 months). At the end of the follow-up, 8 femoral implants remained *in situ* and 3 had been revised; the average implantation time for non-failure cases was 87 ± 7 months (range: 61 to 118 months). The reasons for revision in three implants were; infection, failure of the plate fixation adjacent to the knee and aseptic loosening of the IM stem. The average implantation time for the failed cases was 44 ± 14 months (range: 29 to 71 months); the mean percentage error in resection level for the failed femoral implants was 47.0 ± 29.1% (range: 5.0 to 103.1%) and the mean error in alignment angle was 3.3 ± 1.6° (range: 0° to 5.0°). The mean percentage error in resection level for the implants *in situ* was 20.9 ± 7.7% (range: 0.2 to 64.0%) and the mean error for the inclination angle was 3.7 ± 0.8° degrees (range: 0° to 5.4°).

The mean planned resection level in the tibial group was 38.3 ± 7.4mm (range: 12.0 to 78.5mm). Average time *in situ* in tibial endoprostheses was 60 ± 13 months (range: 20 to 144 months). At the end of the follow-up period, 7 implants remained *in situ*; the mean implantation time for non-failure cases was 76 ± 14 months (range: 28 to 151 months). Three tibial implants were revised, all due to failure of the extra-cortical plate fixation. The mean implantation time for the failed implants was 23 ± 2 months (range: 20 to 27 months). The average percentage error in resection level for all tibial replacements was 18.3 ± 6.8% (range: 1.3 to 65.3%) and the mean error in inclination angle was 2.8 ± 0.4° degrees (range: 0.9° to 4.7°). The average percentage error in resection level for the failed tibial implants was 4.6 ± 1.8% (range: 1.3 to 7.6%) and the mean error in the inclination angle was 2.5 ± 1.1° (range: 0.9° to 2.9°). The mean percentage error in resection level for the implants *in situ* was 24.1 ± 8.8% (range: 6.09 to 65.3%) and the mean error for the inclination angle was 3.0 ± 0.5° degrees (range: 1.5° to 4.3°).

Figure 3.30 to Figure 3.33 represent the relationship between the error in alignment angle and resection error and the time the implant was *in situ* at the time of radiographic analysis for two groups of patients. Results include those whose implants were revised and those whose implants were still *in situ* at the end of the follow-up period. The time that the implants were *in situ* was plotted against the percentage error in resection levels and the inclination angle for both femoral and tibial groups. Spearman's Rank coefficient parameter was calculated to determine whether percentage error in the implantation is associated with the failure of the implant and the longevity of the construct. R^2= 0.998 in failed femoral group for resection error was found but no correlation was found between the duration of implantation and resection error or alignment angle error in any of the other groups.

When the error in alignment angle was plotted against the error in resection levels, no correlation was found. Figure 3.34 and Figure 3.35, show the relationship between the measured alignment error and the resection percentage error.

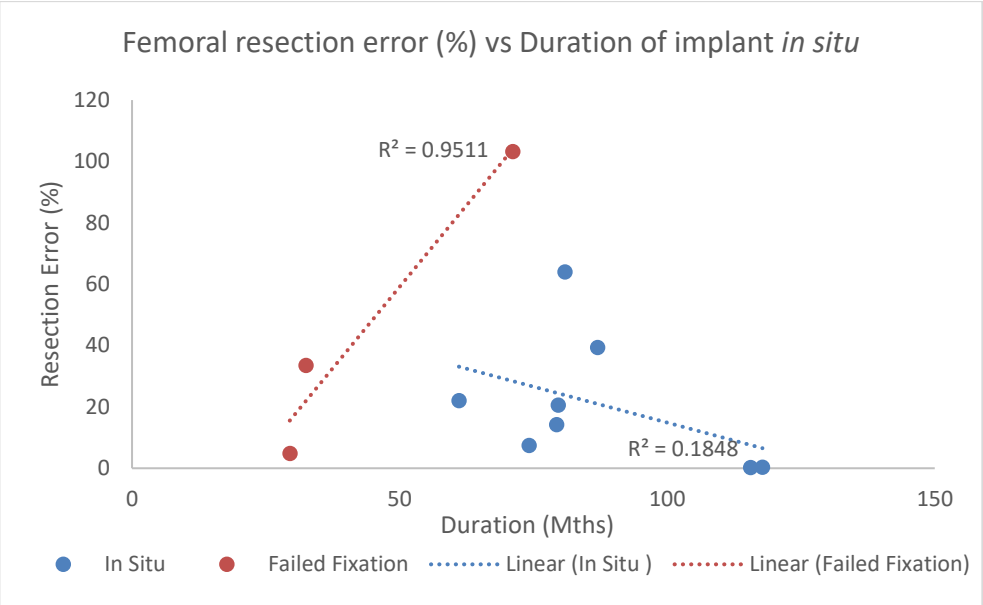

Figure 3.30 Scatter diagram showing femoral resection percentage error against the implantation time for failed fixations and stable fixations.

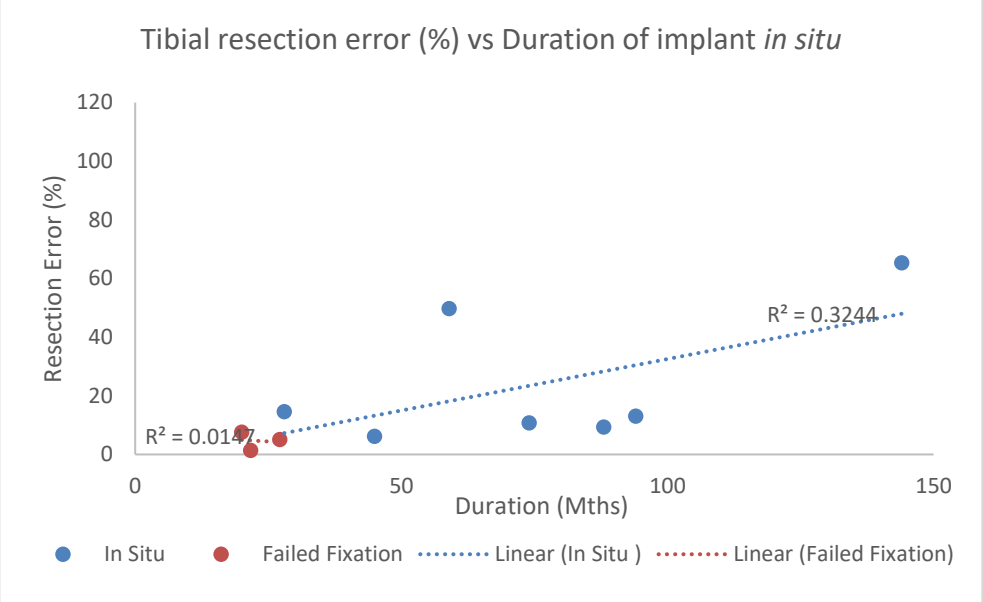

Figure 3.31 Scatter diagram showing tibial resection percentage error against the implantation time for failed fixations and stable fixations.

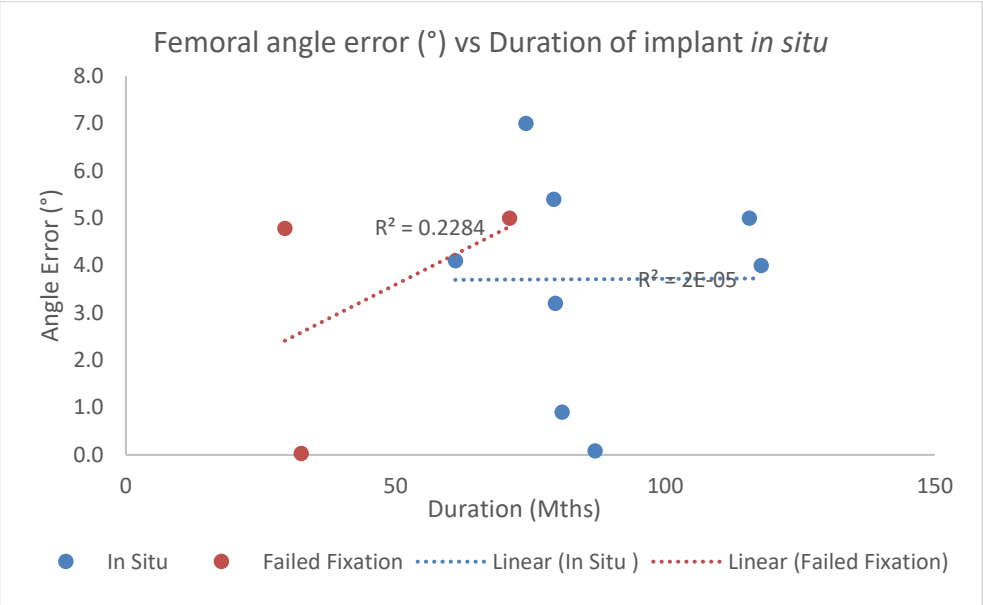

Figure 3.32 Scatter diagram showing femoral alignment angle error against the implantation time for failed and stable fixations.

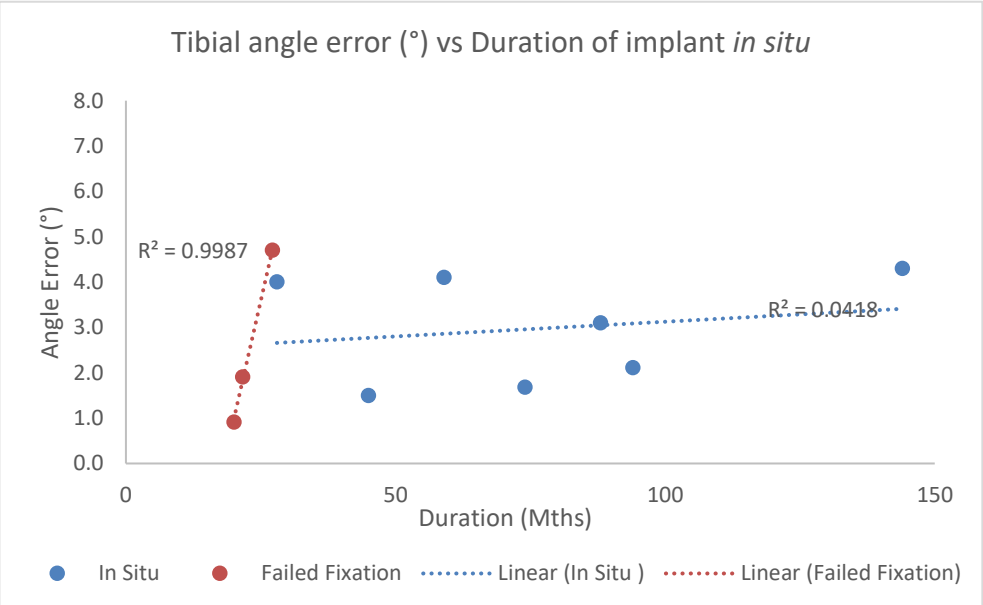

Figure 3.33 Scatter diagram showing tibial alignment angle error against the implantation time for failed and stable fixations.

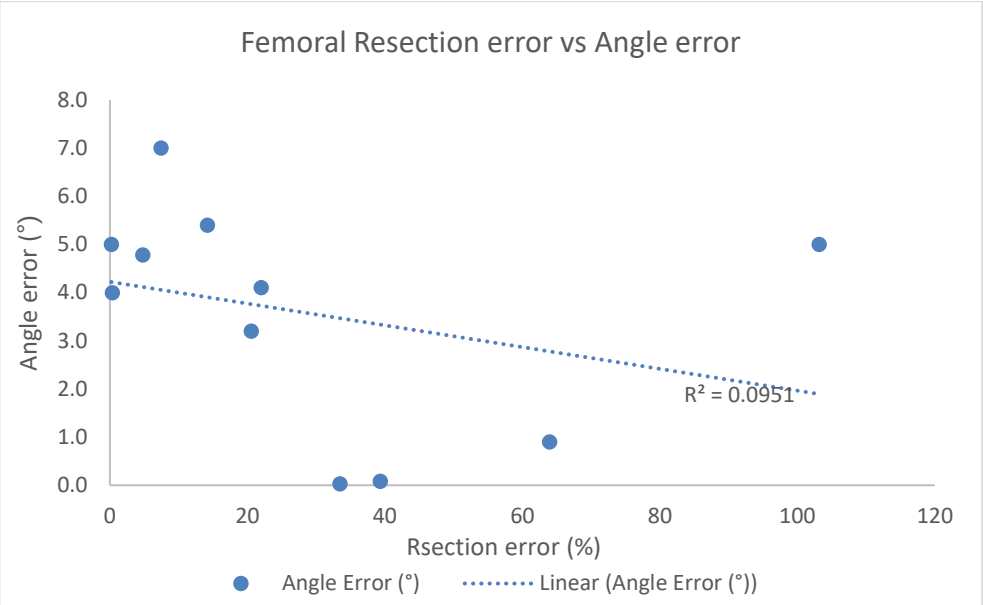

Figure 3.34 Scatter diagram shows the resection percentage error against the error in alignment angle for all femoral implants.

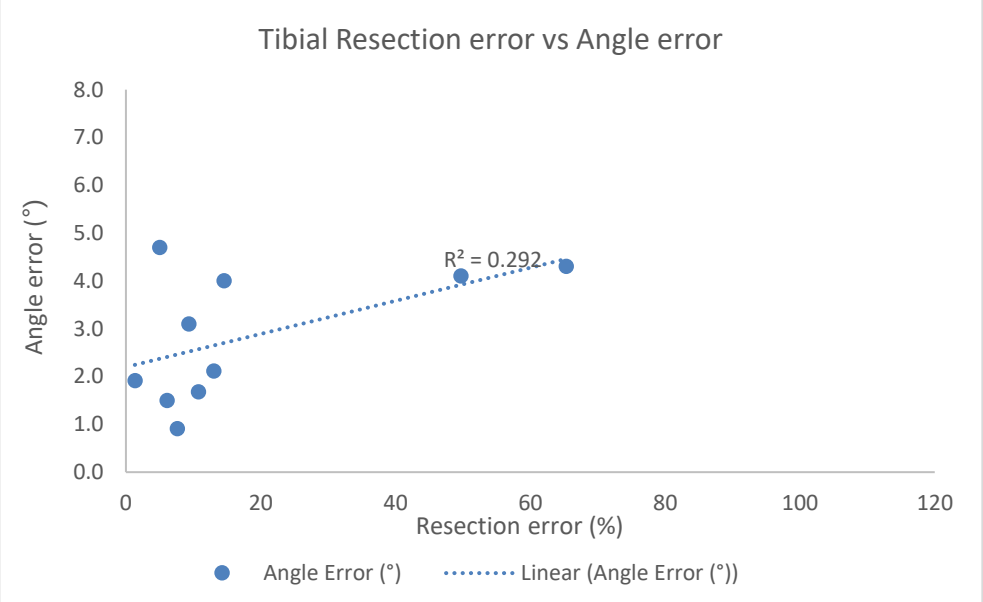

Figure 3.35 Scatter diagram shows the resection percentage error against the error in alignment angle for all proximal tibial implants.

3.6 Discussion

Bone tumours of the proximal tibia and distal femur are often treated by removal of the affected segment of bone and replaced with a conventional, knee sacrificing massive endoprosthesis. Although there are many studies that have investigated the outcomes of using conventional, knee joint sacrificing massive endoprostheses, there are few studies, each with small number of patients that have examined the outcomes of using knee joint-sparing implants that utilise extra-cortical plates. The aim of this chapter was to determine the survival and complication rate in patients treated with massive knee sparing implants and to identify possible contributing factors, such as age, gender and the affected site in implant failure. Post-operative radiographs were also examined to observe changes to the surrounding bone and fixation of the implants. The correlation between implantation accuracy and implant failure was also investigated by quantifying alignment and resection length accuracy in both failed and stable implants.

The overall revision rate in this study was 22.86% at a mean follow-up of 36 ± 11 months with aseptic loosening of the IM stem being the primary mode of failure (6.67%), followed by infection (4.76%) and failure of the extra-cortical plate fixation (4.76%). Probability of survival was estimated to be 39% at 120 months, where the end point was total or partial revision of the implant for any reason. Studies of joint-sacrificing massive endoprostheses with a similar follow-up period have reported infection rates of 3 to 12.5% and aseptic loosening of 3 to 8% (Capanna et al. 2015; Hamilton et al. 2005; Coathup et al. 2013). In a recent study that investigated massive joint-sacrificing implants in the lower extremity, Capanna et al. (2005) reported a 66% survival rate at 120 months, an improved 7% survival rate at ten years when compared with the findings of this study. Although no fracture of the extra-cortical plate was

found in this study, fracture of a fixation screw in one case was a possible contributing factor in failure that resulted in implant revision. There are limited revision options available to patients with a joint sacrificing implants due to the loss of bone stock and the knee joint. However, in patients with a joint-sparing implant, if the joint-spring attachment fails, it can be revised to a conventional joint sacrificing implant.

The overall revision rate was higher in the distal femoral replacements, with a four-fold increase in aseptic loosening and double the number of implant fracture and implant infection when compared with tibial replacements. However, more tibial replacements were revised due to failure of the extra-cortical plate fixation. When patient age was compared, the overall failure rate at 150 months was higher in patients under 21 years of age at the time of surgery than those over the age of 21; this was not significant. A higher failure rate of the extra-cortical plate fixation was also noted in patients over 21 years of age compared with those younger than 21 years. The probability of survival was significant when these two age groups were compared with patients under the age of 21 having a better survival probability at 150 months. In contrast to the findings of this study, Unwin et al. (1996) investigated aseptic loosening in cemented massive bone tumour prostheses of the lower limb and reported that patients under 20 years of age had a worse probability of survival. When the patients age was investigated in combination with resection percentage, under 20 year old patients had the worst probability of survival when aseptic loosening was the end point for both femoral and tibial sites (Unwin et al. 1996). In joint-sparing implants and in juvenile and adolescent patients that the growth plate can be preserved, the affected leg can continue to grow naturally without a need for an extendible implant. This can eliminate failures associated with the extension mechanism and improve the risk of infection caused by key-hole or open surgeries required for extending the implant.

The rate of failures associated with the extra-cortical plate fixation around the knee was higher in male patients compared with the female patients. The probability of survival of the implants at 150 months was 65% higher in female patients than in males. Overall, probability of survival of the implant was higher for female patients for all failure modes, however it was not significant in any of the failure categories investigated.

Aseptic loosening and failure of the extra-cortical plate fixation was more commonly associated with uncemented implants. Radiographic assessment indicated that the majority of the cases reviewed, had a stable extra-cortical plate fixation and bone remodelling that encouraged implant fixation was observed in most cases. However, no correlation between implant failure and implant fixation was found. In a study of eight joint-sparing proximal tibial endoprostheses, Spiegelberg et al. reported two complications, none of which were related to failure of extra-cortical plate fixation. In one case, the limb was amputated due to infection and in the other, the implant was revised to a knee-sacrificing implant due to patient's fall, shortly after surgery (Spiegelberg et al. 2009). Gupta et al. reported on early outcomes following distal femoral joint-sparing surgery at the mean follow-up period of 24 months. This study reported no cases of stem fracture, failure of the implant, aseptic loosening, infection, recurrence of the tumour or amputation (Gupta et al. 2006).

One of the most common complications associated with use of massive implants is infection (Kinkel et al. 2010; Orlic et al. 2006) that can have devastating outcomes for the patient (Racano et al. 2013). Deep infection is often treated by staged revision surgery and intravenous antibiotic treatment and if persistent, amputation may become inevitable (Jeys and Grimer 2009). In a retrospective review of 2174 patients who

received massive endoprostheses for tumour treatment, Henderson et al. reported 534 failures, out of which 182 (34%) failures were due to infection, making infection the primary cause of failure (Henderson et al. 2011). Similarly Hardes et al. reported a 37% infection rate in a follow-up study of patients who underwent extra articular resection of the bone around the knee (Hardes et al. 2013). The failure rate due to infection in our study was significantly lower with 4.7% at a mean follow-up of 48 months. The infection rate reported in this study (4.67%) is comparable to those found in studies of other implant types with a similar follow-up period and patient numbers. Coathup et al. studied the outcome of using distal femoral endoprostheses with a rotating hinge knee and reported a 3% infection rate (Coathup et al. 2013). Sewell et al. reported an infection rate of 5.6% for tibial reconstruction using intercalary diaphyseal endoprosthetic implants after resection of the tumour (Sewell et al. 2011).

In earlier studies, aseptic loosening of the intramedullary (IM) stem was reported as the primary cause of failure in conventional knee sacrificing implants (Unwin et al. 1996). Although design improvements, such as the introduction of a rotating hinge knee design and a hydroxyapatite ingrowth collar have reduced aseptic loosening in megaprostheses (Myers et al. 2007), aseptic loosening remains one of the most common modes of failure in intra-articular massive endoprostheses with incident rates of 2.4% to 17% (Hardes et al. 2013; Pala et al. 2013; Ahlmann et al. 2006; Kinkel et al. 2010). In this study a loosening rate of 6.67% was found, which is within the range reported for massive conventional joint sacrificing implants. This comparable failure rate also indicates that implant attachment by means of extra-cortical plates, can provide a sufficiently secure fixation that does not increase the risk of aseptic loosening of the IM stem.

Local recurrence is considered a failure of local tumour control (Rong-Sen 2005) that has been a concern over the use of joint-sparing reconstruction methods (Agarwal et al. 2010). In our group of patients, one (<1%) patient had a local recurrence and three patients (2.88%) developed metastatic diseases and died. Some studies have indicated an approximately 10% rate of local recurrence amongst bone tumour patients who were treated with conventional massive endoprosthetic replacements (Hamilton et al. 2005; Coathup et al. 2013). Other studies have reported a much higher local recurrence rate (26.14%) and developing metastasis (32.02%) (Fiorenza et al. 2002). Many factors such as aggressiveness of the tumour with wide extension and a poor response to chemotherapy may contribute in causing local recurrence (Rong-Sen 2004). However, careful preoperative planning and assessing individual patients for suitability of receiving a joint-sparing resection can decrease the incidence of local recurrence (Rong-Sen 2005).

Other complications following limb-salvage operations using megaprostheses, such as bone or wound necrosis, dislodgement and dislocation, rotational deformity and periprosthectic fractures were not found in the group of patients studied here. However, the review of the patients' notes and their post-operative radiographic images revealed other complications such as local osteolysis (3 cases), joint contracture (one case), discomfort and irritation caused by plate and screw fixation around the knee (5 cases) and implant fracture (3 cases).

Studies of other intercalary reconstruction methods for treatment of bone tumours, such as devitalized autograft and allografts report similar infection and recurrence rates to those found in this study. However, an overall higher complication rate associated with and isolated to these methods has been reported (Muscolo et al. 2008; Ogura et

al. 2015; Aponte-Tinao et al. 2014). A follow-up study of a similar number of patients to the study presented here and treated for tumours of femur, reported a 17% fracture, 22% non-union, 13% not healing at the host-donor junction and 1% fracture of the fixation implant (Aponte-Tinao et al. 2012). Agrawal et al. 2010, compared various intercalary reconstruction methods, including the use of joint-sparing implants and allografts and reported an improved complication rate and functional outcomes in patients treated with joint-sparing implants (Agarwal et al. 2010).

Radiographic assessment of the femoral implants for accuracy in implantation showed a two-fold increase in resection percentage error in failed implants when compared with that of the stable constructs. The error in alignment angle was also increased in the failed constructs in comparison with the stable femoral fixations with an approximately one degree higher error value. However, a similar trend was not found in tibial implants where the resection percentage error was six-fold higher in implants that were still *in situ* in comparison to that of the failed implants. A Spearman's Rank coefficient test did not indicate any relationship between duration of implantation and error in resection level or implant alignment. R^2=0.998 was found for failed tibial implants, when the correlation between alignment angle error and duration of implantation was assessed, however this could be due to a type two error as a results of the small number of cases assessed. Although there are no studies that have measured accuracy of implantation in joint-sparing implants, there are studies that have used radiographic analysis to assess the success of other orthopaedic reconstruction methods. Freedman and Johnson (1995) radiographically assessed mal-alignment after reconstruction of fractured tibiae following different methods that utilised intramedullary nailing (Freedman and Johnson 1995). Others have assessed stem alignment following hip replacement surgery and its correlation with patient

outcome and implant stability. The results from different studies have been mixed with some studies reporting a correlation between malalignment and success of the implant and others indicating no correlation between the two variables (Khalily and Lester 2002; Min et al. 2008). Computer aided surgery that utilises MRI and CT image, and matches patients anatomy precisely with the pre-operative surgical plans (Wong et al. 2007) can improved resection and implantation accuracy.

This study had several limitations. Firstly, there was no control group with which to make direct comparisons regarding the complications and survival rates of implant fixation using extra-cortical plates and outcomes for patients treated with these implants. Secondly, this was a retrospective and observational analysis of patients treated over a long period of time in several different centres and operated on by different surgeons. Each surgical procedure differed from one patient to another due to variations in the amount of bone and soft tissue resected. The variation could affect the durability and function of each implant. In addition, there are wide variations in patients' height, weight, age, diagnosis, type and dose of adjuvant therapies. When survival analysis was conducted, no confidence interval was calculated to assess the reliability of the results. The radiographic assessment of all cases was also not possible due to the retrospective nature of the study and unavailability of records for the majority of the patients. The radiographic measurement technique was also dependant on angulation and orientation of patients' limbs at the time of imaging and was not controlled. Although all radiographs used were pre-examined for possible rotation, minor rotation or flexion of the knee may have gone undetected. Another limitation was the subjective measurement method used. Additionally, as the images available to us were a mixture of digital and hardcopy images, use of image processing software

was not an option. However, further studies are required to identify which method could provide more accurate results as some significant results were identified.

3.7 Conclusion

In this chapter it was hypothesised that joint-sparing endoprostheses have a comparable complication and local recurrence rate similar to those of conventional, knee sacrificing megaprostheses and other joint-sparing reconstruction methods. It was also hypothesised that inaccurate implantation of joint-sparing implants increased the risk of fixation failure and the duration of implantation is reversely correlated to the implantation error value. The results of the study presented in this chapter supports the hypotheses related to the complication rate of joint-sparing implants outlined earlier. Although there are complications that are isolated to use of joint-sparing implants, the overall patient and implant complication and survival rates are not higher than those treated with intra-articular endoprostheses and are improved compared to use of allografts.

While the limitations of the study does not allow conclusions regarding the group of patients who have an improved response to treatment using joint-sparing implants, the evidence suggest that subjects under age of 21 at the time of surgery, have improved implant survival rates when compared to those over 21. While the younger group of patients respond better to extra-cortical plate fixation, a reduced survival rate after 120 months post-operation requires further investigations. The results also suggested that use of extra-cortical plates may provide a more secure fixation in femoral replacements and female patients than in tibial implants and males patients. However, a longer follow-up period and randomised, controlled studies are required to establish these findings.

Although in this study some correlation between the accuracy of implantation and longevity of fixation in failed implants was determined, a controlled investigation with higher number of cases and improved measurement techniques is required to establish whether there is a relationship between implant durability and resection levels and angle of implantation.

To conclude knee joint-sparing endoprostheses provide a reliable reconstruction method for tumour treatment in a carefully selected group of patients, whose joint can be spared while sufficient surgical margins are allowed.

Chapter 4 Assessment of Knee Proprioception and Function in Patients with Knee Sparing and Knee Sacrificing Massive Bone Tumour Implants

4.1 Introduction

4.1.1 Proprioception

Proprioception is the ability to sense the location, position and movement of the body and its parts (Felson et al. 2009). It has a crucial role in joint stability, postural and motor control (Riemann and Lephart 2002) and hence, it is essential for adequate functioning of the joint structures during day-to-day and sports activities (Safran et al. 2001). Proprioception consists of two components; kinaesthesia and joint position sense (JPS). Kinaesthesia is the awareness of joint movement and is dynamic (Grob et al. 2002) while JPS is awareness of the joint position in space. JPS is a static phenomenon (Grob et al. 2002) that is often tested by examining the accuracy of achieving a previously specified target angle (Suprak et al. 2006; Li et al. 2005). Different measurement methods test different receptor types within the joint muscles and tendons, all of which contribute to proprioception. Kinaesthesia tests Pacinian

corpuscles, which detect movement; whereas JPS tests the Ruffini end organ-like receptors and Golgi tendon organ-like receptors as these provide information regarding the relative position of muscles and joints (Grob et al. 2002).

The knee joint has a wide range of movements, and therefore an appropriate neuroanatomical organization is critical for knee stability and control of its movements. In a recent study, the four main ligaments in the knee, the anterior cruciate ligament (ACL), posterior cruciate ligament (PCL), medial collateral ligament (MCL) and the lateral collateral ligament (LCL) and four tendons, the semitendinosus, gracilis, popliteal, and patellar were harvested from eight fresh frozen cadavers to identify the mechanosensors in the knee. The study found that the mechanoreceptors were usually located close to the bone insertion (Çabuk and Kuşku Çabuk 2016). Free nerve endings followed by Ruffini endings were the most common mechanoreceptors and no Pacini corpuscles were observed. Free nerve endings and Golgi-like endings were most frequent in the PCL and Ruffini endings in the popliteal tendon. The cruciate ligaments had more mechanoreceptors than patellar tendon (Çabuk and Kuşku Çabuk 2016). It is therefore not surprising that proprioception of ACL-injured knees was decreased compared with contralateral intact knees, as determined by both joint movement (kinaesthesia) and joint position(Kim et al. 2016). Proprioception after conventional knee replacement is also compromised and is worse in designs that resect both the ACL and the PCL (Warren et al. 1993).

Treatment of intra-articular bone tumours around the knee by reconstruction of the affected area with conventional massive endoprostheses requires extensive removal of the soft tissues in and around the joint. These include the ligaments, menisci, surrounding muscles and often large sections of the affected bone due to invasion of

the tumour (Stauffer and Ehrlich 1995). Therefore, it is expected that proprioception of the operated knee joint will deteriorate postoperatively (Li et al. 2005) and its alteration can result in poor functional joint stability (Godinho et al. 2014). Additionally, the design of massive intra-articular implants and absence of sufficient soft tissue surrounding the knee joint may reduce the range of motion (ROM) of the knee joint (Yu et al. 2010).

In comparison to a joint sacrificing implant surgical insertion of a knee sparing endoprosthesis can result in retention of the co-lateral ligaments, ACL, PCL, menisci and joint capsule. This may help to retain sensorimotor functions and the functional outcome (Swanik et al. 2004). By preserving the knee, joint-sparing implants may also maintain the pre-operative ROM. In this chapter proprioception and knee ROM in patients with knee joint-sparing implants were compared to healthy subjects and those with conventional knee sacrificing implants.

4.1.2 Functional Assessment

Healthcare professionals commonly use outcome measures in the form of questionnaires to assess the impact of illness on patients (Berber et al. 2011). Standardised questionnaires that are designed to be completed by the patient, minimise any unintentional potential bias by the assessor ("The Oxford Knee Score (OKS)" 2015) and provide a common format for data collection and analysis (Berber et al. 2011).

There are several different functional score assessments available. In orthopaedics, specific measures exist for different anatomical sites and there are specific questionnaires for functional assessment of tumour patients. In this chapter, three

different questionnaires were used to assess patients' function and emotional acceptance in different implant groups and the results were compared.

4.2 Objectives

The aim of this chapter was to investigate proprioception and passive ROM in patients with knee sparing and sacrificing implants and compare their results with healthy subjects. This chapter also aimed to assess and compare functional outcome and patient acceptance in knee joint-sparing patients and conventional joint sacrificing patients, using functional scores.

4.3 Hypothesis

In this chapter, it was hypothesised that:

- Subjects with knee joint-sparing endoprostheses have closer to normal proprioception of the operated knee compare to those with conventional, knee sacrificing implants.
- Knee proprioception in the operated leg is similar to the non-operated leg in patients with knee joint-sparing implants.
- When assessing patients' function using functional scoring systems and health questionnaires, patients with knee sparing endoprostheses produce higher scores compared to those with conventional knee sacrificing implants.
- Passive knee ROM is improved in knee sparing patients compared to knee sacrificing patients.

4.4 Method

4.4.1 Proprioception; Joint Position Sense

The relevant Health Research Authority approval was obtained for this investigation (Reference: 12/LO/0178; Title: "Comparative Study of Gait Analysis and Difference in Balance and Proprioception of the Knee Joint in Patients Having Knee-sparing Prosthesis Against Patients Having Distal Femur or Proximal Tibia Salvaging Procedure").

Twenty oncology patients (10 female, 10 male) at a mean follow-up of 38 months (18 to 84 months) participated. Six patients with a joint sacrificing proximal tibial replacement (PTR), 5 with a joint sacrificing distal femoral replacement (DFR), 4 joint-sparing proximal tibial replacements (JST) and 5 joint-sparing femoral replacements (JSF) were investigated. Ten healthy subjects (7 female, 3 male), with no history of musculoskeletal disease or complications also participated. None of the patients reported any complications with their endoprostheses or any pain in either of their legs at the time of examination and none of the patients had undergone a partial or complete revision surgery.

The subjects were seated in a raised chair, with the seat set at an angle of 15° and the back of the chair set at 105° from the seat of the chair. The depth and height of the chair was adjustable to accommodate for height difference in subjects and to allow for ease of knee movement. The angle of the shank was measured in relation to the horizontal plane using a Delsys EMGworks Trigno Wireless System Accelerometer (Delsys, Boston, USA) which measures acceleration in three planes (x and y axes – in relation to the horizontal, z axis – in relation to gravity). The data was collected and analysed using Delsys EMGworks Acquisition and Analysis software. The knee joint

angle, when at resting position, was measured for each patient and used as the baseline for individual's measurements. The resting position was approximately 90° of knee flexion when the leg was in a 'dangling' position and perpendicular to the horizontal plane. Subjects were blindfolded for the duration of the test and were asked to remove their shoes. The accelerometer was attached to the lateral aspect of the lower shank, using double-sided sticky tape, just above the lateral malleolus, with the x-axis of the accelerometer in line with the tibia. In order to achieve more accurate and reproducible results, active joint movement was measured. Knee proprioceptive acuity was quantified and measured as the error in repositioning of the shank in relation to a previously determined reference angle. Each subject was asked to extend their knee to a set angle decided by the operator. Subjects were asked to hold their leg at the operator-determined angle for approximately 5 seconds and remember the position. Subjects were then asked to move their leg back to the resting position and hold for another 5 seconds. The subjects were then asked to actively repeat the same position, by extending their knee and holding for another 5s. Each set consisted of 6 repetitions; 2 repetition of small angles (approx. 0-20°), 2 medium angles (approx. 25-45°) and 2 large angles (over 45°), from the resting position in a random order. The test was carried out for both the operated and non-operated legs in both implant groups and both left and right legs for healthy subjects. The author carried out all the tests for all the subjects.

4.4.2 Static Measurements; Knee Passive Range of Motion

The same patients who participated in the joint position sense test, were examined for passive ROM of the knee.

During this examination, all patients were asked to lie on a horizontal bed and the measurements were taken using a standard goniometer by a trained physiotherapist. The same person carried out all measurements for all patients. To measure the knee passive ROM, the upper arm of the goniometer was placed along the femur towards the greater trochanter, towards the back of the thigh. The lower arm of the goniometer pointed towards the outer ankle bone and the bottom of the fibula. Two measurements were taken; one with the knee fully extended and one with the knee flexed as much as possible. One set of measurement was taken for each limb of each patient and was recorded.

4.4.3 Functional Assessment

Patients' function was evaluated using 3 different established functional score assessments:

1. The Musculoskeletal Tumour Society scoring system for limb salvage (MSTS), evaluates the functional impairment following tumour treatments (Tunn et al. 2008). The questionnaire includes six scales evaluating pain, function, emotional acceptance, use of supports, walking ability and gait cosmetics with maximum score of 30 (Enneking 1986). Numerical values from 0 to 5 points are assigned to each of the categories, with 0 being the worst and 5 being the best score. These values were added and the functional score was presented as a percentage of the maximum possible score.
2. The revised Oxford Knee Score (OKS) is a patient self-completion questionnaire containing 12 questions on activities of daily living. Each question was assigned a numerical value of 0 to 4, with 0 indicating the poorest and 4 the best function. A maximum score of 48 could be obtained. The OKS

was developed and validated specifically to assess function and pain after total knee arthroplasty and covers pain, function and walking ability ("The Oxford Knee Score (OKS)" 2015).

3. SF-36 (Short Form Health Survey) was developed in 1990 and is a multipurpose health survey with 36 questions (Berber et al. 2011). It provides an 8-scale functional health profile of both physical and mental health outcomes. The form can have various uses including a population survey, assessing the burden of disease, and determining the benefits produced by treatment ("The SF Community - SF-36® Health Survey Update" 2015).

In all three questionnaires, higher scores represented a more improved function. Questionnaires were completed for each patient, either in person or over the telephone. Twenty two oncology patients at a mean follow-up of 63 months (18 to 94 months) participated: 6 patients with a PTR (5 female, 1 male), 5 with a DFR (2 female, 1 male), 5 JST (5 female, 1 male) and 5 JSF (5 male). The scores were calculated using the scoring instruction for each of the questionnaires.

6.1.1 Statistics

The Spearman's Rank coefficient was used to assess the correlation between pairs of continuous variables.

Mann Whitney-U test was used to assess the statistical significance of the results. A p value < 0.05 was considered significant in all tests (version 22.0; IBM SPSS statistics, Chicago, Illinois).

4.5 Results

4.5.1 Proprioception; Joint Position Sense

For each subject the absolute error value in repositioning of the knee for each take was measured and the mean absolute error was calculated for each patient, for both the operated and non-operated legs. JPS for each patient was normalised against the non-operated leg of the patient, resulting in one single value for each patient, called normalised error. In each implant group, the mean error was calculated for the operated and non-operated legs. The variables calculated were the absolute error, the mean absolute error for each leg for each subject, the normalised error, group mean error and standard error for each group.

The group mean error for the operated and non-operated leg for the joint-sparing and sacrificing distal femoral and proximal tibial replacements and the control group are summarised in Figure 4.1. Since there was no significant difference in the mean absolute error values of the left and right legs in the healthy subjects, their results are represented as one set of data.

The JSF group had the largest normalised error while the DFR group exhibited the smallest normalised error amongst the four implant groups. The PTR group had an improved normalised error compared with the JST group. The mean normalised error for the knee sparing proximal tibial implants was 2.11 ± 0.63° and 2.38 ± 0.65° in the knee sparing distal femoral group. The mean normalised error value for the PTRs and DFRs was 1.11 ± 0.39° and 0.82 ± 0.37°, respectively.

The mean absolute error was greatest in the operated leg of the JST group, while the DFRs exhibited an almost identical mean absolute error in both legs and had the

smallest error value when compared with all other four groups examined. The non-operated leg in the JST group and the operated leg in the PTR group presented similar mean errors when compared with the control group. Both the operated and the non-operated legs in the DFR group had improved error values when compared with the control group. When the mean absolute error in the operated leg was compared with the non-operated leg for each group, no significant difference was found. No significant difference was found when normalised error in the knee sparing groups was compared to patients with knee sacrificing implants in the same anatomical location. No significant difference was found when the normalised error in both knee joint-sparing proximal tibial and knee sacrificing PTR groups were compared with the control group. There was also no significant difference in normalised error when both knee sparing distal femoral group and the knee sacrificing DFR group were compared with the control group.

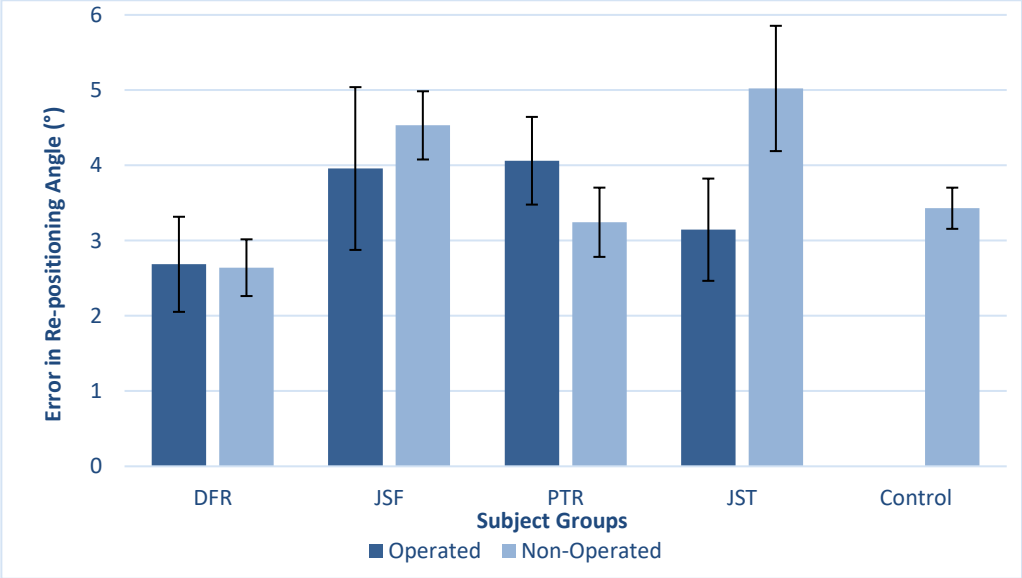

Figure 4.1 Mean absolute error values for the operated and non-operated legs in the DFR, JSF, PTR and JST groups. The mean absolute error in the control group is also provided. Proprioception in the operated legs was the worst in the PTR group; this could be due to removal of the tibial tuberosity that can lead to a poor extensor mechanism.

Data was combined into 2 implant types; joint-sparing and joint sacrificing, regardless of the anatomical location (Figure 4.2). When the mean absolute error in the operated leg was compared to the non-operated leg, no significant difference was found in either of the two groups. A significant difference in mean normalised error was found when the joint-sparing patients (2.24 ± 0.43°) were compared with the knee sacrificing conventional patients (0.98 ± 0.43°; p =0.022). The normalised mean error measured in joint-sparing implants was also significantly different when compared with the control group (p=0.041). There was no significant difference between knee sacrificing implant group and the control group.

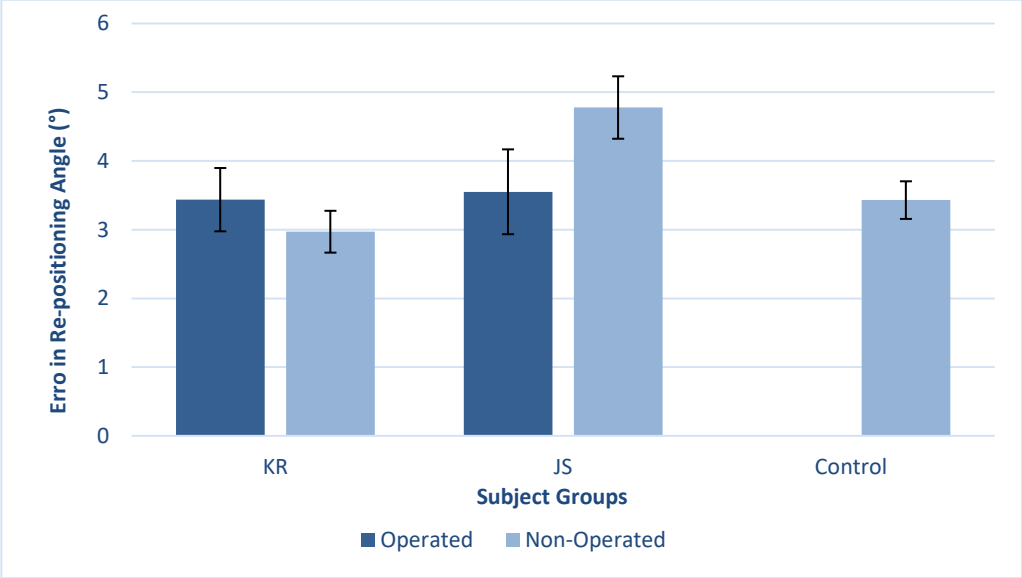

Figure 4.2 Mean absolute error in the operated and non-operated legs, in joint-sparing and conventional joint sacrificing implants. The mean absolute error in the control group was 3.43 ± 0.27° .

A Spearman's Rank coefficient parameter was used to assess the relationship between the mean absolute error in the operated and non-operated leg in each implant group. The R^2 value obtained for each group is provided in Table 4.1. No correlation was found between the mean absolute error in the operated and non-operated legs in any

of the implant groups. The predetermined angle and the repositioned angle were directly related in both the operated and non-operated legs in all the groups ($R^2 > 0.85$). However, there was no significant difference between the two legs in any of the groups and no differences were found between the groups of the same anatomical locations.

Table 4.1 R^2 values in each group; no correlation was found in the error value in repositioning of the joint in the operated and non-operated legs

Type of EPR	Distal Femoral Replacements	Joint-Sparing Femoral implants	Proximal Tibial Replacements	Joint-Sparing Tibial implants
R^2	0.247	0.148	0.288	0.218

4.5.2 Knee Passive Range of Motion

The mean flexion angle in the operated leg in patients with a DFR was 110° (range: 50-145°) and in patients with a JSF implant was 125° (range: 120-135°). The mean knee flexion angle in the non-operated leg in both groups was 137° (DFR range: 120-155°, JSF range: 130-140°). The mean knee flexion angle in patients with a PTR was 103° (range: 60-135°) and the JST group was mean 137° (range: 130-140°). Mean knee flexion angle in the non-operated leg in the PTR group was 142° (range: 135-150°). However, in patients with a joint-sparing tibial replacement the operated leg had a similar ROM to the non-operated leg. All patients were able to achieve full knee extension. Five degrees of hyperextension of the operated knee was noted in one patient with a JST implant. Another two patients with a JSF implant presented 10 degrees of hyperextension of the operated knee.

Passive knee ROM in the operated and the non-operated legs were compared in each group. The knee flexion angle in the operated leg was decreased when compared with the non-operated leg in patients with a knee sacrificing proximal tibial replacement

(p=0.005). The passive knee ROM between the operated and non-operated legs was not significant in other implant groups.

The difference in passive ROM in the operated and the non-operated legs was calculated for each patient and the mean value for each implant group was determined (Figure 4.3). Results for each of the joint-sparing proximal tibial and distal femoral groups were compared with the PTR and DFR groups, respectively. A significant decrease in ROM was measured when the PTRs were compared with the joint-sparing tibial group (p= 0.037). No significant difference was found when the joint sacrificing femoral implants were compared with the JSF group.

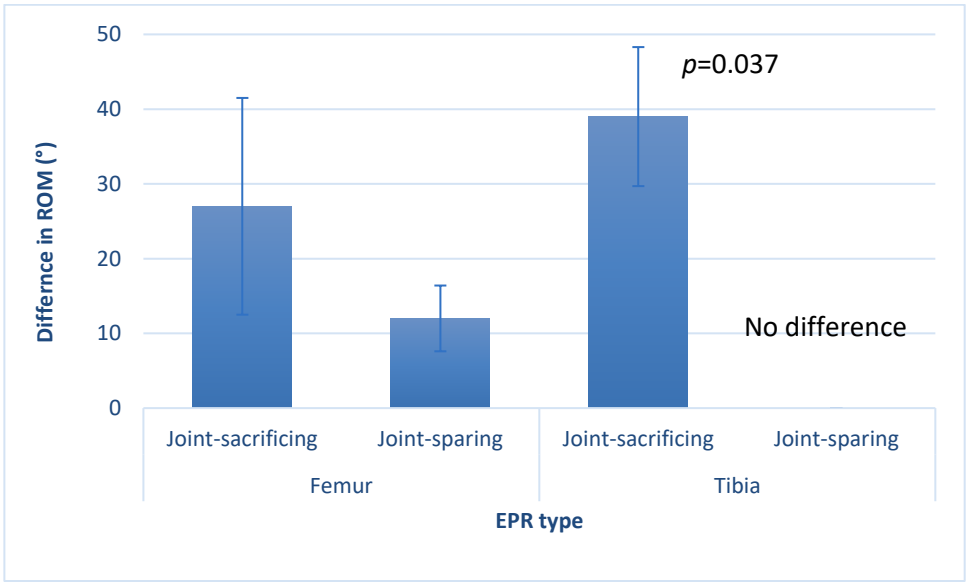

Figure 4.3 Mean difference in knee flexion angle between the operated and the non-operated legs for the DFR, JSF, PTR and JST groups. There was no difference in knee ROM in the operated and non-operated legs in the JST group.

6.1.2 Functional Assessment Questionnaires

The mean functional scores obtained for the Oxford Knee Score (OKS), MSTS and SF-36 in all four implant groups are summarised in Figure 4.4 and Figure 4.5. The results are normalised against the maximum score values of each questionnaire in the form of a percentage. With the exception of the JST group scoring lower than the PTRs in the physical part of the SF-36 questions, both the proximal tibia and distal femoral knee joint-sparing implants scored higher than their corresponding joint sacrificing groups in all four questionnaires.

The mean MSTS score for the JST group was 24.33 ± 2.80 (out of 30) and in the PTR group was 20.17 ± 2.02 (out of 30), the lowest MSTS score. The joint-sparing distal femoral group had the highest MSTS score (26.60 ± 1.75), when compared with the other three implant groups, and their score was 24% higher than the DFRs (20.50 ± 2.11). The mean OK score for the JST group was 40.50 ± 2.79 (out of 48) and in the PTR this score was 36.17 ± 4.31. The JSF group had the highest OK score (42.60 ± 2.77) when compared with the other three patient groups; 26% higher than the DFR group (33.80 ± 2.10), which had the lowest score amongst all four implant groups. The mean Short Form Health Survey Score (SF-36 M) for mental acceptance in the joint-sparing femoral and the DFR groups was 54.50 ± 2.5% and 55.26 ± 1.86%, respectively. The mean score for the joint-sparing proximal tibial replacements was 60.77 ± 2.72%, the highest of all groups, and for the conventional proximal tibial replacements was 52.42 ± 3.42%, the lowest score amongst all implant groups. The mean SF-36 for physical functioning was lower in patients with a joint-sparing tibial implant (45.32 ± 4.83%) when compared with the knee sacrificing proximal tibial

implants (49.13 ± 5.14%). No significant difference was found when the results of joint-sparing groups and the conventional joint sacrificing groups were compared.

The mean score for the joint-sparing and the joint sacrificing groups, regardless of their anatomical location, are summarised in Table 4.2. A significant difference in results of Musculoskeletal Tumour Society Score (MSTS) was found when the two groups were compared (p=0.012). There were no other significant differences when the results of other questionnaires were compared. Overall the functional outcome results were reliable and consistent as the highest and the lowest scores belonged to the same patients in all questionnaires, consistently.

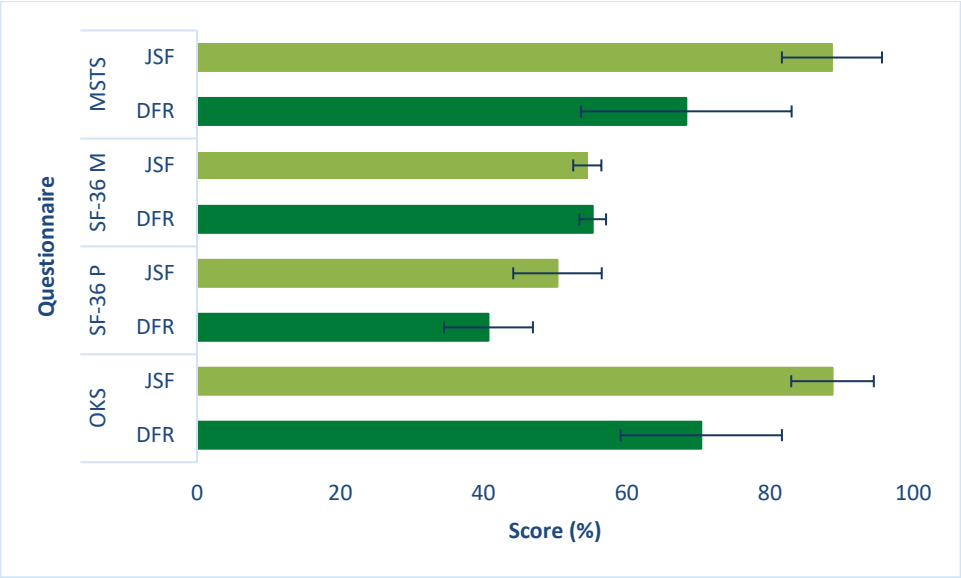

Figure 4.4 Patient functional outcome assessment results using Oxford Knee Score (OKS), SF-36 physical (SF-36 P), SF-36 mental acceptance (SF-36 M) and MSTS for the joint-sparing femoral group (light green) and the conventional joint sacrificing DFRs (dark green). The maximum achievable score for OKS and MSTS are 48 and 30, respectivly.

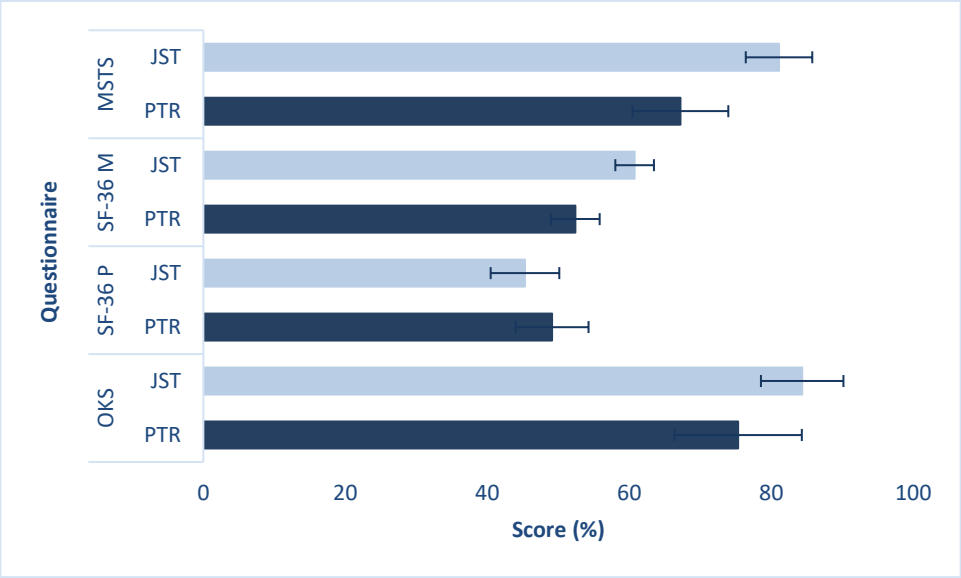

Figure 4.5 Patient functional outcome assessment results using Oxford Knee Score (OKS), SF-36 Physical (SF-36 P), SF-36 Mental acceptance (SF-36 M) and MSTS for the JST (light blue) and the PTR (dark blue) groups. The maximum achievable score for OKS and MSTS are 48 and 30, respectivly.

Table 4.2 Mean scores for Oxford Knee Score (OKS), SF-36 and Musculoskeletal Tumour Society Functional Assessments for the knee joint-sparing and conventional knee sacrificing implant groups.

Functional Assessment Type	OKS	SF-36 (Physical)	SF-36 (Mental)	MSTS
Joint-sparing	41.45 ± 1.90	47.60 ± 2.95	57.92 ± 2.04	25.36 ± 1.11
Joint sacrificing	35.09 ± 3.24	45.30 ± 4.00	53.71 ± 2.00	20.30 ± 1.40

4.6 Discussion

This is the first study that has investigated the proprioception in knee joint-sparing endoprostheses. To my knowledge there is one other study that has investigated knee proprioception as an outcome in patients following limb-salvage bone tumour surgery and insertion of a massive endoprosthesis. The study investigated passive and active repositioning of the knee joint to an angle previously determined (Li et al. 2005). Similar to the study by Li et al. (2005) a non-weight bearing JPS test protocol was used in this chapter. Studies have suggested that weight bearing tests involve more receptors than non-weight bearing tests (Stillman and McMeeken 2001; Garsden and Bullock-Saxton 1999) and can be confounded by the subject's muscle strength and balance (Knoop et al. 2011). Li et al. (2005) reported an absolute error in active repositioning of 2.7 ± 2.1° in the operated knee, and 3.0 ± 1.9° in the contralateral non-operated knee. The mean repositioning error in the control group was 3.2 ± 2.1°. Results presented in this chapter were similar to those reported by Li et al; the mean absolute error value in the operated limb was 3.44 ± 0.46° and in the non-operated leg was 2.97 ± 0.30° in the conventional knee sacrificing group. These values were 3.55 ± 0.62° in the operated and 4.78 ± 0.45° in the non-operated legs in the joint-sparing group and 3.43 ± 0.27° in the control group. However, other studies have reported smaller than one degree error in repositioning of the knee in healthy subjects (Lokhande et al. 2013). In this study it was found that the mean absolute error was higher in the non-operated

leg when compared with the operated leg in joint-sparing patients. Although Li et al. explained the improved proprioception in the operated knee compared with the non-operated knee by a compensatory proprioceptive mechanism, this was not observed in the knee sacrificing group in this study. Other studies have investigated proprioception of the knee joint following tear or damage to knee ligaments that cause alteration in function of the joint using both JPS and threshold detection level methods (Pap et al. 2000, 1999; Lokhande et al. 2013; Godinho et al. 2014; Dhillon et al. 2011). Knee proprioception in total knee arthroplasty (TKA) patients was reported between 4.33° ± 1.52° in designs that preserve the posterior cruciate ligament (PCL) and 4.38° ± 1.39° in implants that do not preserve the ligament, with no significant differences (Lattanzio 1998). Other studies that have compared the knee with injured ligaments with the contralateral intact knee, have found significant differences in proprioception (Godinho et al. 2014). Proprioception in patient groups I investigated in this chapter was improved considering the extent of impairment to the knee joint and the surrounding tissue in sarcoma patients in comparison with the patients undergoing TKA.

Reliability and repeatability of several frequently used methods to quantify proprioception was investigated by Grob et al. (2000). Three commonly used JPS tests: a passive reproduction test, a relative reproduction test and a visual estimation test were investigated and compared for ability to detect passive movement (kinaesthesia) (Grob et al. 2002). However, there was no correlation between the tests for kinaesthesia and JPS or between the different JPS tests. The authors concluded that a subject with a given result in one test may not obtain a similar result in another test for proprioception and proprioceptive ability cannot be inferred from independent tests. Instead, proprioception can be used in combination with other functional tests to

establish patients' ability. Overall, in this study proprioception was more impaired in joint-sparing endoprosthetic groups when compared with the joint sacrificing patients. Other proprioceptive tests are required to confirm this finding and other methods must be employed to assess function. Patients' post-surgery rehabilitation plan, level of activity prior to and post- surgery can be factors that can influence proprioception. Grob et al indicated that different measurement methods, test different receptor types within the joint muscles and tendons, all of which contribute to proprioception (Grob et al. 2002). In sarcoma patients, due to variation in type, size and spread of the tumour, variable amounts of bone and soft tissue is resected in different patients. Therefore a particular test method may be testing the receptors in one patient that have been removed in another. Further study protocols should group patients not only based on the anatomical location and implant group but also based on the amount of soft tissue and bone resected.

The passive range of motion was significantly reduced in the PTR group when compared with the joint-sparing proximal tibial group. This decrease could be associated with the lack of the extensor mechanism that was retained in the JST group and resulted in a reduced flexion/extension power. Other factors such as the extent of the scar tissue or the design of the implant could be contributing factors too. Despite the limited ROM in the operated knee in conventional joint sacrificing implants when compared with the joint-sparing implants of both sites, proprioception in the operated leg was improved in the joint sacrificing group. Li et al indicated that there was a tendency for the group with a smaller range of motion to have better proprioception that could be caused by improved sensory feedback from the stretched tissue surrounding the stiff joint (Li et al. 2005). Further testing and data analysis maybe required to confirm this hypothesis.

In this study overall, the joint-sparing tibial and femoral patients had improved functional outcomes when compared with the conventional implants. The mean Oxford Knee score for joint-sparing tibial replacements was 40.50 ± 2.79 points, and the mean MSTS score was 81.0 ± 1.4%. Spiegelberg et al. investigated the early results of joint-sparing proximal tibial replacements for primary bone tumours and reported similar results to those reported in this chapter; mean OK score of 40 points (36 to 46) and mean Musculoskeletal Tumour Society score of 79% (57% to 90%) (Spiegelberg et al. 2009). Gupta et al., in a follow-up study of knee sparing distal femoral endoprostheses in patients with malignant bone tumours, reported an MSTS score of 80% (57% to 96.7%) (Gupta et al. 2006). The mean MSTS score in joint-sparing femoral replacements in this study was 88.7 ± 2.7%. The improved scores in patients in this study could be a result of the longer follow-up time (mean: 38 month) and a more stable construct compared with the 24 months follow-up in the study by Gupta et al. (2006). In this chapter results demonstrated a mean MSTS score of 20.30 ± 1.40 (67.5%) for patients with joint-sacrificing femoral and tibial replacements. Hardes et al reported a similar MSTS score of 23 (76%) following an endoprosthetic replacement after extra-articular resection of bone and soft-tissue tumours around the knee (Hardes et al. 2013). Similar studies also reported mean MSTS scores of 70 to 89%, with scores ranging from 20% to 100% (Park et al. 2007; Asavamongkolkul et al. 2007; Ilyas et al. 2001; Tunn et al. 2008). Results obtained in this chapter are therefore comparable to those reported in the literature.

The Oxford Knee Score is not commonly used in functional assessment of patients who undergo limb salvage operation following a tumour resection. In a study by Roberts et al., a mean OK score of 42.0 was reported following total knee replacement at five years (Roberts et al. 2015). The mean OK score in the PTR group was 36.17 ±

4.31 and in the DFR group was 33.80 ± 2.10. The lower scores found in the DFR and PTR groups in this chapter may be a result of extensive soft tissue and bone resection that is involved in limb salvage surgery in comparison with a TKA. However, the mean OK score in joint-sparing tibial (40.50 ± 2.79) and femoral (42.60± 2.77) replacements are similar to that reported by Roberts et al. (2015) and approximately 12% and 26% higher than the joint sacrificing endoprosthetic group of the same anatomical location in this study.

Nguyen et al. used SF-36 to assess quality of life in oncology patients who underwent limb reconstruction of the lower limb and compared the results to those with primary and revision total knee replacements. The mean mental component score was 56.6 ± 0.8 and the mean physical component score was 41.2 ± 25.2 at more than three years post-operation (Nguyen et al. 2011). In this chapter scores for the conventional joint sacrificing implants were 53.7 ± 2.0 and 45.3 ± 4.0 and for joint-sparing implants were 57.92 ± 2.04 and 47.60 ± 2.95, respectively. Although overall improved scores were noted for the joint-sparing implants, when compared with the conventional implants in this study and with the study by Nguyen et al., the mental component score of the joint-sparing femoral replacements was lower than the DFRs. These differences, particularly in the mental component of the scores, may be due to the subjective nature of these questionnaires. While the functional scores are commonly used, their results must be analysed and combined with more objective methods to determine function. The treatment regime, such as the type and length of chemotherapy received by the patients may have affected the mental well-being of the patients. Additionally, patients who had received a joint-sparing implant were aware that there was an option for a joint sacrificing implant and this may have led to bias.

This study had various limitations. Small number of patients was one of the main limitations. A sample size calculations indicated that an *n* number of 21, for each group is required to achieve a power of 0.80. The retrospective nature of the study was another limitation and therefore patients could not be assessed at the same follow-up time. A study that investigated patterns of quality of life improvement following an oncologic reconstruction of the lower limb, showed variable average SF-36 scores at different points of the follow up for the same group of patients (Nguyen et al. 2011). Inability to match the patients across groups by age, possible comorbidities, resection levels and time from surgery was another restriction of the study. This is difficult to correct due to the inherent differences in oncologic patients. Additionally there are limited numbers of patients who have received or are suitable to receive a joint-sparing endoprosthesis. The surgical procedure for the patients in this study was carried out by different surgeons; inconsistency in the surgical technique is an additional variable. Time from surgery can affect proprioception and function; a study has suggested that function improves over time (de Visser et al. 2003). A limitation of the proprioception test was that gravity was not eliminated; in future studies weight of the patients' limb could be accounted for. Variability of the results obtained from different proprioception tests indicated that more than one proprioception test could be carried out for a more reliable conclusion (Grob et al. 2002).

4.7 Conclusion

The results presented in this chapter did not confirm the hypothesis that the knee proprioception is improved following insertion of a joint-sparing implant when compared with a conventional knee sacrificing implant. The results also did not confirm that proprioception is closer to that of healthy subjects in patients with a joint-sparing implant. The initial hypothesis that knee proprioception in the operated leg is

similar to the non-operated leg in patients with a knee joint-sparing implant was rejected. Overall, this study showed that proprioception in patients with a proximal tibial replacement, both joint-sparing and sacrificing, is worse when compared with patients with a femoral endoprosthesis. Further studies that investigate proprioception with increased number of patients and other analysis methods, such as balance assessment may be required to establish effects of different implant types on proprioception.

The hypothesis regarding the improved patient outcome and ROM in joint-sparing implants was confirmed. Improvement in functional outcome and passive knee ROM was observed in patients whose limb was reconstructed using knee joint-sparing endoprostheses following tumour resection. Improved knee range of motion in joint-sparing implants may be a possible contributing factor in better functional scores. More detailed investigation with larger numbers of patients is required to assess if there is a correlation between ROM and functional scores. In order to assess and compare function in joint-sparing and joint sacrificing patients, more objective methods such as computerised gait analysis is required.

Chapter 5 Functional Assessment of Patients Following Knee Sparing and Knee Sacrificing Bone Tumour Surgery: an Investigation into Gait Kinematics, Symmetry and Ground Reaction Force

5.1 Introduction

Limb salvage surgery is an invasive procedure that involves the removal of large sections of soft tissue and bone resulting in extended wounds and deep scars (Oren et al. 2004). During this procedure tissues such as muscles, bone, joint surfaces, skin, nerves, vessels and the lymphatic system can be damaged (Oren et al. 2004). Musculoskeletal damage following surgery leads to the sudden and irreversible disruption of gait and in all cases, the body must adapt to the change caused by mass and muscle power asymmetry (de Visser et al. 2003). For example, during a distal femoral replacement (DFR) surgery, often a part or all of the quadriceps are removed. In patients where there is extensive tissue loss, a hinged, fully constrained knee design is used to provide mechanical stability of the limb (Benedetti et al. 2000). Although satisfactory functional results have been reported following tumour resection and the consequent reconstruction of the distal femur using these implants (Capanna et al. 2015; Coathup et al. 2013; Hardes et al. 2013; Orlic et al. 2006), the extensor power

at the knee joint can be substantially decreased when more than two heads of the quadriceps are resected (Capanna et al. 1991). In an experimental study based on a mathematical model, van Krieken et al. (1985) concluded that partial excision of the quadriceps allowed normal gait, whereas complete excision and prosthetic instability resulted in major changes in gait pattern and high joint loads (van Krieken et al. 1985). A study by Benedetti et al. showed that patients who underwent excision of the vastus lateralis and vastus intermedius have a gait pattern that is closer to normal and preservation of the vastus medialis seems to enhance motor control of the knee (Benedetti et al. 2000). In proximal tibial replacements, removal of the tibial tuberosity and inappropriate attachment of the patellar tendon can result in lack of an extensor mechanism which can lead to altered biomechanics of the knee and patient's gait (Oddy et al. 2005).

While questionnaire based functional scores do not provide an objective assessment of limb function in patients (Jang et al. 2012), high performance measuring instruments have enabled accurate kinetic and kinematic gait measurements (Lemoyne et al. 2008). Gait symmetry analysis is a common protocol that is used to evaluate lower limb function (Patterson et al. 2010a; Lythgo et al. 2011; Kim and Eng 2003). Most of these studies focused only on the terminal symmetry of the lower limb during gait motion; however, did not provide detailed information about motions of the whole leg (Lythgo, et al. 2009; Lugade et al. 2010; Patterson et al. 2010b). For a better understanding of changes in kinetics and kinematics of gait and accurate analysis of mutual symmetry of the left and right leg during gait motion, measurement of motion of both legs including the pelvis, hip, knee, and ankle is required (Astephen et al. 2008; Jang et al. 2012). For this reason, in this thesis, the hip and ankle joints, as well as the knee joint were assessed.

While the results of the questionnaire based functional outcome study discussed in Chapter 4 suggested an improved function in the joint-sparing group of patients, patients with conventional knee sacrificing endoprostheses presented an improved proprioception, in terms of joint position sense when compared to patients with a joint-sparing implant. The reason for this is unclear especially when a knee joint replacement associated with a distal femur or a proximal tibia resects all of the knee ligaments, which in the normal knee joint have been shown to provide a proprioception function. Hence a more objective and quantifiable method is required to further investigate the functional outcome of patients following joint-sparing surgery. In this chapter, the mean joint angle and joint symmetry in 8 phases of the gait cycle in three spatial planes, vertical ground reaction force, time in stance and leg length discrepancy in both legs were measured and compared to healthy controls. Increased length of the operated leg has been reported in patients following routine joint replacement surgeries (Perttunen et al. 2004; Lang et al. 2012; Clark et al. 2006) and has been associated with complications such as nerve palsy, lower back pain, and abnormal gait (Clark et al. 2006). It has been demonstrated that mechanical load and isometric torque placed on the longer limb are significantly greater than that of the shorter limb (Gurney 2002). However, there are no studies that have investigated the occurrence of leg length discrepancy following limb salvage surgery and its possible complications.

5.1.1 Kinematics of Normal Gait and the Critical Joint Angles

5.1.1.1 Hip Motion

5.1.1.1.1 Flexion and Extension in Sagittal Plane

At heel strike, the hip is flexed at approximately 25 to 30 degrees in healthy subjects. The hip remains in flexion throughout stance while it steadily extends towards the

neutral position and continues its extension to a position of approximately 10° until Pre-swing (PS). The direction of the movement is then reversed and hip flexion continues during Mid-swing (MSW). During Terminal Swing (TSW), the hip extends to a position of about 30^0 in flexion (Figure 5.1) (Koerner, University of Alberta, and Health Sciences Audiovisual Education 1984).

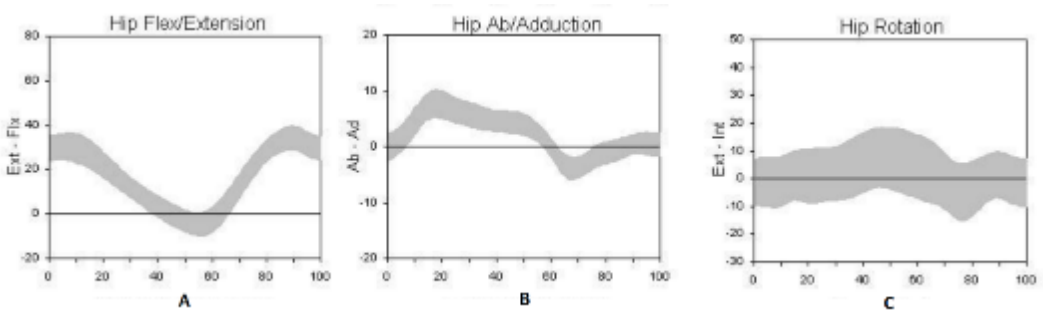

Figure 5.1Trajectory of hip joint angle in [A] sagittal, [B] coronal and [C] horizontal planes in normal adults (http://www.clinicalgaitanalysis.com/data/, accessed on 21 November 2016).

5.1.1.1.2 Internal and External Rotation in Horizontal Plane

The hip rotates ±8° from neutral in a monotonic fashion and peak internal rotation occurs during PS. Peak external rotation occurs at the end of Loading Response (LR) where the hip begins to internally rotate and continues to do so until PS. It then begins to externally rotate until the LR of the contralateral leg (Rancho Los Amigos National Rehabilitation Center 2001).

5.1.1.1.3 Adduction and Abduction in Coronal Plane

During LR, the hip adducts under the control of the gluteus medius and minimus. During mid-stance, the hip begins to abduct until it returns to a neutral position and becomes level with the pelvis by the onset of terminal stance and until the onset of PS. Thereafter, the hip rapidly abducts as the limb is unloaded (Figure 5.1) (Perry 1992).

5.1.1.2 Knee motion

5.1.1.2.1 Flexion and Extension in Sagittal Plane

At initial heel contact the knee is in about 5° of flexion and continues to flex until it reaches approximately 20°. During LR the knee moves approximately 15° (mean joint angle of 10°). At mid-stance, flexion ceases and the knee extends to approximately 8° of flexion (Perry 1992). Knee extension continues at the start of terminal stance and reaches 5° of flexion, before the motion is reversed and the knee begins to flex. During this time the knee excursion is about 3° extending to 7° of flexion (mean angle of 10°). During PS the knee rapidly flexes to about 40° and continues to flex during the Initial Swing (ISW) phase to reach a peak of approximately 60° (Perry 1992). At the end of ISW the knee begins to extend until the end of Terminal Swing (TSW) where the knee reaches neutral position (zero degrees). At the end of TSW the motion is reversed and the knee begins to flex to a position of 5° (Figure 5.2) (Winter 1984).

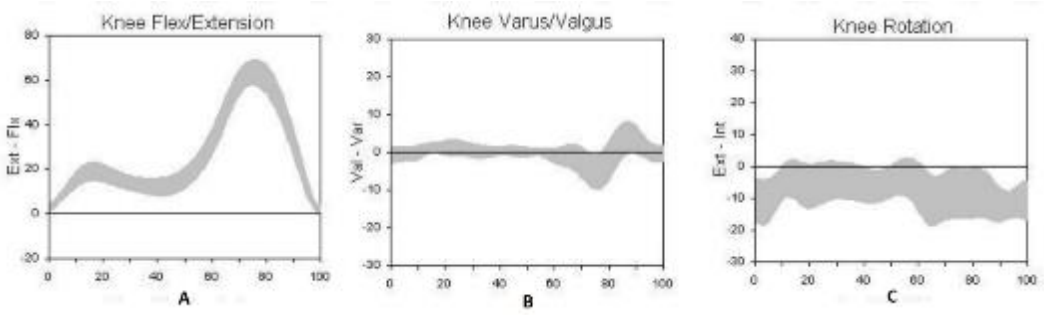

Figure 5.2 Trajectory of knee joint angle in [A] sagittal, [B] coronal and [C] horizontal planes in normal adults (http://www.clinicalgaitanalysis.com/data/, accessed on 21 November 2016).

5.1.1.2.2 Varus/Valgus in Frontal Plane and Rotation in Horizontal Plane

Changes in knee joint angle in the horizontal and coronal planes are not often discussed in the literature as determinants of gait. The trajectory of knee varus and valgus motion in the coronal plane and internal and external rotation in the horizontal plane are

presented in Figure 5.2B and Figure 5.2C, respectively. During normal gait and in the coronal plane, the knee remains close to neutral throughout stance. During ISW, valgus motion of the knee is expected and the knee moves in the varus direction throughout Mid-swing (MSW) until it reaches its peak varus position of approximately 8°. At the start of TSW, the motion is reversed and continues until it reaches a neutral position at the end of TSW. In the horizontal plane and while the direction of movement continually changes, the knee mainly remains externally rotated throughout the gait cycle (Merryweather et al. 2011).

In assessment of patients treated with massive tumour implants around the knee, the most changes in normal gait are expected to be associated with the knee kinematics.

5.1.1.3 Ankle Motion

5.1.1.3.1 Plantarflexion and Dorsiflexion in Sagittal Plane

At initial contact the ankle is in a neutral position to assist with initiation of heel contact. This position also places the ground reaction force behind the ankle creating a plantarflexion moment. During the loading response, the ankle plantar-flexes rapidly to about 8° resulting in a flat foot position, and then reverses and dorsiflexes to a neutral position at the end of the LR phase (mean of 0 degrees) (Gage et al. 1996). During mid-stance, the ankle steadily dorsiflexes to approximately 10°. This is the ankle rocker which allows progression over the weight bearing limb. During terminal stance, the heel begins to rise and the ankle continues to dorsiflex reaching a peak of about 12°. This motion then ceases and just before pre-swing the ankle begins to plantarflex to allow the heel to rise, reaching about 10° of dorsiflexion by the end of terminal stance. Raising the heel off the ground using plantarflexion provides for a more horizontal centre of gravity trajectory (Perry 1992). During PS the ankle rapidly

plantarflexes from 10° in dorsiflexion to 20° of plantarflexion as the weight is shifted onto the contralateral limb. During initial swing, the ankle begins to dorsiflex to stop the contact of the toes with the ground and dorsiflexion is completed as the ankle reaches neutral and remains neutral at MSW and TSW (Figure 5.3A) (Perry 1992).

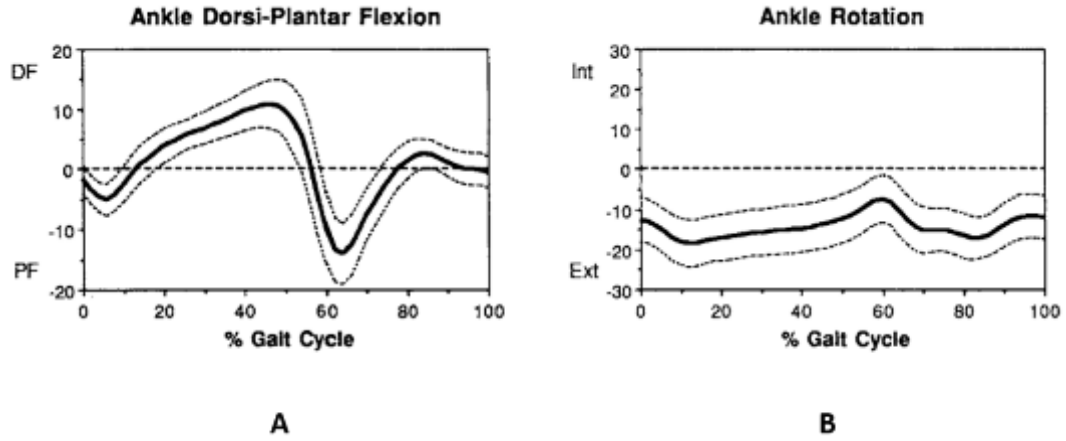

Figure 5.3 Trajectory of ankle joint angles in [A] sagittal plane and [B] horizontal plane, throughout the gait cycle. (Kadaba et al. 1990).

Throughout the gait cycle the ankle joint remains in an externally rotated position (Figure 5.3B). Following LR the ankle internally rotates until the end of PS before it starts to externally rotate. External rotation ceases at the beginning of TSW and the ankle remains relatively steady with slight internal rotation until the end of the cycle (Kadaba et al 1990).

Gait analysis requires the use of markers and the trajectories of these markers when placed on the foot segment often present problems due to their relative proximity to each other. Therefore, often only two markers are placed on the foot and this limits the measurement of ankle joint motion to flexion-extension and internal-external rotation only. The addition of a marker to measure ankle eversion and inversion has been reported to complicate the measurements collected (Kadaba et al. 1990).

5.1.2 Ground Reaction Force

The ground reaction force which acts through the foot during gait, is measured using force plates. Force plate output data provides three ground reaction force vector components; one vertical load and two shear loads acting along the force plate surface (Figure 5.4). The shear forces are resolved into anterior–posterior and medio–lateral directions (Marasovic et al. 2009). The vertical component of ground reaction force is the largest component and accounts for the acceleration of the body's centre of mass in vertical direction during walking (Tongen and Wunderlich 1994). As the heel contacts the ground, there is zero force between the foot and the floor. Immediately after heel strike, the force increases rapidly as the body begins to be supported by the foot. As the centre of mass moves downwards and decelerates, inertial force is added to gravitational force, which means that the vertical force applied to the foot exceeds body weight and peaks at approximately 107% of body weight (Winter 1991). As the gait cycle progresses and during single support, the ground reaction force becomes less than body weight as the centre of mass experiences a downwards acceleration. This gives an upwards inertial force that reduces the ground reaction force to approximately 85% body weight (Marasovic et al. 2009). In the final stage of the stance phase and at push off, a propulsive action generates forces greater than body weight and a second peak appears near the middle of gait cycle. The vertical ground reaction force reaches 105% of body weight. During toe off, the force rapidly decreases and reaches zero at the end of stance phase (Marasovic et al. 2009).

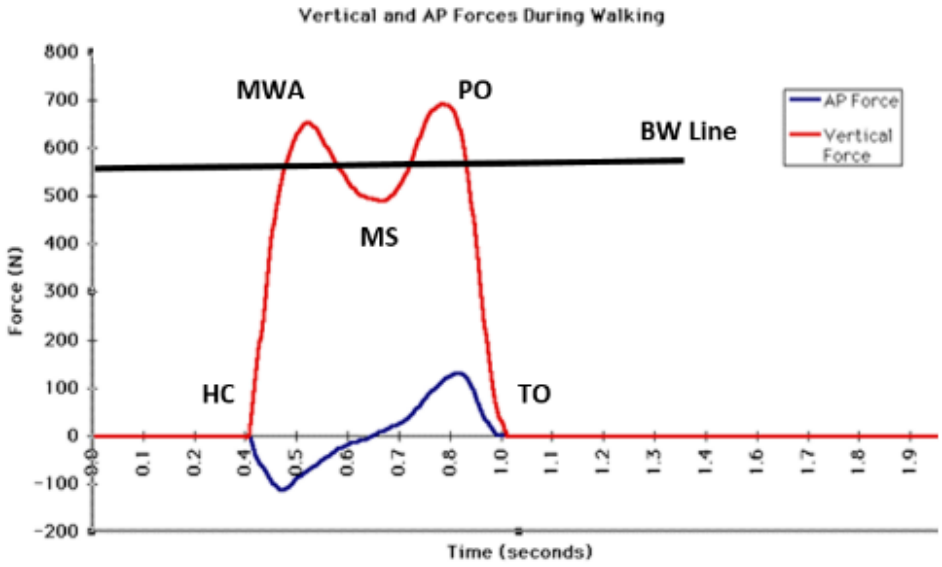

Figure 5.4 Diagram represents change in Vertical Ground Reaction Force (red line) during stance from Heel Contact (HC), through to Toe Off (TO). The black line represents body weight (BW). The blue line presents friction forces. Source: ("Kinetics Methodology Home Page" 2015).

5.1.3 Stair Climbing

Stair climbing is a complex activity that involves horizontal movement and vertical ascent at the same time, while keeping the body balanced (Park et al. 2015). Compared to level walking, higher loads, joint moments and power are generated in the knee during stair climbing (Mündermann et al. 2008; Riener et al. 2002). A study that utilised an instrumented knee prosthesis and simultaneous motion capture, measured the forces generated in the knee joint during walking, chair sit to stand and stand to sit, stair ascending and descending, squatting from a standing position, and golf swings. The results indicated that maximum total compressive load at the knee was highest during stair ascending and descending (Mündermann et al. 2008). During stair climbing the flexor-extensor muscles are also more activated and the absolute demand on the quadriceps muscle is higher (Fenner et al. 2014).

Although limb-salvage surgery is a more complex operation and consists of the removal of a large amount of bone and soft tissue in comparison to routine TKA, a study of patients following TKA indicated no difference before and after operation during walking. However, more significant changes were noted during stair climbing and therefore, in this thesis stair climbing was investigated (Bade et al. 2010).

5.2 Objectives

The aim of this chapter was to determine whether an improved gait is achieved in patients with distal femoral and proximal tibial knee joint-sparing implants when compared with patients with corresponding knee sacrificing endoprostheses. Differences were assessed using computerised gait analysis and through comparison of Vertical Ground Reaction Force (VGRF). This study also aimed to determine if joint-sparing distal femoral and proximal tibial implants improved patient stability during stair climbing.

5.3 Hypothesis

The hypotheses of this chapter was that patients with joint-sparing implants, both proximal tibial and distal femoral, have more normal gait kinematics and force transfer in comparison to those with the corresponding conventional joint-sacrificing knee implants.

Specifically in this chapter I investigated whether:

- There is improved hip, knee and ankle joint symmetry of the operated versus non-operated leg, following implantation of a joint-sparing endoprosthesis compared to a knee sacrificing implant?

- In patients with a joint-sparing implant and during stance, load transfer in both legs is similar to healthy subjects and load transfer in patients with joint-sacrificing implants is more varied and less similar to healthy subjects?
- The time in stance for both the operated and non-operated limb in patients with a joint-sparing implant is similar to healthy subjects and longer in the knee-sacrificing patient group?
- Knee-sparing endoprostheses provide increased overall stability than their knee-sacrificing counterparts during stair climbing?
- Leg length discrepancy is greater in patients with joint sacrificing implants compared to those with a proximal tibial or distal femoral joint-sparing endoprosthesis?

5.4 Method

5.4.1 Patients and Prostheses

The relevant Health Research Authority approval was obtained for this investigation (Reference: 12/LO/0178; Title: Comparative Study of Gait Analysis and Difference In Balance and Proprioception of the Knee Joint in Patients Having Knee Sparing Prosthesis Against Patients Having Distal Femur or Proximal Tibia Salvaging Procedure). Nineteen oncology subjects were investigated at a mean follow-up of 33 months (range: 12 to 84 months). Six patients with a proximal tibial replacement (5 female, 1 male), 5 with a distal femoral replacement (2 female and 3 male), 4 with a joint-sparing tibial (JST) implant (3 female, 1 male) and 4 with a joint-sparing femoral (JSF) implant (all male) were investigated. Three healthy subjects (2 male, 1 female) with no history of musculoskeletal disease or complications also participated in the study. None of the patients in any of the implant groups reported pain in either leg at

the time of examination and had reported no complications associated with their endoprosthesis at least 12 months prior to gait analysis. None of the patients investigated had undergone any revision surgery.

All implants were patient-specific endoprostheses, designed and manufactured by Stanmore Implants Worldwide Ltd (Elstree, UK). Implants were fabricated from medical grade titanium alloy (TiAl6V4). Proximal tibial replacements (PTR) and distal femoral replacements (DFR) were implanted into patients who had undergone intra-articular resection of the knee. These implants included a cobalt chromium molybdenum alloy (Co-Cr-Mo) rotating hinge SMILES knee design on a UHMWPE bearing surface. All implants were fixed using a cemented intra-medullary stem. The design of joint-sparing tibial (JST) and femoral (JSF) endoprostheses are described in Chapters 2 and 3.

5.4.2 Equipment

The data presented in this chapter was collected at the Gait Lab in the Royal National Orthopaedic Hospital, Stanmore. The Gait Lab manager, Matt Thornton, a trained physiotherapist assisted with the data collection and analysis.

5.4.2.1 Optoelectronic 3D Movement Analysis System

The Coda Motion Optoelectronic Movement System (Charnwood Dynamics, UK) was used for data collection. The system included two CODA measurement units, placed on the sides of the walkway to capture the lights emitted by the markers attached to each limb. Each unit is a standalone measurement device capable of tracking 3D marker positions in real time. Three masked linear arrays (MLAs) in each unit, combine to measure X, Y and Z coordinates of each active marker.

The markers used to track movement were “active” markers. They consisted of miniaturized diodes that emit infra-red light that is captured by the measurement unit. All markers were allocated an ID number that was identified in the set up file and did not require post data collection labelling.

An ODIN Software Suit was used for controlling the equipment, controlling the measurement system set-up and handling live streaming of data. The collected data was analysed and output data and reports were produced using this software.

5.4.2.2 Ground Reaction Force

Two force-plates were built into the walkway at approximately half of the length of the walkway and were disguised from the participants to avoid intentional alteration of gait as they approached it. In order to measure gait, a video recording of each participant was taken using four cameras placed at both ends and sides of the walkway. Force-plate data and captured video data was transmitted via the Video Vector System (VVS) software and was combined with the marker data.

5.4.3 Active Marker Placement Protocol for 3D Movement Analysis

5.4.3.1 Static Measurements

To create a 3D model from data collected from each marker, measurements obtained from several anatomical reference points were required. For each participant the following measuremnet were collected prior to marker placement:

- Length of right and left femur, tibia and foot
- Width of right and left knee and ankle
- Range of motion of right and left hip, knee and ankle
- Distance between the right and left anterior superior iliac spine (ASIS) and posterior superior iliac spine (PSIS)

5.4.3.2 Marker Placement

All participants were asked to wear shorts at least 20cm above the knee. Wherever possible, marker placement on clothing was avoided to reduce movement of the markers. For consistency and accuracy, marker placement was carried out by a single qualified physiotherapist. Markers were placed on the foot, tibia, knee and pelvis (Figure 5.5).

5.4.3.2.1 Foot Marker Placement

The foot segment was defined by the centre of the ankle joint, located on the lateral tip of the lateral malleolus of each ankle. The sole of the foot was determined by the position of toe and heel markers. Heel and toe markers were placed on the lateral aspect of the calcaneus and base of the fifth metatarsal respectively. Both markers were placed slightly superiorly to avoid being obscured from view and damage during excessive supination. The markers were attached using double sided sticky tape. Two

imaginary markers were created half an ankle width medial to the heel and toe markers. Imaginary markers are calculated within the acquisition software using the data received from actual markers and the segmental measurement input data for individual participants.

5.4.3.2.2 Tibial Segment

Special wands were used for placement of the tibial markers. Tibial wands were available in two lengths and the size chosen for each participant was based on the length of the shank with a view to avoid the major muscle bulk. The wand was placed perpendicular to the transverse projection of the ankle axis and was aligned by eyeing its direction as parallel to the edge of a customised jig. The jig was designed to align with the tip of the lateral and medial malleoli. The wand was attached to the patient using top and bottom elasticated straps.

5.4.3.2.3 Knee Joint and Femoral Segment

The femoral wand was adjusted with the participant seated. The wand was positioned vertically above the knee, avoiding contact with the major bulk of muscle and soft tissue.

For the knee joint, a plane was defined between the two markers on the femoral wand. An imaginary marker was placed at half of the knee width lateral to the calculated hip joint centre. The knee joint centre was calculated as half the knee width medial to the lateral knee marker in a direction perpendicular to this plane. The lateral knee marker was located on the lateral aspect of the knee joint axis and the joint width was measured as twice the distance between the lateral knee markers to the estimated knee joint

centre. The knee joint marker and the femoral wands were fixed in place using a single elasticated strap.

5.4.3.2.4 Pelvis Segment

Prior to fixing the pelvis marker onto each participant, a Velcro belt of appropriate length was chosen to fit around the patient's pelvic brim. With the belt firmly secured the pelvic frame that housed the pelvis markers and consisted of left and right parts was locked together and attached to the belt. In addition to the pelvis markers a pelvis wand, in some cases was used for additional data; this was however not necessary in all cases.

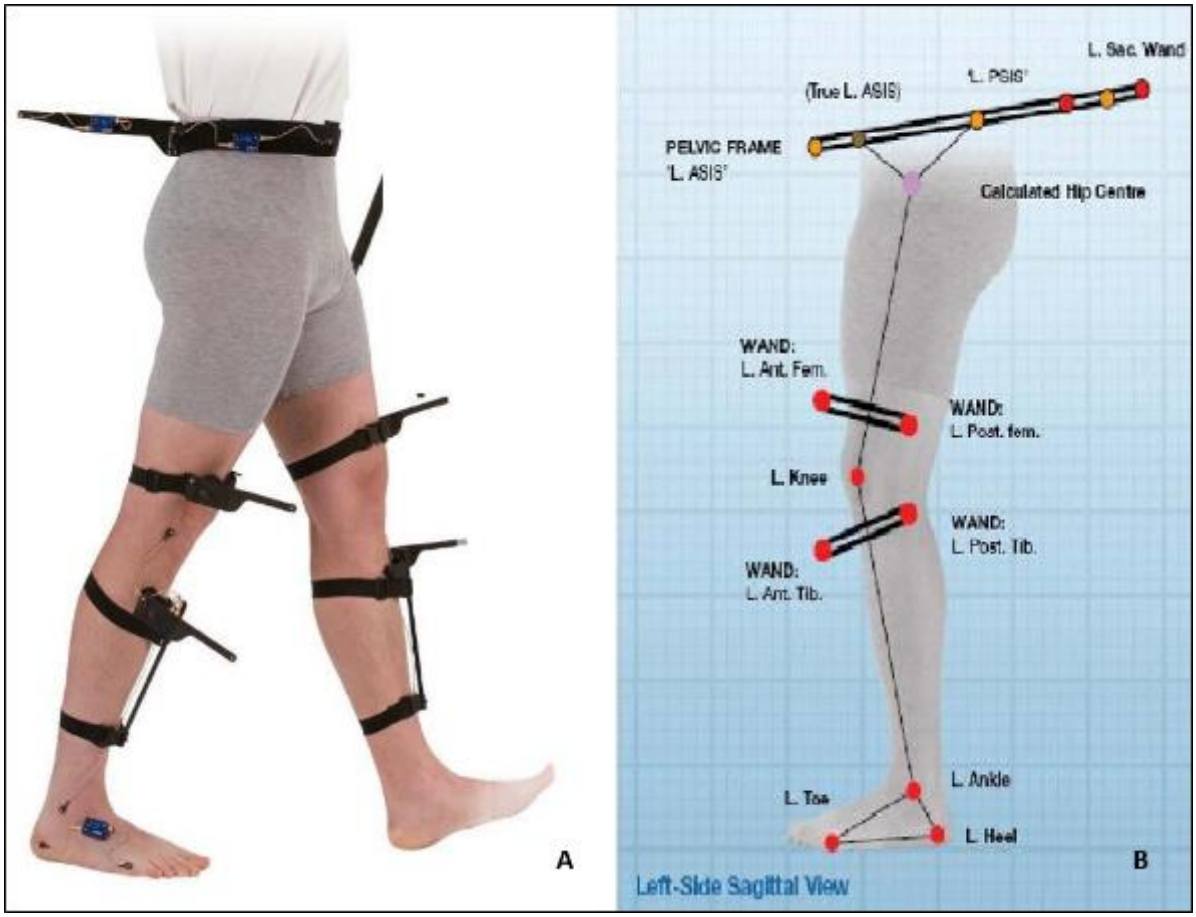

Figure 5.5 Image indicates active marker placement: [A] A participant with markers placed on his legs, feet and pelvic. [B] Schematic of marker placement that form different segments.

5.4.4 Test Protocols Investigated

5.4.4.1 Walking at a Self-Selected Speed

Participants walked barefoot along a walkway approximately 8 meters in length and at a self-selected speed representative of their normal walking pace. The walkway was located between two sensor scanners that recorded the position of each of the attached markers on the participant. Prior to data recording, patients were given time to walk in the lab with the equipment attached to them to become familiar with the testing condition. Patients were asked to walk between 6 and 10 times until sufficient position and ground reaction force data was collected. A minimum of 6 repetitions of uninterrupted position data and 3 sets of data from the force-plates, for each leg were collected.

5.4.4.2 Stability Step Exercise

Patients and healthy controls were asked to participate in a step-up exercise. A plywood box measuring 15mm in thickness and commonly used in physiotherapy, was used. The box was a standard step height of 170mm, 490mm in width and 655mm long. Participants with implants were asked to step-up using their operated leg and step-down using their non-operated leg in a cyclical, continuous manner, at least 6 times and their positional data was recorded by the sensor scanners. Healthy control subjects were asked to step-up with their less dominant leg and step-down with their dominant leg. The participants were given time to practice this routine prior to data collection. The test was repeated 3 times to ensure sufficient data was collected.

5.4.5 Data Analysis

5.4.5.1 Joint Angle Measurement during Gait

For the purpose of this thesis the gait cycle was divided into eight phases. The first phase, Loading Response (LR) was defined as the double support loading from initial contact to opposite toe off and was followed by single support phase. Single support was divided into 3 equal divisions, Initial Single Support (ISS), Mid-Single Support (MSS) and Total Single Support (TSS). The off-loading double support that followed single support, Pre-swing (PS), was followed by swing phase that was also divided into 3 equal divisions; Initial Swing (ISW), Mid-swing (MSW) and Terminal Swing (TSW) (Figure 1.8). Each division was defined by timings of ipsilateral and contralateral contact and lift-off events. This analysis is routinely carried out in the RNOH gait laboratory using a series of macros in Excel (Microsoft Corporation, USA). The mean joint position of the hip, knee and ankle joints in all phases were measured and calculated for the operated and non-operated limb in each participant. Mean joint position was measured in three spatial planes, sagittal, coronal and horizontal and data collected from joint-sparing and conventional joint sacrificing patient groups were compared. Results were also compared to healthy control participants.

5.4.5.2 Measurement of Joint Angle Symmetry during Gait

As a measure of symmetry between the operated and non-operated legs, the average joint position in the operated leg for each patient was normalised against the average joint position in the non-operated leg by calculating the difference. The average of the normalised value for each group was calculated and the distal femoral and proximal tibial joint-sparing and joint sacrificing groups and the control group were compared.

In healthy controls the mean joint position of the non-dominant leg was normalised against the dominant leg; the right leg was the dominant limb in all controls.

5.4.5.3 Ground Reaction Force during Stance

Vertical ground reaction force (VGRF) at 3 points during stance, Maximum Weight Acceptance (MWA), Mid-Stance (MS) and Push-Off (PO) were measured and the average for each leg, in each participant was calculated. The average ground reaction force at each point was normalised against the participant's body weight (BW) and the percentage mean value in the operated and non-operated legs in each group were calculated. The results of proximal tibial and distal femoral joint-sparing implants were compared to the PTR, DFR and control groups.

5.4.5.4 Time in Stance

Time in stance was defined as the time between Heel Contact (HC) and Toe Off (TO). For each leg, a minimum of 3 readings was measured and the mean value was calculated. The average time in stance for the operated and non-operated leg for each implant group was calculated and compared with the equivalent implant group and with the control group.

5.4.5.5 Step Exercise

Patient stability during step exercise was assessed by mapping the trajectory of displacement of the sacrum marker against time in the horizontal (X) and vertical (Y) directions. The marker trajectory in each group, in each direction was examined visually to identify any common trends.

5.4.5.6 Leg Length

The lengths of the operated and non-operated legs were measured using a standard tape measure. Leg length discrepancy was determined by normalising the length of the operated leg against the non-operated leg as a percentage. The average leg length discrepancy for the proximal tibial and distal femoral joint-sparing implants was compared with the corresponding joint sacrificing implants and the control group.

5.4.6 Statistics

A Mann Whitney-U test was used to compare results between groups where a *p* value < 0.05 was considered significant (version 10.1; SPSS, Chicago, Illinois). Results are presented as mean and standard error.

5.5 Results

5.5.1 Mean Joint Angle during Gait

Due to the large amount of data generated in this study, only the results that were statistically significant are reported here. All other data is presented in Appendix.

5.5.1.1 Hip Joint

5.5.1.1.1 Sagittal Plane

The mean hip extension angles measured in the operated and non-operated legs in the distal femoral and proximal tibial joint-sparing and joint sacrificing groups and in the control group are presented in Figure 5.6 and Figure 5.7. The mean hip joint angle measured in the operated leg in the DFR group, at TSS (3.67 ± 3.37°) indicated significantly more flexion of the hip when compared with the control group (-3.12 ± 3.07°; p=0.045). Negative values indicated hip extension in the sagittal plane, while positive values identified hip flexion.

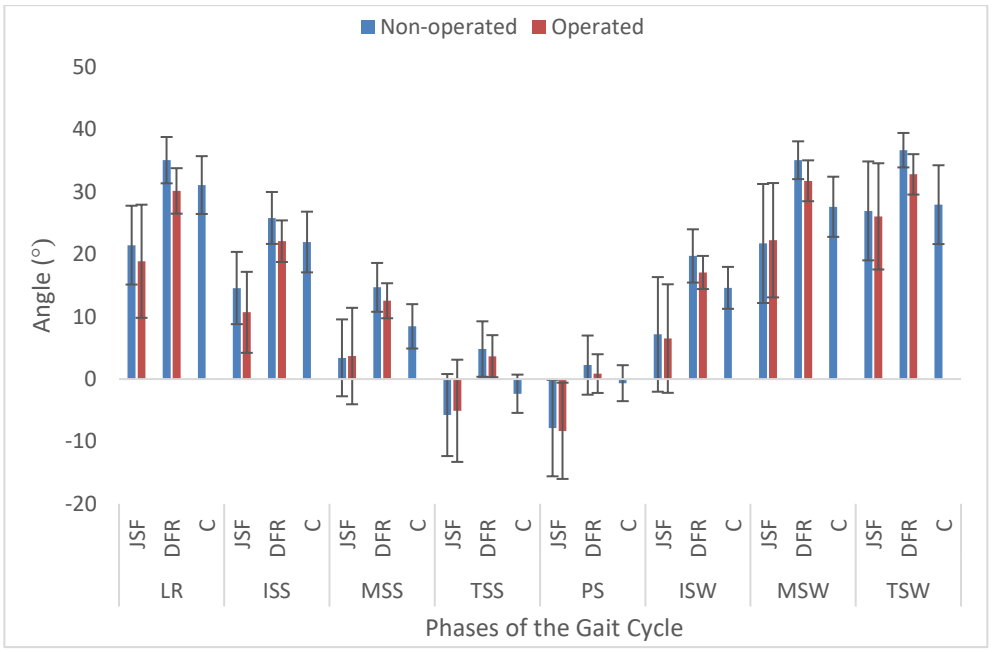

Figure 5.6 Mean hip angles in patients with a femoral replacement in the sagittal plane. The operated and non-operated legs were compared in 8 phases of the gait cycle; Loading Response (LR), Initial Single Support (ISS), Mid- Single Support (MSS), Total Single Support (TSS), Pre-swing (PS), Initial Swing (ISW), Mid- Swing (MSW) and Terminal Swing (TSW). Blue columns represent the control group (C) and the non-operated legs. Red columns represent the operated leg.

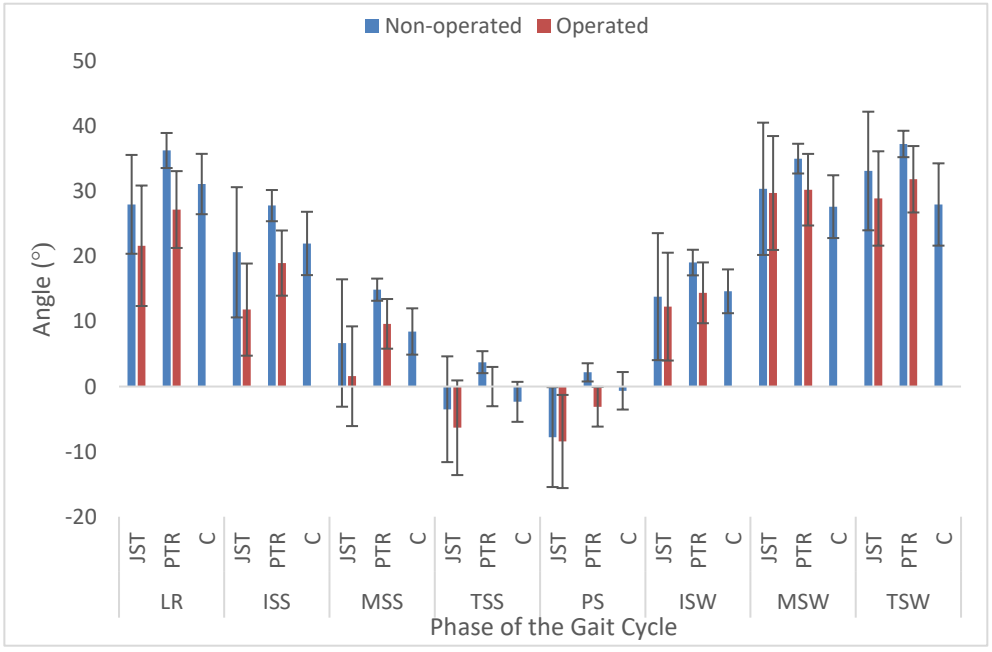

Figure 5.7 Mean hip joint angles in patients with a tibial replacement in 8 phases of the gait cycle in the sagittal plane. The operated and non-operated legs are compared. Negative values indicate hip extension

5.5.1.1.2 Horizontal Plane

The mean hip rotation angle in the non-operated leg at TSS, in the DFR group (5.21 ± 1.26°) was significantly more internally rotated when compared with data obtained from the control group (-2.81 ± 2.23°; p=0.011). Negative values indicated external rotation, and positive values internal rotation of the hip.

The mean hip angle in the horizontal plane measured for the operated leg in the JST implant group (6.93 ± 2.70°) at LR was significantly more internally rotated when compared with the PTRs (-5.57 ± 1.96; p=0.011). The mean hip rotation angles in the non-operated leg in the PTRs at MSS (5.97 ± 2.29°) and TSS (6.82 ± 3.03°) identified a significantly more internal rotation of the hip compared with the control group (p=0.037 and p=0.025, respectively). The mean hip rotation angles at MSS and TSS in the control group were -0.51 ± 2.64° and -2.81 ± 4.88°.

5.5.1.1.3 Coronal Plane

The mean hip abduction angles in the operated leg in the JSF group at MSS and TSS were significantly increased (4.44 ± 1.34° and 1.88 ± 0.39°), when compared with those in the DFR group (-1.30 ± 1.76°; p=0.027 and -1.37 ± 1.13°; p=0.014). Negative values indicated hip abduction in the coronal plane while positive values identified hip adduction.

5.5.1.2 Knee Joint

5.5.1.2.1 Sagittal Plane

There was no significant difference in the mean knee joint angles in the sagittal plane in the operated and the non-operated legs when the distal femoral joint-sparing and

joint sacrificing groups were compared and when they were compared to data obtained from the control group (Figure 5.8).

The mean knee angles measured in the sagittal plane in the operated leg in the JST group were significantly decreased when compared with the control group in all 5 stance phases (Figure 5.9). *P*- values are summarised in Table 5.1

Table 5.1 Mean knee joint angles in the sagittal plane in the operated leg in the proximal tibial joint-sparing group and in the control group with associated *p*-values.

Phase of the Gait Cycle	JST group	Control group	*P* –value
Loading Response	4.56 ± 7.39°	20.00 ± 1.27°	*P* = 0.019
Initial Single Support	6.84 ± 3.89°	25.65 ± 3.05°	*P* = 0.011
Mid- Single Support	3.31 ± 3.54°	18.10 ± 2.00°	*P* = 0.011
Total Single Support	4.26 ± 4.09°	17.42 ± 1.31°	*P* = 0.019
Pre-swing	20.49 ± 5.73°	35.55 ± 1.02°	*P* = 0.011

The mean knee flexion angle measured in the operated leg in the PTRs were significantly decreased when compared with the control groups at; ISS (11.08 ± 3.89°; *p*=0.016), PS (22.90 ± 5.11°; *p*=0.004) and MSW (43.12 ± 7.33°; *p*=0.045). The mean knee joint angle in the sagittal plane in the control group at MSW was 57.87 ± 3.41°. The mean non-operated knee flexion angle in the PTRs (21.19 ± 2.75°) at TSW was significantly increased when compared with the control group (13.56 ± 0.25°; *p*=0.025).

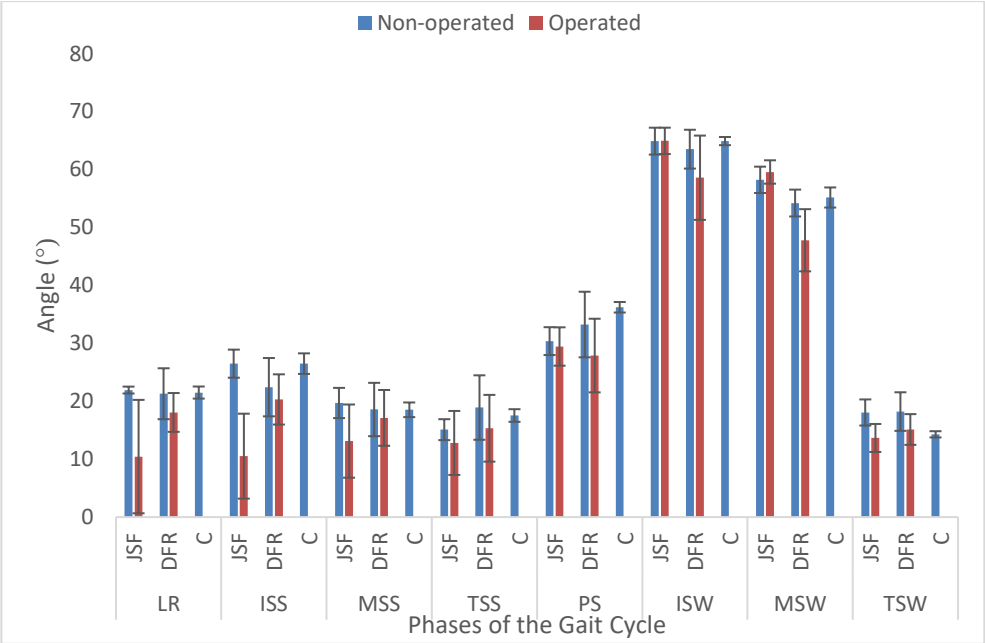

Figure 5.8 Mean knee angles in distal femoral implant groups during the gait cycle in the sagittal plane (flexion-extension). There was no significant difference in knee flexion angles in all phases. Overall, the joint angle during the stance phases of the cycle is more similar in the operated and non-operated legs in the JSF group when compared with the DFRs. This was reversed during the swing phases of the gait cycle.

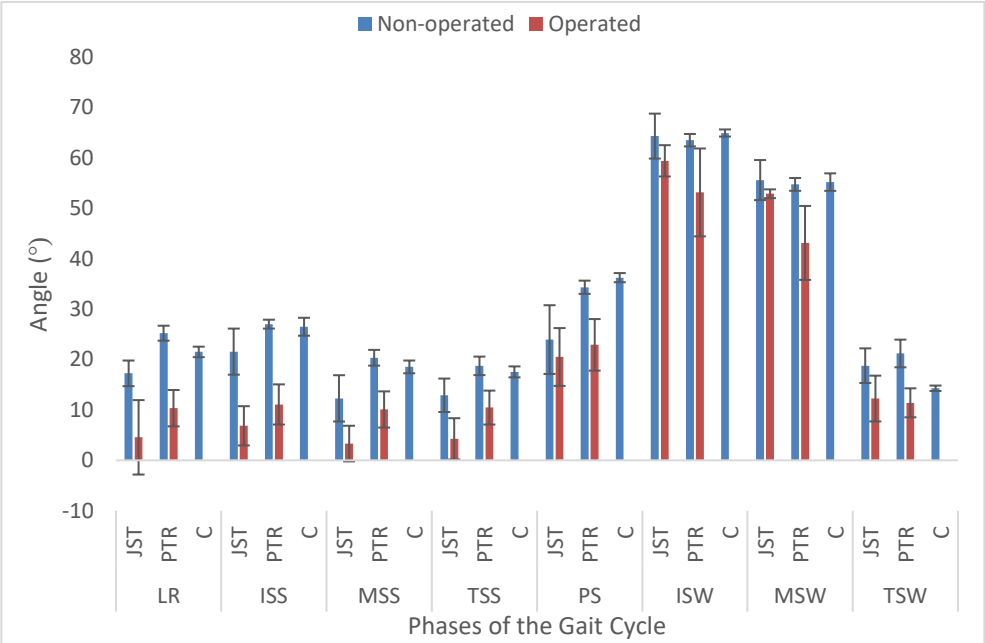

Figure 5.9 Mean knee angles measured in the sagittal plane (flexion-extension), during the gait cycle in the proximal tibial groups. The operated knee in both groups hyperextended when compared with the control group.

5.5.1.2.2 Horizontal Plane

There was no significant difference in the mean internal/external rotation angles measured in the operated and non-operated knees, when the distal femoral and proximal tibial joint-sparing and joint sacrificing groups and the control group were compared.

5.5.1.2.3 Coronal Plane

The mean knee varus/valgus angles measured in the non-operated leg at MSS and MSW, in the DFR group (2.23 ± 1.73° and 2.53 ± 1.3°) were significantly increased (varus) when compared with the JSF group (-1.68 ± 0.86; p=0.027 and -1.68 ± 1.62°; p=0.014).

The mean knee joint angles measured in the coronal plane in the non-operated leg in the JST group were significantly more in varus at MSS (1.09 ± 0.41°) and TSS (1.51 ± 0.42°) when compared with the control group (-0.40 ± 0.35°; p=0.019 and -0.07 ± 0.53°; P=0.019). The mean knee varus angle, measured in the coronal plane in the non-operated leg of the PTRs (1.05± 0.73°) at ISW was significantly increased when compared with the control group (-4.97 ± 2.87°; p=0.033).

5.5.1.3 Ankle Joint

5.5.1.3.1 Sagittal Plane

There was no significant difference in the mean dorsi/plantar flexion ankle joint angles measured in the operated and non-operated legs, in the distal femoral joint-sparing and joint sacrificing groups and the control group (Figure 5.10).

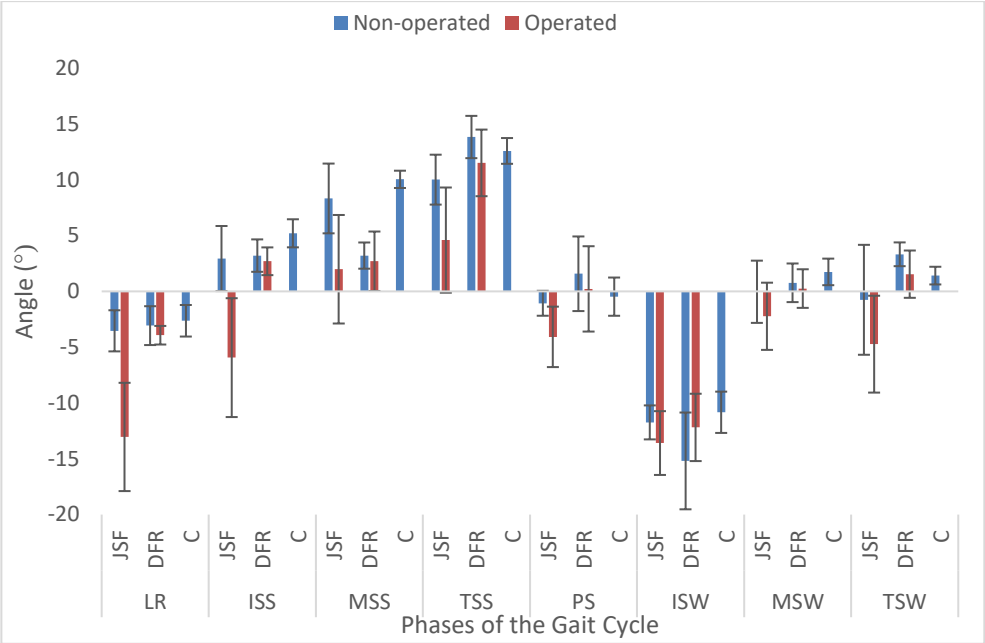

Figure 5.10 Mean ankle angles measured during the 8 phases of the gait cycle in the sagittal plane in the distal femoral groups and the control group. None of the joint angles were significantly different when each of the groups were compared.

The mean ankle joint angles in the sagittal plane (Figure 5.11) measured in the operated leg at ISS and MSS, in the joint-sparing proximal tibial implants (-4.39 ± 3.00° and 1.66 ± 3.65°) were significantly different when compared with the control group (5.21 ± 1.23° and 10.04 ± 0.77°; both p=0.033). At MSS, the mean ankle joint angle measured in the operated leg in the PTRs (5.52 ± 1.81°) was significantly decreased when compared with the control group (p=0.025).

5.5.1.3.2 Horizontal Plane

There was no significant difference in the mean ankle rotation angles measured in the operated and non-operated legs, in the distal femoral and proximal tibial joint-sparing groups where compared with the joint sacrificing and the control groups.

5.5.1.3.3 Coronal Plane

The mean ankle joint angles measured in the operated leg in the DFR group were significantly decreased at PS (4.11 ± 1.79°) and ISW (5.53 ± 1.47°) when compared

with the control group (9.35 ± 2.42° and 10.10 ± 1.18; both p= 0.045). The mean ankle joint angles measured in the non-operated leg were significantly decreased in the DFR group at PS (4.06 ± 0.66°; p=0.028), ISW (5.77 ± 0.90°; p=0.045) and TSW (6.61 ± 0.90°; p=0.028) when compared with the control group. The mean ankle joint angle in the control group at TSW was 8.12 ± 1.48°. The mean ankle joint angle in the operated leg was significantly decreased in the DFR group (-1.90 ± 2.40°) at TSS when compared with the JSF group (2.93 ± 4.59°; p=0.027).

The mean adduction/abduction ankle joint angles measured in the operated leg in the PTR group at LR (1.50 ± 1.90°; p=0.016), PS (1.50 ± 1.70°; p=0.016), ISW (1.55 ± 1.02°; p=0.010), MSW (0.39 ± 1.40°; p=0.006) and TSW (1.31 ± 1.17°; p=0.004) were significantly decreased when compared with the control group. The mean ankle joint angles in the coronal plane in the control group at MSW and TSW were 8.16 ± 1.01° and 8.77 ± 1.46°, respectively.

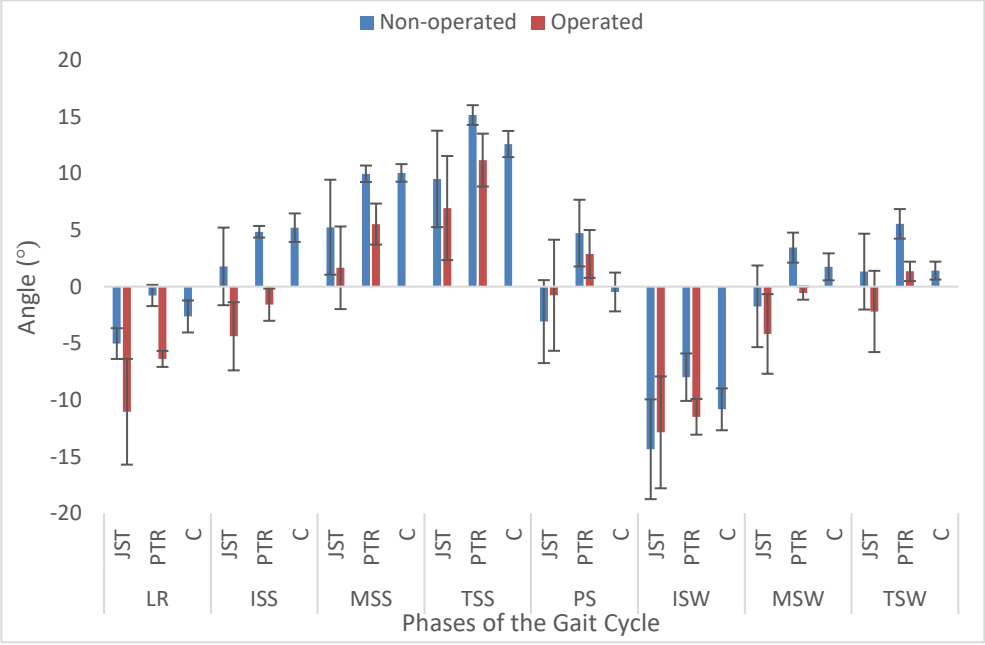

Figure 5.11 Mean ankle angles measured during the 8 phases of the gait cycle in the sagittal plane in proximal tibial groups and the control group. Negative values indicate plantarflexion of the ankle joint.

5.5.2 Joint Symmetry

5.5.2.1 Hip Joint

5.5.2.1.1 Sagittal Plane

The difference between the mean hip joint angles in the operated and the non-operated legs (normalised joint angle), in the joint-sparing tibial replacements (2.84 ± 1.97°; p=0.034) at TSS and in the PTRs (4.77 ± 3.88°; p=0.039) at MSW were significantly increased when compared with the control group (-1.54 ± 0.80° and -3.02 ± 1.40°, respectively).

5.5.2.1.2 Horizontal Plane

The normalised mean hip angle in the JST group (-14.67± 9.60°) at LR indicated a significantly more internally rotated joint in the operated leg when compared with the PTR group (9.60 ± 3.23°; p=0.033).

5.5.2.1.3 Coronal Plane

The normalised mean hip adduction/abduction angles in the coronal plane were not significantly different when the distal femoral and proximal tibial joint-sparing and joint sacrificing groups were compared and when they were compared with the control group.

5.5.2.2 Knee Joint Symmetry

5.5.2.2.1 Sagittal Plane

The normalised mean knee flexion angles in the sagittal plane were not significantly different when the distal femoral and proximal tibial joint-sparing and joint sacrificing groups were compared and when they were compared with the control group (Figure 5.12).

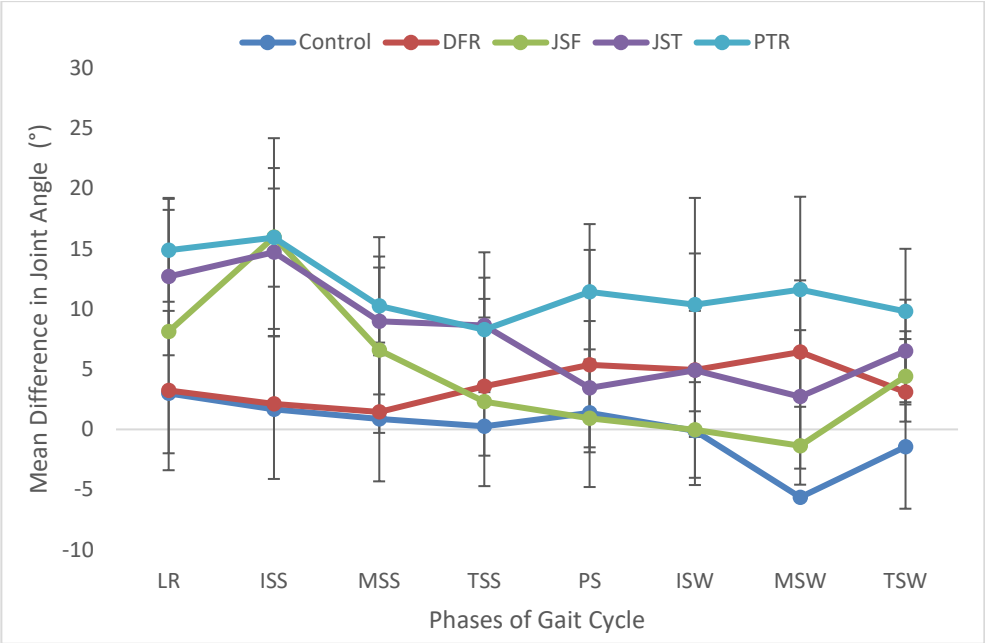

Figure 5.12 Mean differences in knee joint angles in the sagittal plane for the DFF, PTR, JSF and JST groups and the control group. A mean angle difference of zero indicated the symmetry of the joint angles in both legs. In the patient groups the mean difference in joint angle between the operated and non-operated legs and in controls the mean difference in joint angles in the right and left legs are presented as a single value in each phase.

5.5.2.2.2 Horizontal Plane

The normalised mean knee angle measured in the horizontal plane in the PTR group (6.66 ± 7.57°) was significantly different at ISS when compared with the control group (-5.88 ± 7.62°; p=0.039). The results for normalised mean knee rotation angles in all the 5 groups are presented in Figure 5.13.

5.5.2.2.3 Coronal Plane

The normalised mean knee varus/valgus angles in the JST group (-1.83 ± 1.73°) was significantly different (less symmetrical), when compared with the control group (0.32 ± 0.32°; p=0.034) at TSW. The normalised mean knee angles in the coronal plane in the PTR group (-0.44 ± 1.34°) at MSS was also significantly different when compared with the control group (-1.12 ± 1.39°; p=0.033).

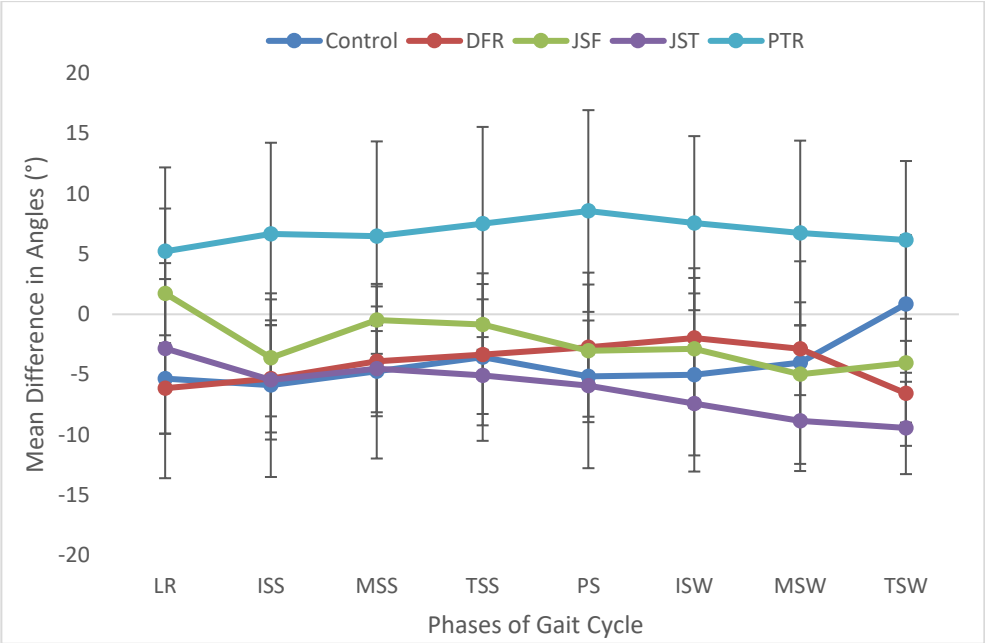

Figure 5.13 Mean differences in knee joint angles in the horizontal plane in the DFR, PTR, JSF, JST, and control groups. The operated knee in the PTR group rotates mainly internally, throughout the gait cycle.

5.5.2.3 Ankle Joint Symmetry

5.5.2.3.1 Sagittal Plane

The normalised mean knee ankle joint angles measured in the sagittal plane were not significantly different when the distal femoral and proximal tibial joint-sparing and joint sacrificing groups were compared and when they were compared with the control group. The results for normalised mean ankle joint angles in the sagittal plane in all the 5 groups are presented in Figure 5.14.

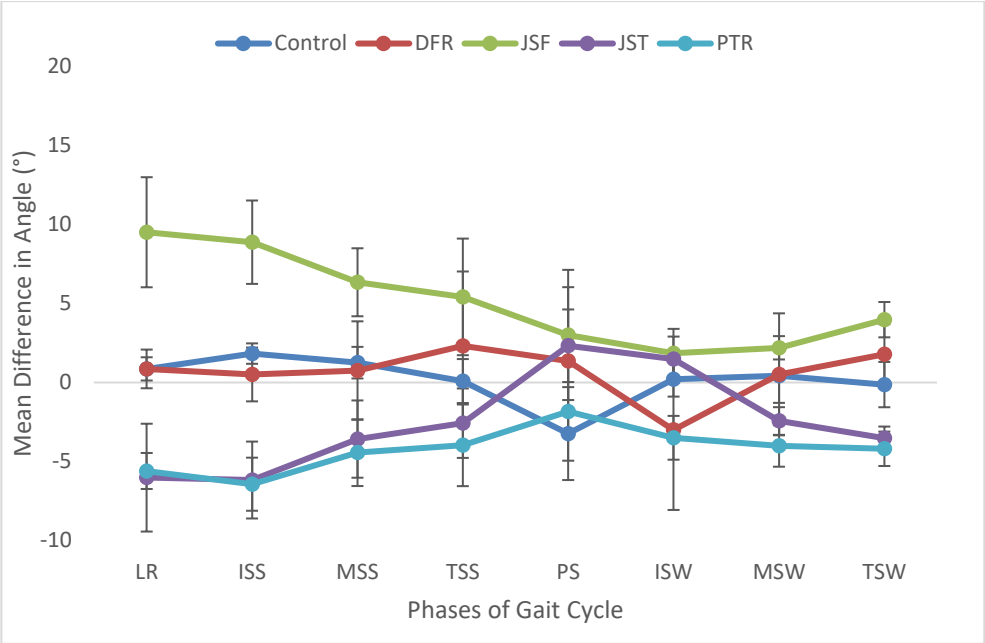

Figure 5.14 Mean difference in ankle joint angles in the sagittal plane in the DFR, PTR, JSF, JST and control groups.

5.5.2.3.2 *Horizontal Plane*

The normalised mean internal/external rotation angles of the ankle joint were significantly less symmetrical in the JSF group (9.50± 10.21°) at LR when compared with the DFR group (-0.17± 1.50°; p=0.027). The normalised mean ankle joint angle in the horizontal plane in the DFR and PTR groups (3.32± 3.76°) were also significantly increased in LR when compared with the control group (1.00 ± 0.84°; p=0.034 and p=0.039, respectively). The results for normalised mean ankle rotation angles in all the 5 groups are presented in (Figure 5.15).

5.5.2.3.3 *Coronal Plane*

The normalised mean ankle joint angles in the coronal plane in the PTR group (4.22 ± 1.93°) was significantly increased at ISW when compared with the control group (-3.13 ± 1.58; p=0.020).

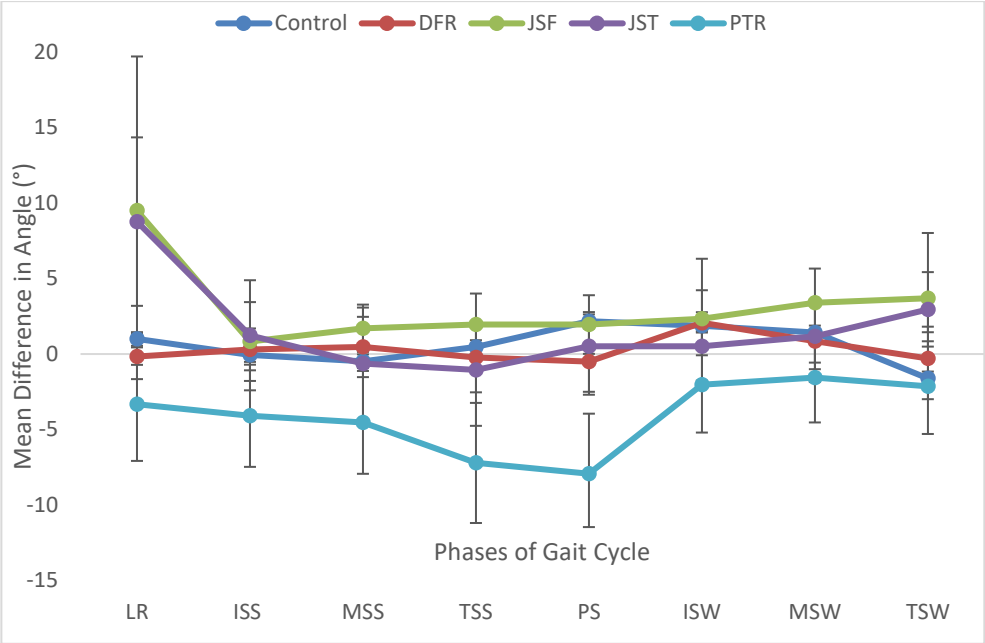

Figure 5.15 Mean difference in ankle joint angles in the horizontal plane in the DFR, PTR, JST, JSF and control groups. The difference in ankle joint angle during LR was significantly different when the JSF and the DFR groups were compared and when the DFR and PTR groups were compared to the control group.

5.5.3 Ground Reaction Force

The normalised mean vertical ground reaction force at the 3 stance points; MWA, MS and PO, in the operated and non-operated legs in the distal femoral and proximal tibial joint-sparing and joint sacrificing groups and in the control group are summarised in Figure 5.16 and Figure 5.17. The normalised mean VGRF in the control group at MWA, MS and PO, were 115.8 ± 3.53% BW, 74.82 ± 3.81% BW and 114.49 ± 4.81% BW, respectively.

The normalised mean VGRF in the operated leg in the DFR group (100.14% BW), at MWA was significantly decreased when compared with the JSF group (111.02% BW; p= 0.025) and when compared with the control group (p=0.006). The normalised mean VGRF in the operated leg in patients the DFR group at MS (88.31 ± 4.39% BW; p=0.045) was significantly increased and was significantly decreased at PO (101.82 ±

2.27% BW; p=0.028) when compared with the control group. The normalised mean VGRT in the operated and the non-operated legs at MS in the JSF group (87.67 ± 4.14% BW; p=0.039 and 87.26 ± 4.71% BW; p=0.020) were significantly increased when compared with the control group.

The normalised mean VGRF in all three stance points was not significantly different in the JST group when compared with the PTR group. The normalised mean VGRF in the operated and non-operated legs at MWA, in the JST group (100.09 ± 1.71% BW and 97.75 ± 3.22% BW; p= 0.020 in both) and in the PTR group (100.10 ± 1.42% BW; p=0.006 and 103.20 ± 2.28% BW; p=0.016) were significantly reduced when compared with the control group. The normalised mean VGRF in the operated leg in the PTR group (85.83 ± 2.41% BW) was significantly increased at MS when compared with the control group (p=0.037).

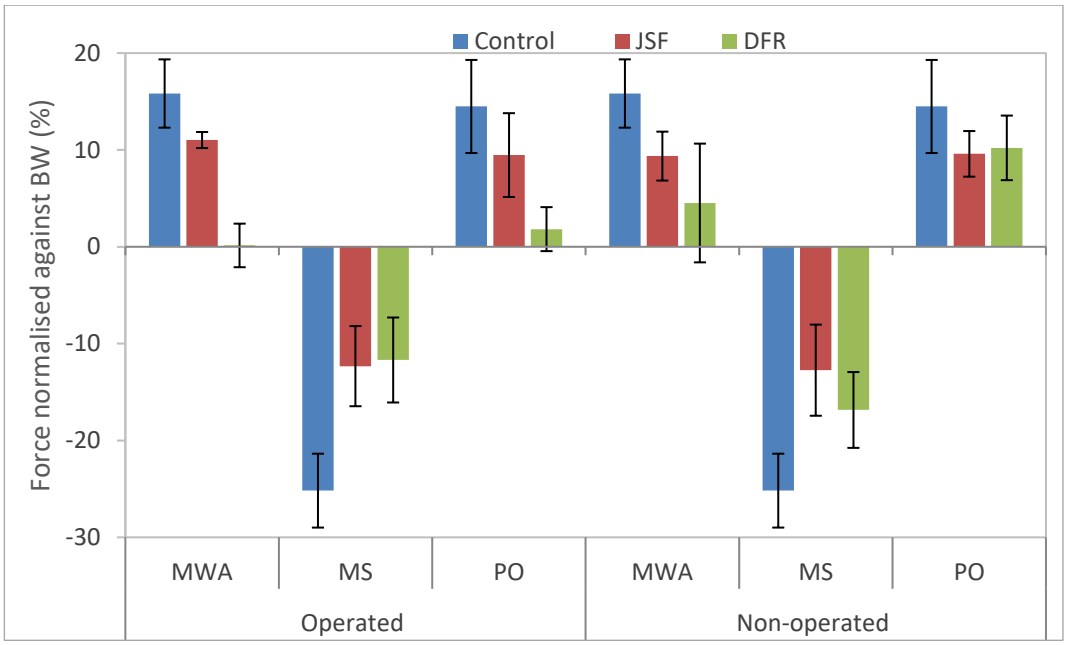

Figure 5.16 Mean ground reaction force, normalised against body weight, in the operated and non-operated legs in the joint-sparing femoral replacements (red), distal femoral replacements (green) and the control group (blue).

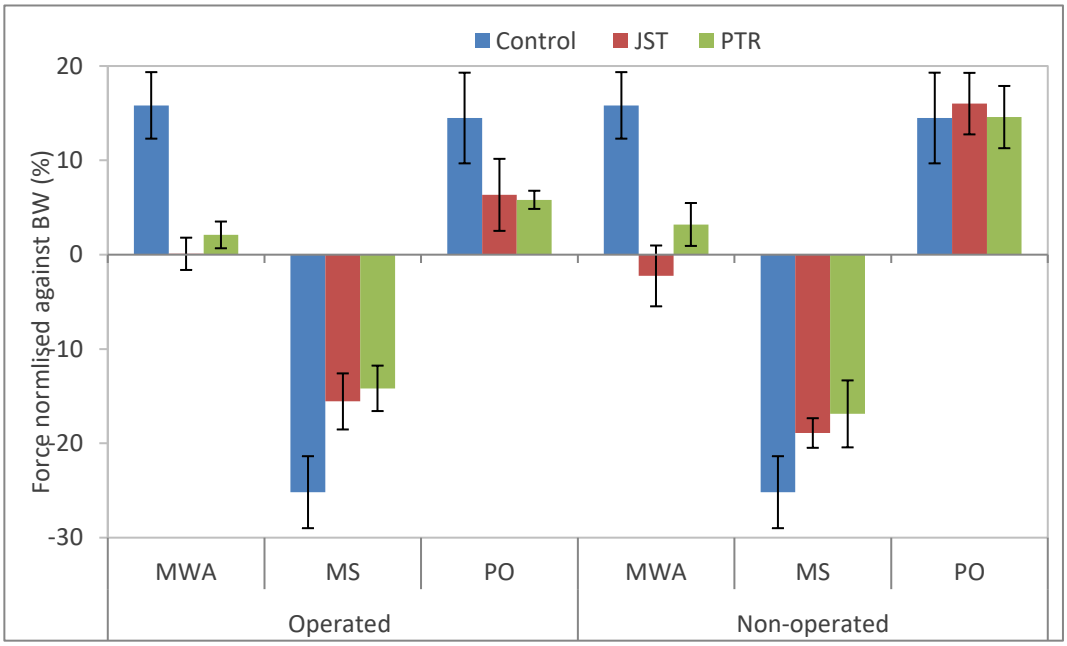

Figure 5.17 Mean ground reaction force normalised against body weight, in both the operated and non-operated legs in the joint-sparing tibial replacements (red) and proximal tibial replacements (green) and in the control group (blue).

5.5.4 Time in Stance

The mean time in stance in the control group was 0.65 ± 0.02 seconds. The mean time in stance in the operated and the non-operated legs in the JSF group was 0.74 ± 0.07s and 0.74 ± 0.05s, and 0.76 ± 0.03s and 0.80 ± 0.09s in the DFR group, respectively. The mean stance time in the operated leg in the DFR group was significantly increased when compared with the control group (p=0.018).

The mean stance time in the operated and the non-operated legs in the JST was 0.79 ± 0.06s and 0.82 ± 0.07s, respectively. The mean stance time in both legs in the JST group was significantly increased when compared with the control group (both, p=0.020). The mean stance time in the operated and the non-operated legs in the PTR group was 0.68 ± 0.02s and 0.75 ± 0.06s, respectively.

5.5.5 Step Exercise

The trajectory of the displacement of the sacrum marker in all patients, during the step up/down exercise was plotted against time and was visually analysed. No particular trend in horizontal or vertical displacement of the sacrum marker in any of the groups was identified. The patients in all groups exhibited a similar displacement pattern in the horizontal (X) direction; however, displacement in the vertical (Y) direction was variable, with no specific pattern.

5.5.6 Leg Length

The mean difference between the right and the left leg length in the distal femoral and proximal tibial joint-sparing and joint sacrificing groups and in the control group is provided in Figure 5.18. The mean leg length discrepancy value was seen to be

increased in the DFR and PTR groups when compared with the JSF, the JST and the control groups however, the results were not significant.

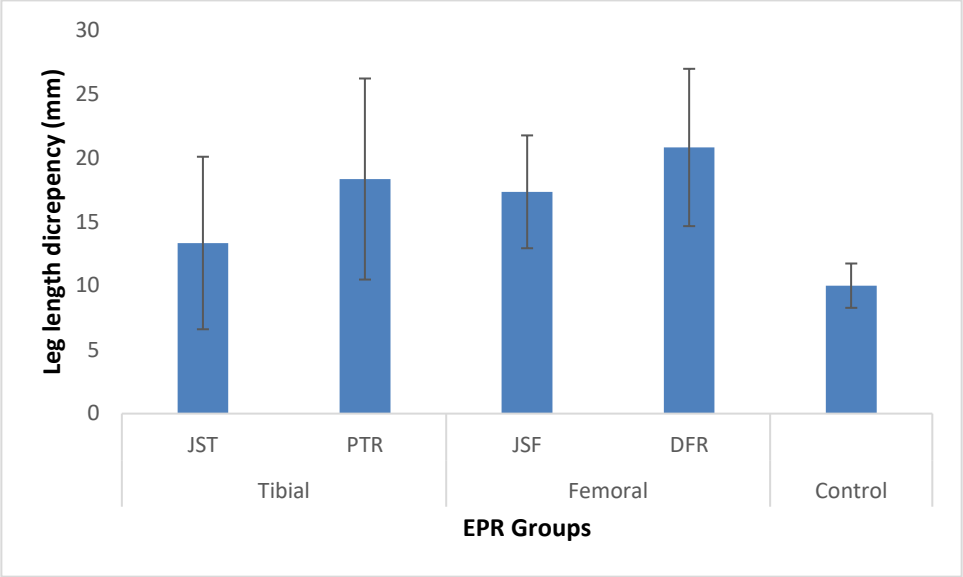

Figure 5.18 Leg length discrepancy values in each of the groups. No significant differences were seen.

5.6 Discussion

Motion analysis and use of kinetic and kinematic gait data is an established quantitative outcome measurement method for severe gait defects, however there are few studies that have utilised this method for assessment of patient outcomes following limb salvage surgery (Bruns et al. 2016; Ochs et al. 2007; De Visser et al. 2000; De Visser et al. 2003; Kawai et al. 2000). The majority of patients undergoing limb salvage surgery for treatment of tumours in the lower extremity are active juvenile or young adults that will be returning to normal life following recovery. Hence, gait assessment is an important component of functional outcome evaluation (Okita et al. 2014). Currently there are no studies that have investigated functional outcome using gait analysis methods in patients following joint-sparing surgery. Measurement of joint angles during gait, symmetry of the operated and the non-operated legs and stance time

that were investigated in this chapter, are widely used to assess recovery following limb salvage surgery for trauma (Archer et al. 2006) and following a tumour resection (Kawamura et al. 1999; De Visser et al. 2003; Ochs et al. 2007). Previous studies have reported reduced function in patients treated with a PTR compared with those treated with a DFR implant (Skaliczki et al. 2005; Tunn et al. 2008). This has been associated with the difficulty to attach the patellar tendon to the implant following removal of the tibial tuberosity, alteration of musculature to provide adequate soft tissue coverage and possible injury to the neurovascular bundle (Ilyas et al. 2000; Anract et al. 2001; Kawai et al. 1999; Dickinson, et al. 2009). Patients treated with a PTR were reported to walk significantly more slowly than those treated with a DFR, however they did not exhibit a different gait pattern (Ochs et al. 2007).

5.6.1 Joint Position in Distal Femoral and Proximal Tibial Replacements

5.6.1.1 Hip

In this chapter, the mean hip joint angle in the sagittal plane in the control group in all phases of the gait cycle were within the values stated in the literature (Winter 1984; Kadaba het al. 1990). The mean hip flexion angle in the sagittal plane, in the PTR and JST groups were similar to normal gait; however, the mean hip joint angle in both groups showed reduced flexion of the hip in the operated leg when compared with the non-operated leg during stance. For example, in the JST group and at the start of stance, the mean hip flexion angle in the operated leg was reduced by approximately 2-folds compared with the non-operated leg. Throughout the gait cycle, the hip flexion angle in the JSF group was smaller than that of the control group and the DFR group. At PS and in the operated and non-operated legs, the mean hip extension angle was approximately 9°, while in normal gait the hip joint is in neutral position during this phase of the cycle. Rompen et al. that investigated hip flexion angle in patients with

massive femoral replacements, reported an overall shift in the flexion-extension pattern of the hip towards more extension throughout the gait cycle (Rompen et al. 2002). However, this was not the case in the study presented here and the mean flexion angle in DFR and PTR patients in both the operated and non-operated legs was increased when compared with the control group and their respective joint-sparing groups. In another study that investigated conventional, joint sacrificing DFRs, subjects exhibited the tendency to flex the hip in the non-operated leg following the initial contact, while the hip in the operated leg extended (Yusuke Okita et al. 2013). However, in this study the joint-sparing and joint sacrificing distal femoral and proximal tibial replacements exhibited less flexion of the operated leg, compared with the non-operated leg. Similarly, Bruns et al. also reported reduced hip ROM at the start of stance and throughout the swing, in both the operated and the non-operated legs in distal femoral implants (Bruns et al. 2016).

In normal gait the peak hip internal rotation is expected to occur during PS (Kirkwood et al. 2007), however in both the operated and non-operated legs in the JSF group, the maximum internal rotation of the hip was reached at MSW. The mean hip angle in the horizontal plane in the JST and PTR groups showed that the hip joint rotated in opposite directions in the operated and non-operated legs at LR. The increased rotation at MSW in the JSF group could be a compensatory mechanism for enabling a more efficient toe-off, while the excessive internal rotation of the hip at LR in the JST and PTR groups could be due to poor control of knee flexion at heel contact. These could also be caused by reduced effectiveness of the extensor mechanism of the knee joint. Disruption to any part of the extensor mechanism, that is the quadriceps muscle and tendon, medial and lateral retinaculum, patellofemoral and patellotibial ligaments, patella, patellar tendon, and tibial tubercle (Vaishya et al. 2016), can be caused during

the removal of a tumour. The mean hip joint angle in the JSF group during stance showed external rotation of the hip, while in the DFR group, the hip joint was mainly internally rotated and close to neutral, however this was not significant.

In the JSF group, the hip in the operated and non-operated legs adducted following LR and reached their maximum adduction angle at ISS, as expected in normal gait. However, the mean hip abduction angle in both legs at PS was over 2-folds higher than the mean hip abduction angle measured in the control group. In the DFR group, the mean hip joint angle in the operated leg, during stance and in the non-operated leg during swing, remained close to the neutral position. This result is in agreement with a study by Bruns et al. where reduced adduction from mid- to terminal stance in patients with a DFR implant and reduced abduction throughout swing in the operated and the non-operated legs was reported (Bruns et al. 2016). In this study and in the JSF and joint sacrificing groups, a similar mean hip joint angle in the coronal plane was measured. In proximal tibial joint-sparing and joint sacrificing groups, the overall joint symmetry was poor. In the PTR group while the hip joint in the operated leg abducted, the hip in the non-operated leg adducted during most of the gait cycle.

In patients with a proximal femoral massive implant, the strength of hip abductor muscles were correlated with the net energy cost and gait symmetry; i.e. the gait in patients with good abductor strength was more symmetrical, and those patients had an improved energy expenditure (Kawai et al. 2000). Decreased strength in hip abduction can be caused by loss of muscle attachment to a metal prosthesis that is less stable (Gitelis et al. 1988; Zehr et al. 1996). In patients with a distal femoral replacement the hip abduction/adduction could be widely varied from one patient to another depending on the size and location of muscle resection, however it may not be

related to preservation of the knee joint and hence, the little difference that was observed in the two distal femoral implant groups investigated in this study.

5.6.1.2 Knee

An investigation of kinematic gait data in patients treated with conventional distal femoral and proximal tibial tumour prostheses revealed that the overall gait pattern in patients with a PTR, was predominantly characterised by a hyperextended knee during stance when compared with patients in the DFR group (Ochs et al. 2007). The mean knee flexion angle in the JST group was significantly different when compared with the PTR group, in several phases of the gait cycle, and with the control group during stance. In Chapter 4 of this thesis, it was established that patients with a JST implant had a normal knee ROM. In this chapter, no significant difference in mean knee flexion angle in the sagittal plane in the distal femoral joint-sparing and joint sacrificing groups was found. However, when the joint-sparing and joint sacrificing distal femoral groups and the control group were compared, the operated knee exhibited decreased flexion. In the JSF group, where the mean knee flexion angle in the operated leg was approximately halved when compared with the non-operated side during loading response until mid-single support. The artificial knee joint has various disadvantages, including a limited range of motion (ROM) (Frink et al. 2005). A study that compared ROM in twenty patients with massive bone tumour implants and twenty matched healthy controls showed that the mean knee flexion angle in the patients, following surgery, was significantly reduced (106.2 ± 13.0°) when compared with the contralateral limb (134.1 ± 7.5°) and with that of the healthy controls (137.7 ± 7.0°) (Tsauo et al. 2006). Okita et al. (2013) investigated gait in patients with a conventional distal femoral replacement and found that of the 8 patients investigated, 5 kept their operated knee extended during early stance, whereas 2 exhibited a normal knee

movement pattern. One patient flexed the ipsilateral knee after initial contact but extended it during late stance, similar to a normal knee (Okita et al. 2013). Other studies have also reported a hyperextension of the knee during LR and mid-Stance in 50% of patients with a DFR and 100% of the patients with a total femoral replacement. Some patients with a DFR, presented a flexed-knee gait pattern that is characterised by continuous flexion during mid-stance (Rompen et al. 2002). When large segments of soft tissue and bone are removed during limb salvage surgery, a substantial decrease in strength of knee extension can occur that is often compensated by the gluteus maximus, biceps femoris, and gastrocnemius muscles, during stance (Kawamura et al. 1999). A simulation study of muscle and joint load transfers following resection of a tumour in the distal femur concluded that as long as the hip extensors and ankle plantar flexors are working, transfer of the forces through the patella tendon can be accommodated in level walking and the patients would have a near normal gait (Van Krieken et al. 1985). Studies that included electromyographic (EMG) analysis of the patients found that during pathologic gait, there is less muscular activity (Winter 1989; De Visser et al. 2000). Hence, in early stance, less knee flexion allows the transfer of weight without the requirement for normal muscle activity (Tsuboyama et al. 1994). This position would reduce the demands on the musculature needed to prevent the knee from collapsing, while full knee extension has the advantage of being the most stable weight-bearing position (Winter 1989; De Visser et al. 2000). In this study, it would have been interesting to also record and analyse EMG activity in order to investigate how the knee was being balanced and if there was a difference in the use of muscles around the knee in patients with a joint-sparing and a joint sacrificing implant. The extensive muscle resection can also cause a loss of proprioceptive feedback that is important for control of locomotion (Winter 1989; Lajoie et al. 1996;

De Visser et al. 2000). This loss of proprioceptive input may be the contributing factor in hyperextension of the knee during stance (De Visser et al. 2000). However, in Chapter 4 of this thesis, the results showed no difference in proprioception between patients with a joint sparing endoprosthesis and patients with a knee joint replacement. In the JSF group of patients, although some muscle attachments are preserved, a large amount of muscle may still be resected.

The mean knee external rotation angle in the operated leg in the joint-sparing and joint sacrificing distal femoral implant groups was reduced at LR and TSW when compared with the non-operated leg and the control group. Throughout the gait cycle, the mean knee rotation angle in the non-operated leg was increased in the DFR group when compared with the control group, while this was decreased in the JSF group. When compared with control data and the PTR group, the mean knee rotation angle measured in the operated and non-operated legs decreased in the JST group, in all phases of the gait cycle. While in the JST group, the knee on the operated side exhibited reduced external rotation when compared with the knee on the non-operated side, the operated knee in the PTR group was more externally rotated compared with the knee on the non-operated side. The mean knee rotation angle, was not significantly different when the joint-sparing and joint sacrificing distal femoral, proximal tibial and control groups were compared. This could be related to subtle rotation of the knee joint during gait that was not detected by the equipment. In knee sacrificing procedures, the anterolateral ligament, as well as the posterior lateral corner (PLC) and posterior cruciate ligament (PCL) that are responsible for knee joint stability, are removed (Wang 2002). It could be argued that in joint-sparing implants these attachments remain intact, and therefore it is expected that in the JST and JSF groups, when compared with the conventional joint sacrificing implants with a rotating hinge knee,

that knee rotation is reduced and the joint is more stable. However, this does not explain the reduced external rotation of the operated knee when compared with the control group and the non-operated knee. While the absence of these ligaments can cause knee instability, most rotating hinge knee implants are designed to increase stability (Myers et al. 2007) in the presence of significant bony and/or soft tissue envelope defects (Morgan, et al. 2005). In the presence of significant instability, implants with more constraint become required. Varus/valgus constrained knee and rotating-hinge knee prostheses are often used to provide stability in the coronal and the sagittal planes when the ligamentous and soft tissue support are severely compromised (Malcolm et al. 2016).

As expected in normal gait, the mean knee varus/valgus angles in the control group were close to neutral from LR to TSS (Winter 1984). In the proximal tibial joint-sparing and joint sacrificing groups and the DFR group, increased knee varus angle in the operated and the non-operated legs was observed during stance, particularly in the operated leg of the JST group. The mean knee varus angle in the coronal plane in the non-operated leg was significantly different at MSS and MSW when the JSF and the DFR patient data were compared. The non-operated side of the JSF group showed valgus movement throughout stance as opposed to varus while the operated leg in the DFR group presented no valgus movement throughout the gait cycle. There is limited data available on knee movement in the coronal plane following limb salvage surgery, however, varus/valgus balance has been studied following total knee arthroplasty (TKA). The knee varus angle and adduction moments are reduced after TKA (Orishimo et al. 2012), though coronal laxity in certain implants can improve ROM and varus/valgus balance (Matsuda et al. 2005). In this study, an increase in varus angle in the DFR and PTR groups was observed and therefore the results are not in

agreement with the findings of studies of TKA patients. The increase in coronal motion of the knee compared with TKA, could be a result of extensive resection of muscles and soft tissue and needs further investigation.

5.6.1.3 Ankle

The mean ankle joint angle in the sagittal plane at each phase within the gait cycle in the control group, was as described in the literature for normal gait (Kadaba, et al. 1990). In the joint-sparing and joint sacrificing distal femoral and proximal tibial groups, the overall mean ankle angle in the non-operated leg was similar to that measured in the control group, however the operated leg presented a different pattern. At LR, the operated leg in the JSF group demonstrated a 13° increase in plantar-flexion when compared with the control group and the non-operated leg. This is in agreement with the findings of gait kinematic studies in patients with conventional lower limb massive tumour implants, where the maximum plantar-flexion angle during early stance was greater in the operated leg compared with the healthy subjects (Okita et al. 2013; Bruns et al. 2016). In this study, the patients in the DFR and JSF groups presented smaller dorsiflexion of the ankle throughout the stance phase of the cycle, as reported in similar studies (Bruns et al. 2016). Okita et al. (2013) reported that during stance, the mean negative ankle joint power of the patients in the operated side was greater than that of the healthy subjects. This implies greater load on the ankle dorsi-flexors during loading response and ankle plantar-flexors during mid-stance (Okita et al. 2013; Carty et al. 2009), as a compensatory mechanism for the decrease in knee flexion during early stance (Kawamura et al. 1999; Okita et al. 2013). Increased load in the ankle of the operated leg was also observed by the longer activation time of the gastrocnemius in patients who underwent endoprosthetic knee replacement, when compared with healthy subjects (Carty et al. 2010).

The ankle in the non-operated leg in the joint-sparing and the joint sacrificing tibial replacements, presented a similar rotation angle to that of the control group, however the symmetry of the ankle joint rotation was poor throughout the gait cycle. At LR and TSS the joint-sparing and joint sacrificing distal femoral replacement groups presented a 2- and 3-fold increase in external rotation of the ankle in the operated and the non-operated legs, compared with the control group. At PS, ISW and MSW, while internal rotation of the ankle in the control group was observed, in the DFR group the ankle joint exhibited little to no rotation of the ankle in both legs and remained close to neutral position. The reduced internal rotation of the ankle in the operated leg in the DRF group cannot be related to damage to muscle and soft tissue structures below the knee and adjacent to the ankle joint as these are limited to fixation of the tibial component in the artificial rotating hinge knee. For fixation of the JSF implants, resection and subsequent reconstruction does not interfere structures in proximal tibial and therefore does not explain the changes in the ankle joint angle. The results of the study indicated poor symmetry of the ankle joint in both femoral replacements. This could be a compensatory mechanism for the reduced knee flexion to increase shock absorption at heel contact. In this study, the ankle rotation angle measured in the control group did not agree with those reported in literature as the ankle was in internal rotation at PS and throughout swing. However, Kadaba et al. reported that although the ankle rotates internally at PS, it remains in external rotation position for the remainder of the gait cycle (Kadaba et al. 1990). This discrepancy may be a result of the combined ankle and subtalar joint complex. The combination of the two joints allowed the transverse plane of rotation to take place proximally while the foot is in a fixed transverse plane position on the floor (Nester et al. 2003). Both the ankle joint and the subtalar joint are necessary parts of this mechanism (Lundberg et al. 1989).

Therefore, the results from one study may be presenting the resultant position of the subtalar and ankle joints while the other may only include the position of the ankle joint.

In the coronal plane while a slight supination of the ankle is expected at LR (approx. 2 degrees) in normal gait, the control group in this study exhibited an 8° mean ankle joint during this phase. As reported in the literature (Winter 1984, 1989), normal gait pronation of the foot is expected following LR and during stance. Results obtained in the control group agree with this. When compared with the DFR group, the overall mean ankle joint angle measured in the JSF group was more similar to the control group; however the DFR group presented a more symmetrical ankle movement. The result of the study presented here is contradictory to that reported in a similar study of patients who had conventional DFRs. In this study, the operated leg showed a significant reduction in pronation of the ankle in comparison to the non-operated leg and to the control group, resulting in a significantly reduced ROM (Bruns et al. 2016). These differences may be caused by the different implant designs investigated, thereby dictating different compensatory mechanisms. Furthermore, there is limited information regarding the kinematics of the ankle joint, particularly following limb salvage procedures. Further investigation with a larger number of patients is required form more conclusive results.

5.6.2 Joint Symmetry

In a study that investigated gait symmetry following limb-salvage surgery for treatment of bone tumours around the knee, Jang et al. (2012) investigated motion of the operated and non-operated legs in the pelvis, hip, knee and ankle in 8 patients and 8 healthy subjects. The results showed that while the moving trajectory of the right

and the left legs in healthy subjects were similar, the movement of the affected and non-affected legs in the patient group were different. The study also found that the moving trajectory of patients was significantly different from that of the healthy subjects (Jang et al. 2012). In the study presented here, patients with a DFR followed by those in the JSF group presented the best joint symmetry in all of the three joints measured and amongst all implant groups investigated. While this result does not support the initial hypothesis, the JSF group exhibited the most symmetrical hip adduction and flexion and knee rotation. Therefore, a larger number of patients is required to assess this hypothesis. The PTR group consistently had the least symmetrical gait amongst all patient groups and the JST group had an improved joint symmetry in comparison. This result supports the initial hypothesis that gait symmetry is improved in patients with a joint-sparing implant when compared with patients with a joint sacrificing endoprosthesis.

5.6.3 Vertical Ground Reaction Force

In all implant groups, a reduced VGRF at MWA and TO, and increased VGRF at MS in the operated and the non-operated legs compared with the control group, was observed. A greater difference was measured in the operated leg in all cases. The distal femoral and proximal tibial joint-sparing groups presented more similar VGRF to the control group, in comparison with the DFR and PTR groups, confirming the hypothesis. Reduced VGRF following limb salvage procedures around the knee has been previously reported (Tsuboyama et al. 1994; Bruns et al. 2016; Okita et al. 2014; Benedetti et al. 2000; Carty et al. 2010, 2009). An evaluation of foot pressure patterns in patients with a DFR showed that the value of force-time integral at heel contact did not change when compared to healthy individuals. In patients with a DFR, the heel has been reported to support the load with a wider contact area and longer contact time

(Tsuboyama et al. 1994) and this may be associated with conservation of muscle energy and interpreted as cautiousness in patients (Bruns et al. 2016). In patients who present a flexed knee gait, the reduced hip abduction torque and changes in the sagittal joint moments have been related to changes in VGRFs (Okita et al. 2013; Carty et al. 2009). Hip abductor muscles are thought to be the primary contributor to the VGRF in healthy individuals (Anderson and Pandy 2003). The reduction in VGRF in patients with a DFR and a PTR in this study, is likely to be related to the reduced knee flexion.

5.6.4 Time in Stance

The data presented in this thesis showed that the stance time in distal femoral and proximal tibial joint-sparing and joint sacrificing groups was increased in both the operated and non-operated sides when compared with the control group. The JST group spent significantly more time in stance when compared to the control and the PTR group, in both the operated and non-operated sides. This result does not support the hypothesis that joint-sparing implants provide a more normal gait than conventional joint sacrificing endoprostheses. In the JSF group, the mean stance time in the operated and non-operated legs was the same and more similar to the control group, while the mean stance time in the operated leg was shorter than in the non-operated leg in the DFR group, thereby supporting the hypothesis. In the DFR, PTR and JST groups, the time in stance in the operated leg was shorter than in the non-operated leg and this is supported by the literature. A study that investigated foot pressure pattern during gait in patients who underwent limb salvage surgery for treatment of bone tumours around the knee, found the duration of foot contact was shortened on the operated side compared to the non-operated side (Tsuboyama et al. 1994). Several other studies have also confirmed the shortened stance time in the operated leg, compared with the non-operated leg that could be associated with

subconscious protection of the "affected" leg by the patients (De Visser et al. 2000; Carty et al. 2009; Kawai et al. 1998; Beebe et al. 2009). Tsauo et al. found that the ratio of extensor strength of the operated to the non-operated knee and isometric hamstring to quadriceps ratio of the operated knee was significantly correlated to the difference in stance time in the operated and non-operated sides (Tsauo et al. 2006). It has been confirmed that the time in stance and swing becomes more symmetrical in the operated and non-operated leg over time (De Visser et al 2003), and may be the reason for the more symmetrical stance time in the JSF group seen in this study. In this chapter, it was important to investigate patients that were pain free as pain can have a significant effect on patients' gait and duration of stance and swing.

5.6.5 Step Exercise

The step exercise was designed to create a simple method to assess stability when using steps. This was done by assessing the trajectory of the sacrum marker. The aim was to create a more challenging scenario for the patients in contrast with the simple level walking. However, the results did not demonstrate any clear pattern. There are relatively few studies that have focused on stair climbing (Kennedy et al. 2007). Human motion analysis during stair climbing, requires more complicated modelling and calculations (Bhatt et al. 2017) and this was not within the capacity of this project.

5.6.6 Leg Length

Equality in leg length was improved in distal femoral and proximal tibial joint-sparing groups, confirming the hypothesis. While leg length discrepancy was not statistically significant when the JST, PTR, DFR and JSF groups were compared with the control group, larger leg length inequality was found in all implant groups in comparison with the healthy subjects. Tsuboyama et al. (1994) reported leg length discrepancy in 8 out

of 20 patients with a DFR. On average the operated leg was 6mm shorter and a positive correlation between the extent of shortening of the operated leg and peak pressure in the heel of the non-operated foot was found (Tsuboyama et al. 1994). Therefore, the greater leg length discrepancy measured in the joint sacrificing groups could be the cause of the poor load transfer in this groups of patients in this study.

5.6.7 Limitations

This study had a number of limitations. Firstly, the patient groups were not matched. Although the distal femoral and proximal tibial joint-sparing groups were compared with patients with a joint sacrificing implant of the same anatomical location, patients' gender, age and time from surgery were not matched. There are many variables involved in limb salvage surgery for bone tumours. The type and length of pre- and post-surgery treatments varies in different patients, which can lead to different functional outcomes. For example, some patients could have a reduced range of motion as a result of any radiotherapy they may have received. Radiotherapy damages the skin, subcutaneous tissues and muscles and can cause fibrosis. It is associated with decreased tissue elasticity and contractures, resulting in joint stiffness (Oren et al. 2004). The post operation rehabilitation plan is also different in patients; for example, the type of physiotherapy exercises, intensity and frequency of the sessions can significantly impact the recovery of the patients (Zhang et al 2016). The patient groups investigated in this study were not matched by time from surgery and it has been found that limb function improves over time (De Visser et al 2003). One of the major variables in oncology patients is the level of resection and the amount of muscle and soft tissue removed during surgery. Patients with larger resections or with more of the soft tissue removed, are expected to have a more impaired function.

An additional limitation of this study was the small number of participants in each group. The values of standard error provided in the results section showed the variability of data obtained. Although a large amount of data was obtained in this study, other gait determinants such as pelvic rotation, pelvic tilt, trunk flexion, pelvis displacement, step and stride lengths and time in swing were not included.

This study was conducted in an experimental setting. All participants had several pieces of equipment that was attached to them, including the markers for data collection and were in a laboratory environment, aware of being observed and this may have affected their gait.

For the purpose of this study an active marker system was used for capturing the spatial data. This equipment may be unable to capture data as accurately as some other motion analysis systems, such as passive marker systems that are available and can detect smaller differences in motion (Richards 1999). The changes in gait in limb salvage patients is subtle and in many cases is undetected by untrained individuals. Therefore, more advanced equipment that can detect small differences in motion may enable a more accurate assessment of joint-sparing implants.

5.7 Conclusion

In summary, the following can be concluded:

- The hypothesis regarding the improved gait in joint-sparing implants compared with the knee sacrificing implants was disproved. Although joint-sparing proximal tibial groups had a more symmetrical gait, the conventional distal femoral group had an improved, more normal gait when compared with the

joint-sparing distal femoral group, with respect to gait symmetry and stance time.

- Gait, both in terms of joint angles and symmetry was worse in proximal tibial implants than in distal femoral implants. Joint sacrificing proximal tibial implants had the worst gait when compared with all the other implant groups.
- Time in stance in the operated leg was shorter than in the non-operated leg, in all implant groups.
- Following limb salvage surgery around the knee, kinematics of all other joints such as the hip and ankle are significantly altered and must be evaluated. All groups of patients use compensatory mechanism for the loss of muscle power and poor extensor mechanism of the knee joint.
- Load transfer is improved in joint-sparing implants when compared with the joint sacrificing implants; the hypothesis regarding VGRF was proved.
- The step exercise was inadequate and did not provide any results that could be conclusive.
- The hypothesis regarding the leg length discrepancy being greater in patients with joint sacrificing implants when compared with the joint-sparing groups was proved, although it was not significant.

In the future, a more comprehensive study with a larger number of patients may identify a more specific trend in the compensatory mechanisms used in patients with joint-sparing and sacrificing implants. Using more advanced equipment may enable us to collect more accurate data that identifies smaller spatial position changes. Combining the gait kinematic data with electromyography (EMG) may also provide valuable information regarding the compensatory mechanisms, detected through different muscular activities.

Chapter 6 Finite Element Analysis of a Knee Sparing Distal Femoral Replacement and Adjacent Residual Bone

6.1 Introduction

Finite Element Analysis (FEA) has become a powerful tool in the field of orthopaedic surgery by assisting surgeons and implant designers to better understand the biomechanical changes that occur in the implant and bone following implantation. For example, FEA has been used to predict changes in stress and strain distribution in the bone adjacent to the implant to prevent complications caused by unsuitable prosthetic design (Herrera et al. 2012). In this chapter, FEA was used to analyse the stress distribution within the distal femoral bone and a joint-sparing distal femoral implant when subject to forces and bending moments associated with loading the implant. FEA was used to investigate the optimum resection level when implanting a distal femoral joint-sparing implant and the changes that occur in the bone and the implant when key design features are altered.

6.2 Objectives

The aim of this chapter was to assess the risk of fracture in extra-cortical plates of different thickness by examining Von Mises stress (VM) and strain (E). This chapter

also aimed to identify the optimal resection level required when inserting a knee sparing implant by investigating Von Mises stresses within the implant and cortical bone and also by measuring Strain Energy Density (SED) within bone adjacent to the plates.

Finally, this chapter aimed to assess whether the use of biomaterials of low stiffness increased the risk of plate fracture and increased stresses within adjacent bone, improving bone formation and implant fixation. This was examined using the VM stress criterion and SED.

6.3 Hypothesis

In this chapter it was hypothesised that:

- The risk of extra-cortical plate fracture in the current design of distal femoral joint-sparing implants is low.
- Reducing the thickness of extra-cortical plates, which can reduce bulkiness around the knee and improve soft tissue coverage, does not result in fracture of the plates.
- Implant resection levels closer to the knee joint, produce lower stresses within cortical bone adjacent to the implant and increase the risk of stress shielding.
- The risk of fracture of the extra-cortical plates is higher when materials with lower Young's modulus, such as porous titanium and PEEK are used as implant material, however it is unlikely.
- Using porous titanium or PEEK, can reduce the risk of stress shielding on the cortical bone adjacent to the plate and encourage bone formation, compared with the knee sparing implants made with solid titanium alloy.

6.4 Method

6.4.1 Geometry

Computer tomography (CT) images were taken of the left femur obtained from a female cadaveric donor with no pathology or history of musculoskeletal disease (Vesalius Clinical Training Centre, University of Bristol, UK). The specimen was submerged in water and 0.5mm thick slices were scanned using a standard clinical CT scanner (Brilliance, Philips Healthcare, UK). Scans through the femur were obtained at a peak voltage of 120kV and a tube current and planned current of 240mA.

The CT images were sent to Stanmore Implants (Elstree, UK) where 4 simplified custom distal femoral joint-sparing implants were designed using CAD software (Unigraphics, Siemens PLM Software). A detailed description of the design of joint-sparing implants is provided in Chapter 2, Section 2.4. One of the four implant designs produced by Stanmore Implants was a control implant. This distal femoral implant was designed using current features where the implant allowed for a 45mm resection level measured from the base of the femoral condyles and was composed of two 3mm thick extra-cortical plates. This model was also used to investigate the effect of material stiffness on the stresses within the bone and implant. The assignment of different material properties was carried out following the mesh generation step, and is explained in Section 6.4.4 of this chapter. The 45mm resection level was based on the average resection level measured in all patients listed within the database held by Stanmore Implants. The metrics of each patient with a joint-sparing distal femoral implant were used and patient data was anonymized. Two other implant models were designed to allow for a 35mm and 55mm resection level where both models also had two extra-cortical plates that were 3mm thick. The fourth implant model was designed

to allow for a 45mm resection level with two extra-cortical plates of 1.5mm thickness. For the purpose of this thesis the bone-implant models were simplified and the extra-cortical plates did not have slots or holes for screw fixation. In reality the implant is fixed to the bone using uni- or bi-cortical screws.

To create the bone-implant model, the CT images of the bone were imported into Mimics® (Materialise, Belgium), an image processing software that can generate 3D models from 2D images. More information about this process is given in Chapter 2, Section 2.4.3. A mask was created from the CT images in order to generate a 3D model that included both the cancellous and cortical bone. Once the 3D bone model was created, the implant model was imported into Mimics® as an STL file. To ensure correct alignment of the 3D bone and the implant models, the 'contour' function of the software that showed the outline of both objects in the plane view, was used to inspect their alignment and contact in 3 spatial planes.

Following alignment of the models, the 3D bone model was cut using the 'poly plane' function of the software in simulation module. Two points on the bone and along the plateau of the implant were chosen to create the cutting plane. The dimensions of the plane were edited to ensure that the cutting plane covered the entire surface of the plateau and a plane thickness of 0.1mm was chosen. The orientation of the plane was adjusted so that it was fully parallel and tangential to the implant plateau and not intersecting the implant. Once the cut was made, the distal and proximal parts of the bone model were split. The distal section that included the femoral condyles was then wrapped, using a closing factor of 0.5mm and saved to be meshed for Finite Element Analysis (FEA). Wrapping is used to enhance complex geometries by closing the gaps between surfaces. For the intact bone model, all the above steps were carried out but

the cut was made 150 mm from the base of the condyles to match the height of the bone-implant model.

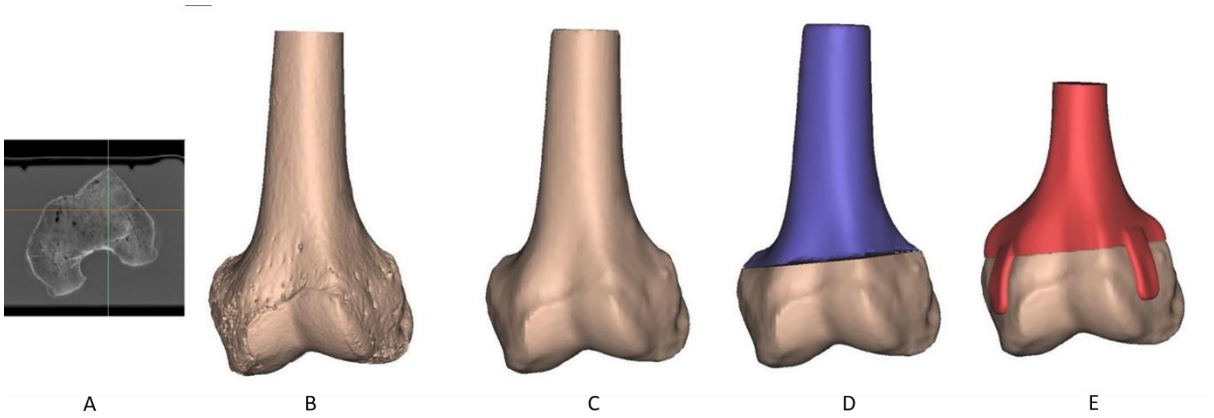

Figure 6.1 [A] A 2D CT image of femoral bone; [B] 3D bone image generated from 2D CT images; [C] wrapped 3D bone prior to cutting for alignment with the implant; [D] 3D bone has been cut and split to two parts; [E] The implant and femoral condyles are aligned.

6.4.2 2D Mesh Generation

The wrapped bone and the implant models were exported from Mimics® into 3-matic® (Materialise, Belgium), a module of Mimics® software that is used for mesh generation and 3D printing. To achieve accurate FE results, a uniform volume mesh of the model was required. The imported wrapped bone and implant model included a rough surface mesh and no volumetric mesh. The bone model was smoothed to eliminate all sharp edges and porous surfaces; a smoothing factor of 0.500mm was used. The number of elements in the mesh was then reduced to prepare both the implant and the bone for a finer mesh. Prior to generating the mesh an "inspection scene" was opened within the software to monitor the quality of the mesh triangles. A shape measure of height to base ratio (Height/Base (N)) and quality value of 0.4 was set within the inspection scene. A regular mesh with nodes roughly on the surface and

even length edges, generate more accurate results, as small displacements are distributed among all sub-items relatively equally. For mesh generation, the "Auto Remesh" function from the remesh module of the software was used and each object was remeshed individually. The auto remesh was carried out in two steps and the set parameters for the first step are given in Table 6.1.

Table 6.1 Auto remesh parameters for the first stage of 2D mesh generating

Shape measure	Height/Base (N)
Shape quality threshold	0.4000
Maximum geometric error	0.2000
Maximum triangle edge length	2.000 mm
Number of iterations	3

In the second step, the maximum geometric error and the maximum triangle edge length were reduced and the number of iterations was increased to generate a finer mesh with fewer distorted, low quality triangles. The auto remesh parameters used are listed in Table 6.2.

Table 6.2 Auto remesh parameters for the second stage of 2D mesh generating

Shape measure	Height/Base (N)
Shape quality threshold	0.4000
Maximum geometric error	0.1000
Maximum triangle edge length	1.000 mm
Number of iterations	5

Once the 2D mesh was generated, all duplicated and overlapping triangles were removed while preserving the quality of the triangles using the "quality preserved reduced triangle" function of the software. All mesh parameters from the previous step remained unchanged (Table 6.2).

To create a single model from two complex geometries, a “non-manifold assembly” was created. Manifold is a geometric topology term that allows disjoint parts to exist in a single logical body. A non-manifold means all disjoint parts will be their own logical body. In a non-manifold assembly, although the objects are part of one assembly with a shared area, each object is its own individual component, with its individual properties. The shared area between the objects is in fact the actual non-manifold condition. In order to create a non-manifold assembly, first the two meshed objects were aligned in such a way that the bone and the implant were intersected and in full contact. This caused the implant model to dig into the bone model in some areas. Once the two meshed objects were aligned, the assembly was created using the “create non-manifold assembly” function of the remesh module.

6.4.3 Generating a Volume Mesh

The finite element mesh is a key factor for an efficient analysis. The type of element and the mesh density affect the accuracy of the results (Ramos and Simões 2006). The mesh element type used in this thesis was a 4-node linear tetrahedral element that is suitable for irregular and complex geometries. This type of element is indicated as “Init” within the 3-matic software. The method used for generating the volume mesh was “Init and Refine” that fills the volume and fits the tetrahedral elements more appropriately. The edge length was controlled to limit the size of tetrahedral elements to set dimensions. For the purpose of this study an “Aspect Ratio” mesh quality assessment method was used and the shape quality threshold was set to 25 (Table 6.3).

Due to the interaction of two independent objects i.e. the bone and implant, at the bone implant interface a finer mesh was generated. The local remesh function was used and area of the bone-implant interface was chosen as the entity to create a local mesh

(Figure 6.2). The parameters chosen for the generation of a local mesh are given in Table 6.4.

Table 6.3 Remesh parameters for the generation of volume mesh

Method	Init and Refine
Shape quality threshold	25.000
Shape measure	Aspect ratio (A)
Maximum edge length	1.000 mm

Table 6.4 Remesh parameters for the generation of local volume mesh at the bone-implant contact

Method	Init and Refine
Shape quality threshold	25.000
Shape measure	Aspect ratio (A)
Maximum edge length	0.500 mm

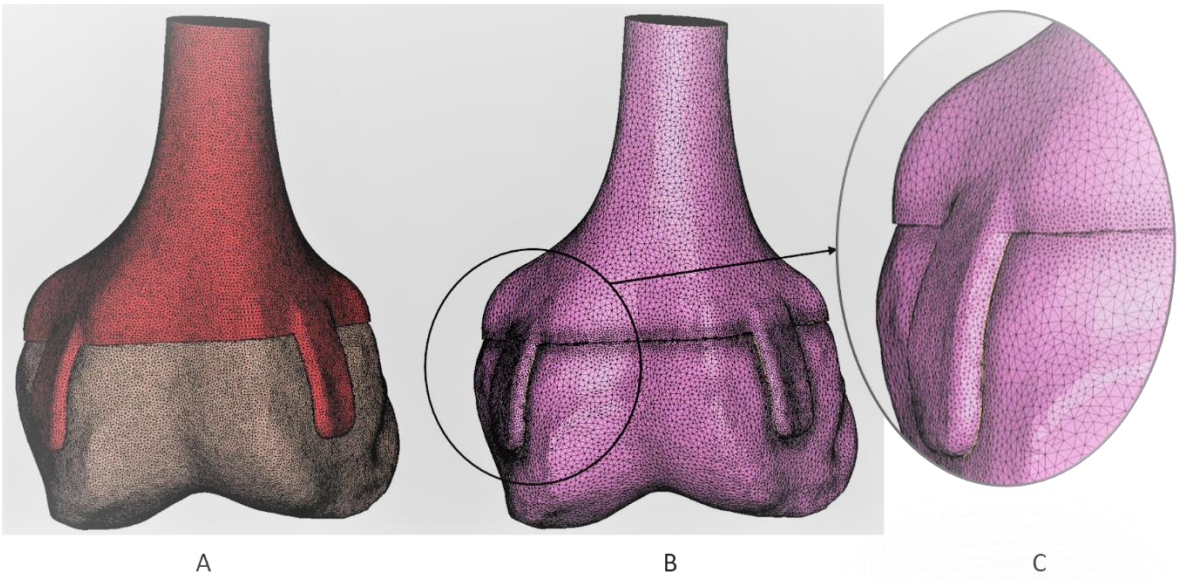

Figure 6.2 [A] The bone and implant are meshed as two individual objects. [B] A non-manifold assembly, consisting of the bone and the implant has been formed and remeshed. [C] A finer local mesh at the bone-implant contact was generated.

6.4.4 Material Assignment

The 3D meshed assembly was imported from 3-matic to Mimics for material assignment. The greyscale values within the CT images were included in the 3D meshed assembly and represented material density. These values were used to assign material properties to each of the elements in the volume mesh. Two quantitative relationship empirical expressions were used to convert the grey value into a density value and elastic modulus value. These expressions are provided in Equations 6.1 and 6.2 (Qiu et al. 2012).

Density = -13.4 + 1017 * HU **Equation 6.1**

Young's modulus = -388.8 + 5925 * Density **Equation 6.2**

Where HU is the Hounsfield Unit.

To simplify the FEA models, the range of grey values of the volume mesh were divided into ten equal-size intervals each representing one material (Figure 6.3). The central grey value of each interval was chosen as a representative for that interval. A Poisson ratio of 0.3 was assigned to all materials in the Material Editor. Figure 6.3 shows an image of the material editor and the relationship between colour and the material property values. The variable material properties of the bone model indicated the inhomogeneous nature of the bone.

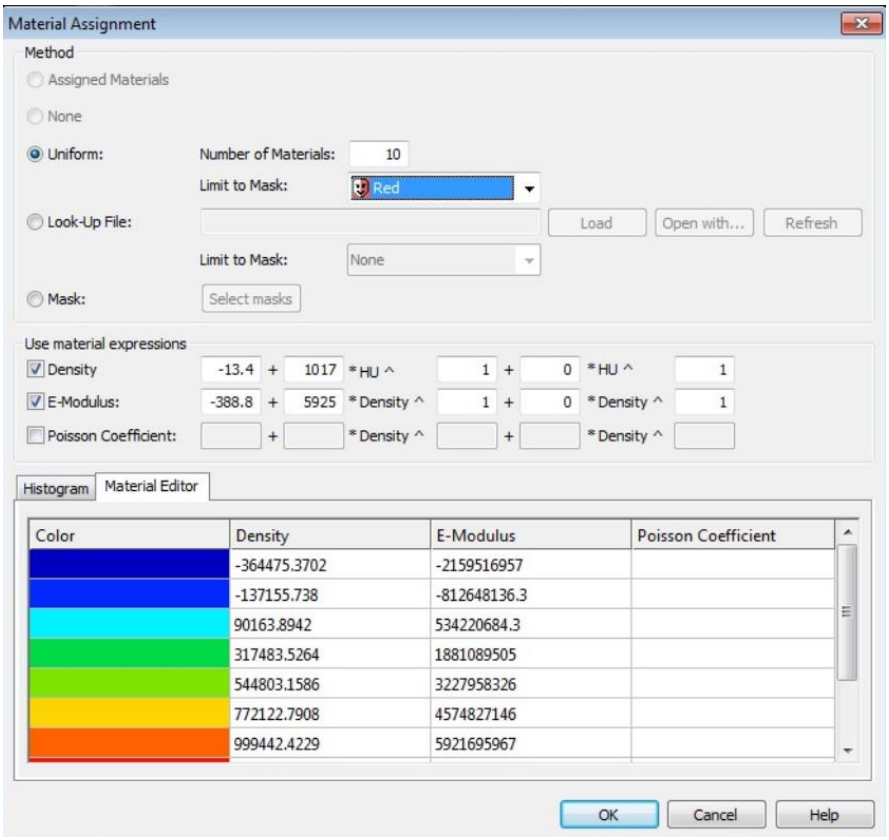

Figure 6.3 Image of the Material Editor window within Mimics. The grey values within the bone volume mesh were divided into 10 equal-size intervals that each represents one material.

Material assignment was applied manually for the implant. The mechanical properties for each type of material are given in Table 6.5.

Table 6.5 Density, Young's Modulus and Poisson's ratio given to each type of material

Material	Density (Kgm^{-3})	Young's Modulus (GPa)	Poisson's Ratio
Titanium Alloy	4430	114.00	0.33
Porous Titanium (30% Porosity)	3100	18.00	0.22
PEEK	1290	3.85	0.40

The final model of a non-manifold assembly composed of a linear tetrahedral elemental volumetric mesh with assigned material properties (Figure 6.4) was

imported to Abaqus/CAE (Dassault Systèmes Simulia Corp.) for Finite Element Analysis.

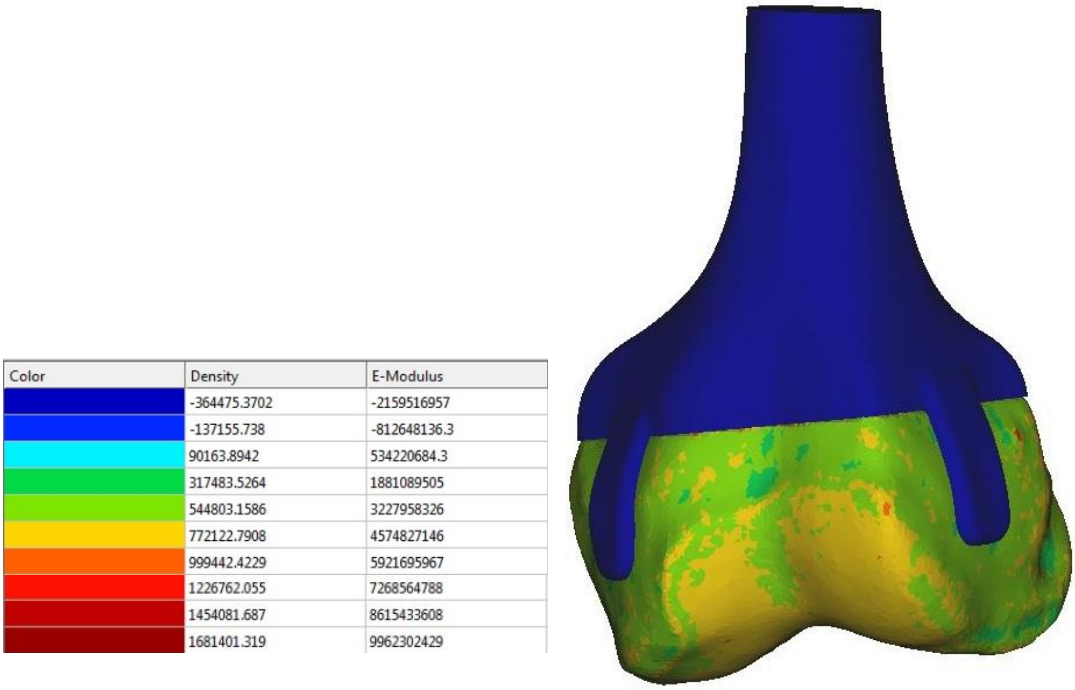

Color	Density	E-Modulus
	-364475.3702	-2159516957
	-137155.738	-812648136.3
	90163.8942	534220684.3
	317483.5264	1881089505
	544803.1586	3227958326
	772122.7908	4574827146
	999442.4229	5921695967
	1226762.055	7268564788
	1454081.687	8615433608
	1681401.319	9962302429

Figure 6.4 Bone-implant model after material assignment. The implant was given the mechanical properties of Ti alloy and has uniform properties throughout the geometry. The voxels of the femoral condyle have different material properties depending on their grey values. Different shades of green, yellow, orange and red indicate different material properties. The scale represents the material properties of the elements within the bone model, only.

6.4.5 Loading Condition

A study carried out by Taylor and Walker (2001), measured the axial force, torque and bending moments in the shaft of the femur using an instrumented massive distal femoral replacement. Forces in the implant were measured for several gait activities including walking and jogging at three intervals over a three year period and their correlation with body weight (BW) was calculated (Figure 6.5).

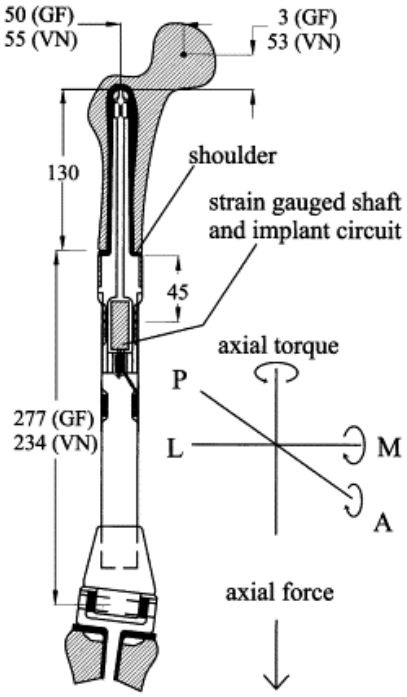

Figure 6.5 Schematic of the instrumented distal femoral replacement used for measurement of forces (Taylor and Walker 2001)

The maximum forces recorded during a gait cycle when the knee is fully extended during walking and jogging at 132 weeks was selected for this study and a body mass of 70kg was assumed. The calculations were made based on the length of the bone-implant model (150mm). A summary of the loads applied is presented in Table 6.6.

As the elements chosen for the FE analysis were linear tetrahedral with no rotational degrees of freedom (DOF), two equal and opposite concentrated forces were applied to represent torsion and bending moments (Figure 6.6).

Although implementation of the bending moments in this way may introduce a shear stress it is assumed to be negligible. The axial load was applied as uniform pressure to the base of the implant (Figure 6.6C).

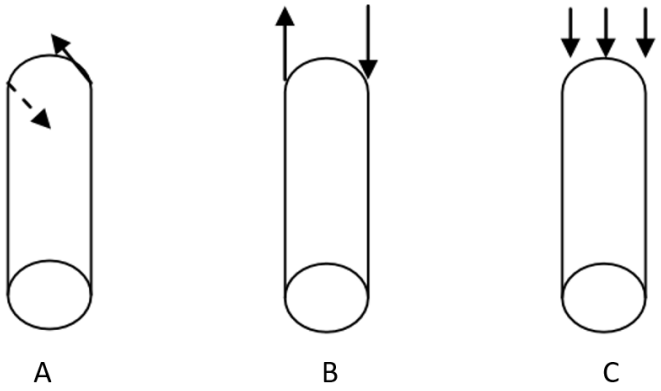

Figure 6.6 Application of [A] torsion and [B] bending moment, using two opposite and equal concentrated forces. [C] Axial force was applied as uniform pressure.

Table 6.6 Loads applied to the FE model, calculated from values by Taylor and Walker study (Taylor and Walker 2001).

Activity	Type of Load	Axial load	AP Bend	ML Bend	Torsion
Walking	Body Weight	3.3 BW	96.0 BWmm	57.0 BWmm	57.0 BWmm
	Newton	2266.11 N	2746.80 Nm	1630.91 Nm	4.12 Nm
	Applied load	**5.01 MPa**	**1428.34 N**	**848.07 N**	**171.80 N**
Jogging	Body Weight	3.82 BW	113.0 BWmm	79.0 BWmm	6.0B Wmm
	Newton	2623.20 N	3233.21 Nm	2260.39 Nm	4.12 Nm
	Applied load	**5.80 MPa**	**1681.27 N**	**1175.40 N**	**171.80 N**

6.4.6 Boundary Conditions

Boundary conditions are applied to mesh nodes to constrain their movement in any or all six degrees of freedom. In applying boundary conditions to a biomechanical FE model, assumptions have to be made based on the part of the human body being modelled and the main areas of interest on the model. For the purpose of this study "ENCASTRE" fixation was selected to fix the model in all 6 degrees of freedom at the distal end of the femoral condyles, eliminating movement in all directions.

ENCASTRE means completely fixed or clamped. This model aimed to mimic the knee joint (Figure 6.7).

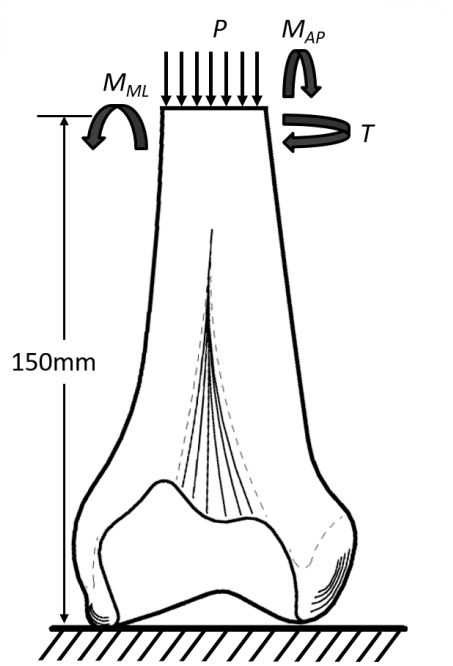

Figure 6.7 Schematic of the loading and boundary conditions applied. M_{ML} and M_{AP} indicate bending moments applied in the M/L and A/P directions, respectively. Torsion (T) and the axial force that was applied as pressure (P) are also indicated. Each model was approximately 150mm high and was constrained (ENCASTRE) at the condyles.

6.4.7 Contact Conditions

A "tie" contact between the bone and the implant model was applied to allow the parts to be effectively fused together, deforming and transferring forces as one.

At the early stages of the study, two other models were assessed:

1. A bone model that included two types of material, namely cancellous and cortical bone. During segmentation of the 2D CT images, two masks were generated, one with a lower threshold value to represent cancellous bone and the other a higher threshold representing cortical bone. The two separate parts

were remeshed and assigned uniform material properties of cancellous and cortical bone before being assembled and imported into Abaqus/CAE. A tie interface was applied between the two parts. However, this model did not generate any results. Although during segmentation of the 2D images the threshold value did not overlap, as Mimics® generated masks based on the average grey value in each pixel, some parts of the geometry were common in both cortical and cancellous bone. Thus, during FE analysis these mesh elements overlapped and the calculations failed. Additionally, due to the large gaps in both geometries, the parts couldn't be wrapped and incorrect results were generated. Therefore, results from this model are not presented in this thesis.

2. The second scenario included introduction of friction between the bone and the implant. In another words a sliding interface, where the two parts move relative to each other. This model aimed to create a near to reality interface condition between the bone and the implant where the bone and the implant were not tied and moved relative to each other. In this case, following the creation of a non-manifold assembly and generating a volume mesh, the non-manifold assembly was separated. This would ensure a perfect contact surface between the bone and the implant while generating two surfaces; one on each part to allow for assignment of contact conditions. Once the material properties were assigned to each part, both parts were imported to Abaqus/CAE. The contact condition of "sliding" was chosen and the bone-implant interface was selected as the contact surface. The mechanical condition of "friction" with a coefficient of friction of 0.3 was selected (Nuno et al., 2001; Completo et al., 2007). The bone contact surface was the "master" and the implant contact surface was the

"slave" surface. The slave surface moves relative to the master surface. A number of nodes on each plate were tied to their corresponding nodes on the bone to represent the screw fixation. Although the FE calculation was completed, the results did not indicate an accurate outcome as large displacement of the implant was observed. Therefore, the results from this model are not presented in this thesis.

6.4.8 Mesh Sensitivity Study

A convergence study was carried out to identify the appropriate mesh size. FEA provides an approximate solution to a problem and therefore, the smaller the elements the more accurate the solution will be, particularly in areas of stress concentration. However, computing a very fine mesh, particularly in a complex geometry with 11 different material properties is time consuming. Therefore, a compromise between accuracy and time taken to compute the results was made.

The same geometry, material and boundary conditions as the control model were used to assess the Von Mises (VM) stresses recorded in areas of interest, i.e. bone adjacent to the implant and the extra-cortical plates. The geometry was meshed with maximum element edge length of 3mm and a varying element size at the bone-implant interface. A permissible relative error of 5% in all 4 areas was used to choose the mesh. The number of elements, included in each model for each element size is provided in Table 6.7.

Figure 6.8 shows the change in VM stress by change in mesh size in four different areas; two on the implant and two on the bone. 'Implant 1' and '2' lines shown in Figure 6.8 indicate the maximum stress on the right and left extra-cortical plates,

respectively and ‘Bone 1’ and ‘2’ represent the maximum stress on the bone elements adjacent to the right and left extra-cortical plates.

The mesh size chosen for this study was the 1.0mm element size, as less than 5% variation was calculated for a mesh size of 0.5mm edge length when compared to 1.0mm edge length.

Table 6.7 Number of elements and their type included in each model for mesh sensitivity study.

Element Size (mm)	No. of Element	Type of Element
0.5	6,266,356	Linear Tetrahedral
1.0	1,177,348	Linear Tetrahedral
1.5	565,160	Linear Tetrahedral
2.0	404,617	Linear Tetrahedral
3.0	334,653	Linear Tetrahedral

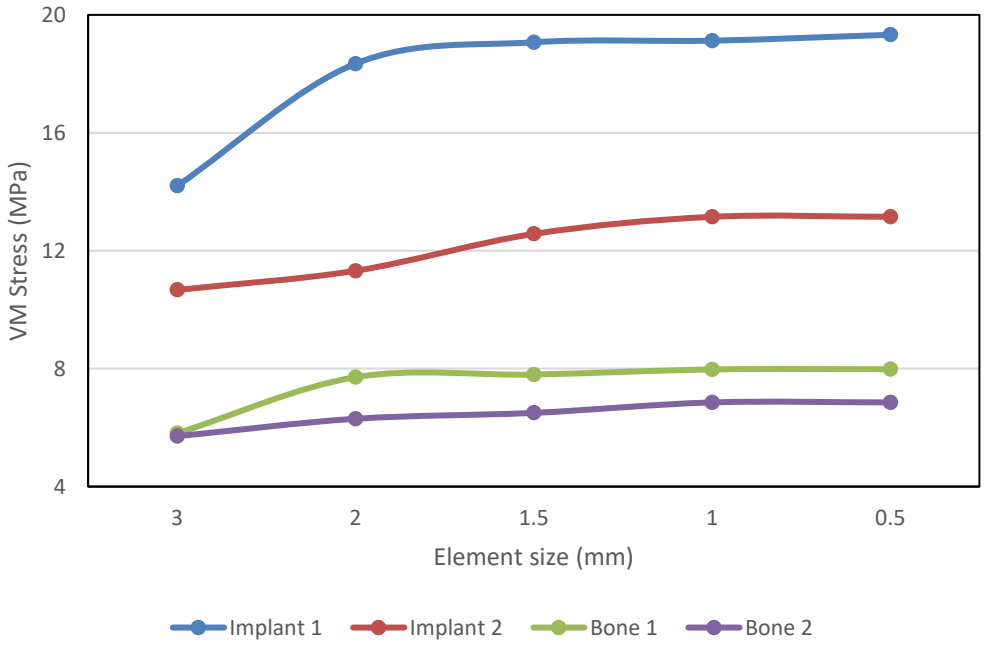

Figure 6.8 Convergence study in Abaqus/CAE, in four high stress areas: right extra-cortical plate adjacent to the bone (Implant 1), left plate adjacent to the bone (Implant 2), cortical bone adjacent to the right plate (Bone 1) and cortical bone adjacent to the left plate (Bone 2). The lines indicate that the 1mm element size was suitable for the study.

6.5 Results

6.5.1 Stress on Implant and Femoral Bone

Analysis of stress distribution in all cases indicated that the anterior side of the implant was under compression loading while the posterior side was in tension. For all 6 models, the maximum Von Mises (VM) values in the medial and lateral side of the bone and implant, in both loading conditions were investigated. The results of this study are presented as Von Mises values as VM stresses provide a single value that takes into account shear stresses as well as normal stresses. Thus, any influence from the shear stresses due to the torsion load would be detected. Von Mises stress can be calculated by the expression provided in Equation 6.3.

$$\boldsymbol{\sigma_e = \frac{1}{\sqrt{2}}[(\sigma_1 - \sigma_2)^2 + (\sigma_2 - \sigma_3)^2 + (\sigma_3 - \sigma_1)^2]^{1/2}} \qquad \textbf{Equation 6.3}$$

Where, σ_e is the Von Mises equivalent stress and σ_1, σ_2 and σ_3 are principal stresses.

The value and location of maximum VM stress in the implant in each model for both walking and jogging loadings are summarised in Table 6.8 to Table 6.11. The maximum VM stress in the intact bone model was 1.19MPa and 1.86MPa when walking and jogging loads were applied, on the anterior surface of cortical bone. In all implant models and for both loading conditions, maximum stresses were observed in the extra-cortical plates and at the plate-shaft interface (Figure 6.10). The highest concentration of stresses were observed at the plate-shaft interface in the model with 1.5mm thick plates, where 24.7MPa in the antero-medial and 16.7MPa in the antero-lateral plate for the walking load and 28.7MPa and 19.0MPa for the jogging load were measured.

When comparing the three resection levels investigated in this Chapter, the 55mm model had the highest concentration of stresses in the antero-medial plate, while the 35mm resection implant had the lowest stress concentration, in both plates and for both loading conditions, indicating a reduced risk of plate fracture. The lowest stresses on the extra-cortical plates were observed in the implant with assigned PEEK material properties where 1.83kPa was measured in the antero-medial plate when subject to walking loading.

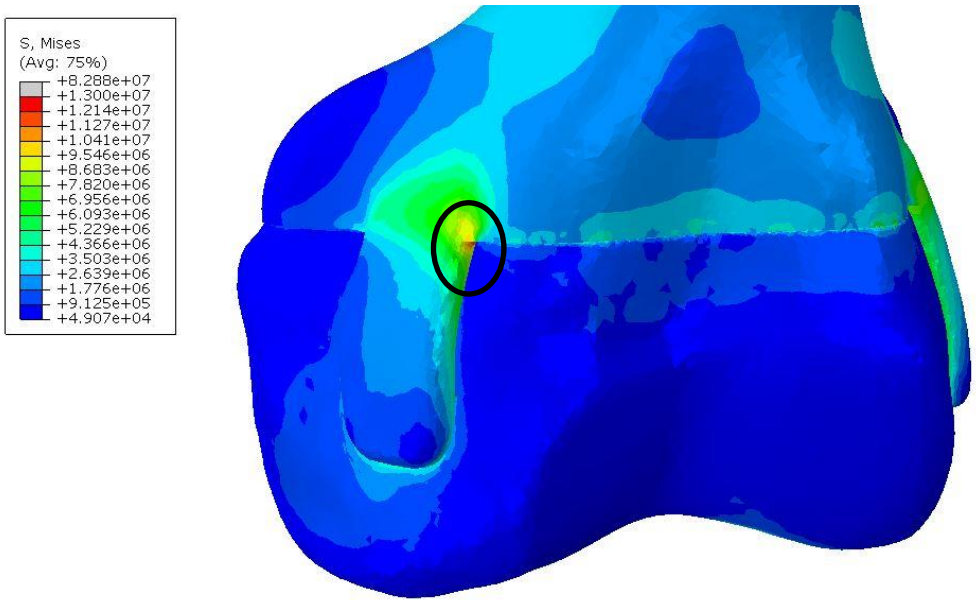

Figure 6.9 VM stress distribution on the standard model under walking loading; low stresses are present on the bone. The highest stress concentration is at the plate-shaft interface.

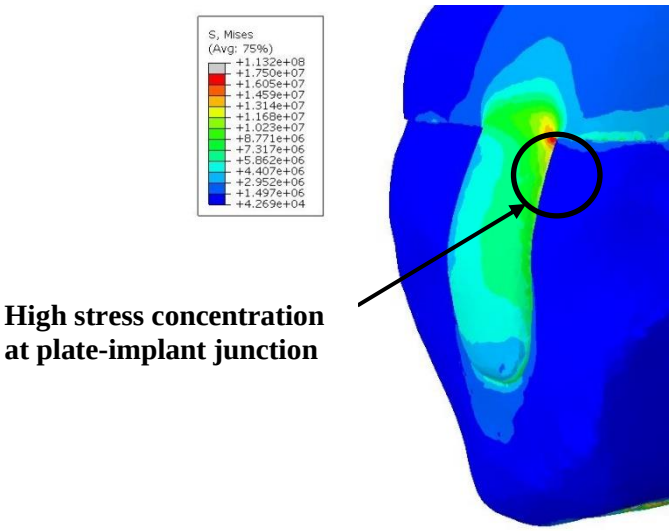

Figure 6.10 Image of the implant with 1.5mm thick extra-cortical plates under walking load. The highest stress concentration of 24.7 MPa was seen at the plate-shaft interface of this model, when subject to jogging loading.

Table 6.8 Maximum VM stresses on the antero-medial plate of each implant for walking load

Model	Load	Part	Max V-Mises (Nm^{-2})	Location
Standard Model	Walking	Implant	1.83E+07	A/M Plate; Plate-shaft interface
55mm Resection	Walking	Implant	2.24 +07	A/M Plate; Plate-shaft interface
35mm Resection	Walking	Implant	1.11E+07	A/M Plate; Plate-shaft interface
Porous Ti Implant	Walking	Implant	5.01E+06	A/M Plate; Plate-shaft interface
PEEK Implant	Walking	Implant	1.83E+03	A/M Plate; Plate-shaft interface
1.5mm Thickness Plates	Walking	Implant	2.47E+07	A/M Plate; Plate-shaft interface

Table 6.9 Maximum VM stresses on the antero-lateral plate of each implant for walking load

Model	Load	Part	Max V-Mises (Nm^{-2})	Location
Standard Model	Walking	Implant	9.77E+06	A/L Plate; Plate-shaft interface
55mm Resection	Walking	Implant	1.19 +07	A/L Plate; Plate-shaft interface
35mm Resection	Walking	Implant	6.78E+06	A/L Plate; Plate-shaft interface
Porous Ti Implant	Walking	Implant	3.97E+06	A/L Plate; Plate-shaft interface
PEEK Implant	Walking	Implant	2.29E+06	A/L Plate; Plate-shaft interface
1.5mm Thickness Plates	Walking	Implant	1.67E+07	A/L Plate; Plate-shaft interface

Table 6.10 Maximum VM stresses on the antero-medial plate of each implant for jogging load

Model	Load	Part	Max V-Mises (Nm^{-2})	Location
Standard Model	Jogging	Implant	2.13E+07	A/M Plate; Plate-shaft interface
55mm Resection	Jogging	Implant	2.27 +07	A/M Plate; Plate-shaft interface
35mm Resection	Jogging	Implant	1.29E+07	A/M Plate; Plate-shaft interface
Porous Ti Implant	Jogging	Implant	5.91E+06	A/M Plate; Plate-shaft interface
PEEK Implant	Jogging	Implant	2.12E+06	A/M Plate; Plate-shaft interface
1.5mm Thickness Plates	Jogging	Implant	2.87E+07	A/M Plate; Plate-shaft interface

Table 6.11 Maximum VM stresses on the antero-lateral plate of each implant for jogging load

Model	Load	Part	Max V-Mises (Nm^{-2})	Location
Standard Model	Jogging	Implant	1.12E+07	A/L Plate; Plate-shaft interface
55mm Resection	Jogging	Implant	1.69E+07	A/L Plate; Plate-shaft interface
35mm Resection	Jogging	Implant	7.70E+06	A/L Plate; Plate-shaft interface
Porous Ti Implant	Jogging	Implant	4.55E+06	A/L Plate; Plate-shaft interface
PEEK Implant	Jogging	Implant	2.65E+06	A/L Plate; Plate-shaft interface
1.5mm Thickness Plates	Jogging	Implant	1.90E+07	A/L Plate; Plate-shaft interface

In all bone-implant models the location of the highest stresses was seen on the implant and areas of bone where the edges of the plates and the plateau of the implant had cut into the bone (Figure 6.11 and Figure 6.12). The results showed that stresses decreased in the femoral condyle compare with the intact bone, except around the areas of the implant that cut into the bone. Highest stress distributions on bone was associated with the PEEK implant (Figure 6.13). In each case maximum stress occured in cortical bone immediately adjacent to the plate. The areas of maximum stress on the bone, in the medial and lateral sides, for both the walking and jogging loading conditions are sumarised in Tables 6.12 to 6.15.

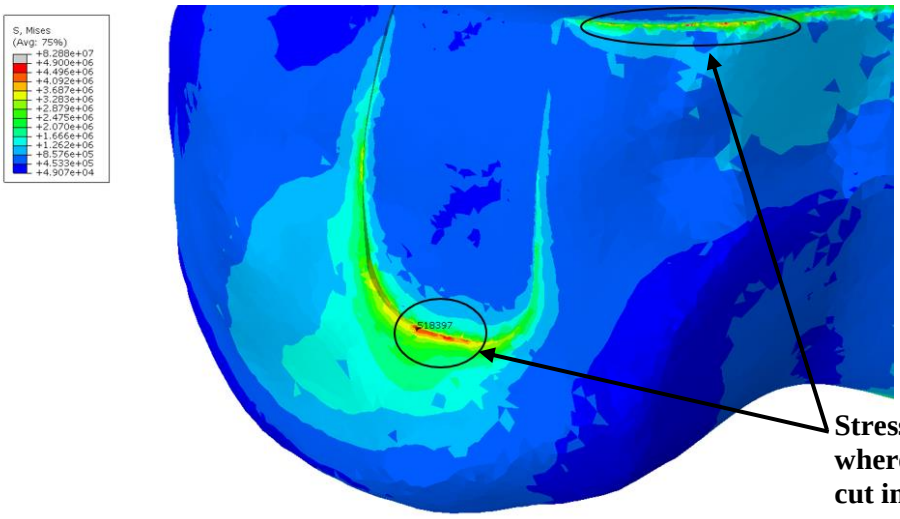

Figure 6.11 Image shows the medial side of the femoral condyle (with the implant removed). Overall low stresses are present on the bone. A high stress concentration is visible at contact areas adjacent to the implant shaft and plates.

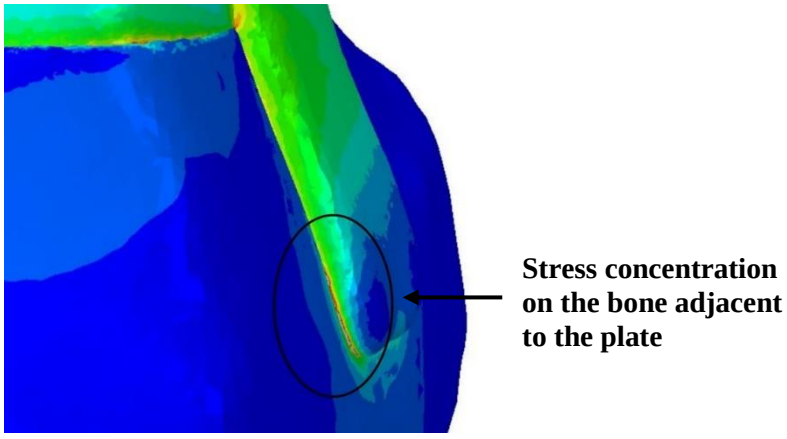

Figure 6.12 Highest stress concentration on the femoral bone adjacent to the extra-cortical plate in implant designed for a 55mm resection level.

Table 6.12 Maximum VM stresses on the antero-medial plate of each implant for walking loading.

Model	Load	Part	Max VM (Nm-2)	Location
Standard Model	Walking	Femoral Condyles	5.10E+06	Bone-plate interface- centre of A/M Plate
55mm Resection	Walking	Femoral Condyles	5.47E+06	Bone-plate Interface- anterior corner of A/M Plate
35mm Resection	Walking	Femoral Condyles	4.34E+06	Bone-plate interface- Posterior corner of A/M Plate
Porous Ti Implant	Walking	Femoral Condyles	3.95E+06	Bone-plate interface- centre of A/M plate
PEEK Implant	Walking	Femoral Condyles	3.22E+06	Bone-plate interface- centre of A/M plate
1.5mm Thickness Plates	Walking	Femoral Condyles	4.94E+06	Bone-plate interface- centre of A/M plate

Table 6.13 Maximum VM stresses for walking loading on the bone adjacent to the antero-lateral plate

Model	Load	Part	Max VM (Nm-2)	Location
Standard Model	Walking	Femoral Condyles	5.04E+06	Bone-plate interface- centre of A/L Plate
55mm Resection	Walking	Femoral Condyles	1.13E+07	Bone-plate interface- anterior corner of A/L Plate
35mm Resection	Walking	Femoral Condyles	5.11E+06	Bone-plate interface- anterior corner of A/L plate
Porous Ti Implant	Walking	Femoral Condyles	3.53E+06	Bone-plate interface- centre of A/L plate
PEEK Implant	Walking	Femoral Condyles	2.07E+06	Bone-plate interface- centre of A/L plate
1.5mm Thickness Plates	Walking	Femoral Condyles	5.80E+06	Bone-plate interface- centre of A/L plate

Table 6.14 Maximum VM stresses for jogging loading on the bone adjacent to the antero-medial plate

Model	Load	Part	Max VM (Nm-2)	Location
Standard Model	Jogging	Femoral Condyles	6.88E+06	Bone-plate interface- centre of A/M plate
55mm Resection	Jogging	Femoral Condyles	7.14E+06	Bone-plate interface- centre of A/M plate
35mm Resection	Jogging	Femoral Condyles	5.03E+06	Bone-plate interface- posterior corner of A/M plate
Porous Ti Implant	Jogging	Femoral Condyles	4.58E+06	Bone-plate interface- centre of A/M plate
PEEK Implant	Jogging	Femoral Condyles	3.74E+06	Bone-plate interface- centre of A/M plate
1.5mm Thickness Plates	Jogging	Femoral Condyles	5.73E+06	Bone-plate interface- centre of A/M plate

Table 6.15 Maximum VM stresses for jogging loading on the bone adjacent to the antero- lateral plate

Model	Load	Part	Max V-Mises (Nm-2)	Location
Standard Model	Jogging	Femoral Condyles	6.45E+06	Bone-plate interface- centre of A/L plate
55mm Resection	Jogging	Femoral Condyles	7.80E+06	Bone-plate interface- anterior corner of A/L plate
35mm Resection	Jogging	Femoral Condyles	5.93E+06	Bone-plate interface- anterior corner of A/L plate
Porous Ti Implant	Jogging	Femoral Condyles	4.09E+06	Bone-plate interface- centre of A/L plate
PEEK Implant	Jogging	Femoral Condyles	2.40E+06	Bone-plate interface- centre of A/L plate
1.5mm Thickness Plates	Jogging	Femoral Condyles	6.73E+06	Bone-plate interface- centre of A/L plate

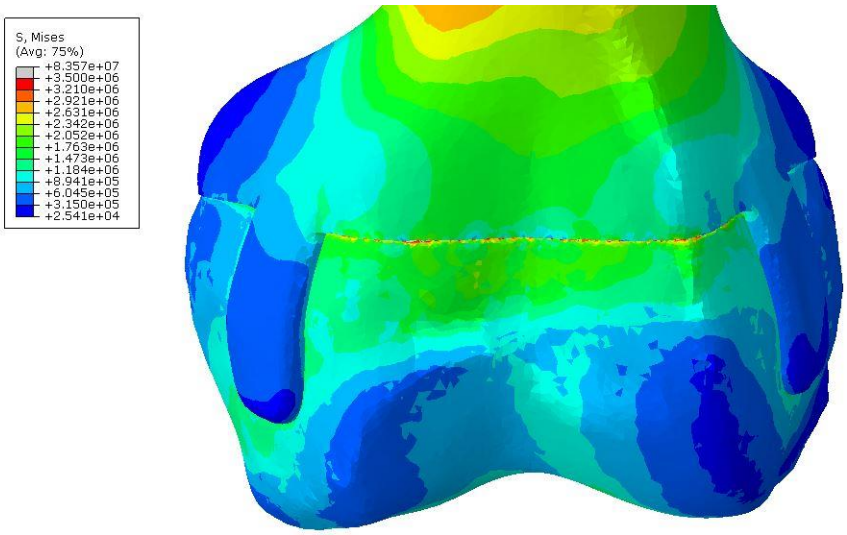

Figure 6.13 Stresses within the bone were increased when the implant material was PEEK.

6.5.2 Maximum Strain in the Implant

A summary of maximum strain in each implant for both loading conditions are provided in Table 6.16. Strain values decreased in resection levels closer to the joint, indicating an overall increase in strength of the bone-implant assembly that could be more durable. The porous titanium implant had the smallest strain values in both loading conditions, followed by PEEK.

Table 6.16 Maximum starin values for all 5 implants when subject to walking and jogging loading.

Model	Load	Max Strain	Load	Max Strain
Standard Model	Walking	2.51E-04	Jogging	2.92E-04
55mm Resection	Walking	2.72E-04	Jogging	2.80E-04
35mm Resection	Walking	1.58E-04	Jogging	1.80E-04
Porous Ti Implant	Walking	3.01E-05	Jogging	3.49E-05
PEEK Implant	Walking	8.32E-05	Jogging	9.64E-05
1.5mm Thickness Plates	Walking	1.36E-04	Jogging	1.58E-04

6.5.3 Strain Energy Density in the Femoral Bone

An increase in SED was noted in all implant cases where the bone and implant came into direct contact, particularly adjacent to the extra-cortical plates. A path made up of the nodes adjacent to the extra-cortical plates was created (Figure 6.14) and the SED values in the bone for each node was plotted against the distance on the path for each loading condition (Figure 6.15 to Figure 6.18). As each node is associated with multiple elements, a single node can have multiple values of strains/SED that are associated with different elements. Therefore, for each node, the average of elemental values was calculated and presented as the nodal solution.

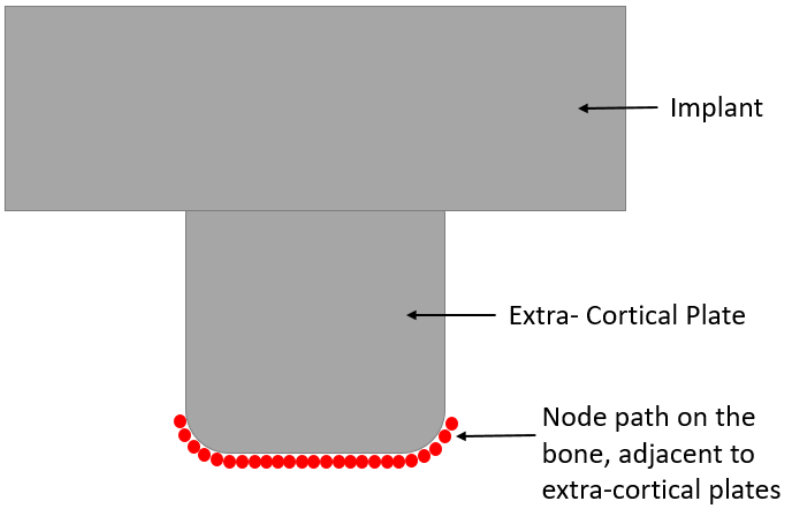

Figure 6.14 Node path along the edge of the plate on the surface of the bone

The PEEK implant model exhibited the lowest values of SED in the bone, while SED in many nodes were highest in the Ti-6AL-4V implant. The SED values in the porous titanium model were more consistent throughout the length of the path. In all scenarios and for all three materials investigated, the value of SED decreased at the edges of the plates.

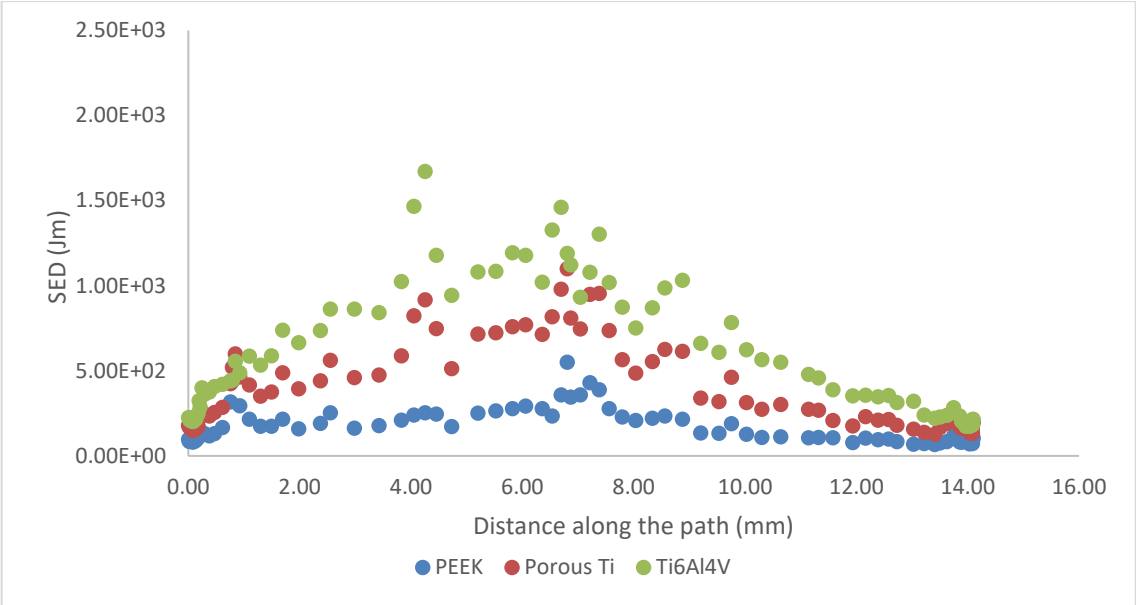

Figure 6.15 SED values for walking load on the bone adjacent to the antero-medial plate.

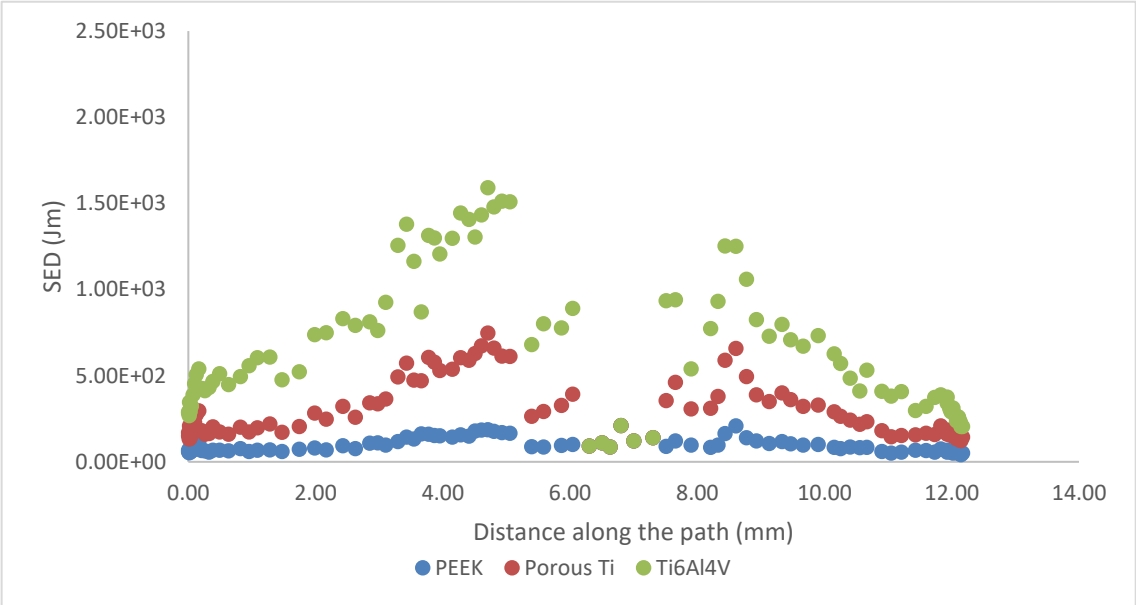

Figure 6.16 SED values for walking load on the bone adjacent to the antero-lateral plate.

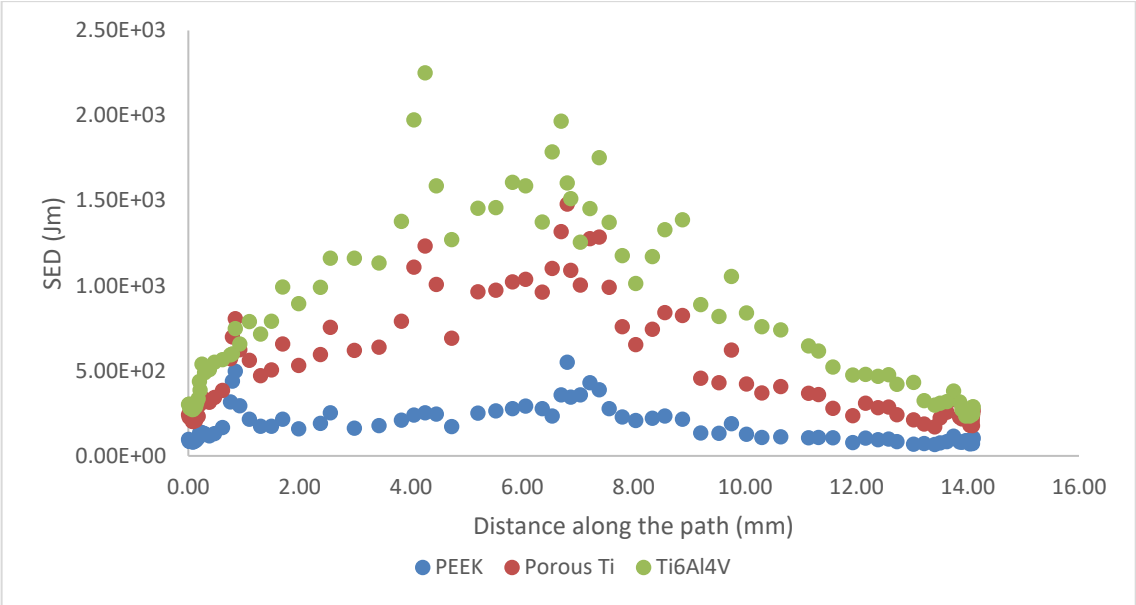

Figure 6.17 SED values for jogging load on the bone adjacent to the antero-medial plate

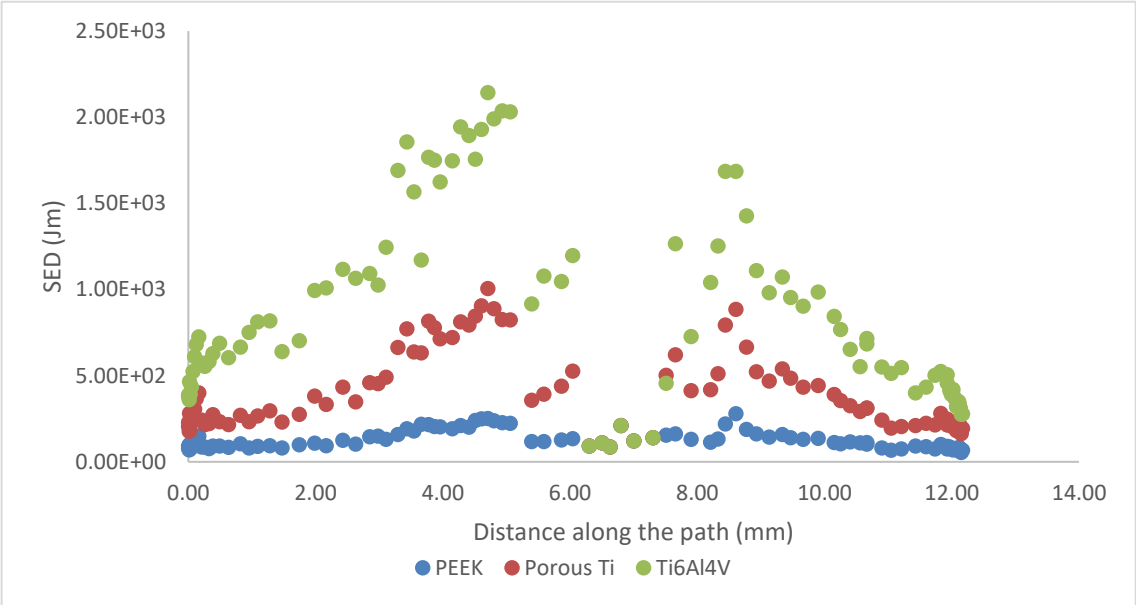

Figure 6.18 SED values for jogging load on the bone adjacent to the antero-lateral plate

A summary of maximum SED values measured on both sides of the models, for all 6 implants investigated and for both loading conditions are provided in Table 6.17 and Table 6.18.

The PEEK implant showed the lowest maximum SED value amongst all implants by a factor of 10 in some cases; the SED of the nodes on the path adjacent to the plates were considerably lower than that of the porous titanium and solid titanium alloy models. When comparing different resection levels, the SED measured on the bone adjacent to the plates in the 55mm model was higher than the control model. The 35mm implant consistently produced lower SED than the other resection levels.

Table 6.17 Maximum SED values for the medial and lateral side of the models when subject to walking load

Model	Medial		Lateral	
	Load	SED (Jm)	Load	SED (Jm)
Standard Model	Walking	2.92E+03	Walking	2.32E+03
55mm Resection	Walking	4.04E+03	Walking	5.21E+03
35mm Resection	Walking	1.69E+03	Walking	1.69E+03
Porous Ti Implant	Walking	5.25E+03	Walking	3.51E+03
PEEK Implant	Walking	8.36E+02	Walking	3.30E+02
1.5mm Thickness Plates	Walking	1.87E+03	Walking	2.83E+03

Table 6.18 Maximum SED values for the medial and lateral sides of the models when subject to jogging load.

Model	Medial		Lateral	
	Load	SED (Jm)	Load	SED (Jm)
Standard Model	Jogging	3.95E+03	Jogging	3.10E+03
55mm Resection	Jogging	4.78E+03	Jogging	6.83E+03
35mm Resection	Jogging	2.41E+03	Jogging	2.27E+03
Porous Ti Implant	Jogging	4.72E+03	Jogging	7.07E+03
PEEK Implant	Jogging	1.13E+03	Jogging	4.45E+02
1.5mm Thickness Plates	Jogging	2.95E+03	Jogging	3.81E+03

6.6 Discussion

The relevant parameters to detect risk of fracture in a structure, depending on the type of loading are: Ultimate Tensile Strength (UTS), Yield strength and Fatigue strength. The known values for these properties for the three materials used in this thesis are given in Table 6.19.

Table 6.19 Ultimate Tensile Strength (UTS), Yield strength and Fatigue strength values for Ti alloy, porous titanium and PEEK.

Parameter Value (MPa)	Ti-6Al-4V	Porous Titanium	PEEK
Ultimate Tensile Strength	900	UKN	110
Yield Strength	830	85	100
Fatigue Strength	510	UKN	103

As the knee joint is exposed to cyclic loading the fatigue strength is more relevant in predicting fatigue failure of the implant. The fatigue strength is a direct predictor of risk of fracture under cyclic loading. If the stress limit is exceeded, a fatigue rupture will occur at some point, however, if the limit is not exceeded the material is expected to resist an infinite number of loading cycles. As the bone implant model presented in this chapter was not an accurate representation of the actual forces applied to the femoral condyles, in order to obtain a more realistic value for the generated stresses, an increase of 20% to the maximum stress in each model can be assumed (Abdoola 2011). By comparing the ultimate tensile strength, yield strength and fatigue strength with the maximum stress values observed in each implant plus a 20% increase, it is clear that the risk of fracture of the extra-cortical plate under a bodyweight load of 687N is low when the implant is made of titanium alloy, porous titanium or PEEK and even when the plate thickness is reduced. The follow-up study of patients with knee sparing distal femoral replacements by Gupta et al. (2006) and those presented in

Chapter 3 of this thesis did not indicate fracture of the extra-cortical plates and confirmed the findings of this chapter for the control implant model.

As expected the stress distribution was highest near the extra-cortical plate attachment; the maximum Von Mises stresses found in all 6 implants was located on the surface of the extra-cortical plates at the junction with the shaft of the implant. The plate-implant interface is a relatively weak part of the implant structure and was expected to present the highest stress concentration. The femoral inclination angle could be a contributing factor in the asymmetry of stress distribution in the antero-medial and antero-lateral plates (Figure 6.19). The 35mm resection level implant presented the smallest stress concentration on the plates while the 55mm resection level implant had the highest concentration of stresses. This could be due to the increased bending forces that are applied to a higher (further from the joint) resection level. In this thesis the two parts of the models i.e. the bone and the implant, were tied. However, in reality there is friction between the two parts that is expected to reduce the stresses on both the implant and the bone.

The stresses on the anterior surface of the intact bone model were increased compared with the stresses in the same location on the bone-implant models. This result was expected, as the higher Young's modulus of the implant compare with the bone would cause the bone to become less loaded and therefore stresses within the bone would decrease.

The stresses within the bone increased around both the extra-cortical plates and at the implant plateau-bone contact regions. These were areas where high SED was recorded. This was expected as stress is directly related to the SED value (Jang et al. 2008).

Therefore, the areas of high stress within the cortical bone immediately adjacent to the plate were not the ideal location for measuring SED to determine possible bone formation. When creating the non-manifold assembly in this study, to ensure the two parts were in full contact, in some areas the implant cut into the bone and caused high stress concentrations. The higher the stiffness of the implant model (Ti alloy), the higher the stresses on the bone model would be; therefore, in future studies, the area on the bone adjacent to the stress concentration zone is more suitable to be investigated to determine the possibility of bone formation. The use of algorithms based on SED, such as those proposed by Huiskes et al. would provide a valuable insight into how bone forms and remodels adjacent to extracortical plates. In such algorithms, strain energy density acts as the stimulus for bone density change and the rate of the bone density change is determined on the basis of the difference between the remodelling stimulus e.g., stress, strain, and strain energy density and its target values (Huiskes et al. 1987, 2000). The radiographic analysis that was conducted and presented in Chapter 3, showed no signs of bone resorption in the bone adjacent to the extra-cortical plates and bone formation was detected in some cases. These results are in line with the FEA results presented in this Chapter, showing high SED values in the bone adjacent to the Ti alloy implant.

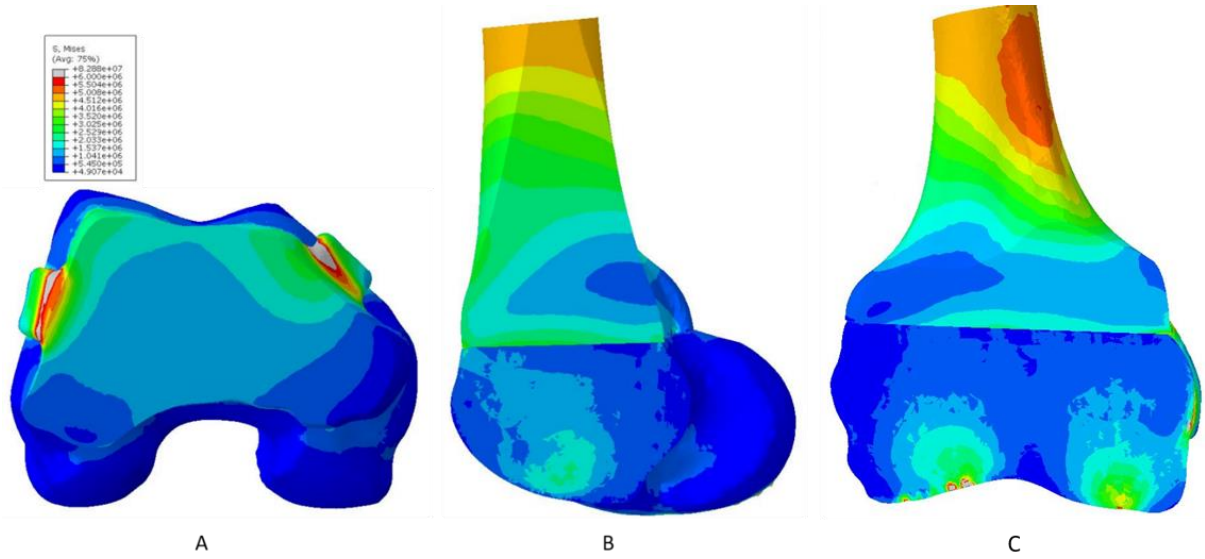

Figure 6.19 Stress distribution in the control model, under walking loading at the centre of the implant; [A] Plane view of the implant with a horizontal cut through the model, [B] M/L view with an axial cut through the model and [C] A/P view with a frontal plane cut through the model

The lowest maximum strain in the implant was observed in the porous titanium model, indicating high strength of the implant. As the 30% porous Ti that was modelled in this study has a similar Young's modulus to cortical bone (18.6 ± 3.5GPa to 20.7 ± 1.9GPa), it can reduce the risk of stress shielding. Therefore, the results of this study indicate that porous titanium is a suitable candidate as an orthopaedic implant (Niinomi 2011). Studies have confirmed the osseoconductivity of porous titanium and its alloys (Simmons et al. 1999; Nouri et al. 2010; Li et al. 2007) that further confirms its suitability as an implant material. However, it must be noted that the fatigue properties of this material depend on the amount of porosity and manufacturing methods used.

In this study, the method used for assigning the material properties of bone was based on the average grey values of the voxels within the volume mesh. While the results of the study were not verified by mechanical testing, this method is an established method

of assigning material properties in biomechanical FE analysis (Taddei et al. 2007; Yosibash et al. 2007; Keyak et al. 2005; Keyak and Falkinstein 2003).

This study had a number of limitations. In clinical practice, the attachment of the implant to the residual bone is through use of cortical screws, whereas in this FE study screw fixation was not modelled due to complexity of their geometry and the complications involved in creating an assembly with multiple parts. The addition of screws through the extra-cortical plates and onto the bone is expected to produce additional stresses on the surrounding bone and plate.

The implant-bone model presented in this study was simplified by eliminating friction between the contact surfaces. Addition of friction increases the calculation time significantly; however, it could generate results that are closer to the physiological loading conditions of the bone and the implant.

The boundary conditions used in this study were not fully representative of the loading condition in patients. The condyles of the bone in this study were fixed and the loads were applied through the shaft of the implant. However, in reality, ligaments in the knee joint exert forces through their attachment sites, located near the femoral condyles. Therefore, additional forces are applied to the joint near the condylar region from the distal part of the femur and via muscle attachments.

Knee sparing implants are custom implants that are designed for individual patients. Therefore, there are unlimited number of possible combinations of resection lengths, number of plates and additional fixation features that could be investigated. While all bones of the same location have common features in all individuals, there are

differences in shape, size and density of each bone. Hence, the results of this study cannot be translated to every case and can significantly vary.

The bone that was used to create the FE model in this study was from a donor with no history of musculoskeletal disease or complications. However, in patients that receive joint-sparing massive implants, the bone properties can be significantly different from a healthy bone due to loss of density associated with the treatments such as chemotherapy and disuse due to pain. Therefore, the model presented in this chapter may not be an accurate representation of the implantation condition.

Due to time restrictions, an experimental validation of the FE model was not carried out. Validation is a process to confirm if the simulation results reflect the real-world outcomes. As FEA is a computational method for estimating solutions for a mathematical problem, a validation test is necessary to determine the reliability of the results and should be carried out in future studies.

6.7 Conclusion

The results presented in this chapter confirmed the hypotheses, which is that the risk of extra-cortical plate fracture in the current design of distal femoral joint-sparing implants is low and a decrease in plate thickness or material stiffness does not cause fracture of the extra-cortical plates. The results also confirmed the hypothesis that the resection levels closer to the knee and lower modulus materials such as PEEK and porous Ti generate lower stresses within the cortical bone immediately adjacent to the plate, while loading the bone more and therefore, are less likely to cause stress shielding of the bone. However, insufficient results were obtained to establish whether bone formation will be encouraged in implants made with less stiff materials than

titanium alloy and therefore, further work is required. This study was a simplified model of a joint-sparing implant and was not validated. Studies with a more realistic model and an experimental validation of the FE model must be carried out in future studies.

Chapter 7 Discussion and Conclusions

In contrast to distal femoral and proximal tibial segmental endoprostheses which use a hinge knee replacement, joint-sparing prostheses are massive implants that replace a segment of bone cancer but where the knee joint can be spared. The implants are fixed to the bone by use of extra-cortical plates. Although knee sparing implants have been used in the treatment of patients for over 13 years, the study presented here is the first to compare the function, safety and the response to plate fixation in joint-sparing prostheses around the knee.

The aim of this thesis was to evaluate patient and implant survival rates and to investigate the perceived advantages and disadvantages of distal femoral and proximal tibial knee sparing massive implants, in terms of gait and proprioception, functional outcome and patient acceptance. Using FEA, this thesis also aimed to investigate the stresses generated on the bone and implant when the bone resection level, plate thickness and implant stiffness was varied.

The following hypotheses were examined in this thesis:

1. *Following bone tumour surgery, knee joint-sparing implants have similar or reduced revision rate when compared to conventional knee sacrificing implants. Extra-cortical plates are a durable method of attaching a joint-sparing prosthesis to the fragmental proximal tibia or distal femur.*
2. *Patients with joint-sparing implants have improved proprioception due to the retention of soft tissues such as the knee ligaments which have been shown to contain sensory nerve endings.*
3. *Patients with joint-sparing implants have improved function and acceptability of their implant compared to patients with knee sacrificing implants.*
4. *Knee joint-sparing massive implants provide a more normal gait in comparison with conventional knee-sacrificing implants.*
5. *FEA shows that extra-cortical plates do not cause stress shielding of the bone.*
6. *Use of materials with a lower Young's modulus, such as porous titanium and PEEK do not increase the risk of implant or plate fracture and can enhance bone formation adjacent to the prosthesis.*

The results of the follow-up study presented in Chapter 3 showed that both patient and implant survival rate in knee sparing proximal tibial and distal femoral implants were comparable with conventional joint sacrificing implants. The recurrence or metastasis in patients with joint-sparing implants was improved compared to recurrence in conventional implants, which has been reported in the literature (Hamilton et al. 2005; Coathup et al. 2013). Revision rates due to aseptic loosening, infection, and fracture of the implant or plates were also similar to those reported for knee sacrificing implants. In this study, aseptic loosening and infection were the primary modes of

failure (6.67% and 4.74%), and this was similar to those reported in studies that investigated conventional joint sacrificing implant survival (Capanna et al. 2015; Henderson et al. 2011; Sewell et al. 2011; Hamilton et al. 2005; Coathup et al. 2013). Five patients underwent revision surgery due to loosening of the extra-cortical plates; however no plate fracture was observed. The revision rate was higher in the distal femoral replacement group and in patients under the age of 21, when compared with patients with a proximal tibial replacement and in patients who were over 21 years of age at the time of surgery. These findings were similar to those reported in patients following knee sacrificing implant surgery (Unwin et al. 1996). The survival rate was significantly higher in patients under the age of 21 when compared with adult patients when the end point was failure due to loosening of extra-cortical plates (p=0.023). Given these results the first hypothesis therefore, can be accepted.

One of the limitations of the follow-up study was that I had to rely on available literature on distal femoral and proximal tibial joint sacrificing implants for comparison data. The patients in this study were not matched with those in the literature with regards to their age, gender, diagnosis and their treatment regime. Additionally, in this study the effect of joint-sparing implants on the growth plate was not investigated. It was not clear in what percentage of the patients the growth plate could be spared, and within that group what percentage of the patients continued to grow naturally.

The results of the proprioception study presented in Chapter 4 of this thesis did not support the second hypothesis. Proprioception was measured in terms of joint position sense (JPS) in 20 oncology patients and 10 healthy subjects. The average error in repositioning angle in the operated leg in each patient was normalised against their

non-operated leg and the average for each group was calculated and compared. The mean absolute error in JPS was greatest in the operated leg in the JST group, while the DFRs exhibited the best JPS. The JPS results in the joint sacrificing distal femoral and proximal tibial groups were similar to those reported in the literature (Li et al. 2005). However, patients with DFRs and PTRs had better proprioception when compared with the JSF and JST groups. This result was surprising as proprioception is associated with nerve endings that are in tendons and ligaments that would have been resected during reconstruction procedures with a DFR or a PTR.

The results of 3 established patient questionnaires confirmed the third hypothesis, as the patients with a joint-sparing distal femoral or proximal tibial implant showed improved functional outcome and acceptance when compared with patients with a conventional DFR and PTR. The results were aligned with other functional outcome studies of joint-sparing implants (Gupta et al. 2006; Spiegelberg et al. 2009). The passive knee ROM was identical in both legs in the JST group and significantly improved when compared with the PTR group (p=0.037). Similarly, the JSF group had an improved ROM, when compared with the DFR group, however this was not significant. The reduced knee motion could be associated with the design of the rotating hinge knee or the extent of scar tissue in the joint sacrificing groups.

In Chapter 5, while some gait kinematics were more normal in joint-sparing patients, this was not observed consistently throughout the study and in some cases patients with a knee sacrificing implant showed improved gait when compared with those with a joint-sparing implant. Using optoelectronic gait analysis and force plates, gait in terms of the mean hip, knee, and ankle joint angles, joint angle symmetry, time in stance and vertical ground reaction force (VGRF) were assessed. Symmetry in leg

length was also analysed. A more symmetrical gait and one that was more normal was observed in patients with a JST replacement when compared with the PTR group. However, the DFRs showed a more symmetrical gait pattern, when compared with the JSF group. The measured VGRF indicated that load transfer in the joint-sparing groups was more normal when compared with the joint sacrificing groups. The JSF group had a similar stance time to the control group, compared with the DFRs. However, time in stance in the JST group was significantly increased when compared with the control group (p=0.020). This was not the case in the PTR group. Leg length discrepancy in joint sacrificing implants was greater, however this was not significant. While some results confirmed the hypothesis of this study, further investigation with a higher number of patients and more accurate equipment for data capture and analysis is required to assess gait in patients with joint-sparing implants.

The gait analysis study presented here had a number of limitations. Firstly, the number of patients in each group was small. Secondly, the patient groups were not matched. Although the distal femoral and proximal tibial joint-sparing groups were compared with patients with joint sacrificing implants of the same anatomical location, patients' gender, age, time from surgery, resection levels and treatment regime were not matched.

In Chapter 6, Finite Element Analysis of a bone-implant model was carried out and results showed a low risk of plate fracture in the current design of the implant. Stresses and Strain Energy Density within the cortical bone adjacent to the plates were increased, indicating a low risk of stress shielding. This result was also confirmed by the results of the retrospective radiographic assessment of the joint-sparing implants, in Chapter 3 of this thesis.

The bone and implant response when subject to everyday (walking) and extreme (jogging) loading was estimated in order to potentially improve the design of the implant in distal femoral joint-sparing implants. A simplified model of a JSF implant was parametrised to identify the optimum design. The rationale for this was that the bony reaction to the extra-cortical plates seen in clinical radiographs was often negligible, while in the animal study carried out by Coathup et al. (2000), the extra-cortical plates became buried within the bone. This may be associated with the stiffness and the positioning of the plates on the metaphysis. The plates in the study by Coathup et al. were longer, and were attached to the diapahyseal of the bone (Coathup et al. 2000). The variables investigated in this study included the resection level, material used and extra-cortical plate thickness. The stresses within the bone and the implant, strain on the implant and the SED on the bone were assessed. The results of this study indicated that a decrease in plate thickness would not significantly compromise the strength of the plate and result in fracture. This could be a design improvement as reducing plate thickness would reduce stress shielding within adjacent bone and also lessen the bulkiness of the implant around the knee joint where adequate soft tissue coverage is often a problem. Using less stiff plates may encourage a greater bony reaction which would enhance implant fixation. The SED values found in this study indicate that bone formation may increase, adjacent to porous titanium when compared with the solid Ti alloy implant.

These implants are currently manufactured from titanium alloy and this study also investigated the use of materials of lower stiffness. PEEK and 30% percent porous titanium have Young's moduli that are similar to natural bone (Oh et al. 2002). Osseoconductivity of porous titanium has also been previously confirmed (Simmons et al. 1999; Nouri et al. 2010; Li et al. 2007). In orthopaedic applications, the ideal

biomedical implant material is required to have high strength and a low Young's modulus (Niinomi 2011).The results of this study indicated that both PEEK and porous Ti can be suitable materials for fabrication of a joint-sparing implant.

Three different resection levels were also investigated and results showed that a resection level closer to the joint line reduced stresses within bone and the extra-cortical plates, thereby reducing the risk of plate fracture. However, insufficient evidence was obtained to confirm that stress shielding is more likely when a higher bone resection level is made.

The FEA study had a number of limitations. Firstly, it was simplified and elements such as friction and screw fixation were eliminated. The forces and the boundary conditions were also simplified and were not a true representation of the forces that are applied to the femoral condyles. Secondly, an experimental validation of the FE model was not carried out in order to confirm if the simulation results reflect the real-world outcomes. A validation test is necessary to determine the reliability of the results and should be carried out in the future. Additionally, to investigate the bony reaction to the extra-cortical plates, the use of algorithms based on SED, such as those proposed by Huiskes et al (2000) would provide a valuable insight and could be used in future studies.

7.1 Conclusion

Knee joint-sparing endoprostheses provide a reliable reconstruction method for tumour treatment in a carefully selected group of patients, whose joint can be spared while sufficient surgical margins are allowed.

While subjective functional assessments indicated an improved function in patients with a joint-sparing implant, the more objective assessment methods produced mixed results. Knee proprioception was not improved in joint-sparing implants when compared with the patients with a knee sacrificing implant and with the healthy subjects. While joint sacrificing implants had improved joint angles and joint symmetry in some phases of the gait, overall the load transfer and time in stance was improved and closer to normal in joint-sparing implants. Overall, JST implants had better function than PTRs while this was reversed in the femoral replacement groups. Therefore, each anatomical location should be investigated individually due to their substantial differences.

Finally, while the results of the FEA indicated that the risk of stress shielding within the bone and plate fracture in the current design of the joint-sparing implants is low, there are design improvements that can be made. Lower resection levels and use of lower modulus materials such as porous titanium require further investigation.

7.2 Further work

A randomised controlled study is required to establish the findings of the follow-up study. A prospective radiographic analysis that utilises a less subjective image analysis technique can be used to assess the relationship between the implantation accuracy and implant survival.

Further studies that investigate proprioception with an increased number of patients and other analysis methods such as balance assessment may be required to establish the effect of different implant types on patients' proprioception.

Further gait assessment, where the patient groups are matched with respect to their age, gender, time from surgery and resection levels are required to establish the differences in gait in both implant types and in each anatomical location. Also, a longitudinal study could reveal information about the difference in recovery time in patients with joint-sparing and joint sacrificing groups and how the gait in each group improves over time.

A Finite Element model with constraints, loading and contact conditions that is closer to the actual bone-implant interaction may provide a more real world representative results.

References

Abdoola T. Bone remodeling around metalic implants. [Department of Mechanical Engineering]: University College London; 2011.

Agarwal M, Puri A, Gulia A, Reddy K. Joint-sparing or physeal-sparing diaphyseal resections: the challenge of holding small fragments. Clin Orthop. 2010 Nov;468(11):2924–32.

Ahlmann ER, Menendez LR, Kermani C, Gotha H. Survivorship and clinical outcome of modular endoprosthetic reconstruction for neoplastic disease of the lower limb. J Bone Joint Surg Br. 2006 Jun;88(6):790–5.

Akahane T, Shimizu T, Isobe K, Yoshimura Y, Fujioka F, Kato H. Evaluation of postoperative general quality of life for patients with osteosarcoma around the knee joint. J Pediatr Orthop Part B. 2007 Jul;16(4):269–72.

Albrektsson T, Johansson C. Osteoinduction, osteoconduction and osseointegration. Eur Spine J. 2001 Oct;10(Suppl 2):S96–101.

American Cancer Society | Information and Resources for Cancer: Breast, Colon, Lung, Prostate, Skin [Internet]. [cited 2014 Jan 18]. Available from: http://www.cancer.org/index

Amin NH, Omiyi D, Kuczynski B, Cushner FD, Scuderi GR. The Risk of a Deep Infection Associated With Intraarticular Injections Before a Total Knee Arthroplasty. J Arthroplasty. 2016 Jan;31(1):240-4

Anderson FC, Pandy MG. Individual muscle contributions to support in normal walking. Gait Posture. 2003 Apr;17(2):159–69.

Anderson KC, Buehler KC, Markel DC. Computer assisted navigation in total knee arthroplasty: comparison with conventional methods. J Arthroplasty. 2005 Oct;20(7 Suppl 3):132–8.

Aponte-Tinao L, Ayerza MA, Muscolo DL, Farfalli GL. Survival, Recurrence, and Function After Epiphyseal Preservation and Allograft Reconstruction in Osteosarcoma of the Knee. Clin Orthop Relat Res. 2014 Oct 29;473(5):1789–96.

Aponte-Tinao L, Farfalli GL, Ritacco LE, Ayerza MA, Muscolo DL. Intercalary Femur Allografts Are an Acceptable Alternative After Tumor Resection. Clin Orthop. 2012 Mar;470(3):728–34.

Archer KR, Castillo RC, MacKenzie EJ, Bosse MJ. Gait Symmetry and Walking Speed Analysis Following Lower-Extremity Trauma. Phys Ther. 2006 Dec 1;86(12):1630–40.

Arpaci F, Ataergin S, Ozet A, Erler K, Basbozkurt M, Ozcan A, et al. The feasibility of neoadjuvant high-dose chemotherapy and autologous peripheral blood stem cell transplantation in patients with nonmetastatic high grade localized osteosarcoma. Cancer. 2005 Sep 1;104(5):1058–65.

Asavamongkolkul A, Waikakul S, Phimolsarnti R, Kiatisevi P, Wangsaturaka P. Endoprosthetic reconstruction for malignant bone and soft-tissue tumors. J Med Assoc Thail Chotmaihet Thangphaet. 2007 Apr;90(4):706–17.

Aspenberg P, Goodman S, Toksvig-Larsen S, Ryd L, Albrektsson T. Intermittent micromotion inhibits bone ingrowth. Titanium implants in rabbits. Acta Orthop Scand. 1992 Apr;63(2):141–5.

Astephen JL, Deluzio KJ, Caldwell GE, Dunbar MJ. Biomechanical changes at the hip, knee, and ankle joints during gait are associated with knee osteoarthritis severity. J Orthop Res Off Publ Orthop Res Soc. 2008 Mar;26(3):332–41.

Bade MJ, Kohrt WM, Stevens-Lapsley JE. Outcomes before and after total knee arthroplasty compared to healthy adults. J Orthop Sports Phys Ther. 2010 Sep;40(9):559-67.

Barfeie A, Wilson J, Rees J. Implant surface characteristics and their effect on osseointegration. Br Dent J. 2015 Mar 13;218(5):E9–E9.

Beebe K, Song KJ, Ross E, Tuy B, Patterson F, Benevenia J. Functional outcomes after limb-salvage surgery and endoprosthetic reconstruction with an expandable prosthesis: a report of 4 cases. Arch Phys Med Rehabil. 2009 Jun;90(6):1039–47.

Bellemans J. Osseointegration in porous coated knee arthroplasty. The influence of component coating type in sheep. Acta Orthop Scand Suppl. 1999 Oct;288:1–35.

Benedetti MG, Catani F, Donati D, Simoncini L, Giannini S. Muscle performance about the knee joint in patients who had distal femoral replacement after resection of a bone tumor. An objective study with use of gait analysis. J Bone Joint Surg Am. 2000 Nov;82–A(11):1619–25.

Berber O, Sturridge SN, Vanhegan I, Cannon SR, Blunn GW. The Use of a Novel 'Conservative Hip Replacement' to Reconstruct an Osteoarthritic Hip With an Occluded Femoral Canal. J Arthroplasty. 2011 Dec;26(8):1571.e9-10.

Berrey BH, Lord CF, Gebhardt MC, Mankin HJ. Fractures of allografts. Frequency, treatment, and end-results. J Bone Joint Surg Am. 1990 Jul;72(6):825–33.

Bhangu AA, Kramer MJ, Grimer RJ, O'Donnell RJ. Early distal femoral endoprosthetic survival: cemented stems versus the Compress® implant. Int Orthop. 2006 Dec;30(6):465–72.

Bhatt R, Xiang Y, Kim J, Mathai A, Penmatsa R. Dynamic Optimization of Human Stair-Climbing Motion. SAE Technical Paper 2008-01-1931, 2008

Biemond JE, Aquarius R, Verdonschot N, Buma P. Frictional and bone ingrowth properties of engineered surface topographies produced by electron beam technology. Arch Orthop Trauma Surg. 2011 May;131(5):711–8.

Biswas D, Haughom B, Mayle RE, Della Valle CJ. Case Report: Failure of Rotating-hinge Total Knee Prosthesis by Disengagement of the Hinge-post Extension. Clin Orthop. 2013 Apr;471(4):1389–92.

Blunn G, Coathup M. Fixation of Endoprostheses in Tumour Replacement. In: European Surgical Orthopaedics and Traumatology. 1st ed. Springer Reference; 2014. p. 4119–33.

Blunn GW, Briggs TW, Cannon SR, Walker PS, Unwin PS, Culligan S, et al. Cementless fixation for primary segmental bone tumor endoprostheses. Clin Orthop. 2000 Mar;(372):223–30.

Blunn GW, Wait ME. Remodelling of bone around intramedullary stems in growing patients. J Orthop Res Off Publ Orthop Res Soc. 1991 Nov;9(6):809–19.

Boffetta P, Boccia S, Vecchia CL. A Quick Guide to Cancer Epidemiology. Springer Science & Business Media; 2014. 110 p.

Bosetti C, Bertuccio P, Chatenoud L, Negri E, Levi F, La Vecchia C. Childhood cancer mortality in Europe, 1970-2007. Eur J Cancer Oxf Engl 1990. 2010 Jan;46(2):384–94.

Bozic KJ, Grosso LM, Lin Z, Parzynski CS, Suter LG, Krumholz HM, et al. Variation in Hospital-Level Risk-Standardized Complication Rates Following Elective Primary Total Hip and Knee Arthroplasty. J Bone Jt Surg. 2014 Apr 16;96(8):640–7.

Brand RA. Biographical Sketch: Julius Wolff, 1836–1902. Clin Orthop. 2010 Apr;468(4):1047.

Brånemark PI, Adell R, Albrektsson T, Lekholm U, Lundkvist S, Rockler B. Osseointegrated titanium fixtures in the treatment of edentulousness. Biomaterials. 1983 Jan;4(1):25–8.

Bruns J, Raabe K, Deuretzbacher G. Gait analysis in tumor patients after distal femoral resection and implantation of a megaprosthesis. Acta Orthop Belg. 2016 Aug;82(2):287–97.

Burchardt H. Biology of bone transplantation. Orthop Clin North Am. 1987 Apr;18(2):187–96.

Burrows HJ, Wilson JN, Scales JT. Excision of Tumours of Humerus and Femur, with Restoration by Internal Prostheses. Bone Jt J. 1975 May 1;57–B(2):148–59.

Çabuk H, Kuşku Çabuk F. Mechanoreceptors of the ligaments and tendons around the knee. Clin Anat N Y N. 2016 Sep;29(6):789–95.

Cancer of the Bones and Joints - SEER Stat Fact Sheets [Internet]. [cited 2011 Oct 20]. Available from: http://seer.cancer.gov/statfacts/html/bones.html

Capanna DR, Bufalini C, Campanacci M. A new technique for reconstructions of large metadiaphyseal bone defects. Orthop Traumatol. 1993 Sep;2(3):159–77.

Capanna R, Campanacci DA, Belot N, Beltrami G, Manfrini M, Innocenti M, et al. A new reconstructive technique for intercalary defects of long bones: the association of massive allograft with vascularized fibular autograft. Long-term results and comparison with alternative techniques. Orthop Clin North Am. 2007 Jan;38(1):51–60.

Capanna R, Morris HG, Campanacci D, Del Ben M, Campanacci M. Modular uncemented prosthetic reconstruction after resection of tumours of the distal femur. J Bone Joint Surg Br. 1994 Mar;76(2):178–86.

Capanna R, Ruggieri P, Biagini R, Ferraro A, DeCristofaro R, McDonald D, et al. The effect of quadriceps excision on functional results after distal femoral resection and prosthetic replacement of bone tumors. Clin Orthop. 1991 Jun;(267):186–96.

Capanna R, Scoccianti G, Frenos F, Vilardi A, Beltrami G, Campanacci DA. What was the survival of megaprostheses in lower limb reconstructions after tumor resections? Clin Orthop. 2015 Mar;473(3):820–30.

Carter DR. Skeletal Function and Form: Mechanobiology of Skeletal Development, Aging, and Regeneration. 1 Reissue edition. Cambridge, U.K.; New York: Cambridge University Press; 2008. 332 p.

Carty CP, Bennett MB, Dickinson IC, Steadman P. Assessment of kinematic and kinetic patterns following limb salvage procedures for bone sarcoma. Gait Posture. 2009 Nov;30(4):547–51.

Carty CP, Bennett MB, Dickinson IC, Steadman P. Electromyographic assessment of Gait function following limb salvage procedures for bone sarcoma. J Electromyogr Kinesiol. 2010 Jun;20(3):502–7.

Cedars-Sinai [Internet]. [cited 2015 Jun 25]. Available from: http://www.cedars-sinai.edu/Patients/Programs-and-Services/Imaging-Center/For-Physicians/Musculoskeletal-Radiology/Exhibits-and-Presentations/Knee-Arthroplasty/Aseptic-Loosening.aspx

Chang DW, Weber KL. Use of a vascularized fibula bone flap and intercalary allograft for diaphyseal reconstruction after resection of primary extremity bone sarcomas. Plast Reconstr Surg. 2005 Dec;116(7):1918–25.

Chao EY, Sim FH. Composite fixation of salvage prostheses for the hip and knee. Clin Orthop. 1992 Mar;(276):91–101.

Chao EY, Sim FH. Composite fixation of segmental bone/joint defect replacement (SDR) prostheses. Biological and biomechanical justifications. Chir Organi Mov. 1990;75(1 Suppl):171–3.

Chao EY. A composite fixation principle for modular segmental defect replacement (SDR) prostheses. Orthop Clin North Am. 1989 Jul;20(3):439–53.

Chao EYS, Fuchs B, Rowland CM, Ilstrup DM, Pritchard DJ, Sim FH. Long-term results of segmental prosthesis fixation by extracortical bone-bridging and ingrowth. J Bone Joint Surg Am. 2004 May;86–A(5):948–55.

Cherian JJ, Kapadia BH, Banerjee S, Jauregui JJ, Issa K, Mont MA. Mechanical, Anatomical, and Kinematic Axis in TKA: Concepts and Practical Applications. Curr Rev Musculoskelet Med. 2014 Jun;7(2):89.

Clark CR, Huddleston HD, Schoch III EP, Thomas BJ. Leg-Length Discrepancy After Total Hip Arthroplasty. J Am Acad Orthop Surg. 2006 Jan;14(1):38–45.

Clatworthy MG, Gross AE. The allograft prosthetic composite: when and how. Orthopedics. 2001 Sep;24(9):897–8.

Coathup MJ, Bates P, Cool P, Walker PS, Blumenthal N, Cobb JP, et al. Osseo-mechanical induction of extra-cortical plates with reference to their surface properties and geometric designs. Biomaterials. 1999 Apr;20(8):793–800.

Coathup MJ, Batta V, Pollock RC, Aston WJ, Cannon SR, Skinner JA, et al. Long-Term Survival of Cemented Distal Femoral Endoprostheses with a Hydroxyapatite-

Coated CollarA Histological Study and a Radiographic Follow-up. J Bone Jt Surg. 2013 Sep 4;95(17):1569–75.

Coathup MJ, Cobb JP, Walker PS, Blunn GW. Plate fixation of prostheses after segmental resection for bone tumours. J Orthop Res Off Publ Orthop Res Soc. 2000 Nov;18(6):865–72.

Coathup MJ, Sanghrajka A, Aston WJ, Gikas PD, Pollock RC, Cannon SR, et al. Hydroxyapatite-coated collars reduce radiolucent line progression in cemented distal femoral bone tumor implants. Clin Orthop. 2015 Apr;473(4):1505–14.

Cobb JP, Ashwood N, Robbins G, Witt JD, Unwin PS, Blunn G. Triplate fixation: a new technique in limb-salvage surgery. J Bone Joint Surg Br. 2005 Apr;87(4):534–9.

Completo A., Fonseca F., Simoes J.A., Experimental Validation of Intact and Implanted Distal Femur Finite Element Models. J Biomech. 2007;40(11):2467-76.

Cordey J, Perren SM, Steinemann SG. Stress protection due to plates: myth or reality? A parametric analysis made using the composite beam theory. Injury. 2000 Sep;31 Suppl 3:C1-13.

Croci AT, Camargo OP, Baptista AM, Caiero MT. The use of a modular titanium endoprosthesis in skeletal reconstructions after bone tumor resections: method presentation and analysis of 37 cases. Rev Hosp Clínicas. 2000 Oct;55(5):169–76.

Davidson AW, Hong A, McCarthy SW, Stalley PD. En-bloc resection, extracorporeal irradiation, and re-implantation in limb salvage for bony malignancies. J Bone Joint Surg Br. 2005 Jun;87(6):851–7.

De Boer HH, Wood MB. Bone changes in the vascularised fibular graft. J Bone Joint Surg Br. 1989 May;71(3):374–8.

De Visser E, Mulder T, Schreuder HW, Veth RP, Duysens J. Gait and electromyographic analysis of patients recovering after limb-saving surgery. Clin Biomech Bristol Avon. 2000 Oct;15(8):592–9.

De Visser E, Veth RPH, Schreuder HWB, Duysens J, Mulder T. Reorganization of gait after limb-saving surgery of the lower limb. Am J Phys Med Rehabil. 2003 Nov;82(11):825–31.

Deijkers RLM, Bloem RM, Kroon HM, Van Lent JB, Brand R, Taminiau AHM. Epidiaphyseal versus other intercalary allografts for tumors of the lower limb. Clin Orthop. 2005 Oct;439:151–60. D

Dhillon MS, Bali K, Prabhakar S. Proprioception in anterior cruciate ligament deficient knees and its relevance in anterior cruciate ligament reconstruction. Indian J Orthop. 2011;45(4):294–300.

Dorfman HD, Czerniak B. Bone cancers. Cancer. 1995 Jan 1;75(1 Suppl):203–10.

Drnovsek N, Novak S, Dragin U, Ceh M, Gorensek M, Gradisar M. Bioactive glass enhances bone ingrowth into the porous titanium coating on orthopaedic implants. Int Orthop. 2012 Aug;36(8):1739–45.

Dunlop JWC, Hartmann MA, Bréchet YJ, Fratzl P, Weinkamer R. New Suggestions for the Mechanical Control of Bone Remodeling. Calcif Tissue Int. 2009 Jul;85(1):45.

Ek EW, Rozen WM, Ek ET, Rudiger HA. Surgical options for reconstruction of the extensor mechanism of the knee after limb-sparing sarcoma surgery: an evidence-based review. Arch Orthop Trauma Surg. 2011 Apr;131(4):487–95.

Enneking WF, Dunham W, Gebhardt MC, Malawar M, Pritchard DJ. A system for the functional evaluation of reconstructive procedures after surgical treatment of tumors of the musculoskeletal system. Clin Orthop. 1993 Jan;(286):241–6.

Enneking WF. A system of staging musculoskeletal neoplasms. Clin Orthop. 1986 Mar;(204):9–24.

Enneking WF. An abbreviated history of orthopaedic oncology in North America. Clin Orthop. 2000 May;(374):115–24.

Esiashvili N, Goodman M, Marcus RB Jr. Changes in incidence and survival of Ewing sarcoma patients over the past 3 decades: Surveillance Epidemiology and End Results data. J Pediatr Hematol Oncol. 2008 Jun;30(6):425–30.

Fan JP, Tsui CP, Tang CY, Chow CL. Influence of interphase layer on the overall elasto-plastic behaviors of HA/PEEK biocomposite. Biomaterials. 2004 Oct;25(23):5363–73.

Farfalli GL, Boland PJ, Morris CD, Athanasian EA, Healey JH. Early Equivalence of Uncemented Press-fit and Compress® Femoral Fixation. Clin Orthop. 2009 Nov;467(11):2792–9.

Felson DT, Gross KD, Nevitt MC, Yang M, Lane NE, Torner JC, et al. The effects of impaired joint position sense on the development and progression of pain and structural damage in knee osteoarthritis. Arthritis Rheum. 2009 Aug 15;61(8):1070–6.

Feng X, McDonald JM. Disorders of Bone Remodeling. Annu Rev Pathol. 2011;6:121.

Fenner V, Behrend H, Kuster MS. Whole Body Gait Function during Stair Ascending and Level Walking in Patients Following Total Knee Arthroplasty. Int J Phys Med Rehabil. 2014 Sep;2(5):2-9

Fish DJ, Nielsen J-P. Clinical Assessment of Human Gait. J Prosthet Orthot. 1993;5(2):39–48.

Freedman EL, Johnson EE. Radiographic analysis of tibial fracture malalignment following intramedullary nailing. Clin Orthop. 1995 Jun;(315):25–33.

Frink SJ, Rutledge J, Lewis VO, Lin PP, Yasko AW. Favorable long-term results of prosthetic arthroplasty of the knee for distal femur neoplasms. Clin Orthop. 2005 Sep;438:65–70.

Fromme P, Blunn GW, Aston WJ, Abdoola T, Koris J, Coathup MJ. The effect of bone growth onto massive prostheses collars in protecting the implant from fracture. Med Eng Phys. 2017 Mar 1;41:19–25.

Frost HM. Bone ‘mass’ and the ‘mechanostat’: a proposal. Anat Rec. 1987 Sep;219(1):1–9.

Frost HM. Skeletal structural adaptations to mechanical usage (SATMU): 2. Redefining Wolff's Law: The remodeling problem. Anat Rec. 1990 Apr 1;226(4):414–22.

Fuchs B, Sim F h. Rotationplasty about the knee: Clin Anat. 2004;17(4):345–353.

Fyhrie DP, Carter DR. A unifying principle relating stress to trabecular bone morphology. J Orthop Res Off Publ Orthop Res Soc. 1986;4(3):304–17.

Gage JR, DeLuca PA, Renshaw TS. Gait analysis: principle and applications with emphasis on its use in cerebral palsy. Instr Course Lect. 1996;45:491–507.

Gage JR. Gait analysis. An essential tool in the treatment of cerebral palsy. Clin Orthop. 1993 Mar;(288):126–34.

Ganesh V, Ramakrishna K, Ghista DN. Biomechanics of bone-fracture fixation by stiffness-graded plates in comparison with stainless-steel plates. Biomed Eng OnLine. 2005 Jul 27;4:46.

Gehrke T, Alijanipour P, Parvizi J. The management of an infected total knee arthroplasty. Bone Jt J. 2015 Jan 10;97–B(10 Supple A):20–9.

Geller DS, Gorlick R. Osteosarcoma: a review of diagnosis, management, and treatment strategies. Clin Adv Hematol Oncol HO. 2010 Oct;8(10):705–18.

Gillespy T, Manfrini M, Ruggieri P, Spanier SS, Pettersson H, Springfield DS. Staging of intraosseous extent of osteosarcoma: correlation of preoperative CT and MR imaging with pathologic macroslides. Radiology. 1988 Jun 1;167(3):765–7.

Gitelis S, Heligman D, Quill G, Piasecki P. The use of large allografts for tumor reconstruction and salvage of the failed total hip arthroplasty. Clin Orthop. 1988 Jun;(231):62–70.

Godinho P, Nicoliche E, Cossich V, de Sousa EB, Velasques B, Salles JI. Proprioceptive deficit in patients with complete tearing of the anterior cruciate ligament. Rev Bras Ortop. 2014 Dec;49(6):613–8.

Goodship AE, Cunningham JL, Kenwright J. Strain rate and timing of stimulation in mechanical modulation of fracture healing. Clin Orthop. 1998 Oct;(355 Suppl):S105-115.

Gorlick R, Janeway K, Lessnick S, Randall RL, Marina N, COG Bone Tumor Committee. Children's Oncology Group's 2013 blueprint for research: bone tumors. Pediatr Blood Cancer. 2013 Jun;60(6):1009–15.

Gorlick R, Khanna C. Osteosarcoma. J Bone Miner Res Off J Am Soc Bone Miner Res. 2010 Apr;25(4):683–91.

Grimer RJ, Carter SR, Pynsent PB. The cost-effectiveness of limb salvage for bone tumours. J Bone Joint Surg Br. 1997 Jul;79(4):558–61.

Grimer RJ, Carter SR, Tillman RM, Sneath RS, Walker PS, Unwin PS, et al. Endoprosthetic replacement of the proximal tibia. J Bone Joint Surg Br. 1999 May;81(3):488–94.

Grimer RJ. Surgical options for children with osteosarcoma. Lancet Oncol. 2005 Feb;6(2):85–92.

Grob KR, Kuster MS, Higgins SA, Lloyd DG, Yata H. Lack of correlation between different measurements of proprioception in the knee. J Bone Joint Surg Br. 2002 May;84(4):614–8.

Gupta A, Pollock R, Cannon SR, Briggs TWR, Skinner J, Blunn G. A knee-sparing distal femoral endoprosthesis using hydroxyapatite-coated extracortical plates. Preliminary results. J Bone Joint Surg Br. 2006 Oct;88(10):1367–72.

Gupta SK, Alassaf N, Harrop AR, Kiefer GN. Principles of rotationplasty. J Am Acad Orthop Surg. 2012 Oct;20(10):657–67.

Gurney B. Leg length discrepancy. Gait Posture. 2002 Apr;15(2):195–206.

Ha SW, Kirch M, Birchler F, Eckert KL, Mayer J, Wintermantel E, et al. Surface activation of polyetheretherketone (PEEK) and formation of calcium phosphate coatings by precipitation. J Mater Sci Mater Med. 1997 Nov;8(11):683–90.

Hacking SA, Boyraz P, Powers BM, Sen-Gupta E, Kucharski W, Brown CA, et al. Surface roughness enhances the osseointegration of titanium headposts in non-human primates. J Neurosci Methods. 2012 Nov 15;211(2):237–44.

Hadjidakis DJ, Androulakis II. Bone Remodeling. Ann N Y Acad Sci. 2006 Dec 1;1092(1):385–96.

Hamilton P, Dunstan E, Maruthainar K, Unwin P, Cannon S, Briggs T. Uncemented Massive Endoprostheses for Primary Bone Tumours: A 7 Year Follow Up. J Bone Joint Surg Br. 2005 Jan 3;87–B(SUPP I):5–5.

Hardes J, Henrichs MP, Gosheger G, Gebert C, Höll S, Dieckmann R, et al. Endoprosthetic replacement after extra-articular resection of bone and soft-tissue tumours around the knee. Bone Jt J. 2013 Oct;95–B(10):1425–31.

Hardes J, von Eiff C, Streitbuerger A, Balke M, Budny T, Henrichs MP, et al. Reduction of periprosthetic infection with silver-coated megaprostheses in patients with bone sarcoma. J Surg Oncol. 2010 Apr 1;101(5):389–95.

Hay R. Infection in the Cancer Patient: A Practical Guide. OUP Oxford; 2006. 292 p.

Heck DA, Chao EY, Sim FH, Pritchard DJ, Shives TC. Titanium fibermetal segmental replacement prostheses. A radiographic analysis and review of current status. Clin Orthop. 1986 Mar;(204):266–85.

Hefti F. Pediatric Orthopedics in Practice. Springer; 2015. 912 p.

Heise U, Minet-Sommer S. [The Borggreve rotation-plasty. A surgical method in therapy of malignant bone tumors and functional results]. Z Für Orthop Ihre Grenzgeb. 1993 Oct;131(5):452–60.

Hench LL, Jones JR. Biomaterials, Artificial Organs and Tissue Engineering. CRC Press; 2005. 297 p.

Henderson ER, Groundland JS, Pala E, Dennis JA, Wooten R, Cheong D, et al. Failure mode classification for tumor endoprostheses: retrospective review of five institutions and a literature review. J Bone Joint Surg Am. 2011 Mar 2;93(5):418–29.

Henshaw R, Malawer M. Review of Endoprosthetic Reconstruction in Limb-sparing Surgery. In: Musculoskeletal Cancer Surgery; 2001 p. 383–403.

Herrera A, Ibarz E, Cegoñino J, Lobo-Escolar A, Puértolas S, López E, et al. Applications of finite element simulation in orthopedic and trauma surgery. World J Orthop. 2012 Apr 18;3(4):25–41.

Huang M-S, Chen L-K, Ou K-L, Cheng H-Y, Wang C-S. Rapid Osseointegration on Titanium Implant With Innovative Nanoporous Surface Modification: Animal Model and Clinical Trial. Implant Dent. 2015 Aug;24(4):441-7.

Huiskes R, Ruimerman R, van Lenthe GH, Janssen JD. Effects of mechanical forces on maintenance and adaptation of form in trabecular bone. Nature. 2000 Jun 8;405(6787):704–6.

Huiskes R, Weinans H, Grootenboer HJ, Dalstra M, Fudala B, Slooff TJ. Adaptive bone-remodeling theory applied to prosthetic-design analysis. J Biomech. 1987;20(11–12):1135–50.

Hwang JS, Mehta AD, Yoon RS, Beebe KS. From amputation to limb salvage reconstruction: evolution and role of the endoprosthesis in musculoskeletal oncology. J Orthop Traumatol Off J Ital Soc Orthop Traumatol. 2014 Jun;15(2):81–6.

Ilyas I, Kurar A, Moreau PG, Younge DA. Modular megaprosthesis for distal femoral tumors. Int Orthop. 2001;25(6):375–7.

Jan van der Woude H, Smithuis R. Bone tumor - well-defined osteolytic tumors and tumor-like lesions [Internet]. 2014. Available from:

http://www.radiologyassistant.nl/en/p4bc6176e56228/bone-tumor-well-defined-osteolytic-tumors-and-tumor-like-lesions.html

Jang IG, Kim IY, Kwak BM. Analogy of Strain Energy Density Based Bone-Remodeling Algorithm and Structural Topology Optimization. J Biomech Eng. 2008 Nov 26;131(1):011012-011012-7.

Jang IG, Nam KW, Park HS, Jo YH, Kang HG, Park JY, et al. Gait symmetry analysis protocol for whole leg movement symmetry evaluation. J Mech Med Biol. 2012 May 20;12(04):1250073.

Jansson E, Källtorp M, Johansson A, Tengvall P, Thomsen P. On the formation of fibrous capsule and fluid space around machined and porous blood plasma clot coated titanium. J Mater Sci Mater Med. 2001 Dec;12(10–12):1019–24.

Jeys L, Grimer R. The long-term risks of infection and amputation with limb salvage surgery using endoprostheses. Recent Results Cancer Res Fortschritte Krebsforsch Prog Dans Rech Sur Cancer. 2009;179:75–84.

Jeys LM, Grimer RJ, Carter SR, Tillman RM. Periprosthetic infection in patients treated for an orthopaedic oncological condition. J Bone Joint Surg Am. 2005 Apr;87(4):842–9.

Jeys LM, Grimer RJ, Carter SR, Tillman RM. Risk of amputation following limb salvage surgery with endoprosthetic replacement, in a consecutive series of 1261 patients. Int Orthop. 2003;27(3):160–3.

Jeys LM, Kulkarni A, Grimer RJ, Carter SR, Tillman RM, Abudu A. Endoprosthetic reconstruction for the treatment of musculoskeletal tumors of the appendicular skeleton and pelvis. J Bone Joint Surg Am. 2008 Jun;90(6):1265–71.

Kadaba MP, Ramakrishnan HK, Wootten ME. Measurement of lower extremity kinematics during level walking. J Orthop Res Off Publ Orthop Res Soc. 1990 May;8(3):383–92.

Kawaguchi N, Ahmed AR, Matsumoto S, Manabe J, Matsushita Y. The concept of curative margin in surgery for bone and soft tissue sarcoma. Clin Orthop. 2004 Feb;(419):165–72.

Kawai A, Backus SI, Otis JC, Healey JH. Interrelationships of clinical outcome, length of resection, and energy cost of walking after prosthetic knee replacement following resection of a malignant tumor of the distal aspect of the femur. J Bone Joint Surg Am. 1998 Jun;80(6):822–31.

Kawai A, Backus SI, Otis JC, Inoue H, Healey JH. Gait characteristics of patients after proximal femoral replacement for malignant bone tumour. J Bone Joint Surg Br. 2000 Jul;82(5):666–9.

Kawamura H, Fuchioka S, Inoue S, Kuratsu S, Yoshikawa H, Katou K, et al. Restoring normal gait after limb salvage procedures in malignant bone tumours of the knee. Scand J Rehabil Med. 1999 Jun;31(2):77–81.

Kennedy RA, Boreham CAG, Murphy MH, Young IS, Mutrie N. Evaluating the effects of a low volume stairclimbing programme on measures of health-related fitness in sedentary office workers. J Sports Sci Med. 2007;6(4):448–54.

Kent PM, Trafton LW. Clinical presentation of bone tumors in children and young adults. Curr Probl Cancer. 2013 Aug;37(4):167–71.

Kershaw CJ, Themen AEC. The Attenborough knee. A four- to ten-year review. Bone Jt J. 1988 Feb 1;70(1):89–93.

Kester MA, Cook SD, Harding AF, Rodriguez RP, Pipkin CS. An evaluation of the mechanical failure modalities of a rotating hinge knee prosthesis. Clin Orthop. 1988 Mar;(228):156–63.

Keyak JH, Falkinstein Y. Comparison of in situ and in vitro CT scan-based finite element model predictions of proximal femoral fracture load. Med Eng Phys. 2003 Nov;25(9):781–7.

Keyak JH, Kaneko TS, Tehranzadeh J, Skinner HB. Predicting proximal femoral strength using structural engineering models. Clin Orthop. 2005 Aug;(437):219–28.

Khalily C, Lester DK. Results of a tapered cementless femoral stem implanted in varus. J Arthroplasty. 2002 Jun;17(4):463–6.

Kilgore C. Gait Analysis Called Useful Outcomes Tool [Internet]. Clinical Rounds Pediatric News. 2005 [cited 2015 Aug 24]. Available from: http://www.internalmedicinenews.com/fileadmin/content_pdf/ped/archive_pdf/vol39iss4/70114_main.pdf

Kim CM, Eng JJ. Symmetry in vertical ground reaction force is accompanied by symmetry in temporal but not distance variables of gait in persons with stroke. Gait Posture. 2003 Aug;18(1):23–8.

Kim H-J, Lee J-H, Lee D-H. Proprioception in Patients With Anterior Cruciate Ligament Tears. Am J Sports Med. 2016 Dec 1;363546516682231.

Kinetics Methodology Home Page [Internet]. [cited 2015 Oct 2]. Available from: http://faculty.educ.ubc.ca/sanderson/courses/HKIN363/LABS/biomech/knmethod/ktcmeth.htm

Kinkel S, Lehner B, Kleinhans JA, Jakubowitz E, Ewerbeck V, Heisel C. Medium to long-term results after reconstruction of bone defects at the knee with tumor endoprostheses. J Surg Oncol. 2010 Feb 1;101(2):166–9.

Kirkwood RN, Gomes H de A, Sampaio RF, Culham E, Costigan P. Biomechanical analysis of hip and knee joints during gait in elderly subjects. Acta Ortopédica Bras. 2007;15(5):267–71.

Koefoed M, Ito H, Gromov K, Reynolds DG, Awad HA, Rubery PT, et al. Biological Effects of rAAV-caAlk2 Coating on Structural Allograft healing. Mol Ther. 2005 Aug;12(2):212–8.

Koerner I, University of Alberta, Health Sciences Audiovisual Education. Observation of human gait. Edmonton, Alta.: Health Sciences Audiovisual Education; 1984.

Kurtz SM, Devine JN. PEEK Biomaterials in Trauma, Orthopedic, and Spinal Implants. Biomaterials. 2007 Nov;28(32):4845.

Kurtz SM, Lau E, Watson H, Schmier JK, Parvizi J. Economic Burden of Periprosthetic Joint Infection in the United States. J Arthroplasty. 2012 Sep;27(8, Supplement):61–65.e1.

Kurtz SM, Ong KL, Lau E, Bozic KJ, Berry D, Parvizi J. Prosthetic Joint Infection Risk after TKA in the Medicare Population. Clin Orthop Relat Res. 2009 Aug 8;468(1):52–6.

Kurtz SM. PEEK Biomaterials Handbook. William Andrew; 2011. 309 p.

Laine T, Lund T, Ylikoski M, Lohikoski J, Schlenzka D. Accuracy of pedicle screw insertion with and without computer assistance: a randomised controlled clinical study in 100 consecutive patients. Eur Spine J. 2000 Jun;9(3):235-40.

Lajoie Y, Teasdale N, Cole JD, Burnett M, Bard C, Fleury M, et al. Gait of a deafferented subject without large myelinated sensory fibers below the neck. Neurology. 1996 Jan 7;47(1):109–15.

Lang JE, Scott RD, Lonner JH, Bono JV, Hunter DJ, Li L. Magnitude of limb lengthening after primary total knee arthroplasty. J Arthroplasty. 2012 Mar;27(3):341–6.

Larsson S, Kim W, Caja VL, Egger EL, Inoue N, Chao EY. Effect of early axial dynamization on tibial bone healing: a study in dogs. Clin Orthop. 2001 Jul;(388):240–51.

Le Vu B, de Vathaire F, Shamsaldin A, Hawkins MM, Grimaud E, Hardiman C, et al. Radiation dose, chemotherapy and risk of osteosarcoma after solid tumours during childhood. Int J Cancer J Int Cancer. 1998 Jul 29;77(3):370–7.

Lemoyne R, Coroian C, Mastroianni T, Grundfest W. Accelerometers for quantification of gait and movement disorders: a perspective review. J Mech Med Biol. 2008 Jun 1;08(02):137–52.

Levine D, Richards J, Whittles MW. Whittles's Gait Anlysis. 5th ed. Elsevier Ltd.; 2012.

Li J, Wang Z, Guo Z, Chen G-J, Fu J, Pei G-X. The use of allograft shell with intramedullary vascularized fibula graft for intercalary reconstruction after diaphyseal resection for lower extremity bony malignancy. J Surg Oncol. 2010 Oct 1;102(5):368–74.

Li JP, Habibovic P, van den Doel M, Wilson CE, de Wijn JR, van Blitterswijk CA, et al. Bone ingrowth in porous titanium implants produced by 3D fiber deposition. Biomaterials. 2007 Jun;28(18):2810–20.

Li W-C, Yang R-S, Tsauo J-Y. Knee proprioception in patients with osteosarcoma around the knee after modular endoprosthetic reconstruction. J Bone Joint Surg Am. 2005 Apr;87(4):850–6.

Liedert A, Kaspar D, Augat P, Ignatius A, Claes L. Mechanobiology of Bone Tissue and Bone Cells. In: Kamkin A, Kiseleva I, editors. Mechanosensitivity in Cells and Tissues. Moscow: Academia; 2005

Lietman SA, Joyce MJ. Bone sarcomas: Overview of management, with a focus on surgical treatment considerations. Cleve Clin J Med. 2010 Jan 3;77(Suppl 1):S8–12.

Lin S-J, Lee C-Y, Huang K-C, Peng K-T, Huang T-W, Lee MS, et al. Improved femoral component rotation in advanced genu valgum deformity using computer-assisted measured resection total knee arthroplasty. J Orthop Surg. 2015;10(1):135.

Lokhande MV, Shetye J, Mehta A, Deo MV. Assessment of Knee Joint Proprioception in Weight Bearing and in Non-Weight Bearing Positions in Normal Subjects. JKIMSU, Vol. 2, No. 2, July-Dec. 2013

Lugade V, Wu A, Jewett B, Collis D, Chou L-S. Gait asymmetry following an anterior and anterolateral approach to total hip arthroplasty. Clin Biomech Bristol Avon. 2010 Aug;25(7):675–80.

Lundberg A, Svensson OK, Bylund C, Selvik G. Kinematics of the ankle/foot complex--Part 3: Influence of leg rotation. Foot Ankle. 1989 Jun;9(6):304–9.

Lythgo N, Wilson C, Galea M. Basic gait and symmetry measures for primary school-aged children and young adults. II: walking at slow, free and fast speed. Gait Posture. 2011 Jan;33(1):29–35.

Lythgo N, Wilson C, Galea M. Basic gait and symmetry measures for primary school-aged children and young adults whilst walking barefoot and with shoes. Gait Posture. 2009 Nov;30(4):502–6.

Malawer M, Henshaw RM, Kellar-Graney K. Overview of Endoprosthetic Reconstruction. In: Operative Techniques in Orthopaedic Surgical Oncology. Wolters Kluwer; 2001.

Malawer MM, Sugarbaker PH. Musculoskeletal Cancer Surgery: Treatment of Sarcomas and Allied Diseases. Springer; 2001. 648 p.

Malcolm TL, Bederman SS, Schwarzkopf R. Outcomes of Varus Valgus Constrained Versus Rotating-Hinge Implants in Total Knee Arthroplasty. Orthopedics. 2016 Feb;39(1):e140-148.

Manning DW, Chiang PP, Freiberg AA. Hinge Implants. In: Revision Total Knee Arthroplasty. 2005. p. 219–36.

Marasovic T, Cecic M, Zanchi V. Analysis and Interpretation of Ground Reaction Forces in Normal Gait. WSEAS Trans Math. 2009 Sep;8(9):1105–14.

Marina N, Gebhardt M, Teot L, Gorlick R. Biology and therapeutic advances for pediatric osteosarcoma. The oncologist. 2004;9(4):422–41.

Martini FH. Fundamentals of Anatomy and Physiology. Seventh. Pearson; 2006.

Maruthainar K, Dunstan ER, Hamilton PD, Unwin P, Cannon SR, Briggs TWRB. Massive endoprostheses for giant cell tumours of the distal femur: A 12-year follow-up. The Knee. 2006 Oct;13(5):378–81.

Matena J, Petersen S, Gieseke M, Teske M, Beyerbach M, Kampmann A, et al. Comparison of Selective Laser Melted Titanium and Magnesium Implants Coated with PCL. Int J Mol Sci. 2015 Jun 10;16(6):13287–301.

Matsuda Y, Ishii Y, Noguchi H, Ishii R. Varus-valgus balance and range of movement after total knee arthroplasty. J Bone Joint Surg Br. 2005 Jun;87(6):804–8.

Matthews LS, Goldstein SA, Kolowich PA, Kaufer H. Spherocentric arthroplasty of the knee. A long-term and final follow-up evaluation. Clin Orthop. 1986 Apr;(205):58–66.

Mattos CBRD, Binitie O, Dormans JP. Pathological fractures in children. Bone Jt Res. 2012 Jan 10;1(10):272–80.

Mavrogenis AF, Angelini A, Pala E, Sakellariou VI, Ruggieri P, Papagelopoulos PJ. Reconstruction of the Extensor Mechanism After Major Knee Resection. Orthopedics. 2012 May 1;35(5):e672–80.

Mavrogenis AF, Papagelopoulos PJ, Coll-Mesa L, Pala E, Guerra G, Ruggieri P. Infected Tumor Prostheses. Orthopedics. 2011 Dec 1;34(12):991–8.

Meirelles L, Brånemark P-I, Albrektsson T, Feng C, Johansson C. Histological evaluation of bone formation adjacent to dental implants with a novel apical chamber design: preliminary data in the rabbit model. Clin Implant Dent Relat Res. 2015 Jun;17(3):453–60.

Merryweather A, Yoo B, Bloswick D. Gait Characteristics Associated with Trip-Induced Falls on Level and Sloped Irregular Surfaces. Minerals. 2011 Nov 23;1(1):109–21.

Meswania JM, Taylor SJG, Blunn GW. Design and characterization of a novel permanent magnet synchronous motor used in a growing prosthesis for young patients with bone cancer. Proc Inst Mech Eng [H]. 2008 Apr;222(3):393–402.

Min B-W, Song K-S, Bae K-C, Cho C-H, Kang C-H, Kim S-Y. The effect of stem alignment on results of total hip arthroplasty with a cementless tapered-wedge femoral component. J Arthroplasty. 2008 Apr;23(3):418–23.

Mirabello L, Troisi RJ, Savage SA. International osteosarcoma incidence patterns in children and adolescents, middle ages and elderly persons. Int J Cancer J Int Cancer. 2009 Jul 1;125(1):229–34.

Morgan H, Battista V, Leopold SS. Constraint in primary total knee arthroplasty. J Am Acad Orthop Surg. 2005 Dec;13(8):515–24.

Morii T, Yabe H, Morioka H, Beppu Y, Chuman H, Kawai A, et al. Postoperative deep infection in tumor endoprosthesis reconstruction around the knee. J Orthop Sci Off J Jpn Orthop Assoc. 2010 May;15(3):331–9.

Mündermann A, Dyrby CO, D'Lima DD, Colwell CW, Andriacchi TP. In vivo knee loading characteristics during activities of daily living as measured by an instrumented total knee replacement. J Orthop Res Off Publ Orthop Res Soc. 2008 Sep;26(9):1167–72.

Murray DG, Wilde AH, Werner F, Foster D. Herbert total knee prosthesis: combined laboratory and clinical assessment. J Bone Joint Surg Am. 1977 Dec;59(8):1026–32.

Murray DW, Fitzpatrick R, Rogers K, Pandit H, Beard DJ, Carr AJ, et al. The use of the Oxford hip and knee scores. J Bone Joint Surg Br. 2007 Aug;89(8):1010–4.

Muscolo DL, Ayerza MA, Aponte-Tinao L, Farfalli G. Allograft Reconstruction After Sarcoma Resection in Children Younger Than 10 Years Old. Clin Orthop. 2008 Aug;466(8):1856–62.

Myers GJC, Abudu AT, Carter SR, Tillman RM, Grimer RJ. Endoprosthetic replacement of the distal femur for bone tumours: long-term results. J Bone Joint Surg Br. 2007 Apr;89(4):521–6.

Myers GJC, Abudu AT, Carter SR, Tillman RM, Grimer RJ. The long-term results of endoprosthetic replacement of the proximal tibia for bone tumours. J Bone Joint Surg Br. 2007 Dec;89(12):1632–7.

Nackaerts O, Maes F, Yan H, Couto Souza P, Pauwels R, Jacobs R. Analysis of intensity variability in multislice and cone beam computed tomography. Clin Oral Implants Res. 2011 Aug;22(8):873–9.

Nagarajan R, Neglia JP, Clohisy DR, Robison LL. Limb salvage and amputation in survivors of pediatric lower-extremity bone tumors: what are the long-term implications? J Clin Oncol Off J Am Soc Clin Oncol. 2002 Nov 15;20(22):4493–501.

Nester CJ, Findlow AF, Bowker P, Bowden PD. Transverse plane motion at the ankle joint. Foot Ankle Int. 2003 Feb;24(2):164–8.

Nguyen MP, Buckwalter JA, Miller BJ. Patterns of Improvement Following Oncologic Reconstructrion Compared to Total Knee Arthroplasty and Revision Knee Arthroplasty. Iowa Orthop J. 2011;31:160–5.

Niinomi M. Low Modulus Titanium Alloys for Inhibiting Bone Atrophy. 2011 [cited 2017 Jan 31]; Available from: http://www.intechopen.com/books/biomaterials-science-and-engineering/low-modulus-titanium-alloys-for-inhibiting-bone-atrophy

Niinomi M. Mechanical biocompatibilities of titanium alloys for biomedical applications. J Mech Behav Biomed Mater. 2008 Jan;1(1):30–42.

Nouri A, Hodgson PD, Wen C. Biomimetic Porous Titanium Scaffolds for Orthopedic and Dental Applications. Iowa Orthop J. 2010 March;30(21): 144-149.

Nuno N., Amabili R., Groppetti R., Rossi A., Static coefficient of friction between Ti6Al-4V and PMMA for cemented hip and knee implants. J Biomed Mater Res. 2002 Jan;59(1):191-200.

O'Donnell RJ. Compressive Osseointegration of Tibial Implants in Primary Cancer Reconstruction. Clin Orthop. 2009 Nov;467(11):2807–12.

Ochs BG, Simank HG, Kopp-Schneider A, Rupp R, Schablowski-Trautmann M. [Gait analysis in limb-preserving tumour surgery--kinematic gait patterns after resection of malignant bone tumours near the knee joint]. Z Orthopadie Unfallchirurgie. 2007 Dec;145(6):763–71.

Oddy MJ, Pendegrass CJ, Goodship AE, Cannon SR, Briggs TWR, Blunn GW. Extensor mechanism reconstruction after proximal tibial replacement. J Bone Joint Surg Br. 2005 Jun;87(6):873–8.

Office of the Surgeon General (US). The Basics of Bone in Health and Disease [Internet]. Office of the Surgeon General (US); 2004 [cited 2017 Jan 31]. Available from: https://www.ncbi.nlm.nih.gov/books/NBK45504/

Ogura K, Miyamoto S, Sakuraba M, Fujiwara T, Chuman H, Kawai A. Intercalary Reconstruction after Wide Resection of Malignant Bone Tumors of the Lower Extremity Using a Composite Graft with a Devitalized Autograft and a Vascularized Fibula. Sarcoma 2015; 2015: 861575.

Oh I-H, Nomura N, Hanada S. Microstructures and Mechanical Properties of Porous Titanium Compacts Prepared by Powder Sintering. Mater Trans. 2002;43(3):443–6.

Ohyama T, Uchida T, Shibuya N, Nakabayashi S, Ishigami T, Ogawa T. High bone-implant contact achieved by photofunctionalization to reduce periimplant stress: a three-dimensional finite element analysis. Implant Dent. 2013 Feb;22(1):102–8.

Okita Y, Tatematsu N, Nagai K, Nakayama T, Nakamata T, Okamoto T, et al. The effect of walking speed on gait kinematics and kinetics after endoprosthetic knee replacement following bone tumor resection. Gait Posture. 2014 Sep;40(4):622–7.

Okita Y, Tatematsu N, Nagai K, Nakayama T, Nakamata T, Okamoto T, et al. Compensation by nonoperated joints in the lower limbs during walking after

endoprosthetic knee replacement following bone tumor resection. Clin Biomech. 2013 Oct;28(8):898–903.

Okita Y, Tatematsu N, Nagai K, Nakayama T, Nakamata T, Okamoto T, et al. Characteristics of flexed knee gait and functional outcome of a patient who underwent knee reconstruction with a hingeless prosthesis for bone tumor resection: a case report with gait analysis and comparison with healthy subjects. Eur J Phys Rehabil Med. 2013 December;49(6):849-55

Oren R, Zagury A, Katzir O, Kollender Y, Meller I. Principles of Rehabilitation after Limb-sparing Surgery for Cancer. In: Musculoskeletal Cancer Surgery; pp 583-593

Orishimo KF, Kremenic IJ, Deshmukh AJ, Nicholas SJ, Rodriguez JA. Does total knee arthroplasty change frontal plane knee biomechanics during gait? Clin Orthop. 2012 Apr;470(4):1171–6.

Orlic D, Smerdelj M, Kolundzic R, Bergovec M. Lower limb salvage surgery: modular endoprosthesis in bone tumour treatment. Int Orthop. 2006 Dec;30(6):458–64.

Pakuła G, Słowiński J, Scigała K. Biomechanics of distal femoral fracture fixed with an angular stable LISS plate. Acta Bioeng Biomech Wroc Univ Technol. 2013;15(4):57–65.

Pala E, Henderson ER, Calabrò T, Angelini A, Abati CN, Trovarelli G, et al. Survival of current production tumor endoprostheses: complications, functional results, and a comparative statistical analysis. J Surg Oncol. 2013 Nov;108(6):403–8.

Pap G, Machner A, Nebelung W, Awiszus F. Detailed analysis of proprioception in normal and ACL-deficient knees. J Bone Joint Surg Br. 1999 Sep;81(5):764–8.

Pap G, Meyer M, Weiler HT, Machner A, Awiszus F. Proprioception after total knee arthroplasty: a comparison with clinical outcome. Acta Orthop Scand. 2000 Apr;71(2):153–9.

Park DH, Jaiswal PK, Al-Hakim W, Aston WJS, Pollock RC, Skinner JA, et al. The Use of Massive Endoprostheses for the Treatment of Bone Metastases. Sarcoma. 2007; 2007: 62151.

Park K-H, Kim D-Y, Kim T-H. The effect of step climbing exercise on balance and step length in chronic stroke patients. J Phys Ther Sci. 2015 Nov;27(11):3515–8.

Patterson KK, Gage WH, Brooks D, Black SE, McIlroy WE. Evaluation of gait symmetry after stroke: a comparison of current methods and recommendations for standardization. Gait Posture. 2010 Feb;31(2):241–6.

Pendegrass CJ, Oddy MJ, Cannon SR, Briggs T, Goodship AE, Blunn GW. A histomorphological study of tendon reconstruction to a hydroxyapatite-coated implant: regeneration of a neo-enthesis in vivo. J Orthop Res Off Publ Orthop Res Soc. 2004 Nov;22(6):1316–24.

Perry J. Gait Analysis: Normal and Pathological Function. SLACK; 1992. 566 p.

Perttunen JR, Anttila E, Södergård J, Merikanto J, Komi PV. Gait asymmetry in patients with limb length discrepancy. Scand J Med Sci Sports. 2004 Feb;14(1):49–56.

Petrovic L, Pohle D, Münstedt H, Rechtenwald T, Schlegel KA, Rupprecht S. Effect of betaTCP filled polyetheretherketone on osteoblast cell proliferation in vitro. J Biomed Sci. 2006 Jan;13(1):41–6.

Pilliar RM, Lee JM, Maniatopoulos C. Observations on the effect of movement on bone ingrowth into porous-surfaced implants. Clin Orthop. 1986 Jul;(208):108–13.

Pizzo PA, Poplack DG. Principles and Practice of Pediatric Oncology. Lippincott Williams & Wilkins; 2006. 1816 p.

Plasma Spray - Thermal Spray Coating Process [Internet]. [cited 2015 Jun 21]. Available from: http://www.gordonengland.co.uk/ps.htm

Plötz W, Rechl H, Burgkart R, Messmer C, Schelter R, Hipp E, et al. Limb salvage with tumor endoprostheses for malignant tumors of the knee. Clin Orthop. 2002 Dec;(405):207–15.

Pour AE, Parvizi J, Slenker N, Purtill JJ, Sharkey PF. Rotating hinged total knee replacement: use with caution. J Bone Joint Surg Am. 2007 Aug;89(8):1735–41.

Puri A, Subin BS, Agarwal MG. Fibular centralisation for the reconstruction of defects of the tibial diaphysis and distal metaphysis after excision of bone tumours. J Bone Joint Surg Br. 2009 Feb;91(2):234–9.

Puri A. Tips and tricks of limb salvage: Proximal tibia. Indian J Orthop. 2014;48(3):296–300.

Qiu S, Gui L, Wang M, Chen Y, Niu F, Liu J, et al. Biomechanical analysis of reduction malarplasty with L-shaped osteotomy. J Craniofac Surg. 2012 May;23(3):749–54.

Qureshi A, Zahid KF, Ibrahim SI, Burney I. Osteosarcoma arising on a background of Paget's disease report of an unusual case. BMJ Case Rep. 2013;2013.

Racano A, Pazionis T, Farrokhyar F, Benjamin Deheshi MD Ms, Michelle Ghert MD F. High Infection Rate Outcomes in Long-bone Tumor Surgery with Endoprosthetic Reconstruction in Adults: A Systematic Review. Clin Orthop Relat Res. 2013 Jun 1;471(6):2017–27.

Ramos A, Simões JA. Tetrahedral versus hexahedral finite elements in numerical modelling of the proximal femur. Med Eng Phys. 2006 Nov;28(9):916–24.

Rana K, Wadhwa V, Bhargava EK, Batra V, Mandal S. Ewing's Sarcoma Multifocal Metastases to Temporal and Occipital Bone: A Rare Presentation. J Clin Diagn Res JCDR. 2015 Jun;9(6):MD04-MD05.

Rancho Los Amigos National Rehabilitation Center. Observational Gait Analysis. Los Amigos Research and Education Institute, Rancho Los Amigos National Rehabilitation Center; 2001. 72 p.

Ratner BD, Hoffman AS, Schoen FJ, Lemons JE. Biomaterials Science: An Introduction to Materials in Medicine. Academic Press; 2012. 1610 p.

Refaat Y, Gunnoe J, Hornicek FJ, Mankin HJ. Comparison of quality of life after amputation or limb salvage. Clin Orthop. 2002 Apr;(397):298–305.

Rennie May. Polyetheretherketones. In: Encyclopedia of Polymer Science and Technology. John Wiley & Sons, Inc.; 2002

Research Council [Internet]. GCMAS. [cited 2015 Aug 24]. Available from: http://www.gcmas.org/research

Revell PA. The combined role of wear particles, macrophages and lymphocytes in the loosening of total joint prostheses. J R Soc Interface. 2008 Nov 6;5(28):1263–78.

Rho JY, Ashman RB, Turner CH. Young's modulus of trabecular and cortical bone material: ultrasonic and microtensile measurements. J Biomech. 1993 Feb;26(2):111–9.

Riemann BL, Lephart SM. The sensorimotor system, part I: the physiologic basis of functional joint stability. J Athl Train. 2002 Jan;37(1):71–9.

Riener R, Rabuffetti M, Frigo C. Stair ascent and descent at different inclinations. Gait Posture. 2002 Feb;15(1):32–44.

Rödl RW, Ozaki T, Hoffmann C, Böttner F, Lindner N, Winkelmann W. Osteoarticular allograft in surgery for high-grade malignant tumours of bone. J Bone Joint Surg Br. 2000 Sep;82–B(7):1006–10.

Rompen JC, Ham SJ, Halbertsma JPK, Horn JRV. Gait and function in patients with a femoral endoprosthesis after tumor resection. Acta Orthop Scand. 2002 Jan 1;73(4):439–46.

Rong-Sen Y. Limb Salvage Operations for Patients with Malignant Bone Tumors in the Extremities. Tzu Chi Med J. 2005 May 2;6(17):389–96.

Safran MR, Borsa PA, Lephart SM, Fu FH, Warner JJ. Shoulder proprioception in baseball pitchers. J Shoulder Elb Surg Am Shoulder Elb Surg Al. 2001 Oct;10(5):438–44.

Sanghrajka A, Amin A, Briggs TWR, Cannon SR, Blunn G, Unwin P. The Effect of a Hydroxyapatite-Coated, Grooved Femoral Collar on Radiographic Loosening of Distal Femoral Endoprostheses. J Bone Joint Surg Br. 2005 Jan 3;87–B(SUPP I):77–77.

Saurabh M, Yadav Y. Literature Review on Finite Element Method. International Journal of Enhanced Research in Science, Technology & Engineering. 2016 Mar;5(3):267–9.

Schwartz AJ, Kabo JM, Eilber FC, Eilber FR, Eckardt JJ. Endoprosthetic reconstruction after resection of musculoskeletal. Am J Orthop Belle Mead NJ. 2014 Mar;43(3):122–7.

Schwartz HS. Orthopaedic Knowledge Update: Musculoskeletal Tumors 2. 2nd edition. Rosemont, IL: Amer Academy of Orthopaedic; 2007. 426 p.

Schwarzkopf R, Chaudhry S, Kummer FJ, Marwin SE. Failure of the tibial insert in a rotating hinge total knee arthroplasty. J Arthroplasty. 2011 Sep;26(6):977.e5-8.

Sewell MD, Hanna SA, McGrath A, Aston WJS, Blunn GW, Pollock RC, et al. Intercalary diaphyseal endoprosthetic reconstruction for malignant tibial bone tumours. J Bone Joint Surg Br. 2011 Aug;93(8):1111–7.

Sharma DN, Rastogi S, Bakhshi S, Rath GK, Julka PK, Laviraj MA, et al. Role of extracorporeal irradiation in malignant bone tumors. Indian J Cancer. 2013 Jan 10;50(4):306.

Sharma S, Turcotte RE, Isler MH, Wong C. Cemented rotating hinge endoprosthesis for limb salvage of distal femur tumors. Clin Orthop. 2006 Sep;450:28–32.

Shaw JA, Balcom W, Greer RB. Total knee arthroplasty using the kinematic rotating hinge prosthesis. Orthopedics. 1989 May;12(5):647–54.

Sheehan JM. Arthroplasty of the knee. Clin Orthop. 1979 Dec;(145):101–9.

Shindell R, Neumann R, Connolly JF, Jardon OM. Evaluation of the Noiles hinged knee prosthesis. A five-year study of seventeen knees. J Bone Joint Surg Am. 1986 Apr;68(4):579–85.

Siegel R, Naishadham D, Jemal A. Cancer statistics, 2013. CA Cancer J Clin. 2013;63(1):11–30.

Simmons CA, Valiquette N, Pilliar RM. Osseointegration of sintered porous-surfaced and plasma spray-coated implants: An animal model study of early postimplantation healing response and mechanical stability. J Biomed Mater Res. 1999 Nov;47(2):127–38.

Simon MA, Aschliman MA, Thomas N, Mankin HJ. Limb-salvage treatment versus amputation for osteosarcoma of the distal end of the femur. 1986. J Bone Joint Surg Am. 2005 Dec;87(12):2822.

Simon U, Augat P, Ignatius A, Claes L. Influence of the stiffness of bone defect implants on the mechanical conditions at the interface--a finite element analysis with contact. J Biomech. 2003 Aug;36(8):1079–86.

Singh VA, Nagalingam J, Saad M, Pailoor J. Which is the best method of sterilization of tumour bone for reimplantation? A biomechanical and histopathological study. Biomed Eng Online. 2010;9:48.

Spiegelberg BGI, Sewell MD, Aston WJS, Blunn GW, Pollock R, Cannon SR, et al. The early results of joint-sparing proximal tibial replacement for primary bone tumours, using extracortical plate fixation. J Bone Joint Surg Br. 2009 Oct;91(10):1373–7.

Springer BD, Sim FH, Hanssen AD, Lewallen DG. The modular segmental kinematic rotating hinge for nonneoplastic limb salvage. Clin Orthop. 2004 Apr;(421):181–7.

Stauffer RN, Ehrlich MG. Advances in Operative Orthopaedics. Mosby Incorporated; 1995. 328 p.

Sumitomo N, Noritake K, Hattori T, Morikawa K, Niwa S, Sato K, et al. Experiment study on fracture fixation with low rigidity titanium alloy. J Mater Sci Mater Med. 2008 Apr 1;19(4):1581–6.

Suprak DN, Osternig LR, van Donkelaar P, Karduna AR. Shoulder joint position sense improves with elevation angle in a novel, unconstrained task. J Orthop Res. 2006 Mar 1;24(3):559–68.

Swanik CB, Lephart SM, Rubash HE. Proprioception, Kinesthesia, and Balance After Total Knee Arthroplasty with Cruciate-Retaining and Posterior Stabilized Prostheses. J Bone Jt Surg. 2004 Feb 1;86(2):328–34.

Taddei F, Schileo E, Helgason B, Cristofolini L, Viceconti M. The material mapping strategy influences the accuracy of CT-based finite element models of bones: an evaluation against experimental measurements. Med Eng Phys. 2007 Nov;29(9):973–9.

Tanzer M, Turcotte R, Harvey E, Bobyn JD. Extracortical bone bridging in tumor endoprostheses. Radiographic and histologic analysis. J Bone Joint Surg Am. 2003 Dec;85–A(12):2365–70.

Taylor GI, Miller GD, Ham FJ. The free vascularized bone graft. A clinical extension of microvascular techniques. Plast Reconstr Surg. 1975 May;55(5):533–44.

Taylor SJ, Perry JS, Meswania JM, Donaldson N, Walker PS, Cannon SR. Telemetry of forces from proximal femoral replacements and relevance to fixation. J Biomech. 1997 Mar;30(3):225–34.

Taylor SJ, Walker PS. Forces and moments telemetered from two distal femoral replacements during various activities. J Biomech. 2001 Jul;34(7):839–48.

Teo HEL, Peh WCG. Primary bone tumors of adulthood. Cancer Imaging. 2004 Mar 31;4(2):74–83.

The Oxford Knee Score (OKS) [Internet]. Isis Innovation. [cited 2015 Sep 28]. Available from: http://isis-innovation.com/outcome-measures/oxford-knee-score-oks/

The SF Community - SF-36® Health Survey Update [Internet]. [cited 2015 Sep 15]. Available from: http://www.sf-36.org/tools/sf36.shtml

Tipton S, Sutherland J, Schwarzkopf R. Change in Limb Length After Total Knee Arthroplasty. Geriatr Orthop Surg Rehabil. 2015 Sep;6(3):197–201.

Titus V, Clayer M. Protecting a Patellar Ligament Reconstruction after Proximal Tibial Resection: A Simplified Approach. Clin Orthop. 2008 Jul;466(7):1749–54.

Tongen A, Wunderlich RE. The biomechanics of walking and running. ResearchGate. 1994 Nov 1;13(4):843–63.

Tortora GJ, Grabowski SR. Principles of anatomy and physiology. HarperCollinsCollege; 1993. 1168 p.

Tsauo J-Y, Li W-C, Yang R-S. Functional outcomes after endoprosthetic knee reconstruction following resection of osteosarcoma near the knee. Disabil Rehabil. 2006 Jan 15;28(1):61–6.

Tsili MC. Theoretical solutions for internal bone remodeling of diaphyseal shafts using adaptive elasticity theory. J Biomech. 2000 Feb;33(2):235–9.

Tsuboyama T, Windhager R, Bochdansky T, Yamamuro T, Kotz R. Gait after knee arthroplasty for femoral tumor. Foot pressure patterns recorded in 20 patients. Acta Orthop Scand. 1994 Feb;65(1):51–4.

Tsuchiya H, Morsy AF, Matsubara H, Watanabe K, Abdel-Wanis ME, Tomita K. Treatment of benign bone tumours using external fixation. J Bone Joint Surg Br. 2007 Jan 8;89–B(8):1077–83.

Tsui YC, Doyle C, Clyne TW. Plasma sprayed hydroxyapatite coatings on titanium substrates Part 1: Mechanical properties and residual stress levels. Biomaterials. 1998 Nov;19(22):2015–29.

Tunn PU, Pomraenke D, Goerling U, Hohenberger P. Functional outcome after endoprosthetic limb-salvage therapy of primary bone tumours—a comparative analysis using the MSTS score, the TESS and the RNL index. Int Orthop. 2008 Oct;32(5):619–25.

Turner MJ, Clough RW, Martin H., Topp LJ. Stiffness and Deflection Analysis of Complex Structures. J Aeronaut Sci. 1956 Sep 1;23(9):805–23.

Unwin PS, Cannon SR, Grimer RJ, Kemp HB, Sneath RS, Walker PS. Aseptic loosening in cemented custom-made prosthetic replacements for bone tumours of the lower limb. J Bone Joint Surg Br. 1996 Jan;78(1):5–13.

Unwin PS, Cobb JP, Walker PS. Distal femoral arthroplasty using custom-made prostheses. The first 218 cases. J Arthroplasty. 1993 Jun;8(3):259–68.

Unwin PS, Walker PS, Blunn GW. A radiographic and retrieval study, comparing porous collared and hydroxyapatite coated segmental femoral replacements. In 1995.

Unwin PS. Modular or Custom-made reconstruction? Poster presented at: The Asia Pacific Musculoskeletal Tumour Society; 2006; Chaing Mai, Thailand.

Vaishya R, Agarwal AK, Vijay V. Extensor Mechanism Disruption after Total Knee Arthroplasty: A Case Series and Review of Literature. Cureus. 2016 Feb; 8(2): e479

van Krieken FM, den Heeten GJ, Pedersen DR, Brand RA, Crowninshield RD. Prediction of muscle and joint loads after segmental femur replacement for osteosarcoma. Clin Orthop. 1985 Sep;(198):273–83.

Veenstra KM, Sprangers MA, van der Eyken JW, Taminiau AH. Quality of life in survivors with a Van Ness-Borggreve rotationplasty after bone tumour resection. J Surg Oncol. 2000 Apr;73(4):192–7.

Veth R, van Hoesel R, Pruszczynski M, Hoogenhout J, Schreuder B, Wobbes T. Limb salvage in musculoskeletal oncology. Lancet Oncol. 2003 Jun;4(6):343–50.

Wang C-J. Injuries to the posterior cruciate ligament and posterolateral instabilities of the knee. Chang Gung Med J. 2002 May;25(5):288–97.

Ward WG, Johnston KS, Dorey FJ, Eckardt JJ. Extramedullary porous coating to prevent diaphyseal osteolysis and radiolucent lines around proximal tibial replacements. A preliminary report. J Bone Joint Surg Am. 1993 Jul;75(7):976–87.

Ward WG, Johnston KS, Dorey FJ, Eckardt JJ. Loosening of massive proximal femoral cemented endoprostheses. Radiographic evidence of loosening mechanism. J Arthroplasty. 1997 Oct;12(7):741–50.

Warren PJ, Olanlokun TK, Cobb AG, Bentley G. Proprioception after knee arthroplasty. The influence of prosthetic design. Clin Orthop. 1993 Dec;(297):182–7.

Weber K, Damron TA, Frassica FJ, Sim FH. Malignant bone tumors. Instr Course Lect. 2008;57:673–88.

Wiesel SW. Operative Techniques in Orthopaedic Surgery. Lippincott Williams & Wilkins; 2012. 1184 p.

Winter DA. Biomechanics of Normal and Pathological Gait. J Mot Behav. 1989 Dec 1;21(4):337–55.

Winter DA. Kinematic and kinetic patterns in human gait: Variability and compensating effects. Hum Mov Sci. 1984 Jun;3(1–2):51–76.

Winter DA. The Biomechanics and Motor Control of Human Gait: Normal, Elderly and Pathological. University of Waterloo Press; 1991. 164 p.

Wodajo FM, Bickels J, Wittig J, Malawer M. Complex reconstruction in the management of extremity sarcomas. Curr Opin Oncol. 2003 Jul;15(4):304–12.

Wolff J. The Law of Bone Remodelling. Springer Science & Business Media; 2012. 310 p.

Wong KC, Kumta SM, Chiu KH, Antonio GE, Unwin P, Leung KS. Precision tumour resection and reconstruction using image-guided computer navigation. J Bone Joint Surg Br. 2007 Jan 7;89–B(7):943–7.

Wong KC, Kumta SM, Sze KY, Wong CM. Use of a patient-specific CAD/CAM surgical jig in extremity bone tumor resection and custom prosthetic reconstruction. Comput Aided Surg Off J Int Soc Comput Aided Surg. 2012;17(6):284–93.

Wong KC, Kumta SM. Joint-preserving Tumor Resection and Reconstruction Using Image-guided Computer Navigation. Clin Orthop. 2013 Mar;471(3):762–73.

Wong K-C, Kumta S-M. Use of Computer Navigation in Orthopedic Oncology. Curr Surg Rep. 2014; 2(4): 47.

Wyatt M, Hooper G, Frampton C, Rothwell A. Survival outcomes of cemented compared to uncemented stems in primary total hip replacement. World J Orthop. 2014 Nov 18;5(5):591–6.

Yosibash Z, Trabelsi N, Milgrom C. Reliable simulations of the human proximal femur by high-order finite element analysis validated by experimental observations. J Biomech. 2007;40(16):3688–99.

Yu S, Hariram KP, Kumar R, Cheang P, Aik KK. In vitro apatite formation and its growth kinetics on hydroxyapatite/polyetheretherketone biocomposites. Biomaterials. 2005 May;26(15):2343–52.

Yu X, Xu M, Song R, Fu Z, Liu X. Long-term outcome of giant cell tumors of bone around the knee treated by en bloc resection of tumor and reconstruction with prosthesis. Orthop Surg. 2010 Aug;2(3):211–7.

Zehr RJ, Enneking WF, Scarborough MT. Allograft-prosthesis composite versus megaprosthesis in proximal femoral reconstruction. Clin Orthop. 1996 Jan;(322):207–23.

Zhang X, Xie C, Lin AS, Ito H, Awad H, Lieberman JR, et al. Periosteal Progenitor Cell Fate in Segmental Cortical Bone Graft Transplantations: Implications for Functional Tissue Engineering. J Bone Miner Res Off J Am Soc Bone Miner Res. 2005 Dec;20(12):2124–37.

Appendix

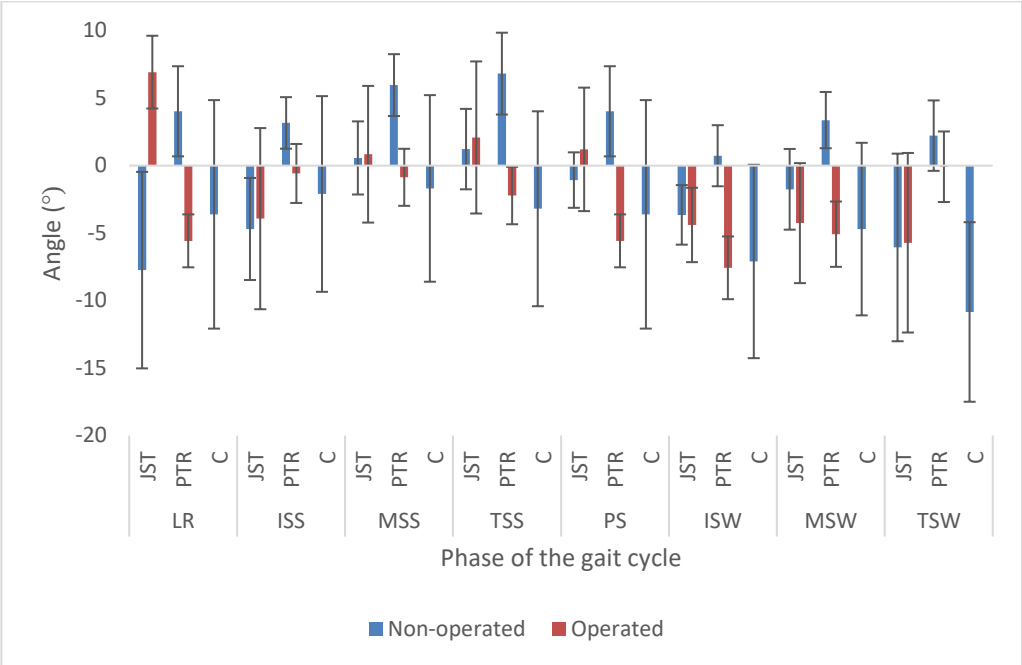

Appendix 1 Mean hip joint angles in the horizontal plane for proximal tibial joint-sparing and joint sacrificing groups and the control group.

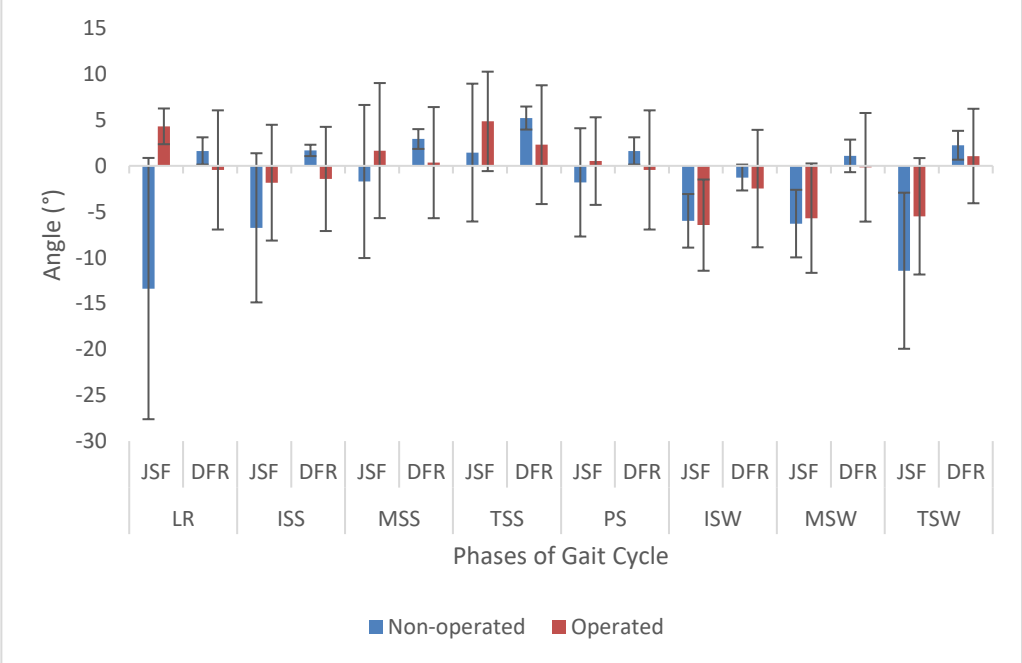

Appendix 2 Mean hip joint angle in the horizontal plane for distal femoral joint-sparing and joint sacrificing groups.

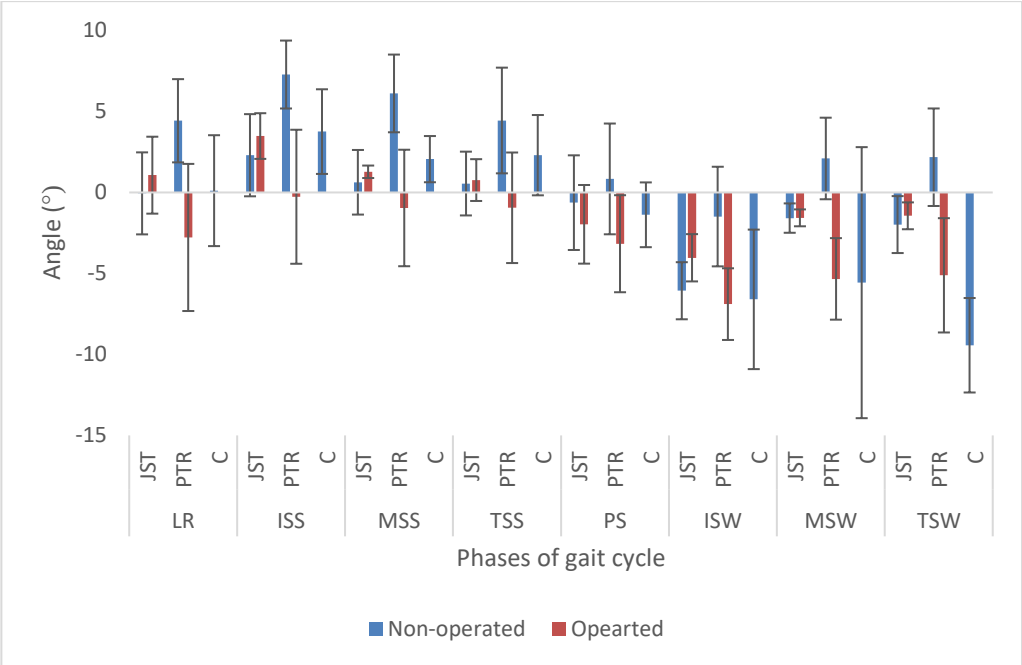

Appendix 3 Mean hip angle in the coronal plane in the proximal tibial joint-sparing and joint sacrificing groups and in the control group.

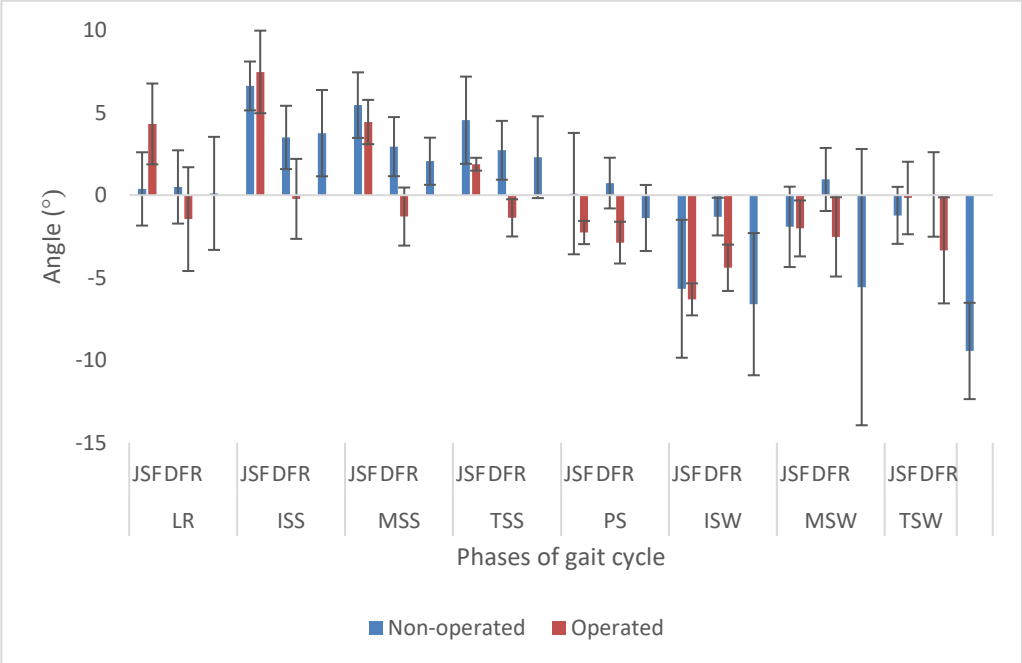

Appendix 4 Mean hip angle in the coronal plane in the distal femoral joint-sparing and joint sacrificing groups and in the control group.

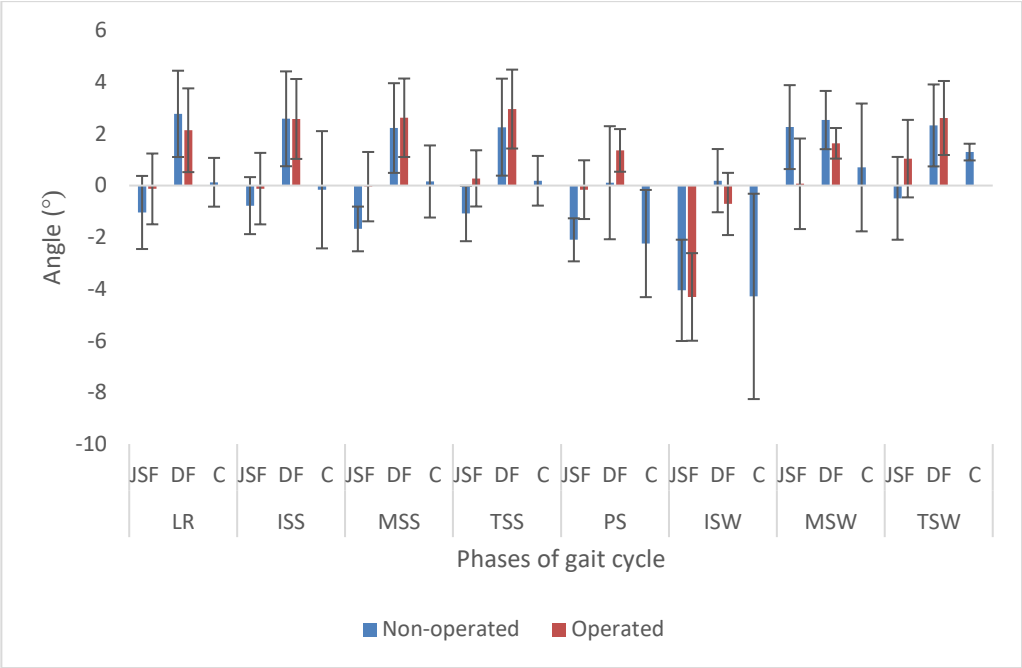

Appendix 5 Mean knee angle in the coronal plane in the distal femoral joint-sparing and joint sacrificing groups and in the control group.

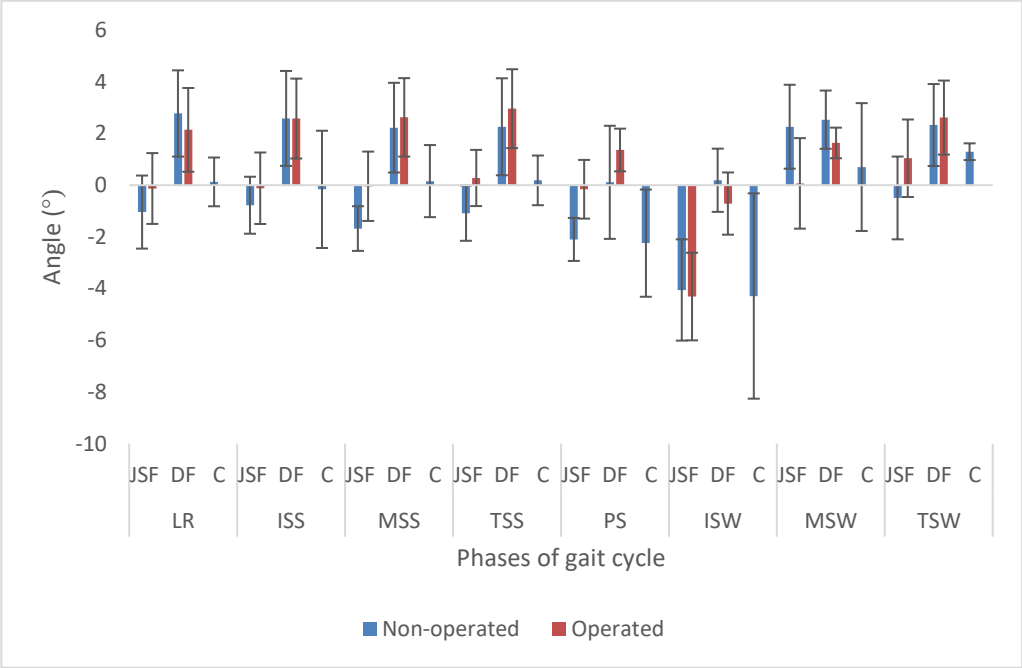

Appendix 6 Mean knee angle in the coronal plane in the proximal tibial joint-sparing and joint sacrificing groups and in the control group.

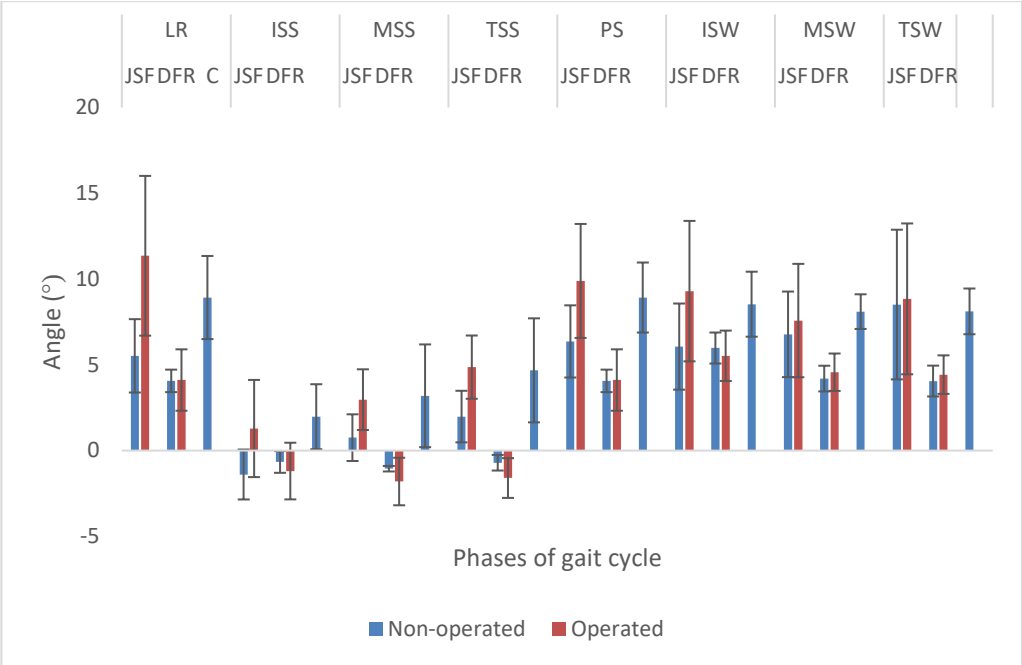

Appendix 7 Mean ankle angle in the coronal plane in the distal femoral joint-sparing and joint sacrificing groups and in the control group.

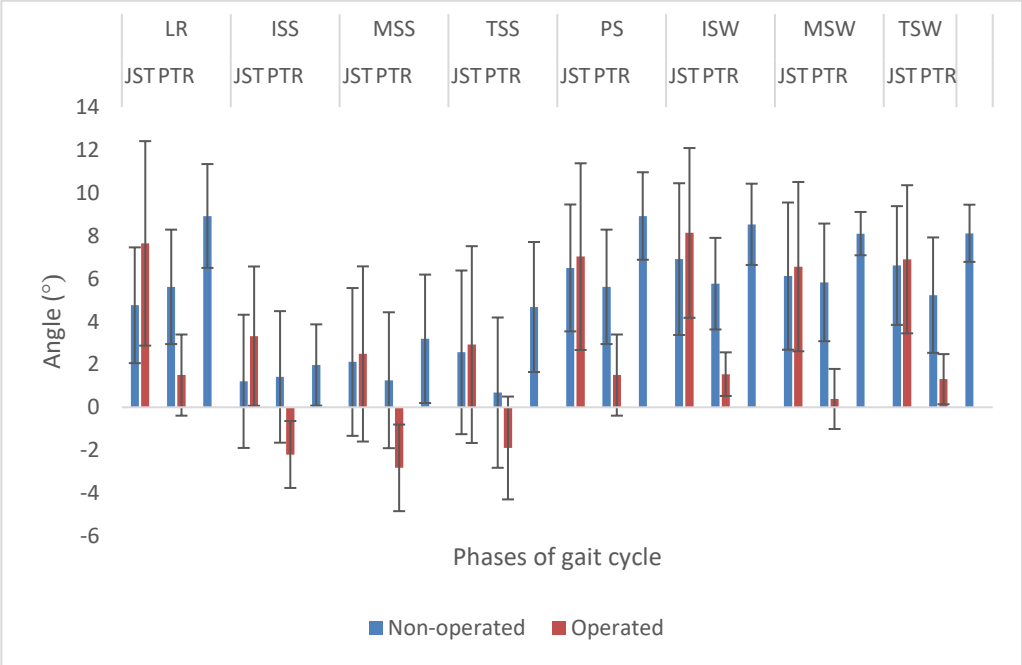

Appendix 8 Mean ankle angle in the coronal plane in the proximal tibial joint-sparing and joint sacrificing groups and in the control group.

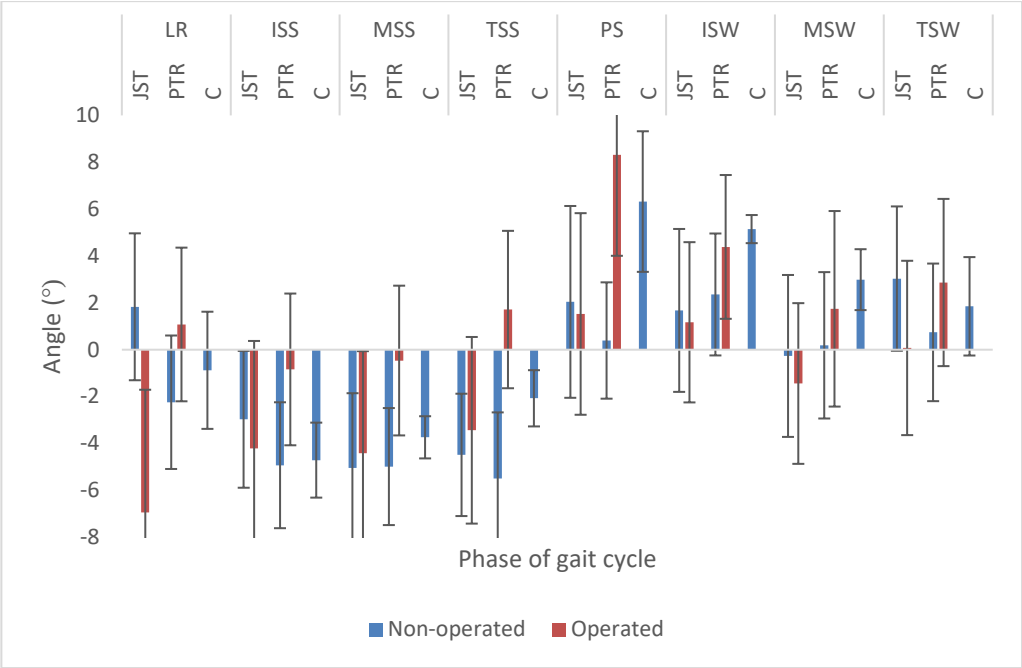

Appendix 9 Mean ankle angle in the horizontal plane in the proximal tibial joint-sparing and joint sacrificing groups and in the control group.

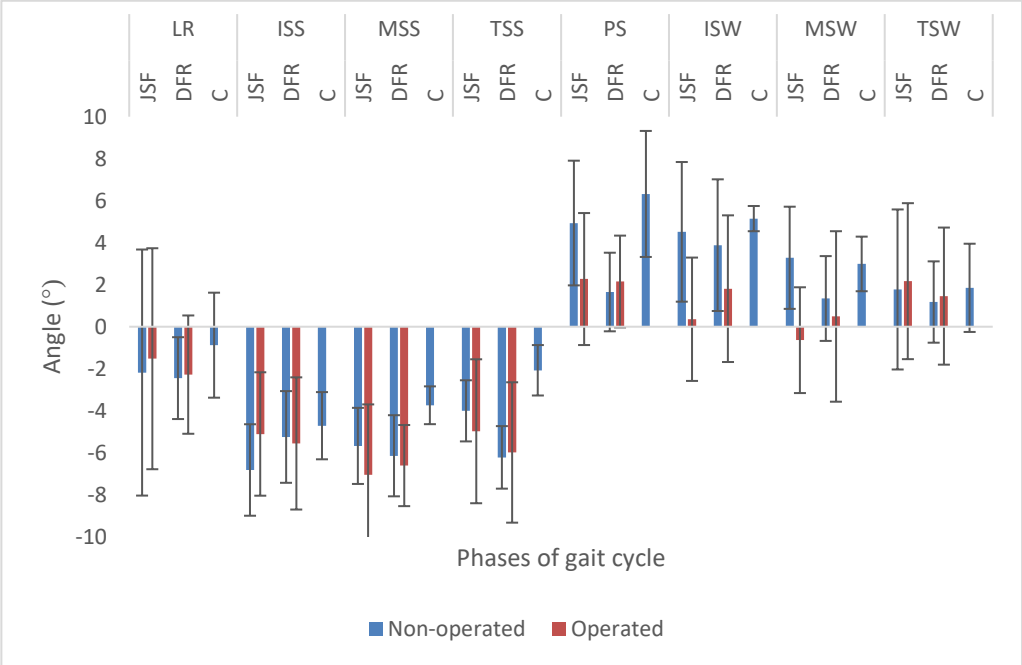

Appendix 10 Mean ankle angle in the horizontal plane in the distal femoral joint-sparing and joint sacrificing groups and in the control group.